PPPL-Q--45

DE89 008659

# Annual Report Covering the Period October 1, 1986 to September 30, 1987

**Princeton University**
**Plasma Physics Laboratory**
**Princeton, New Jersey 08543**

**PPPL-Q-45**



**Unless otherwise designated, the work in this report is funded by the United States Department of Energy under Contract DE-AC02-76-CHO-3073.**

**Printed in the United States of America**

# Contents


| | |
|---|---|
| *Preface* | 1 |
| Principal Parameters Achieved in Experimental Devices (FY87) | 3 |
| Tokamak Fusion Test Reactor | 5 |
| Princeton Beta Experiment-Modification | 40 |
| S-1 Spheromak | 52 |
| Current-Drive Experiment | 58 |
| X-Ray Laser Studies | 60 |
| Theoretical Division | 67 |
| Tokamak Modeling | 79 |
| Compact Ignition Tokamak | 86 |
| Engineering Department | 90 |
| Project Planning and Safety Office | 108 |
| Quality Assurance and Reliability | 110 |
| Administrative Operations | 112 |
| PPPL Patent Invention Disclosures (FY87) | 124 |
| Graduate Education: Plasma Physics | 126 |
| Graduate Education: Plasma Science and Fusion Technology | 129 |
| Section Coordinators | 131 |
| *Glossary of Abbreviations, Acronyms, Symbols* | 132 |
| Princeton Plasma Physics Laboratory Reports (FY87) | 140 |

# Preface

During 1987, the Tokamak Fusion Test Reactor (TFTR) extended its studies of the high-temperature, enhanced-confinement plasma regime. The neutral-beam-heating pulse was lengthened to 2 seconds, and central ion temperatures approaching 30 keV were measured, along with a Lawson parameter $n\tau_E$ above $10^{13}$ $cm^{-3}$ sec. To facilitate further advances in TFTR plasma parameters, the neutral-beam system is being converted to tangentially balanced injection, at a power level of 27 MW. In addition, 4 MW of ICRF power will be available for deposition in the plasma core. A detailed plan has been prepared for deuterium-tritium operation, with the objective of producing about 100 discharges in the range $Q_{DT} = 0.5\text{-}1.0$.

The conceptual design of the Compact Ignition Tokamak (CIT) has been developed by a national design team. An increase of the major radius to 1.75 m has permitted substantial enhancements in the experimental capabilities and the mechanical reliability of the device. The CIT Project became a federal budget line item in FY88, but full authorization of construction is not anticipated until FY89-90—with a corresponding delay of experimental operations to FY95-96.

The Princeton Beta Experiment-Modification (PBX-M) was completed at the end of FY87 and will study more strongly indented bean-shaped plasmas with conducting plates for kink-mode stabilization. The main objectives are to raise first-stability regime $\beta$-values towards the 10% level and begin the exploration of the second stability regime.

The S-1 Spheromak has increased its plasma temperature and has provided new results on self-stabilizing dynamo mechanisms. Adiabatic compression experiments will be carried out during the last quarter of calendar 1987, and the S-1 facility will then be shut down. The Current Drive Experiment (CDX) is producing and studying tokamak discharges generated by an external electron gun in a vacuum magnetic field.

The X-Ray Laser program has begun to use its 182-Å beam for microscopy. A new experimental facility is being completed, which has more powerful magnets and includes a $CO_2$ and a Nd-Yag laser for plasma heating, as well as a 1-TW picosecond laser for excitation of multiphoton processes.

The Theoretical Division has increased its contributions to the design of the CIT device and the physics of burning-plasma phenomena in general. Areas of principal activity are: (1) MHD equilibria and stability; (2) kinetic microinstability theory; (3) diagnostics and data analysis; (4) turbulence and transport, and (5) space plasma physics.

## PRINCIPAL PARAMETERS ACHIEVED IN EXPERIMENTAL DEVICES (Fiscal Year 1987)

| Parameters | Tokamak Facilities | | | Alternate Concept Facilities | |
|---|---|---|---|---|---|
| | TFTR | PLT** | PBX-M | S-1 | CDX |
| R (m) | 2.48 | 1.32 | 1.65 | 0.40 | 0.59 |
| a (m) | 0.83 | 0.42 | 0.3 | 0.25 | 0.1 |
| $I_p$ (MA) | 2.5 | 0.7 | 0.8 | 0.55 | — |
| $B_T$ (T) | 5.2 | 3.4 | 2.2 | 0.4 | 0.57 |
| $\tau_{AUX}$ (sec) | 2.0 | 0.5 | 0.5 | — | dc |
| $P_{AUX}$ (MW) | | | | | |
| NB | 22 (110 kV) | — | 7 (40 kV) | — | — |
| ICRF | 7 (40-80 MHz)*** | 5.0 (30 MHz) | 2.0 (40-80 MHz)***,[a] | — | 0.002 |
| LH | — | 1.0 (2.45 GHz) | 2.0 (4.6 GHz)*** | — | — |
| ECRH | — | 0.05 (60 GHz) | — | — | 0.002 |
| n(0) ($cm^{-3}$)* | $4.0 \times 10^{14}$ | $0.8 \times 10^{14}$ | — | $3 \times 10^{14}$ | $3 \times 10^{13}$ |
| $T_i(0)$ (keV)* | 27 | 5.0 | — | 0.15 | 0.04 |
| $\tau_E$ (msec)* | 500 | 40 | — | 0.1 | 0.2 |

* These highest values of n, T, and $\tau$ were not achieved simultaneously.
** Inactive.
*** Under construction.
[a] Ion Bernstein Wave Heating (IBWH)

# TOKAMAK FUSION TEST REACTOR

## SUMMARY

The research program for the Tokamak Fusion Test Reactor (TFTR) made very significant progress this year on two parallel fronts. Both point toward the goal of operation of TFTR in breakeven deuterium-tritium (D-T) fusion experiments in 1990. The first effort was in enhancing the neutral-beam-heating capability and subsequent plasma studies, while the second was in developing and starting to implement a coherent plan for achieving D-T operation. This program ranges in aspect from assessing the scientific merit and feasibility, to specification of the configuration changes required for the tritium and neutron environments of this operation.

The capability of the four neutral heating beams was enhanced by replacing the ion sources. The new Long-Pulse Ion Sources (LPIS) have a two-second pulse length and provide a better high-energy species component than the previous sources which had a half-second pulse length. A power level of 22 MW lasting for half a second was achieved and 3 MW for 0.9 sec could be obtained from one source of the eleven on the tokamak. But in practice, the operation of the heating beams at full capability was constrained either because the best plasma performance occurred with balanced co- and counter-injected power or because a new constraint limiting the total number of neutrons emitted during a shot was applied to keep the incremental nuclear activation of the tokamak components down. During this run, three beamlines (with eight sources) pointed in the co-direction and only one (with three sources) in the counter-direction so that the supershot plasmas, which showed best confinement properties, made use of only about half of the available power. With co-injection (i.e., neutral-beam power applied tangentially in the direction of the plasma current) only, the plasma gains momentum from the beam particles and moves rapidly in the co-direction. This momentum gain becomes negligible for balanced injection and becomes large in the opposite direction for counter-injection alone. Also, with a large fraction of the neutrons arising from beam-beam and beam-plasma interactions and the neutron source strength often reaching its maximum long before the full two-second time interval, the heating could be terminated early without loss of physics information.

During the experimental studies of the supershot plasma regime, yet higher record ion temperatures of about 30 keV were reached, about 50% higher than last year's achievement. It was particularly gratifying to be able to cross-check the temperatures between measurements by a charge-exchange recombination spectrometer and an X-ray crystal spectrometer. The former instrument yielded radial profiles the ion temperature (and of the toroidal component of plasma motion induced by unbalanced beams) and has led to a better knowledge of the ion confinement. These beam-fueled discharges have very peaked density profiles as have the high density discharges fueled by pellets. The study of these discharges and the understanding of the plasma behavior as the balance of the heating was changed made up most of the experimental program.

The major changes in the configuration of the auxiliary heating, started near the end of the year, were guided by these results. One of the neutral-beam lines is being relocated so that it will point in the counter- rather than co-direction. Effectively, the power available for supershot studies will be doubled. Further, two ion-cyclotron radio-frequency (ICRF) antennae are being built to provide 4 MW of power for heating the center of the plasma.

The installation of these antennae is indicated in the TFTR Research Plan, revised in April 1987 and shown in Fig. 1. The approach to fabrication of these antennae is important. One of them was built at the Princeton Plasma Physics Laboratory (PPPL), the other at the Oak Ridge National Laboratory (ORNL). While they both have been thoroughly reviewed for engineering feasibility and quality, they deliberately have some different components. Conditioning and operating of the two antennas on TFTR will provide prototyping data for the Compact Ignition Tokamak (CIT) Project, which is presently based on using ICRF for its auxiliary heating.

The second major effort lay in the preparation of a plan mapping out the program of work necessary for achieving plasma breakeven $Q_{DT} \sim 1$ ($Q_{DT} \equiv$ power from fusion reactions/power delivered to the plasma) in 1990. A draft of this "D-T Plan"[1] was completed in April 1987. It is being revised as a result of analysis and design activity which was inspired by this first detailed global look at the D-T program. In September, a "Report on the Scientific Technical Merit of Deuterium-Tritium Operation in TFTR" was presented by Panel XVII of the Magnetic Fusion Advisory Committee (MFAC)[2] after a very thorough examination of the TFTR program. The report emphatically endorsed carrying out an experimental program of approximately 100 discharges with D-T plasmas for $Q_{DT} \sim 1$ on TFTR. The report endorses the importance of the physics aspects of the program, in particular, the ability to do studies of the alpha particles for $Q_{DT}$

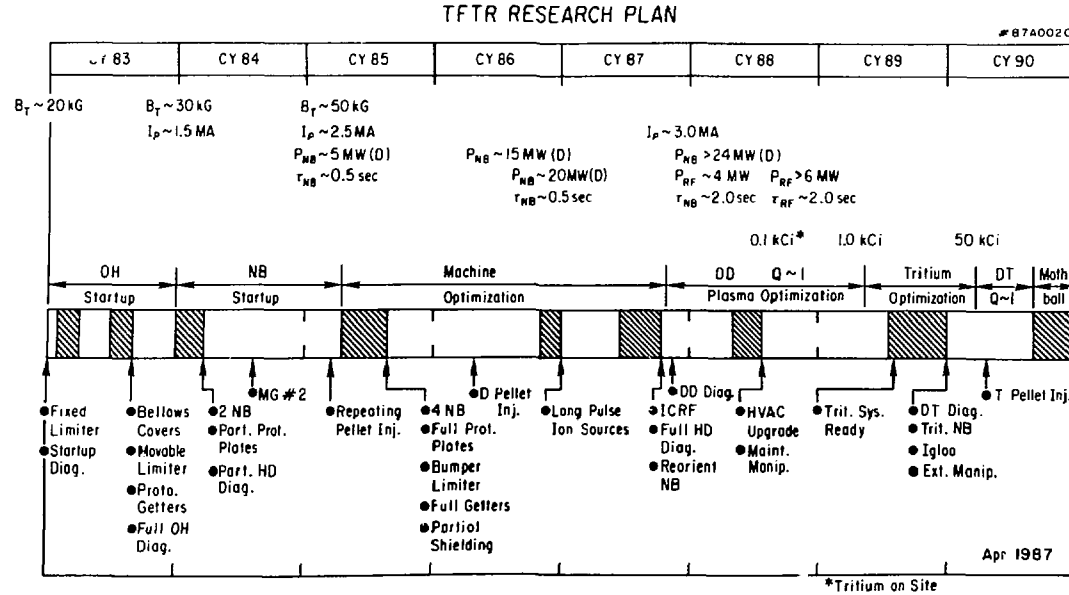


*Figure 1. The Tokamak Fusion Test Reactor Research Plan, revised in April 1987.*

$\geq$ 0.5, and the technical benefits of a fully working tritium-compatible and radiation-hardened tokamak for the fusion program. The benefits for future devices, in particular CIT, are spelled out clearly for diagnostics in a radiation enviornment, for understanding of tritium retention on wall surfaces, and for a limited remote-handling capability.

In the latter part of the year, it became apparent that significantly more work than originally estimated will be necessary for implementing D-T operation. Preparation of components close to the tokamak for installation of the enclosing concrete igloo shield, both to improve reliability and to reduce interferences, and changes at the interface ducts of the neutral beams fall within this additional scope. The additional manpower and funding required may cause an extension of the TFTR program. This extension is presently under consideration.

The details of the experimental program and the main features of the operation of TFTR and its preparation for later programs are given in the following sections.

## PHYSICS PROGRAM

The principle TFTR research objective is demonstration of fusion "energy breakeven," which means the generation of hot, dense plasmas whose ratio ($Q_{DT}$) of fusion power production to input power exceeds unity. Here, the subscript "D-T" on Q signifies that actual break-even experiments, now scheduled for FY90, will be carried out with a mixture of deuterium (D) and tritium (T) fuel. All experiments up to that time will operate without tritium, to allow the crucial scientific issues of plasma heating and stability to be studied without introducing the technical complications of tritium handling and heavy neutron shielding.

Achieving $Q_{DT} \geq 1$ in TFTR will require intense plasma heating to produce high ion temperatures ($T_i \approx 20$ keV) and simultaneously good plasma confinement, such that the product of energy confinement time and central density $[n_e(0)\tau_E]$ exceeds about 2.5 $\times 10^{19}$ sec m$^{-3}$. These conditions have already been obtained separately in TFTR: the required ion temperatures, in low-density plasmas heated with 10-20 MW of neutral-beam injection, and the required $n(0)\tau_E$ product, in high-density plasmas fueled by rapid injection of frozen deuterium pellets. The plasma conditions of temperature, density, and confinement time obtained (simultaneously) so far in the low-density experiments would yield $Q_{DT} \approx 0.25$ if an optimum fraction of the deuterium fuel were replaced by tritium.

The physics program in FY87 explored a number of plasma regimes that hold promise for attaining the conditions necessary to achieve $Q_{DT} \sim 1$ in 1990. Record ion temperatures, $T_i \approx 30$ keV, and record values of the product $n_e(0)\tau_E(a)T_i(0) \approx 3 \times 10^{20}$ keV sec m$^{-3}$ were obtained in the supershot regime for which near-balanced neutral beams are injected into a low-density target plasma of modest current ($I_p <$ 1.1 MA). The improved performance resulted in part from more deeply penetrating beams ($E_b$ up to 120 keV) having an improved species mix (67% of beam current in the full energy component). The new beam sources also provided longer pulses (0.5-2.0 sec) making possible studies of current ramps to extend the range of plasma currents which sustain the

favorable profiles [broad $T_e(r)$, peaked $n_e(r)$] characteristic of supershots. In preparation for a beamline reorientation, starting in July 1987, to provide more balanced injection, special emphasis was given to studies of the effects of beam directedness (co, counter, and balanced) and plasma rotation on energy confinement and neutron emissivity. Measurements of the particle confinement time showed little variation over the range of plasma currents $I_p$ = 1.0-1.3 MA, suggesting that changes in particle transport are not responsible for the loss of favorable supershot conditions at higher $I_p$.

Charge-exchange recombination spectroscopic measurements of ion temperature and rotation speed profiles provided new insights into fundamental transport mechanisms. The ion temperature profiles over a wide range of auxiliary heating conditions are significantly narrower than expected from neoclassical transport. Transport simulations of the $T_e(r)$, $T_i(r)$, and $v_\phi(r)$ profiles indicate that the heat and momentum diffusivities $\chi_e$, $\chi_i$, and $\chi_\phi$ are all comparable in magnitude and have similar shapes in minor radius. Experiments with off-axis beam heating confirm that ion heat transport is enhanced above neoclassical levels during auxiliary central heating; $\eta_i$ modes[3] are considered a possible driving mechanism. Edge turbulence also correlates with electron energy confinement in L-mode (low-mode) discharges, but no clear relationship emerges in supershots.

A second approach to $Q_{DT} \sim 1$ is high-current, high-density pellet-fueled discharges. The favorable peaked $n_e(r)$ profiles and long pump-out times observed previously in ohmic-heated pellet-fueled discharges were found to persist with up to 10 MW of neutral-beam power, which thus represent ideal target plasmas for central ICRH heating. The densities presently achieved with pellet injection are already in the optimum range for maximizing $Q_{DT}$ with 27 MW of near-perpendicular injection and 7 MW of centrally deposited ICRH power. Projections of energy confinement times based on beam-heated, high-current TFTR discharges extrapolate to $Q_{DT} \geq 0.5$ at $I_p$ = 3 MA, if the confinement is L-mode with $\tau_E \sim 120$ msec.

A new class of phenomena, called the "q-transition," was observed at specific $q_\psi(a)$ values (2.6, 3.1, 4.0) with neutral-beam power greater than 6 MW. The q-transition shares many features of the enhanced confinement H-mode (high-mode), which is typically seen in tokamaks with divertors, and which has also been observed in the JFT-2M tokamak which has a limiter. Thus far, enhancements in energy confinement during q-transitions have been limited to approximately 20%.

Finally, a plasma scenario (the "alpha storage mode") was devised to maximize the collective alpha-particle effects which can be studied in TFTR at $Q_{DT} \sim 1$. Ignition levels of $n_\alpha/n_e$ and $\beta_\alpha/\beta$ can be obtained in TFTR with $Q_{DT} \sim 1$ by operating at the highest possible electron temperature which is usually obtained at the lowest possible density. Significant alpha-heating ($P_\alpha/P_{tot} \approx 0.5$) can be studied on a transient basis by rapidly increasing the density in a $Q_{DT} \sim 1$ plasma following beam turn-off.

## Enhanced-Confinement Regime

An enhanced regime of plasma confinement, known as the "supershot" regime, was first identified in June 1986.[4,5] Supershots were obtained by injecting near-balanced beam power above a certain power threshold ($P_b \gtrsim 10$ MW) into a low-current ($I_p$ = 0.8-1.0 MA), low-density target plasma, with wall recycling suppressed by prior conditioning of the carbon tiles through repetitive ohmic discharges in helium or low-density deuterium. Supershot performance was characterized by high energy-confinement times $\tau_E < 180$ msec [about three times larger than L-mode scaling,[6] profile modifications [broad $T_e(r)$, narrow $n_e(r)$]], high central ion temperatures up to 20 keV, and large neutron emissivity, up to $1.2 \times 10^{16}$ sec$^{-1}$. A tantalizing feature of the supershot regime is that it first appears at low plasma current, 0.7-0.8 MA, only about 30% of the present TFTR capability of 2.5 MA. Because standard L-mode scaling of energy confinement[6] improved linearly with $I_p$, there is potential for substantial increases in $\tau_E$, which would extrapolate to $Q_{DT} = 1$, if the favorable $I_p$ scaling could be retained in supershots. Higher plasma currents will be required, in any event, as the beam power is increased in order to avoid coherent MHD activity ($m/n$ = 3/2, 2/1) that spoils confinement as the value of $\epsilon\beta_p$ approaches 0.7 (Refs. 7-8) and to remain below the Troyon $\beta$-limit.[9] However, simply raising the flattop plasma current prior to neutral injection has not proven to be an avenue to improved performance, because the favorable confinement times and profile shapes are progressively lost for $I_p \geq 1.1$ MA.

Using the SURVEY code, computer projections of attainable $Q_{DT}$ indicate that the temperatures ($T_i \approx 30$ keV, $T_e < 9$ keV) and global energy confinement times ($\tau_E < 180$ msec) already obtained with supershots are adequate to reach $Q_{DT}$ = 0.5 with full beam power, if the density can be doubled and $Z_{eff}$ reduced from 3.5 to 1.5. The favorable confinement times must be sustained as the balanced beam power is doubled over the present levels, as the density is doubled, and as the plasma current is increased to at least 1.6 MA (to remain below the Troyon $\beta$-limit). Figure 2 sketches the parameter space presently accessible to the supershot regime. Due to the soft transport (and occasionally disruptive) limit imposed by $\epsilon\beta_p \lesssim 0.7$ (Refs. 7-8) the supershot confinement times can be maintained at successively higher beam powers as the plasma current is increased. Correspondingly, the minimum beam power required to achieve the supershot regime appears to increase with plasma current. These correlations suggest a technique whereby beam power and $I_p$ are programmed to ramp up simultaneously to maintain the desirable supershot profile shapes and to avoid the deleterious coherent MHD. As discussed below, initial ramp experiments have shown promise in extending stable operation to higher beam power, but the available beam configuration on TFTR during this year

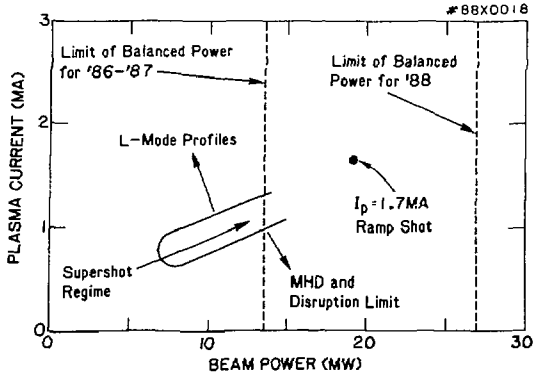


*Figure 2. The TFTR operating diagram for well-degassed limiters and balanced injection. A discharge with the current ramped to $I_p$ = 1.7 MA with unbalanced injection of 19 MW is shown for comparison.*

(two co-beamlines, one counter-beamline) only allowed balanced injection up to 13 MW. The full benefit of dual current/beam power ramps will be realized in experiments next year following reorientation of the beamlines to provide 27 MW of balanced power.

Figure 3 illustrates a discharge in which the $I_p$ was ramped continuously from 1.0 to 1.7 MA as the heating power was increased stepwise from 8.8 to 18.9 MW. Unlike a supershot at constant $I_p$ = 1.0 MA with 19 MW of injection, which would suffer a decline in stored energy and neutron emission after 400-500 msec of beam heating due to coherent MHD, the ramped shot shows a continuous increase in stored energy and neutron emission as more beam power is applied. In addition, the electron density profile is modestly more peaked than that obtained in a discharge at the same power level but at a constant $I_p$ = 1.7 MA, although not as peaked as typical supershots at lower $I_p$.

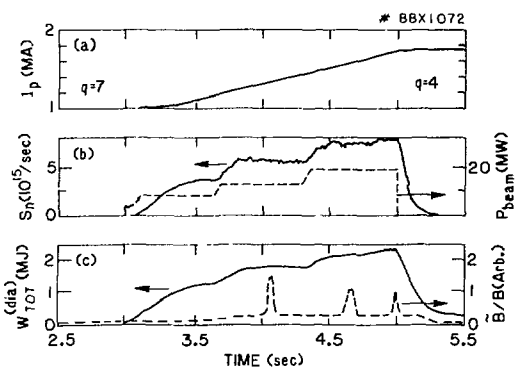


*Figure 3. Waveforms of plasma current, neutron source strength, beam power, plasma stored energy, and amplitude of edge MHD during current ramp to 1.7 MA with $P_b$ increased in steps to 19 MW.*

Current ramps modestly improve the total stored plasma energy as well as preserving the more favorable profile shapes at higher current. Figure 4 illustrates the variation of total stored plasma energy with beam power for ramped discharges at 1.3 and 1.7 MA versus unramped discharges ($I_p$ = 1.0-1.8 MA). Despite limited experimental time at high beam power, these initial experiments with current programming have demonstrated improvements in global energy confinement times of up to 20% at $I_p$ = 1.3 MA.

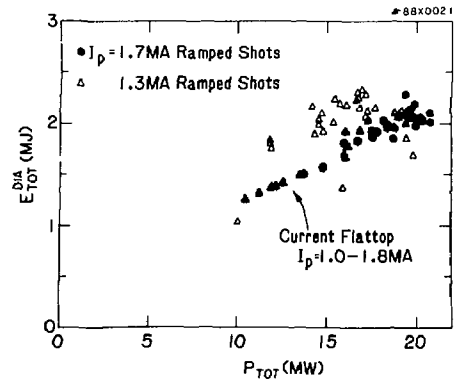


*Figure 4. Plasma stored energy plotted versus total input power for conditioned current-flattop discharges with $I_p$ = 1.0-1.8 MA (shaded region) and for current ramp discharges to $I_p$ = 1.3 and 1.7 MA.*

## Effects of Beam Directedness and Plasma Rotation on Supershots

It was reported previously that the supershot energy confinement time and neutron yield depends critically on the fraction of beam power injected in the co- and counter-directions.[5] These results were extended to higher powers and to a wider range of the balance parameter $(P_{co} - P_{cntr})/(P_{co} + P_{cntr})$, including unidirectional injection up to 11 MW with co-injection and 14 MW with counter-injection.[10] The variation of fusion gain $Q_{DD}$, central electron temperature, and global energy confinement time with the balance parameter is illustrated in Fig. 5 for conditioned discharges with $I_p$ = 0.9 MA. Despite modest scatter in the data at fixed balance parameter, which presumably reflects differences in wall conditioning and recycling, the optimum confinement times are obtained for balance parameters in the range 0.0 - 0.3, corresponding to balanced injection or a slight excess of co-power. It is also clear that unidirectional co-injection yields higher $Q_{DD}$, higher central electron temperatures, and higher confinement times than unidirectional counter-injection. This result cannot be attributed to enhanced orbit losses during counter injection, which are calculated to represent less than 5% of the total injected power at $I_p$ = 0.9 MA. The central ion temperatures also show a distinct

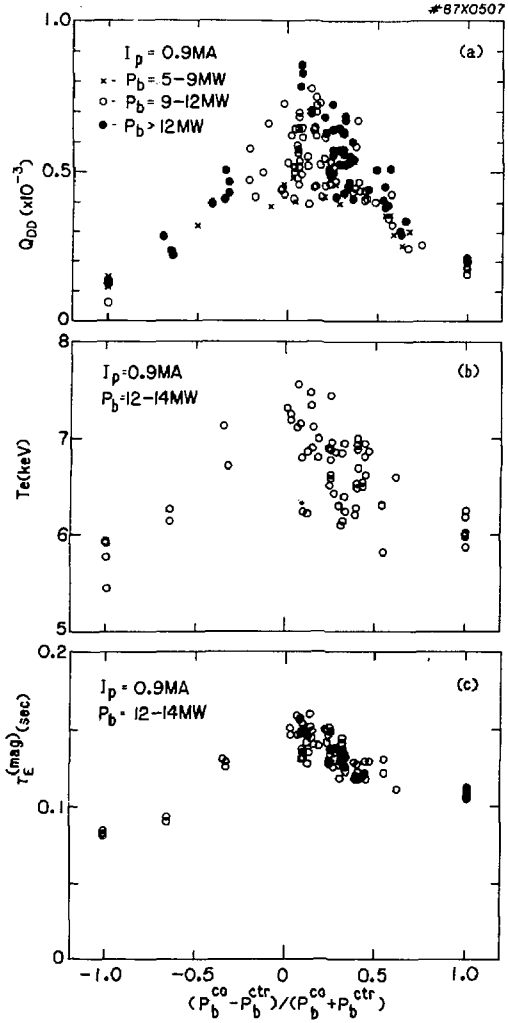


*Figure 5. (a) Fusion Power gain $Q_{dd}$, (b) central electron temperature, and (c) global energy confinement time as a function of the beam balance parameter.*

difference between co- and counter-injection (Fig. 6). There is considerable scatter in the ion temperatures achieved with balanced injection which partially overlaps the co-injection results, but the highest ion temperatures ($T_i$ > 20 keV) are obtained only with balanced injection.

The degraded performance of unbalanced injection is attributed, at least in part, to classical effects associated with beam-induced plasma rotation,[11] which can reach speeds in excess of 8 × $10^5$ m/sec at steady state for 11 MW of unidirectional injection.[10] A deuterium beam ion at 100 keV injected tangentially into a plasma moving at this speed has a kinetic energy in the plasma frame of only 55 keV, which reduces the rate coefficient for neutron yield from

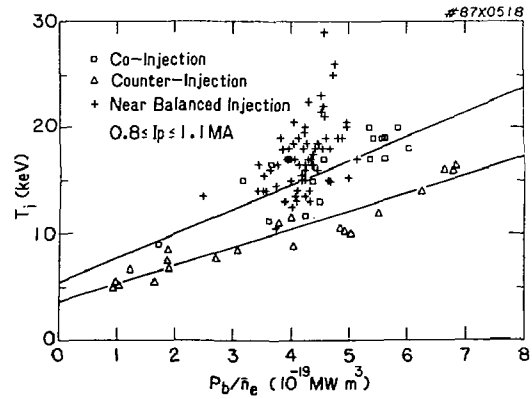


*Figure 6. Central ion temperature from Doppler broadening measurements of the NiXXVII $K_\alpha$ line from discharges with co-, counter-, and near-balanced injection as a function of $P_b/\bar{n}_e$. The beam power ranged from 3 to 14 MW, and $\bar{n}_e$ was in the range from 2 to 3.5 × $10^{19}$ $m^{-3}$. The solid lines represent linear least-squares fits to the data points with co- and counter-injection, respectively.*

beam-target reactions by a factor of four and causes less power to be delivered to electrons. Also, as a result of the reduced beam neutral energy in the plasma frame, the mean free path for ionization by proton collisions and charge-exchange is reduced about 40%. Consequently, the peaked heating profiles obtained in balanced supershots, which contribute to the favorable peaked density profiles and central ion heating, are broadened considerably.

Figure 7 shows a SNAP code comparison of the radial profiles for transfer of beam power to ions and electrons and the power flow from plasma rotation to viscous heating with and without a strong plasma

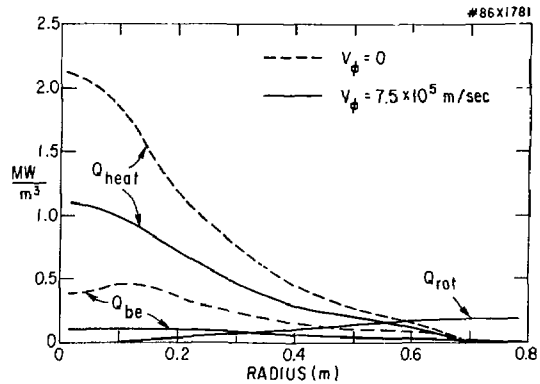


*Figure 7. SNAP-code calculations of radial profiles for beam power deposition into ions plus electrons ($Q_{heat}$), electrons along ($Q_{be}$) and power flow from beam-driven rotation into viscous heating ($Q_{rot}$). The calculations are performed for deuterium beams with $P_b$ = 12 MW for (a) balanced injection and zero rotation and (b) co-injection with $v_\phi(0)$ = 7.5 × $10^5$ m/sec with a parabolic density and velocity profile.*

rotation of $7.5 \times 10^5$ m/sec. The beam power invested in plasma rotation is, in this calculation, largely returned to the thermal plasma in the form of "edge" viscous heating.[11] Without plasma rotation, the heating efficiency of the plasma core is greatly improved, especially for the electrons.

## Analysis of Ion Temperature and Velocity Profile Measurements

Radial profile measurements of ion temperature and toroidal rotation speed were obtained for the first time on TFTR from the multi-sightline charge-exchange recombination spectrometer (CHERS). Measurements of ion temperature by CHERS and from the Doppler shift of intrinsic nickel $K_\alpha$ impurity lines measured by the horizontal X-ray crystal spectrometer yielded ion temperatures of 30 keV in TFTR. This represents a 50% increase over the 20 keV temperatures obtained during 1986.

The ion temperature profiles measured by CHERS for the three cases of balanced-injection supershots, high-power L-mode discharges, and conditioned co-injection discharges were found to be significantly narrower than would be expected from an ion power balance based on neoclassical ion thermal transport. Instead, the ion temperature profiles for these conditions were more consistent with power balance calculations which invoke an ion thermal diffusivity roughly equal to the electron thermal diffusivity in both magnitude and radial variation. The observation that $\chi_i \approx \chi_e$ during auxiliary heating may narrow the search for theoretical mechanisms controlling anomalous transport in tokamaks. In this regard, an investigation is underway into the $T_i(r)$ profiles that would be calculated with ion heat transport driven by $\eta_i$ modes.[3] The observation of narrow $T_i(r)$ profiles also has implications for $Q_{DT}$ projections in TFTR; for example, the $T_e(0)$ required to attain $Q_{DT} > 0.5$ is higher by several keV than projections based on neoclassical $T_i(r)$ profiles.

Figure 8(a) shows the measured ion temperature profile for a supershot with near-balanced injection ($I_p$ = 0.9 MA, $P_{inj}$ = 13.6 MW, $\bar{n}_e = 2.5 \times 10^{19}$ m$^{-3}$). Power balance calculations were performed by the one-dimensional SNAP kinetic analysis code assuming a particle confinement time of 100 msec, and assuming that energy transport due to particle convection is given by $\Gamma_{heat} = 1.5 \times T_i \times \Gamma_{particle}$. As shown in Fig. 8(b), the inferred ion thermal diffusivity $\chi_i$ was somewhat larger than the electron thermal diffusivity $\chi_e$ and showed a similar variation in minor radius. The inferred $\chi_i$ was much larger than the neoclassical ($\chi_i^{neo}$) value throughout the entire plasma and had a different shape. These observations are consistent with previous ion power balance analyses on the D-III tokamak.[12] Owing to the higher electron temperature in TFTR, the electron-ion power coupling is a small term in the ion power balance; within $r < a/2$, the dominant power losses are ion conduction and convection.

The SNAP code was also used in a predictive mode to calculate an expected ion temperature profile,

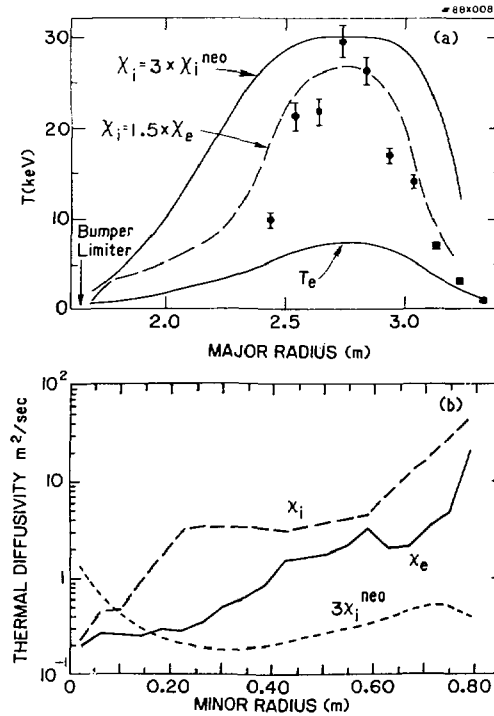


*Figure 8. (a) Ion temperature profile measured by CHERS versus calculated profiles based on $\chi_i = 3 \times \chi_i^{neo}$ (solid) and $\chi_i = 1.5 \times \chi_e$ (dashed) in a supershot with 13.6 MW of balanced injection. The lowest solid curve represents $T_e(R)$. (b) Ion $\chi_i$ and electron $\chi_e$ thermal diffusivity inferred from the measured temperature profiles. The neoclassical $\chi_i^{neo}(r)$ is much lower and has a different radial shape.*

given the measured $T_e(r)$ and a specific model for ion energy transport. The calculated ion temperature profile using $\chi_i(r) = 1.5 \times \chi_e(r)$ was in reasonable agreement with the measured $T_i(r)$, Fig. 8(a), in contrast to the neoclassical model ($\chi_i = 3 \times \chi_i^{neo}$) which predicted an overly broad $T_i(r)$ profile.

Figure 9(a) shows the measured ion temperature and rotation speed profiles as a function of minor radius for a co-injection, 11-MW discharge at $I_p$ = 0.9 MA, $\bar{n}_e = 1.7 \times 10^{19}$ m$^{-3}$. The strong rotation in this discharge [$v\phi(0) \approx 8 \times 10^5$ m/sec] significantly alters the calculated beam power deposition and the ion power balance. Beam slowing down times are reduced substantially because the beam ions have a reduced velocity in the plasma frame of reference; consequently, less beam power is delivered to the electrons. Indeed in the plasma frame at the magnetic axis, the beam component at one-third energy ($E_0$ /3 = 32 keV) is less than the mean thermal ion energy ($1.5 \times T_i \approx 30$ keV), so this component is thermalized immediately. A considerable fraction of the beam power (about 30%) is invested in pushing the plasma, and is returned to the thermal components as viscous heating.[11] This viscous heating, which is largest at

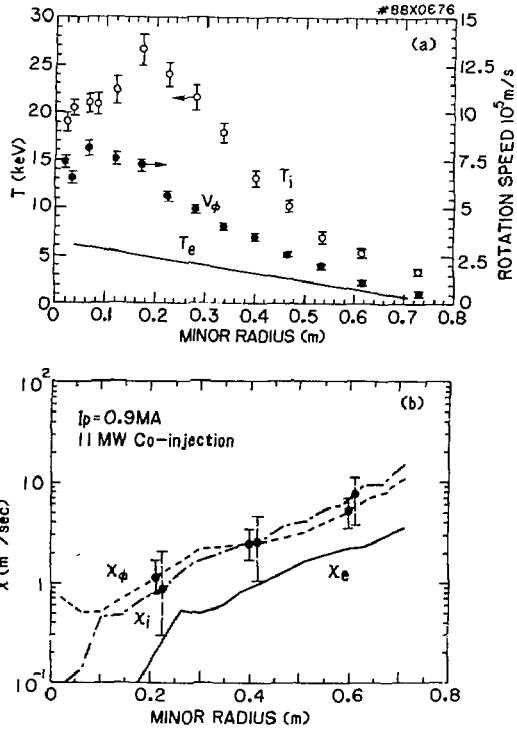


*Figure 9. (a) Measured profiles of $T_i(r)$, $T_e(r)$, v (r) for an 11 MW, co-injection discharge. (b) Inferred ion $\chi_i$ and electron $\chi_e$ thermal diffusivities and the ion momentum $\chi_\phi$ diffusivity as a function of minor radius.*

the point of maximum velocity gradient, peaks off-axis and may be responsible for the appearance of the off-axis peak in ion temperature at $r_{minor} \approx 0.2$ m.

The inferred thermal diffusivities for electrons and ions, together with the momentum diffusivity inferred from a momentum power balance, are shown in Fig. 9(b). An important result is that the momentum diffusivity is comparable in magnitude to the ion thermal diffusivity, and it has a similar variation with minor radius. Within $r < 2a/3$, the momentum balance is strongly dominated by viscosity, with convection and charge-exchange losses remaining relatively small. The thermal momentum confinement time for this discharge was 36 msec, about 2/3 of the thermal energy confinement time of 57 msec (the total energy confinement time, including the significant beam contribution, was 129 msec). In other co-injection discharges at different powers and plasma currents, and in supershots, the thermal momentum confinement time ranged from 34 to 102 msec, but it always remained a constant fraction (0.5-0.7) of the thermal energy confinement time. This systematic correlation between $\tau_\phi$ and $\tau_E$ points toward a transport mechanism that affects heat and momentum transport similarly.

# Effects of Plasma Rotation on Impurity Metal Accumulation

Beam directionality and/or the associated toroidal plasma rotation have been found to affect central metal concentrations. Total central metal concentrations of chromium, iron, and nickel measured with the horizontal X-ray pulse-height analysis diagnostic were significantly higher ($\Sigma n_m/n_e$ = 0.1-0.4%) in nearly balanced 0.8-1.0 MA supershots than in shots with pure co-injection (typically, $\Sigma n_m/n_e$ = 0.02-0.1%). With balanced injection, the metal concentrations increased only slightly with energy confinement time $\tau_E$ (0.09- 0.18 sec). The increase was more dramatic for pure co-injection, reaching values near 0.2% for $\tau_E > 0.14$ sec. A more informative indication of the effects of beam directionality is obtained by dividing the central metal density during neutral-beam injection into that observed in the ohmic-heating phase of the discharge. This normalization removes the effects of gradual changes (factors up to about 5) in the metal contamination on the graphite limiter throughout the run period, and it shows whether the metal densities (rather than concentration) actually increased or decreased during injection. As the beam power per particle ($P_b/\bar{n}_e$) increases, the metal density normalized to that in the ohmic phase increases from about 2 to 6 for nearly balanced shots, but decreases from approximately 2 to 0.4 for co-injected shots (Fig. 10). A new theory based on the effect of beam-driven plasma rotation on the orbits of impurity ions[13] suggests that edge impurities are poorly confined during co-rotation, leading to a smaller influx to the plasma core, in qualitative agreement with experiment.

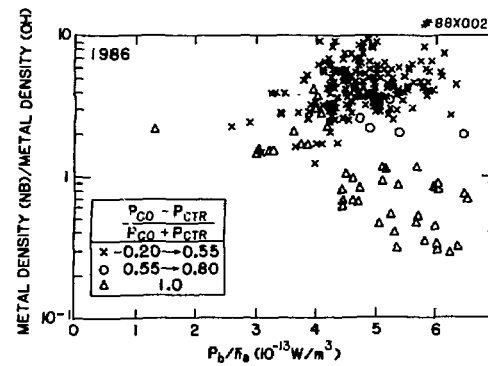


*Figure 10. Metal densities during neutral-beam injection, relative to their value in the ohmic-heating phase, for balanced and unbalanced injection. The scatter in the data for each range of balance parameter $[(P_{co}-P_{cntr})/(P_{co}+P_{cntr})]$ is indicative of the measurement uncertainty.*

## Wall Conditioning for Supershots

Because of the importance of low recycling conditions for obtaining supershot discharges in TFTR, we continued to study and quantify the effects of helium discharge conditioning on the hydrogen recycling and retention properties of the graphite inner wall limiter.[14-16] The helium conditioning technique was found to be an effective means of lowering the recycling coefficient of the bumper limiter, from values of near unity when the limiter surface is saturated with hydrogen to values as low as 0.5 after conditioning.[14] The conditioning process induces a pumping effect in the limiter which was quantified using particle balance measurements.[15,16]

By comparison of the gas input to the integrated particle outgassing for an identical series of ohmic discharges, the saturable pumping capacity of the bumper limiter was measured to be approximately 100 Torr-liters or $7 \times 10^{21}$ D atoms (Fig. 11). This quantity of gas is equal to the estimated saturation capacity of the high flux area of the limiter surface[15] assuming the same value of the hydrogen-to-carbon saturation ratio that is observed in laboratory measurements (approximately 0.4).

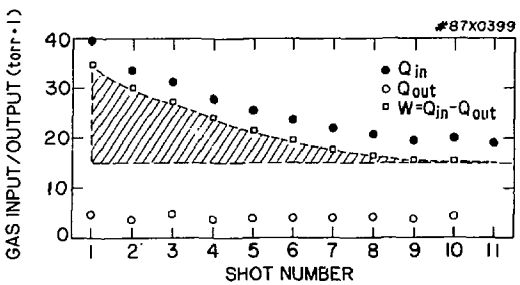


*Figure 11. The required gas fueling ($Q_{in}$), integrated vessel outgassing after a discharge ($Q_{out}$ from t = 0 to 80 sec), and the wall loading ($W = Q_{in}-Q_{out}$) during the wall loading sequence. The wall loading indicated in the cross-hatched area of the figure corresponds to a saturable wall pumping effect which sums to approximately 100 Torrliters.*

## D-T Retention Studies

Particle balance measurements and hydrogen retention measurements in wall and limiter samples removed from TFTR[17] were used to investigate the limiter pumping processes, and also to estimate tritium inventory in the TFTR first-wall structures during the D-T operational phase.[17] Measurements in TFTR first-wall samples show approximately $10^{17}$ deuterium atoms per $cm^2$ retained within carbon films redeposited on vacuum vessel wall areas and approximately $10^{18}$ deuterium atoms per $cm^2$ retained in the near-surface of plasma-facing areas of the bumper limiter. Less than 1 ppm (parts per million) deuterium was found in the bulk of the bumper limiter by depth profiling measurements. By integrating these local measurements over the total first-wall area, it is estimated that approximately 10% of the deuterium throughput was retained in the vessel for the 1985-1987 operation period. Similar calculations performed with retained tritium show that approximately 50% of tritons generated by D-D fusion reactions (approximately $6 \times 10^{18}$) were retained in the near-surface region of the bumper limiter.

The deuterium retention measurements were used to estimate the in-vessel tritium inventory for the specific discharge scenarios which have been proposed for the D-T operational phase. The current estimates[1] are yielding values close to the present on-site limit of 5 grams tritium.

## Magnetic Fluctuations in L-Mode and Supershot Discharges

A broadband spectrum of magnetic fluctuations is observed on the 20-coil Mirnov array during TFTR discharges. Over a broad frequency range, 1-1000 kHz, the amplitude spectra decrease with frequency as 1/f at all poloidal and toroidal locations. Coarse identification of the poloidal mode number is derived from the lack of correlation among the Mirnov coils spaced apart poloidally by 22.5°, which suggests $m > 16$. Evidence from gas puffing and impurity injection experiments indicates that the fluctuations originate within the outer edge of the plasma. Extrapolation of the fluctuation level to the plasma edge gives an rms (root-mean-square) fluctuation level of $\tilde{B}_\theta/B_T$ up to $2 \times 10^{-4}$ in the plasma edge. Theoretical estimates of energy transport driven by these fluctuations[18] suggest that they are large enough to be responsible for the observed anomalous energy loss. Preliminary work has shown a clear, linear correlation between the magnetic fluctuation level and inverse global electron energy confinement for L-mode and ohmic plasmas (Fig. 12). This relationship is violated in supershots with enhanced

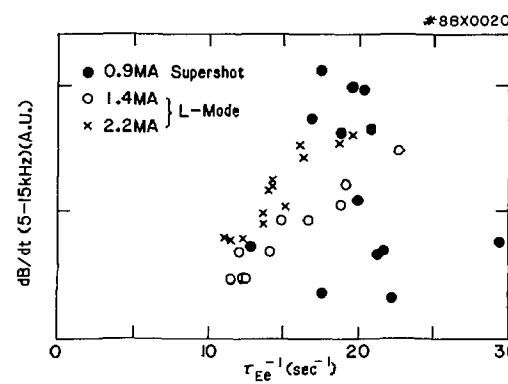


*Figure 12. Correlation between inverse electron energy confinement time in L-mode discharges and the measured edge fluctuation level. Supershots exhibit no clear relationship between $\tau_{Ee}^{-1}$ and the magnitude of edge fluctuations.*

confinement. For these, the measured fluctuation level is the same or lower than the scaling would predict for a given $\tau_{Ee}$. These results suggest that magnetic turbulence might be the cause of the anomalous transport, but other mechanisms cannot be ruled out with the data presently available. Future work will focus on measurements of the poloidal and toroidal correlation lengths with an expanded set of coils installed during the extended maintenance period.

## Profile Heating Experiments

The radial profile of neutral-beam power deposition in TFTR can be changed dramatically through selective injection of more perpendicularly or more tangentially oriented beam sources, which span a wide range of injection angles (tangency radii $R_t$ = 1.73 - 2.84 m). The most tangential source, which aims well outside the magnetic axis, can deliver heating profiles which are nearly hollow, providing little power deposition in the plasma core ($r < 0.40$ m for $R_o$ = 2.36 m) unless the fast-beam ions diffuse radially as they slow down. The off-axis heating experiments are of particular interest because they can reverse, at least temporarily, the usual physical situation wherein power and momentum transport is everywhere outward directed. Several experiments were performed. The recent beamline reorientation with more perpendicular sightlines precludes further off-axis experiments.

The first local measurements of fast-ion radial diffusion were obtained by injecting the single most-tangential beam source ($R_t$ = 2.84 m) into a modestly reduced-aperture plasma [R/a = (2.36 m/0.70 m)] to create a hollow annular ring of fast ions in the region $r > 0.4$ m. Charge-exchange (CX) observations of the fast neutral flux along horizontal sightlines near the inner edge of this annular ring ($R_t \approx R_o$ - 0.4 m) measured the density of ions which diffused radially into the hollow core as they slowed down. An upper bound on the fast-ion radial diffusivity can be obtained by comparing the relative shapes of the CX flux as a function of viewing position near $E = E_{beam}$ (for which there is little slowing down and correspondingly little time for radial diffusion) with that at $E > E_{beam}/2$. Figure 13 illustrates the normalized CX flux as a function of viewing position at E = 90 keV and E = 60 keV for a co-injection discharge with $I_p$ = 1.2 MA, $P_b$ = 2.1 MW, $E_b$ = 95 keV, $T_{eo}$ = 5.0 keV, and $\bar{n}_e = 1.5 \times 10^{19}$ m$^{-3}$. Also shown is the expected shape of the CX flux as calculated by a Fokker-Planck code including three levels of radial diffusion, taken to be independent of space and energy (D = 0.0, 0.1, and 0.5 m$^2$/sec). The data at 60 keV is bracketed by the simulations with D = 0.0 and D = 0.1 m$^2$/sec, which represents a very low rate of radial diffusion for fast ions. For comparison, the electron thermal diffusivity for this discharge as inferred from the measured $T_e(r)$ and $T_i(r)$ profiles was a factor of about 10 higher, $\chi_e \approx 1$ m$^2$/sec at $r \approx 0.5$ m. Even the fast-ion diffusivity of 0.5 m$^2$/sec would cause only a 13% loss of beam power under typical TFTR supershot conditions. Thus, these experiments

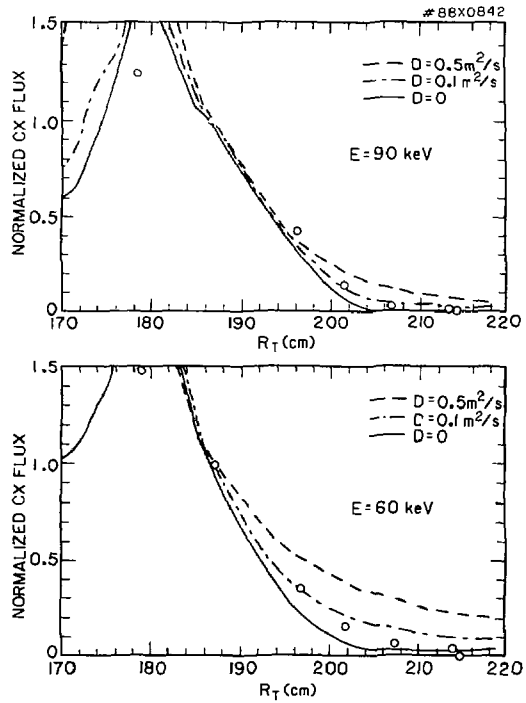


*Figure 13. Measured and calculated neutral particle flux as a function of viewing tangency radius near the inner edge of the annular ring of fast ions, at E = 90 keV (near $E_b$ = 90 keV), and at E = 60 keV.*

indicate that fast ions do not suffer any serious anomalous radial diffusion as they slow down under quiescent MHD conditions with edge neutral-beam heating.

The capability to control radial deposition of beam power, and hence beam torque, was also used to investigate the physical mechanism controlling radial transport of toroidal momentum.[19] Unidirectional co-beam power ($P_b \approx 2.3$ MW) was injected in three 100-msec pulses separated by two 100-msec off-periods for both the center- and edge-weighted deposition profiles. The central rotation speed during central weighted heating shows a clear modulation which is correlated with the beam timing [Fig. 14(a)]. By contrast, the rotation speed during edge heating rises more or less monotonically throughout the entire 500 msec of modulated beam injection to a final speed approximately 2/3 of that attained with central heating [Fig. 14(b)]. This is the qualitative behavior one would expect if momentum transport were predominantly diffusive in character, allowing an inverted rotation speed profile [$v_\phi$(edge) > $v_\phi$(central)] to relax to a flatter profile during the beam-off periods. Local damping mechanisms such as ripple damping would not transport momentum to the plasma center during edge heating. The time history of central rotation speed can be reproduced for both experiments by a transport simulation invoking only the calculated

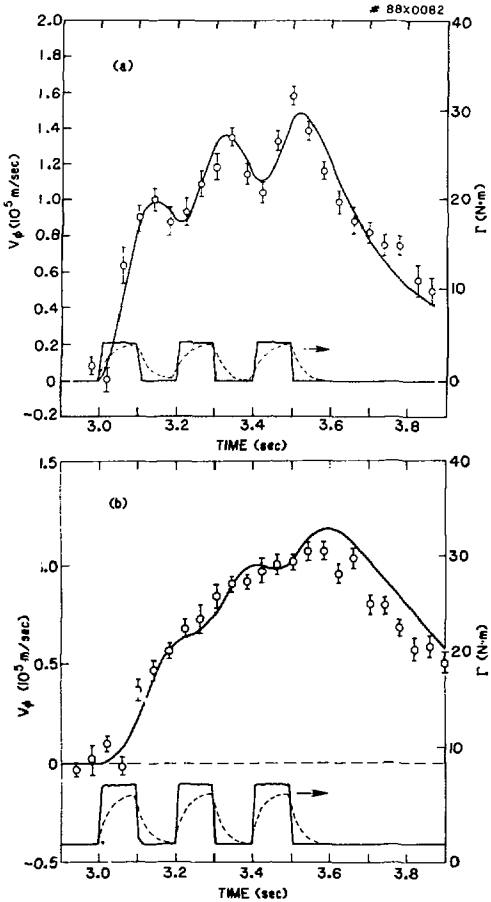


*Figure 14. Time history of central rotation speed measured by Doppler shift of TiXXI $K_\alpha$ emission during modulated central heating (a) and edge heating (b). The solid lines represent transport simulations assuming $\chi_\phi$ = 7.0 m²/sec (central heating) and $\chi_\phi$ = 3.0 m²/sec (edge heating).*

torque deposition rate and a radial momentum diffusivity which is assumed to be either flat or which increases with radius as $\chi_\phi \propto [1+(2r/a)]$. The inferred magnitude of momentum diffusivity is found to be twice as high in the central-heating experiment, e.g., $\chi_\phi$ = 7.0 m²/sec versus $\chi_\phi$ = 3.0 m²/sec for the edge-heating experiment. Measurements of the time evolution of the velocity profile by the CHERS (charge-exchange recombination spectrometer) diagnostic in edge-heating experiments confirmed that the velocity is peaked at the edge shortly after beam turn-on, then relaxes to a flatter profile.

The capability to modify the heating profile was used to investigate the mechanism(s) contributing to the apparent resiliency of $T_e(r)$ in tokamaks during auxiliary heating.[20] Experiments were conducted in deuterium plasmas at $R_o$ = 2.36 m, a = 0.70 m, $B_T$ = 4.9 T, $I_p$ = 1.2 MA, with 2.8 MW of neutral beams directed to provide central ($R_t$ = 1.9 m) or edge ($R_t$ = 2.75 m) heating profiles. Beam fueling increased the electron density from 2.6 × 10¹⁹ m⁻³ to 3.4 × 10¹⁹ m⁻³ in both cases during the 500-msec beam pulse. The central ion temperature as measured by X-ray crystal spectroscopy increased from an initial value of 2.2 keV up to 3.5 keV in the central-heating case, but only to 2.9 keV in the edge-heating case.

The electron and ion power balance in these discharges was analyzed using the TRANSP code. Using a neoclassical model for ion heat transport ($\chi_i = \chi_i^{neo}$), the central ion temperature calculated by TRANSP agrees with the measured value for edge heating, but it overestimates the central temperature (4.5 versus 3.5 keV) for central heating. This suggests that anomalous ion thermal transport may play a role, and $\eta_i$ modes[3] are a natural candidate because TRANSP calculates much more peaked $T_i(r)$ profiles with central than with edge heating (using $\chi_i = \chi_i^{neo}$). The calculated central ion temperature using $\chi_i = \chi_i^{neo} + \chi_i(\eta_i)$ agrees with the measured values for both experiments, while the inferred $\chi_e(r)$ is very similar for the edge and central experiments outside r = 0.4 m. Inclusion of $\chi_i(\eta_i)$ has no effect on the deduced $\chi_e$ in the core region or $T_i(0)$ of the edge heating case, because the hollow heating profile did not drive $\eta_i$ past threshold in the central region. These results imply that the observed resiliency of the measured electron temperature profile in the face of very different heating profiles could at least in part be explained by a mechanism in the ion channel which tends to maintain itself at marginal stability.

## Pellet-Injection Results

Combined neutral beam and ICRF heating of high $I_p$, pellet-fueled discharges is another approach to attaining high $Q_{DT}$ in TFTR. Auxiliary heating of pellet-fueled target ohmic-heated plasmas exploits the favorable fusion yield of peaked $n_D(r)$ profiles for a given global $\tau_E$. Previous experiments[21] demonstrated the capability of producing suitable high-density ohmic-heated target plasmas with peaked $n_e(r)$ profiles and slow post-pellet density decay times. This year's experiments explored the effects of modest levels of neutral-beam injection ($P_b$ < 10 MW) on density pumpout and profile shapes. Modeling efforts concentrated on simulating particle transport and identifying the optimum density to maximize $Q_{DT}$ for fixed $\tau_E$.

High current operation is envisioned for pellet experiments both to sustain the high-density ohmic-heated plasma during pellet fueling and to exploit the favorable $I_p$ dependence of energy confinement in L-mode scaling. For gas-fueled discharges, beam power scans of total stored energy at $I_p$ = 1.4 and 2.2 MA in TFTR show an improvement in energy confinement with increasing plasma current. The results can be expressed by either an "incremental" confinement time, $W_{tot} = W_o + \tau_{inc} \times P_{tot}$ (with $\tau_{inc} \propto I_p$) (Ref. 5), or by standard Goldston L-mode scaling,[6]

$\tau_E = 1.16 \times \tau_E^{L\text{-MODE}}$. These two representations yield similar projections when extrapolated to $I_p$ = 3.0 MA and $P_{tot}$ = 30 MW: the former yields $\tau_E$ = 150 msec and the latter 120 msec. Modest improvements over L-mode scaling have also been considered ($\tau_E$ = 150-200 msec) based on the observation that central $\tau_E$ ($r < a/2$) can be nearly twice that of the global $\tau_E$.

Projections of $Q_{DT}$ by the SURVEY code indicate that energy breakeven ($Q_{DT}$ = 1) can be attained with $\tau_E$ = 200 msec at an optimum density of $\bar{n}_e = 8 \times 10^{19}$ m$^{-3}$ with a peaking factor, $p = n_e(0)/\bar{n}_e$, of 2.3. As shown in Fig. 15, the $Q_{DT}$ performance improves considerably with the peaking factor. The density for optimum $Q_{DT}$ increases modestly with assumed $\tau_E$ and tends to be a weak function of $\bar{n}_e$ near the optimum value.

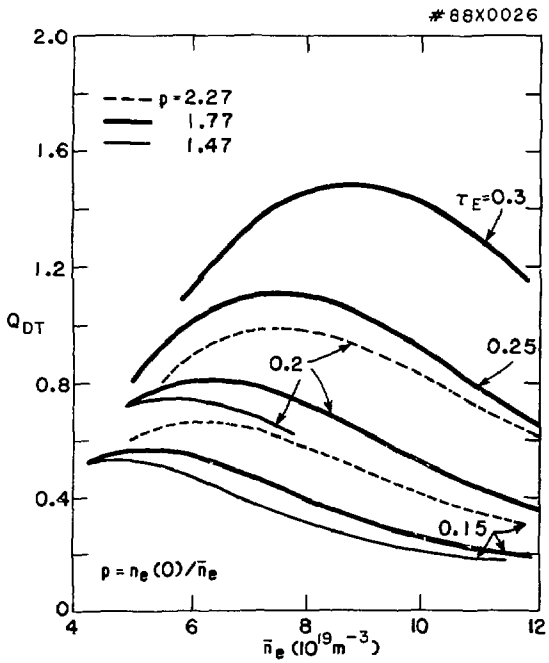


*Figure 15. SURVEY-code projections of $Q_{DT}$ performance in TFTR as a function of $\bar{n}_e$ assuming various peaking factors, $p = n_e(0)/\bar{n}_e$, and assuming various global energy confinement times.*

Figure 16 illustrates the time evolution of density during 5 MW of neutral injection following injection of a single pellet that raised $\bar{n}_e$ to 1.4 × 10$^{20}$ m$^{-3}$. The profile shapes may be characterized as a strongly peaked central core, which decays in time, superimposed on a relatively high edge pedestal, which remains roughly constant during neutral-beam heating. The peaking factor decreases from an initial high value of 2.3 to approximately 1.8 after 1.0 sec of beam heating. In the same time interval, the line-averaged density decays from 1.4 × 10$^{20}$ m$^{-3}$ to 8 × 10$^{19}$ m$^{-3}$, which is above the density for optimum $Q_{DT}$ at $\tau_E$ = 150 msec but which approaches the optimum density for $\tau_E$ = 200 msec. A similar

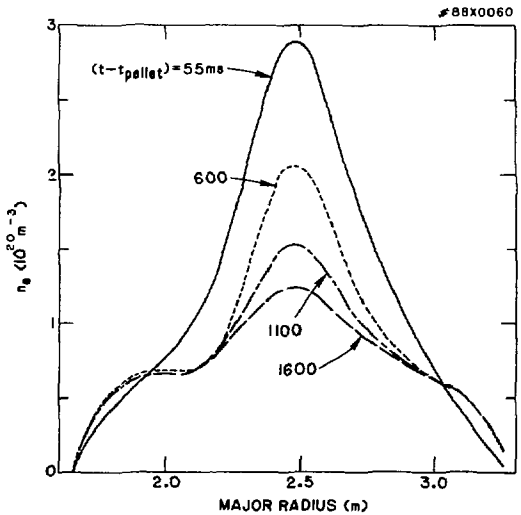


*Figure 16. Evolution of the electron density profile following injection of a single pellet into an ohmic-heated, $I_p$ = 1.8 MA target discharge; 5 MW of counter-beam are injected throughout the post-pellet phase.*

experiment at $P_b$ = 10 MW found $\bar{n}_e$ = 6.6 × 10$^{19}$ m$^{-3}$ and p = 1.65 after 700 msec of neutral injection. Thus, at least to the level of 10 MW, acceptably peaked profiles and sufficiently long density pump-out times have been observed. More aggressive wall conditioning, more deeply penetrating beams, and use of smaller minor radius target plasmas before heating may reduce the edge pedestal on electron density, thereby increasing the peaking factor still further and, in the case of wall conditioning, decreasing $\bar{n}_e$ closer to optimum levels.

Sawteeth are suppressed during reheat of a pellet-fueled plasma ($I_p$ = 1.8, $\bar{n}_e = 1.1 \times 10^{20}$ m$^{-3}$ with 10 MW of co-injection, allowing the stored electron energy in the core ($r < 30$ cm) to rise with time despite the decaying $\bar{n}_e$. However, the electron heating during reheat (0.6 to 3.5 keV) is limited by power deposition in the core [$P_{beam}$ ($r < 30$ cm) = 1.6 MW at 500 msec into beam pulse, when $\bar{n}_e = 7.5 \times 10^{19}$ m$^{-3}$] and is insufficient for $Q_{DT}$ = 1, which requires $T_{eo}$ in the range 7-10 keV. The desire for improved core heating during high-density-pellet experiments was a significant factor in the decision to install ICRF heating on TFTR, and to reorient the beamlines to provide more perpendicular injection (these modifications are also beneficial to supershot performance). Code simulations indicate that for the same density profile obtained experimentally with 10 MW of beam power, the auxiliary core-heating power can be increased by a factor of five, from 1.6 to 8 MW, using 27 MW of neutral injection ($D^o \approx 110$ keV) in the balanced configuration and 4 MW of ion cyclotron resonant heating (ICRH). This provides the basis for attaining $Q_{DT} \approx 1$ with only modest enhancements over L-mode energy scaling.

## Transitions Related to Edge Safety Factor

Spurred by the observation of H-mode transitions in JFT-2M,[22] experiments have been performed in TFTR to study the possibility of attaining enhanced confinement of the H-mode regime in a limiter configuration. In the former, the safety factor at the plasma edge q (a) was low, so TFTR was operated at low toroidal field ($B_T$ = 2.8-4.3 T), and the plasma current was ramped to sample a range of $q_\psi$(a) values continuously. For these experiments, the limiter had not been conditioned to the degree necessary for achieving supershots. A new class of phenomena, dubbed the "q-transition," was observed when $q_\psi$(a) reached special values of 2.6, 3.1, or 4.0 during neutral injection greater than 6 MW (Fig. 17). Significant changes are seen in a number of observed parameters: the emission of $H_\alpha$ light drops by about factor 2, $\bar{n}_e$ rises by about 50%, the electron density profile broadens, the edge electron temperature drops, the flux of fast neutral particles ($E < E_b$) drops dramatically (a factor of about 10), and the beam-driven toroidal plasma rotation (during co-injection) decreases by a factor of about 2. A transient rise in thermal energy confinement occurs, with $\tau_E$ increasing up to 20% for periods of approximately 200 msec. The plasma $Z_{eff}$ rises typically from 3 to 3.5, and spectroscopic measurements indicate that most of the electron density rise is due to carbon influx. Magnetic fluctuations measured by Mirnov coils tend to decrease during q-transitions. Slowly rotating coherent edge modes were identified with $m/n \approx q_\psi(a)$. Periodic bursts are observed on the $H_\alpha$ detectors and sometimes on the Mirnov coils, but these apparently do not represent edge relaxation modes as are typically seen in H-mode discharges.

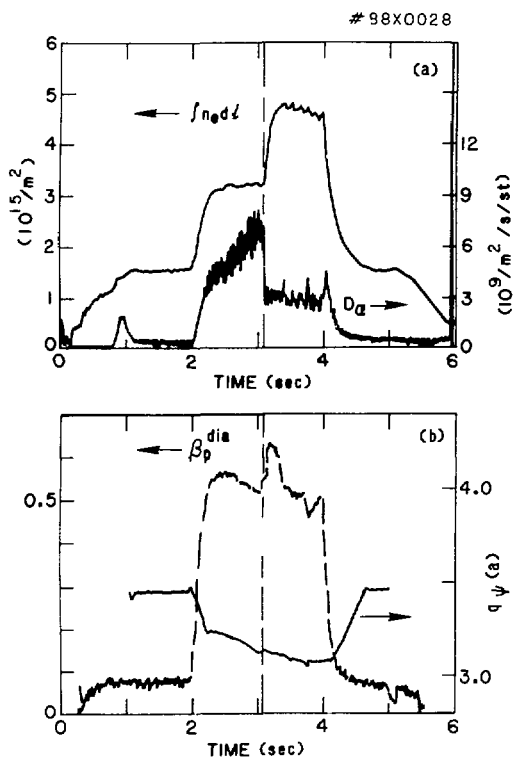


*Figure 17. Plasma waveforms during a q-transition. (a) Line-integrated electron density and $D_\alpha$ emission. (b) Diamagnetic poloidal beta and $q_\psi$ (a). The q-transition occurs at t = 3.1 sec.*

## Ohmic-Heating Experiments

The existing data base ($\bar{n}_e < 5 \times 10^{19}$ m$^{-3}$, $0.6 < I_p < 2.2$ MA) of energy confinement scaling in ohmically heated discharges was extended to higher density this year using helium plasmas.[23] The maximum density was nearly twice that previously sustained in gas-fueled deuterium discharges. Density scans ($1.0 \times 10^{19} < \bar{n}_e < 9.0 \times 10^{19}$ m$^{-3}$) at several levels of plasma current ($I_p$ = 1.0, 1.4, 1.8, and 2.2 MA) explored both the linear and the saturated regime of confinement. The upper density limit for these experiments was set by increases in edge radiation associated with MARFE-like behavior. At the lower densities, the measured global energy confinement time fits the previous TFTR prescription, $\tau_E \propto \bar{n}_e q_\psi(a)$. At higher densities, the confinement time rolls over to a saturated value of 0.4 - 0.44 sec, similar to the previous results in deuterium discharges. Very little, if any, dependence of $\tau_E$ on plasma current is seen in the high-density saturated regime. Future analysis will focus on the ion power balance for these discharges to determine whether electron or ion heat conduction dominates the heat transport.

By measuring the inward propagation of small density perturbations ($\Delta n_e/n_e < 8\%$) created by small puffs of neutral gas with the ten-channel multichannel infrared interferometer (MIRI) diagnostic, information about both particle diffusion and convection has been obtained in ohmic discharges.[24] Figure 18 illustrates the measured time evolution of the increment in density following a gas puff into a low-density target plasma ($\bar{n}_e = 1.2 \times 10^{19}$ m$^{-3}$, $I_p$ = 1.4 MA, $B_T$ = 4.8 T). Transport modeling of the density propagation is consistent with low values of inward convection velocity and particle diffusivity at the plasma center (D = 0.4 m$^2$/sec, v = 0.1 m/sec), which increase rapidly in the outer half of the plasma (D = 1.0 m$^2$/sec, v = 4 m/sec at r/a = 0.75). The response of the temperature to these gas puffs was surprising: although the density perturbation was kept as low as 5%, the electron and ion temperature decreased by typically 15%. The ion temperature response is particularly interesting because time-dependent transport calculations by the TRANSP code using a neoclassical model for $\chi_i$ predicted an increase in $T_i(0)$ following the puff. There is better agreement with temperature calculations based on ion heat transport driven by $\eta_i$ modes.[3]

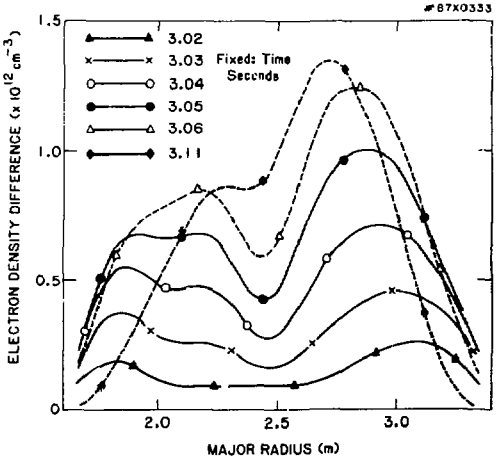


*Figure 18. Incremental density wave as measured by ten-channel infrared interferometer. The gas puff was introduced at 3.00-3.05 sec.*

## Impurity Transport in Ohmic Discharges

Impurity transport in ohmically heated TFTR plasmas was studied using MIST code modeling of time evolution and intensities from laser-blowoff injection of impurities, as measured by vacuum ultraviolet spectroscopy and soft X-ray pulse-height analysis. The particle diffusivity and inward convective velocity were determined for various elements (Ge, Cu, Ni, and Mo) in deuterium and helium discharges over a wide range of $I_p$ (0.8-2.5 MA) and $\bar{n}_e$ (0.6 - 6.0 × $10^{19}$ $m^{-3}$), and a limited range in plasma size ($R$ = 2.36-2.59 m, $a$ = 0.71-0.83 m) and toroidal field ($B_T$ = 3.9-4.9 T). All of the inferred diffusivities lie in the range 0.5 - 1.5 $m^2$/sec, the same magnitude as those for a helium puff into beam-heated TFTR plasmas measured by Strachan and Chan[25] using a thermonuclear technique, and as measured by modeling the time evolutions of the $n_e$ profile following a deuterium puff into ohmically heated plasma. At constant $I_P$ (1.4 MA) and $\bar{n}_e$ (1.8 - 2.2 × $10^{19}$ $m^{-3}$), there is no significant dependence of D on the charge ($Z$ = 22-42) or mass ($m$ = 48-96) of the injected element. Comparison of germanium injection into deuterium and helium discharges at 1.4 MA and $\bar{n}_e$ = 1.2 × $10^{19}$ $m^{-3}$ shows no significant dependence of D on the working gas, in contrast to similar experiment in Alcator[26] at lower $Z_{eff}$. For fixed $\bar{n}_e$, there appears to be no significant variation of D with plasma current over the range 1.0-1.8 MA at low $\bar{n}_e$ and over the range 2.2-2.5 MA at high $\bar{n}_e$, also in contrast to the observation of increased impurity confinement with $I_p$ on Alcator.[26]

## Alpha-Particle Physics: The "Alpha Storage Mode"

The focus of physics studies during deuterium-tritium (D-T) operation in TFTR will be exploration of collective alpha-particle effects, including alpha-driven instabilities and alpha-heating physics. A scenario called the "alpha storage mode" has been devised to maximize these alpha-particle effects, which should make possible meaningful studies of collective phenomena when $Q_{DT}$ exceeds 0.5. As shown in Fig. 19, the first phase of this scenario

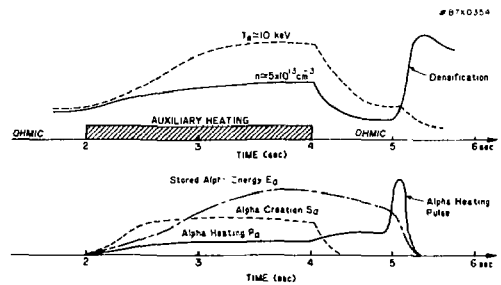


*Figure 19. Time history of temperature, density, and stored energy in the alpha storage mode. A pellet is injected 1 sec after beam turn-off to thermalize the alpha population rapidly.*

involves running with $Q_{DT} \approx 1$ at the lowest possible density and highest possible electron temperature in order to maximize the alpha slowing down time, thus storing up the alpha population and maximizing the parameter $n_\alpha/n_e$. Interestingly, TFTR can achieve ignition-level values of $n_\alpha/n_e \approx 1\%$, since for a 50:50 mix of D/T, $n_\alpha/n_e$ scales approximately as

$$n_\alpha n_e \propto T_e^{3/2} T_i^2 \Omega$$

where $\Omega$ = total fusion rate/thermonuclear fusion rate. At $Q_{DT}$ = 0.5-1.0 conditions ($T_e$ = 10 keV, $T_i$ = 30 keV, and $\Omega \simeq 2$), TFTR should have a level of $n_\alpha/n_e$ about 50% higher than an ignited thermonuclear plasma at $T_e = T_i$ = 20 keV and $\Omega$ = 1, where all parameters refer to central values. Another important alpha instability parameter, $\beta_\alpha/\beta$, scales as (at constant B):

$$\beta_\alpha/\beta = (n_\alpha/n_e)\,[\langle E_\alpha \rangle/(T_e + T_i)] \gtrsim 0.1$$

where the average alpha energy $\langle E_\alpha \rangle$ is approximately independent of temperature. For the plasma parameters cited above, the normalized alpha pressure $\beta_\alpha/\beta$ for TFTR is also higher than for a typical ignited plasma.

Figure 19 also illustrates how alpha-particle heating can be explored in this scenario through rapid plasma densification of the post-beam plasma. During neutral injection, the alpha-heating power is always small compared to the total heating rate even in the plasma center ($P_\alpha/P_{tot}$ = 30-40% at $Q_{DT}$ = 1.0). However, following beam turn-off the fast-ion beam population slows down more rapidly than the alpha population [$\tau_{slow}^{(\alpha)}/\tau_{slow}$(120 keV $D^+$) = 3.5 at $T_e$ = 10 keV]. In this post-beam phase, the slowly thermalizing alpha population can have an energy content similar to the ohmic plasma. Rapid plasma densification with pellets or gas puff can rapidly thermalize the fast alpha population, providing a powerful, albeit transient, alpha-heating pulse. Both the total energy stored in the alpha population and the effective confinement time under alpha-heated conditions might be assessed in such an experiment.

# HEATING SYSTEMS

The TFTR Heating Systems Division was formed as part of the reorganization of the project at the beginning of FY87. The division responsibilities include the neutral-beam heating system, the radio-frequency (rf) heating system and the motor generator and field coil power systems. Highlights of the year's activities are: successful modification of the beamlines and power systems to operate all of the long-pulse ion sources designed by the Lawrence Berkeley Laboratory (LBL), reliable routine operation of the motor generator and the field coil power conversion systems at design rated levels, and design and fabrication of a 9-MW ion cyclotron radio-frequency (ICRF) system for TFTR.

The long-pulse ion sources (LPIS) were provided as part of the common LPIS program managed by Lawrence Livermore National Laboratory (LLNL). The ICRF project included a collaborative effort with the Oak Ridge National Laboratory (ORNL), whereby ORNL designed, built, and tested one of the two rf launchers to be installed on TFTR.

## Neutral-Beam Operations

Modifications of the TFTR neutral-beam injection systems began in the fall of 1986, in preparation for operation of the long-pulse ion sources developed at the Lawrence Berkeley Laboratory. The sources were fabricated by RCA and will provide 27 MW of power to TFTR for 2 sec. A cutaway view of the source is shown in Fig. 20. Neutral-beam injection began in March of 1987, quickly realizing 15 MW of injected power for 2 sec from nine ion sources. Administrative restrictions were then placed on beam pulse lengths to minimize neutron production, while meeting the experimental requirements of the physics program. During this operating period, a record injection level of 22 MW for over 0.5 sec (Fig. 21) was achieved. The injected energy for a single shot exceed 32 MJ using nine sources. One ion source operated at the

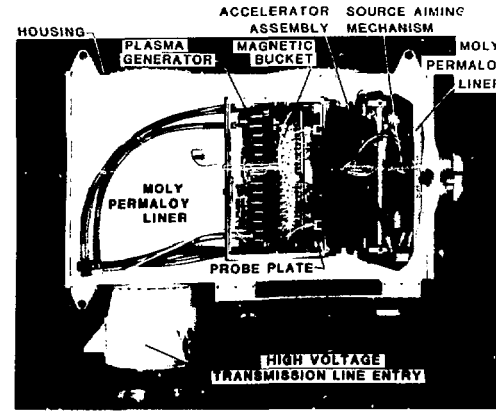


*Figure 20. Cutaway view of a long-pulse ion source installed in its housing. (87E1292)*

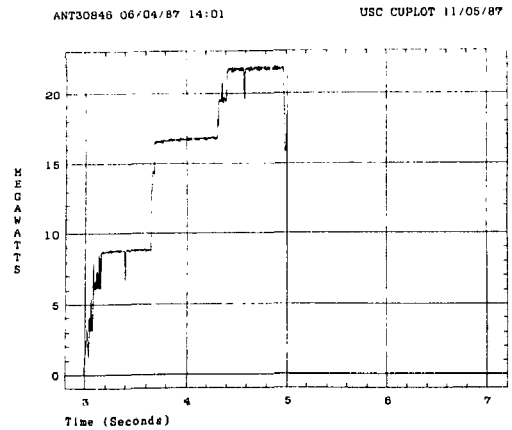


*Figure 21. Stepped power profile obtained with nine long-pulse sources. (88X3008)*

maximum design criteria of 120 kV, while injecting 3 MW of neutral power for 0.9 sec (Fig. 22).

The neutral-beam power subsystems were also modified to achieve successful LPIS operation. Phase control was added to the filament low-voltage power supply in order to maintain constant ion source filament heating during the arc pulse and beam extraction. Phase control was also added to the arc low-voltage power supply to decrease the arc turn-off time and to provide future flexibility of arc control. The parallel arc voltage rectifiers were reconnected in series to provide the higher arc voltages required for LPIS operation. For the first time, all modulator/regulator control parameters [high-voltage switch tube (HVST) filament current, etc.] had to be operated at their specified values in order to provide 120-kV, 2-sec beam pulses; this indicated that the modulator/regulators are evolving into a reliable component of the overall power system.

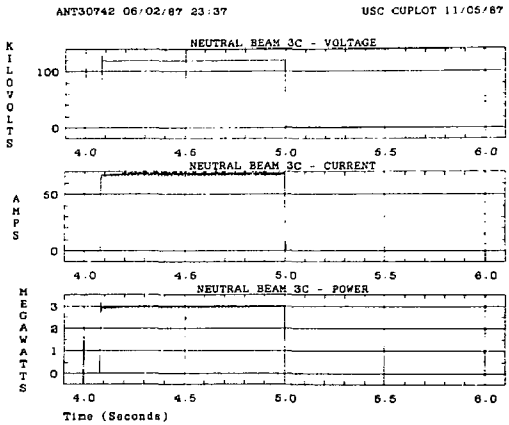


*Figure 22. One ion source operated at 120 kV, delivering 3 MW of neutral-beam power. Traces of voltage, current, and power are shown. (88X3007)*

## Neutral-Beam Project Engineering

The LPIS plasma generator includes a one-foot long bucket with magnetic cusps formed by rows of samarium-cobalt magnets with alternating magnetic poles. There are thirty-two 0.060-inch diameter tungsten filaments with optimal placement and shapes based on a design from the Japan Atomic Energy Research Institute (JAERI).

The LPIS accelerated grids are actively cooled and the extracted ion current density was reduced from short-pulse ion source levels. These improvements have helped to eliminate accelerator damage associated with overheating of the grid rails, typical of short-pulse ion sources.

Several water-cooled copper beam-defining apertures were redesigned to handle the increased power loads deposited by the larger-area long-pulse ion sources. Even so, cracks (apparently due to thermal fatigue) appeared in the steel attachment ducts between the ion sources and the beamlines. The cross-sectional area of this duct will be enlarged and a water-cooled copper liner installed to address this problem.

The gimbal mechanisms which provide precise aiming of the ion sources are being upgraded to support the increased load of the long-pulse ion sources. Additional thermocouples are being added to verify proper source alignment and beam divergence.

The ion deflection magnet was modified to spread the ion energy over a wider area on the full-energy ion dump. However, these dumps developed radial cracks around the thermocouple plugs. Thermal fatigue analysis suggests a lifetime of 1,000-3,000 full-energy two-second pulses. Evaluation is underway to produce an appropriate course of action.

Increased attenuation for the TFTR poloidal magnetic fields was provided by adding an additional layer of low-carbon steel around the neutralizers, by adding a layer of lower permeability shielding between the neutralizers and bending magnets, and by increasing the effectiveness of the lattice-type shielding bars in this region. The resulting lower magnetic fields will reduce the power deposition on the ion deflection magnets.

New calorimeter vacuum bellows were installed with a theoretical fatigue lifetime in excess of 20,000 cycles. However, three of the eight new bellows developed vacuum leaks after only 200-300 cycles. This problem is being studied for causes and solutions. Additional thermal shields and a continuous flow of warm, dry nitrogen were added to avoid thermal and condensation problems.

## Neutral-Beam Systems Engineering

In prior years the beams were operated through local control centers using one operator for each of the 12 sources. All of these local control and monitoring functions are now available through the Central Instrumentation, Control, and Data Acquisition (CICADA) computer system. Figure 23 shows the neutral-beam operating stations in the TFTR control room. By using the data acquisition, processing, and display capabilities of the computer system three sources can be controlled from each station by one operator. About three months of experience has been gained using the computer system to operate the beams. Several computer enhancements are also under development, including improvement of response and the use of "expert" system software.

*Figure 23. Neutral-beam operating consoles in the TFTR control room. (85E1164)*

Installation and checkout of the majority of the neutral-beam instrumentation and control system components were completed by the year's end. The system requires approximately 5,000 control and monitoring signals for the source power supplies, 1,500 for beam physics diagnostics, and 2,000 for

the beamlines and the water, vacuum, and cryogenic services.

Because of the very high levels of power generated by the beams, a significant part of the control system consists of equipment interlocks and protection subsystems. Over 1,800 signals are monitored and logically combined to permit or inhibit operation of the beams. Critical subsystems, such as the vacuum vessel, are protected with several layers of redundancy. A real-time scanning system currently under development will monitor an additional 1,500 thermocouples on the vacuum vessel wall armor and beamline calorimeters, ion dumps, and scrapers.

Damage to a beamline vacuum valve, caused by failure of protective interlock system, was addressed by an improved design of the interlock system and more rigorous installation and operating procedures.

## Neutral-Beam Performance and Diagnostics

A major portion of effort during the first five months of this fiscal year was devoted to finding a workable operation mode for the first LBL long-pulse ion source on the TFTR neural-beam test stand. Progress was initially slow due to, among other factors, the difficulty of operating with the cathodes running in an emission-limited mode, where the arc characteristics are dependent upon the temperatures of the filaments, which in turn are affected by the arc. The previous short-pulse ion sources had been able to run satisfactorily with the filaments part way into the space-charge-limited regime, and thus were in some respects more straightforward to run. Nonetheless, after considerable experimentation with conditioning and running techniques, 2-sec operation at 119 kV with deuterium was achieved before terminating operation on the test stand.

During this period the atomic and molecular species mix was also measured, primarily through doppler shift spectroscopy with an optical multichannel analyzer (OMA). A substantial improvement in the beam energy mix relative to what had been obtained with the earlier short pulse sources was achieved. At an accelerating potential of 100 kV, the neutral-particle current fractions computed from species measurements on the test stand with a long-pulse ion source were 46% for the full-energy, 28% for the half energy, and 26% for the one-third energy, with the full-energy component thus carrying 67% of the total neutral power. By comparison, the corresponding neutral-particle current fractions for the short-pulse ion sources were 32% for the one-third energy with the full-energy component carrying 53% of the neutral power. During subsequent measurements on several long-pulse ion sources running on the TFTR beamlines, measured species mixes with the OMA were measured which varied around those obtained on the test stand, but which tended to run slightly higher (suggesting that at 100 kV, for instance, the neutral-particle current fractions were about 50%, 28%, and 22% for the full, half, and one-third energy components, respectively).

Another characteristic in which the long-pulse ion sources showed marked improvement over their predecessors was their divergence. The perpendicular divergence of the short-pulse ion sources typically ran in the range of 1.6°-2.0° during most of the operation, as measured by the thermocouple arrays on the beamline calorimeters. With the long-pulse ion sources, the measured perpendicular divergence was typically in the range of 0.8°-1.1°, and the true divergence may in fact be even smaller since the width of the beam footprint on the calorimeter is dominated by the source extractor geometry at small beamlet divergence angles. This improvement is probably due to the fact that, with their much deeper arc chambers and the addition of magnetic multicusp confinement, the long-pulse ion sources have very uniform plasma density profiles near the extraction plane. The Langmuir probes indicate that the uniformity is typically good to about ±3% across the region illuminating the grids. With the short-pulse ion sources this uniformity was seldom better than ±10%, and was often worse. The improved uniformity probably also accounts for the fact that the long-pulse ion souces, once they are well conditioned, exhibit a wider minimum in the divergence versus perveance curve than did the short-pulse ion sources. This wider perveance curve is a significant benefit of the change to these new sources, since it means, for instance, that there is now a modicum of choice in the voltage required for a given beam power and, more importantly, during tritium-beam operation it may mean that the current relative to a deuterium beam does not need to be reduced by the full factor of 2/3 that would be implied by the mass effect upon the perveance.

Experiments were also conducted on the test stand to ascertain how few conditioning shots could be tolerated. With a well-conditioned source, it appeared that one shot per half hour, preceded by a filament-only shot, was sufficient at 105 kV; there was one case of a 14-hour overnight wait before the successful firing of a 105-kV shot after only hi-potting the source and firing filament-only shots.

At 105 kV, the gas was changed from deuterium to hydrogen, and back again, while observing the beam with the OMA. It was found that two seconds of arc operation prior to extraction are sufficient to make a nearly complete (better than 95%) changeover in the beam isotope without any other arc shots. This means that there should be no need to consume tritium in noninjection shots, even if conditioning with deuterium is done between tritium-injection shots. Figure 24 shows OMA data for the first shot with deuterium after running hydrogen; showing the nearly complete changeover in isotope is apparent.

During fiscal year 1987 members of the beam group presented invited talks at the *Ninth Conference on Applications of Accelerators* and at the *14th IEEE International Conference on Plasma Science* meeting in June. Presentations were also given at the positive ion workshop held in Japan as well as one on negative

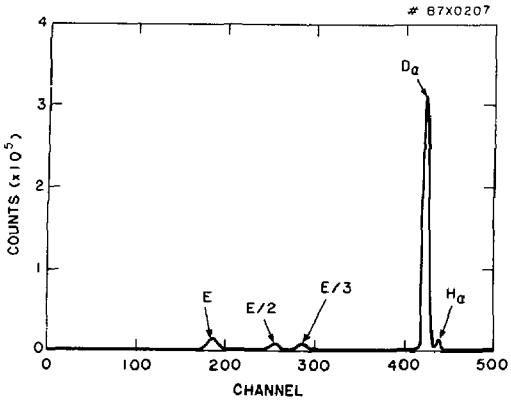


*Figure 24. An optical multichannel analyzer trace showing the full (E), one-half (E/2), and one-third (E/3) energy components as well as the unshifted deuterium ($D_\alpha$) and hydrogen ($H_\alpha$) peaks obtained on the first deuterium pulse after a sequence of hydrogen pulses.*

ions. A number of papers were given at the *IEEE 12th Symposium on Progress in Fusion Engineering.*

The program was enriched by substantial international exchanges. During the fiscal year two Soviet physicists, one physicist from JT-60 (JAERI Tokamak-60), and one from JET (Joint European Torus) were hosted for periods of a month each, and physicists from our group spent two weeks at JT-60 and two months at JET. PPPL also hosted an IAEA workshop with JT-60 personnel on neutral-beam technology.

## TFTR Power Systems

In general, the TFTR power systems activities for 1987 were focused toward realization of the best possible use of the equipment in terms of performance and reliability. A full preventive maintenance program is in place. Miscellaneous minor defects in various control circuits were cleaned up, thereby eliminating all known nuisance causes of downtime. Although not yet implemented, enhanced protection systems for certain equipment are under development; this will lead to the full utilization of installed equipment capability.

It is expected that fiscal year 1988 will see the completion of all major engineering tasks, and that operation should become fully routine. A small engineering workload will always exist (to cover operations and contingencies), but it is expected that time will become available for engineering work toward the adaption of the TFTR power systems equipment for the Compact Ignition Tokamak (CIT). Additionally, during fiscal year 1988 the operation of the TFTR ion cyclotron radio-frequency equipment will become part of the power systems branch work scope. This will complement the skills and existing work scope of the staff well; cross training will lead to the development of a common base of personnel to cover the work.

## Motor-Generator System

The motor generator system is at a mature state; overall performance and reliability have been excellent for the past two years. Maintenance work is performed on a subcontract basis by the equipment manufacturer, General Electric (GE), which ensures continuing reliable operation. Maintenance inspection this year revealed problems with the thrust bearing (uneven babbit wear) and motor-to-generator shaft gusset welds (cracks). These problems are the result of design/manufacturing defects which have become apparent only after an extended period of operation. Corrective actions are being undertaken in collaboration with the manufacturer.

Studies were completed that define the envelope of pulsed power which can be safely and reliably extracted from the generators under different conditions of speed and load power factor (versus the generator nameplate which addresses only a single point of speed and power factor). A load monitor is under development which will enforce the restrictions defined by the envelope. This will lead (under certain conditions) to the availability of power in excess of that presently taken.

## Energy Conversion System

The energy conversion system (ECS) operated at or near full rating for the past two years. A high level of reliability was demonstrated during operation in 1987. Availability typically exceeded 95% (Fig. 25). For example, during the last two weeks of the run period (June 22-July 2, 1987) there was only a single and short downtime.

During the last run period, it was possible to focus attention on several nuisance causes of downtime having to do with minor defects in control circuitry. During the machine opening in the summer (1987) these problems were investigated in depth and

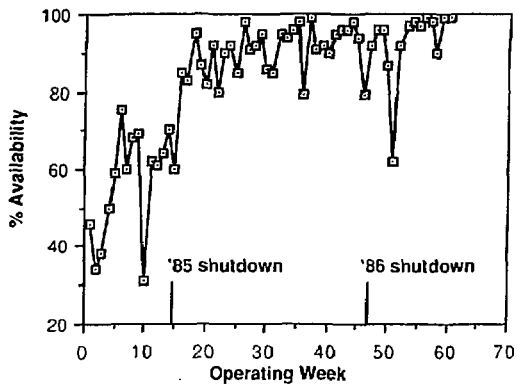


*Figure 25. Availability of the energy conversion system equipment versus time. The dramatic improvement in availability is attributed to a comprehensive reliability upgrade program. (88X3009)*

resolved via minor modifications. Reliability improvements should result.

The reversing switches (used in the ohmic-heating system), having logged over ten thousand operations, are beginning to show wearout on some mechanical parts. Since they experience a mechanical operation each shot, to minimize downtime and to ensure proper preventive maintenance of the complicated switch actuating mechanism, a contract was let with the manufacturer (Westinghouse) which provides not only for preventive maintenance but also for emergency repair service. For the other emergency conversion system equipment, there is a preventive maintenance program in place which is manned internally.

The only remaining upgrade activities involved the ohmic-heating system. A modification undertaken early in the year involved the rearrangement and addition to the ac (alternating current) feeders to the power supplies. As a result, the common impedance of the system was reduced so that better voltage regulation (less voltage drop with load) was obtained. Plasma experiments with low-voltage start-up (using power supplies only, i.e., without interrupters) show promise. With the future implementation of improved protection (power diode thermal protection, optimization of existing power supply thermal protection) plus the development of control software designed specifically for the low-voltage start-up mode, the energy conversion system will be ready for upgraded ohmic-heating operation. The goal is to provide a 3.0-MA capability for the plasma current.

## ICRF Heating

Substantial progress toward applying 9 MW of ion cyclotron radio-frequency (ICRF) source power to heat the TFTR plasma was achieved during this year. Two antennae capable of delivering the entire 9 MW were designed jointly by PPPL and ORNL and were constructed and tested, one at PPPL and the other at ORNL. These antennae were designed and thoroughly analyzed to meet the stringent requirements of D-T operation with full beam power (about 27 MW) and full ICRF power (about 8-9 MW) delivered to the plasma. The modifications required for the four radio-frequency (rf) sources [two previously used on the Princeton Large Torus (PLT) and two originally Fusion Material Irradiation Test (FMIT) units] were specified. The modifications to the two PLT units to provide 47 MHz, 3 MW, 2 sec pulse duration sources were completed in support of antenna testing on the PPPL Radio-Frequency Test Facility (RFTF) and of TFTR operations to begin in January 1988. The other two sources will be modified, with kits purchased from the Continental Electronics Corporation, to operate between 40 MHz and 80 MHz at 1.5 MW powers and for 2 sec pulse durations. All parts for these modifications were fabricated. The full, total source capability of 9 MW will be achieved in FY89 when budget allocations are available for supporting the labor required for assembly. Finally, the remaining components of the ICRF system, including transmission lines and matching components, switches, local and TFTR source controls, and computer processor monitoring and controls, are nearing completion to support the 47 MHz, 6 MW system checkout and operation on TFTR.

Collaboration efforts between PPPL and ORNL to produce full-power antennae for TFTR deuterium-tritium operation has proven to be very successful. Members of the JET, JT-60, and ASDEX (Axially Symmetric Divertor Experiment) radio-frequency groups contributed to this success by freely sharing their design ideas with us. The resulting PPPL and ORNL antennas are shown in Figs. 26 and 27, respectively. Large teams from both laboratories contributed to the design and analyses for both antennas, to assure that they will function properly under the extreme thermal and mechanical stresses

*Figure 26. The TFTR ion cyclotron radio-frequency launchers are shown as installed in TFTR. The titanium-carbon-coated Faraday shield rods can be seen on the launcher on the right which was built by PPPL. (88E0450)*

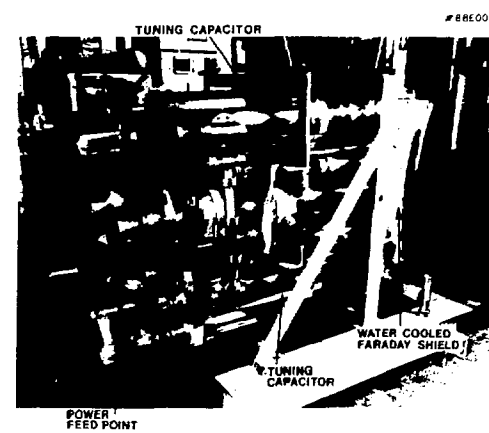


*Figure 27. The TFTR ion cyclotron radio-frequency launcher designed and built by Oak Ridge National Laboratory. This design incorporates a water-cooled Faraday shield and an off-center fed current strap with integral tuning capacitors. (88E0002)*

which occur during TFTR operation. Furthermore, considerable effort was directed toward incorporating some distinctive individual features into each antenna which may be contrasted to determine their potential importance in antenna designs for CIT. Most notably, the PPPL design has slotted walls, a slotted septum, and titanium-carbon Faraday shield rods. Whereas, the ORNL design has solid walls, a solid septum, and graphite-coated, water-cooled Faraday shield tubes. The relative effects of spectral differences, outgassing, and impurity generation on antenna performance will be of primary importance for future designs. Also, the PPPL design incorporates rf feeds at the high-voltage ends of the current straps, whereas the ORNL design utilizes central strap feed at the matched impedance point. The relative ease of achieving full-power performance for the two designs will be compared and should serve to guide the choice of the excitation method for CIT.

The antennas were tested to full design voltage and current on the rf test facilities at PPPL and ORNL. We are now looking forward to beginning operations on TFTR and accomplishing the goal of optimizing wave coupling and rf power deposition in support of achieving $Q \sim 1$ conditions. Computer simulations suggest that approximately 7 MW of ICRF heating in conjunction with intense neutral-beam heating may have dramatic effects on Q, if the power deposition is focused at the center of the plasma. Another exciting prospect is the actual exploration, for the first time, of ICRF heating effects in the D-T regime in preparation for heating CIT to ignition.

# TFTR DIAGNOSTICS

For FY87, TFTR Diagnostics had two distinct phases. During the first half of the year, TFTR was not operating and this period was used to repair, improve, and perform routine maintenance which was not possible during the extensive operation in 1986. The second part of the year was a period of intensive data acquisition and analysis with frequent two-shift operation.

Table I gives a complete list of diagnostics which were operational in fiscal year 1987. The diagnostics are listed so as to identify the principal plasma measurements for which they were used. Readers seeking additional details of the experimental techniques will find an excellent collection of articles in Ref. 27. Some areas of major concentration were confirmation of high ion temperatures, improved fusion product diagnostics, and shielding of diagnostics for future D-T operation.

**Table I. Operational Diagnostics in FY87.**

| Principal Plasma Parameter Measured | Diagnostic | Location of Measurement |
|---|---|---|
| Ion Temperature | Diagnostic Neutral Beam (DNB) | Horizontal Midplane |
| | Charge-Exchange Recombination Spectrometer (CHERS) | 4 Locations |
| | Charge-Exchange (CX) | 3 Horizontal Chords, 1 Vertical |
| | X-Ray Crystal Spectrometer | Horizontal Midplane, 3 Vertical |
| | Soft X-Ray Monochromator Spectrometer (SOXMOS) | Horizontal Midplane |
| Electron Density | 1-mm Microwave Interferometer | Horizontal Midplane |
| | Multichannel FIR Interferometer | 10 Vertical Chords |
| Electron Temperature | TV Thomson Scattering | Dual Multipoint Radial Profile |
| | ECE Heterodyne Radiometer | Radial Profile |
| | X-Ray Pulse-Height Analyzer | Horizontal Midplane |
| | ECE Fourier-Transform Spectrometer | Radial Profile |
| Impurity Concentration | Multichannel Visible Impurity Photometric Spectrometer (VIPS) | 2 Horizontal Midplane |
| | Hydrogen Alpha Interference Filter Array (HAIFA) | 18 Chord array, 4 Toroidal Locations |
| | Pellet Polychrometer | 1 Location |
| | UV Survey Spectrometer (SPRED) | Horizontal Midplane |
| Radiated Power | Bolometer Arrays | 19 Horizontal, 19 Vertical Chords |
| | Wide-Angle Bolometers | 6 Toroidal Locations |
| | Tangential Bolometers | 2 Opposing Horizontal Views |
| Fusion Products | Epithermal Neutrons | 4 Toroidal Locations |
| | Proton Detectors | 4 Vertical Locations |

Continued

Table I. Operational Diagnostics in FY87 (Continued).

| Principal Plasma Parameter Measured | Diagnostic | Location of Measurement |
|---|---|---|
| Fusion Products | Neutron Activation System | 2 Toroidal Locations |
| | Two-Channel Collimator | 1 Toroidal Location |
| | Neutron Fluctuation Detector | 1 Location |
| Magnetic Properties | Rogowski Loops | 2 Toroidal Locations |
| | Voltage Loops | 6 Poloidal Locations + Saddle |
| | $B_\theta/B_p$ Loops | 2 Sets of 26 Pairs, External |
| | Diamagnetic Loops | 2 Toroidal Locations |
| Plasma Edge/Wall | Plasma TV/IR TV | Periscopes at 3 Toroidal Locations |
| | Neutral-Beam Pyrometer | 2 Toroidal Locations |
| | Probes | 2 Horizontal, 1 Vertical |
| Miscellaneous | Hard X-Ray Monitors | 5 Wall Locations |
| | Torus Pressure Gauges | 2 Toroidal Locations |
| | Residual Gas Analyzers | 2 Toroidal Locations |
| | Vacuum Vessel Illumination | 3 Toroidal Locations |
| | Laser Impurity Injector | 1 Toroidal Location |
| | Glow-Discharge Probes | 2 Mechanisms |

## Diagnostic Neutral Beam

Improvements to the diagnostic neutral beam (DNB) are continuing to raise its reliability and performance.[28] The beam has been brought up to 61 kV/13 A for 50 msec; ion source conditioning to raise these parameters to 80 kV for 500 msec design goal is in progress. The capability for beam modulation needed during the next run period is being installed.

The radio-frequency plasma generator in the ion source continues to perform very well. An inspection after six months of continuous TFTR injection revealed no apparent wear. Diagnostics have been temporarily added to the beamline to aid in determining beam species, neutralization, and divergence behavior.

After beam realignment, the charge-exchange neutral-particle analyzer spectra showed good DNB signal enhancement up to moderate plasma density and heating beam power for the available DNB energies. Charge-exchange recombination spectroscopy spectra also showed good DNB signals for a variety of discharge and heating conditions. Signals are expected to increase as the DNB power is increased.

## Charge-Exchange Recombination Spectrometer

Several improvements were made to the TFTR CHarge-Exchange Recombination Spectrometer (CHERS) diagnostic system during FY87. The main purposes of this system are the measurement of the radial profiles of the plasma ion temperature and rotation velocity. A redesigned, fiber optically coupled, two-dimensional, solid-state detector was installed to provide better optical coupling to the imaging spectrometer system. In addition, the new compact detector design allowed more efficient magnetic shielding. Also, new fiber optically coupled sightlines, which allow horizontal viewing access to one of the heating neutral beams as the excitation source for the CHERS diagnostic, were installed at one of the windows of the plasma TV system. The use of both the DNB and heating beams for CHERS measurements resulted in the acquisition of radially resolved ion temperature measurements in the majority of discharges during the second half of the 1987 run period. The optics using the heating beam provide spatial points every 10 cm in the plasma, while using the DNB allowed a finer resolution of 5 cm. As the diagnostic hardware development for the CHERS system has been completed, substantial efforts have been invested in providing data acquisition and analysis software. So far, the main progress has been in the development of the data reduction and fitting routines for interactive analysis of the CHERS data. Full automation of the analysis procedure will be developed in the next fiscal year.

As mentioned above, the CHERS diagnostic system has allowed measurements of the plasma ion temperature and toroidal rotation velocity profile under a wide variety of discharge conditions. Usually, visible spectral lines emitted by hydrogen-like carbon ($C^{+5}$) were used for these measurements, since carbon was the predominant impurity species in the discharge. The first priority of these measurements was to confirm the high central ion temperatures indicated by the nickel $K_\alpha$ line broadening measurements from the X-ray crystal spectrometer diagnostic and charge-exchange data obtained from fast ion measurements. In general, it was found that these measurement techniques agree within experimental

error. For example, Fig. 28 shows a comparison of the peak ion temperature measured from the CHERS radial ion temperature profile with the near-central ion temperature measured with the X-ray crystal spectrometer. Since the line integrated $K_\alpha$ emission has some spatial extent over the peaked profile in the core plasma region, it is expected that, on average, the CHERS central ion temperature values should be slightly higher than the $K_\alpha$ values, as is seen in the data in Fig. 28. Reasonable agreement with the X-ray crystal spectrometer diagnostic is also obtained for measurements of the central rotation velocity. With the acquisition of radially resolved measurements from CHERS, ion temperature and rotation velocity profiles can be constructed as shown in Fig. 29. Here, very high rotation speeds and somewhat broadened and centrally lowered ion temperature profiles are evident for the case of unbalanced neutral injection, while the highest central ion temperature values are obtained with balanced injection, which results in minimal toroidal rotation speeds. These and other similar measurements have been used to commence a detailed study of the thermal ion energy transport in TFTR discharges, as described in the Physics Program.

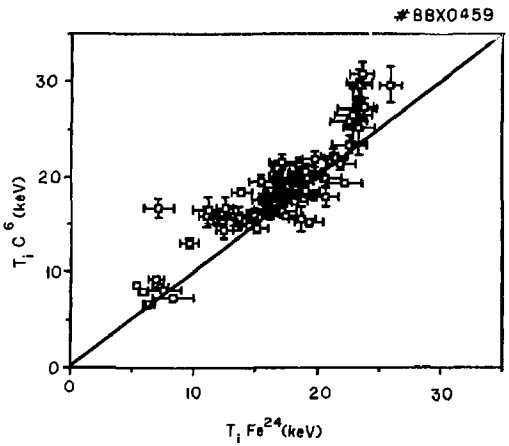


*Figure 28. Comparison of peak charge-exchange recombination spectrometer ion temperatures with ion temperatures measured with the X-ray crystal spectrometer near the plasma center.*

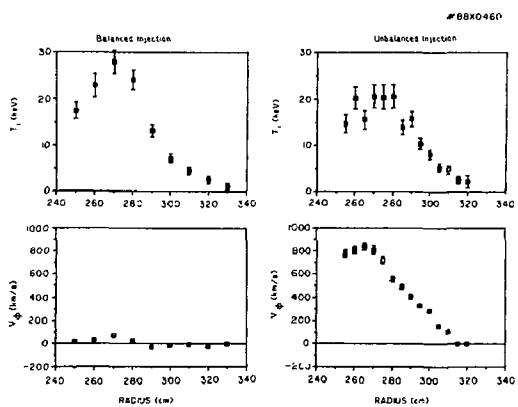


*Figure 29. The charge-exchange recombination spectrometer (CHERS) radial ion temperature ($T_i$) and rotation velocity profiles ($v_\phi$) observed with balanced and unbalanced neutral-beam injection.*

## Charge-Exchange

The vertical charge-exchange system was expanded by the addition of a second E||B analyzer and six small cylindrical-plate electrostatic analyzers.[29] A neutron/gamma radiation shield (see Fig. 30) installed on one of the three E||B analyzers in the horizontally scanning charge-exchange system provided more than a hundred-fold improvement in the signal-to-noise ratio, which extended the operational capability to discharges with neutron yields in excess of $10^{16}$ sec$^{-1}$.

*Figure 30. Photograph showing the extensive shielding (large box in center of photograph) installed on one of the horizontal charge-exchange analyzers. An unshielded analyzer is visible on the left. (86E0936)*

Charge-exchange measurement of the ion temperature with deuterium neutral-beam heating of deuterium plasmas in TFTR is difficult because the charge-exchange energy spectrum is dominated by the beam slowing-down spectrum, and the residual hydrogen flux [$H/(H+D) \leq 5\%$] is insufficient to obtain a measurement of the thermal distribution. With the guidance of Fokker-Planck code simulations, a technique was advanced which enabled the plasma ion temperature to be deduced from the deuterium beam slowing-down spectrum at energies in excess of the neutral-beam-injection energy.[30] Above the neutral-beam-injection energy, the slope of the ion energy spectrum is determined by collisions with both the plasma ions and electrons. Neglecting small toroidal electric fields effects, the ion temperature $T_i$ is given by

$$T_i = T_{eff} + (T_{eff} - T_e)\left(\frac{E}{E_c}\right)^{1.5},$$

where $T_{eff}$ is the slope of the beam spectrum above the injection energy, $T_e$ is the electron temperature, and $E_c$ is the critical energy above which the effect of the electron drag on the beam ions is more important than the ion energy diffusion. Application of this technique requires that the tangency radius of the charge-exchange sightline be close to the average tangency radius of the beam injectors. A representative deuterium charge-exchange spectrum is shown in Fig. 31 where a linear least-squares fit to the data (open circles) above the beam-injection energy yields $T_{eff}$. Figure 32 shows the favorable agreement of the derived charge-exchange ion temperature, corrected for toroidal rotation effects (solid circles), with X-ray Doppler broadening (NiXXVII) measurements (open circles).

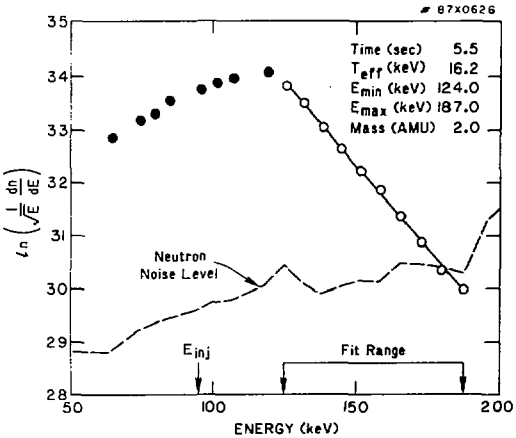


*Figure 31. Energy dependence of the observed charge-exchange neutral flux. The ion temperature can be determined from the slowing-down spectrum of fast ions.*

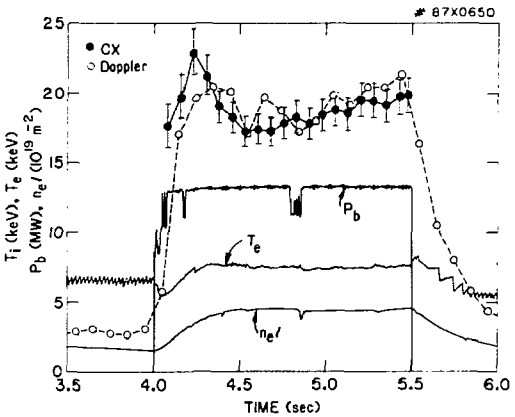


*Figure 32. Ion temperature measured by the charge-exchange system compared with X-ray crystal measurements.*

# X-Ray Crystal Spectroscopy

Four crystal spectrometers with one horizontal and three vertical sightlines were used to measure the Doppler broadening and shift of X-ray lines from helium-like metal impurity ions in TFTR.[31] The horizontal spectrometer was reconfigured to record spectra of NiXXVII, and shielding against neutrons and gammas was improved to allow reliable ion temperature measurements at total neutron source rates greater than $10^{16}$ $sec^{-1}$. Measurements of the ion temperature and the toroidal plasma rotation velocity were made for a variety of neutral-beam-heating plasma conditions including unidirectional co- or counter-injection up to 13 MW and combined co- and counter-injection up to 18 MW.

Figure 33 presents the time evolution of the observed central ion temperature from a supershot discharge with ion temperatures approaching 30 keV soon after the start of the neutral-beam injection. The subsequent decrease of the ion temperature is correlated to the onset of MHD activity at 4.4 sec. Also shown is the entire satellite spectrum of NiXXVII before and during neutral-beam injection. Changes of the ionization equilibrium of the nickel charge states due to charge-exchange recombination with the

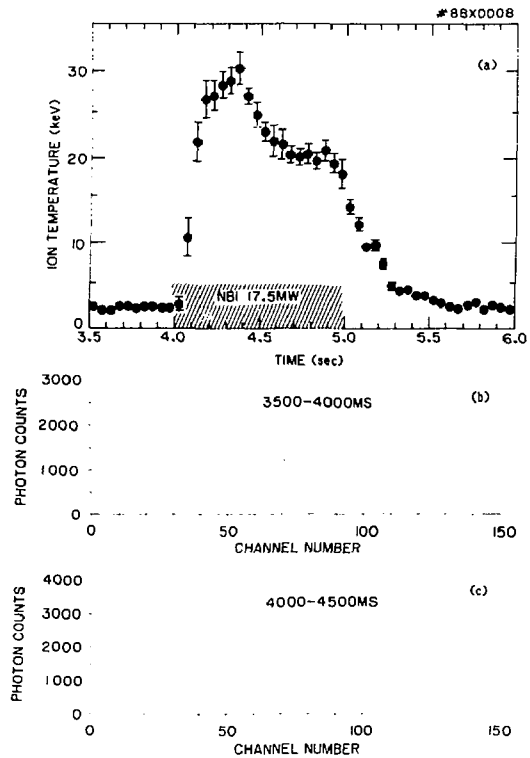


*Figure 33. The X-ray crystal ion temperatures and satellite spectrum of NiXXVII obtained during a TFTR supershot.*

injected hydrogen neutrals can be inferred from the line ratios. A detailed comparison of the experimental NiXXVII spectra with atomic theories is given in Ref. 32. Results on the scaling of the ion temperature and toroidal plasma rotation velocity with beam power and plasma density are presented in Refs. 10 and 19.

## Multichannel Infrared Interferometer

The ten-channel far-infrared interferometer (MIRI) system continued to measure density profiles in a reliable fashion and appears to be ready to enter the D-T phase of TFTR operation.[33]

In addition, initial attempts to measure multichannel Faraday rotation signals met with some success.[34] During the fall '87 opening, wire grid polarizers will be installed in an effort to improve the quality of the polarimetry signals by improving the quality of the beam polarization. Some improvements to the far-infrared lasers will also be attempted. Further, the polarimetry analysis software is nearing completion.

## Thomson Scattering

The dual multipoint Thomson scattering system was used extensively to provide 76-point radial profiles of electron temperature and density at two times in the discharge. Work continued on preparation for D-T operation with new capabilities for remote steering of the laser beams and readout of beam position.

It is common after long operating periods when the tokamak is under vacuum that diagnostic recalibrations requiring access to the inside of the machine will lead to data correction. After the last major opening a chromatic metallic coating was discovered on the Thomson scattering viewing window which resulted in a significant $T_e$ correction. After two years of running with the graphite inner wall limiter, no significant chromatic coating was found when the machine was opened in July '87. However, in repeating the spectral calibration, a mistake was found in the old calibration which resulted in a 15-20% upward correction in the temperature with no significant change in the shapes of $T_e(r)$ or $n_e(r)$. At peak temperatures of 6-8 keV, there is now good agreement between Thomson scattering and the electron cyclotron diagnostics.

Manpower limitations and high noise levels in the detector have frustrated efforts to provide edge profiles of temperature and density and central q values. The edge system diverts light from 10-12 cm of the 2-m radial field of one of the main systems and analyses it with a higher dispersion spectrometer and a more sensitive detector. The same diversion optics and detector can be used with a Fabry-Perot for central q measurements.[35] Initial attempts to measure q were unsuccessful during the last run, probably also because of poor detector performance.

## Electron Cyclotron Emission

A grating polychromator based on the Ebert-Fastie grating monochromator[36] was built to follow the evolution of the electron temperature profile and electron temperature fluctuations in TFTR plasmas. These quantities are monitored at twenty locations simultaneously across 70% of the plasma column with excellent spatial (3-cm radial resolution and 5-cm antenna spot size) and temporal (1 microsecond amplifier risetime) resolution. Some typical results of electron temperature as a function of time during high-power neutral-beam injection are shown in Fig. 34.

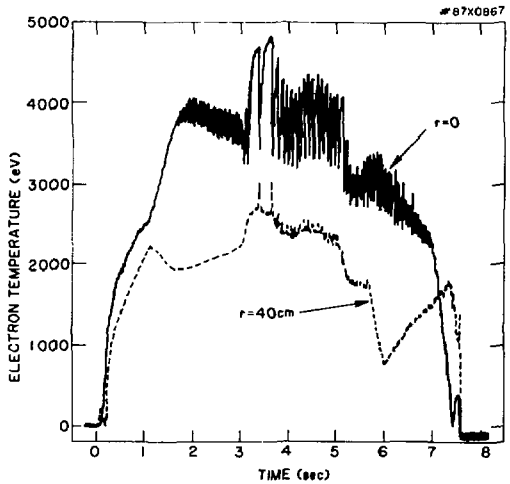


*Figure 34. Time evolution of the electron temperature measured with the electron cyclotron emission (ECE) grating polychrometer. A central and outer channel are shown.*

## Spectroscopy

Activity on hardware this year centered on three areas: implementing an array of tangentially-viewing visible bremsstrahlung detectors, expansion of the $H_\alpha$ system, and determining the spectrometer shielding requirements for D-T operation. The tangential visible bremsstrahlung system was designed and procurement was started for the major components. This will allow determination of $Z_{eff}$ profiles for discharges cleaning on the bumper limiter. The $H_\alpha$ measurement capabilities of the $H_\alpha$ interference array (HAIFA) were expanded by the installation of a 5-channel poloidal array looking in the upper half-plane of TFTR at the inner limiter. During the coming run, the HAIFA system will be further expanded by adding $H_\alpha$ channels in the lower half-plane, and including a system of bandpass filters for carbon spectral lines so that carbon generation and influx, in a fashion similar to hydrogen, can be investigated.

Neutron and gamma ray noise in multichannel detectors of the type used in the survey spectrometer (SPRED), soft X-ray monochromator spectrometer (SOXMOS), and the visible impurity photometric spectrometer (VIPS) was measured during TFTR supershots and the results extrapolated to estimate the noise expected during D-T operation with the igloo in place. Temporary neutron and gamma shielding which consisted of lead and borated polyethylene was installed around the SPRED detector and proved to be effective. These results, combined with shielding calculations, will be important in designing spectrometer shielding for D-T operation.

Progress in data analysis continued. Intrinsic impurity measurements[37] continued to be performed for a variety of TFTR plasmas. Impurity transport was measured in ohmic- and beam-heated discharges via MIST impurity transport code modeling of VUV (visible ultraviolet) lines emitted by impurities injected by a laser-blowoff system. The SOXMOS was routinely used to measure the central ion temperature in supershots from the Doppler broadening of the FeXXIV 192 Å line. The new $H_\alpha$ measurements, together with the DEGAS neutral transport code, have opened an interesting new opportunity for the investigation of fuel recycling and limiter conditioning. It was already known that these are critical parameters for achieving the supershot mode of operation. Analysis shows that, among other things, the recycling coefficient of the limiter is a dynamic quantity during a shot.

## Bolometer

An important diagnostic for the analysis of the energy balance in TFTR is the bolometric measurement of the total radiated power.[38] To improve coverage of the radiation loss profile, and in particular to overcome the background from a bright cloud of radiation in front of the inner bumper limiter, a tangentially viewing bolometer array and an oppositely viewing single unit were designed and are being fabricated. The single unit will make it possible to separate the signal from the loss of charge-exchanged circulating beam ions.

## Fusion Products

In 1987 the highest neutron source strength, S, and fusion power gain, Q, continued to be realized in the beam-fueled, low initial plasma-density supershot regime at low plasma current. Some TFTR effort was directed toward extending the supershot regime to higher currents by ramping the current during neutral-beam injection. That technique was effective in producing the highest total neutron production per shot during the 2-sec beam pulses made possible with the new ion sources. As indicated in Fig. 35, up to $1.2 \times 10^{16}$ D-D neutrons per pulse were produced, representing a total D-D fusion yield of 14 kJ.

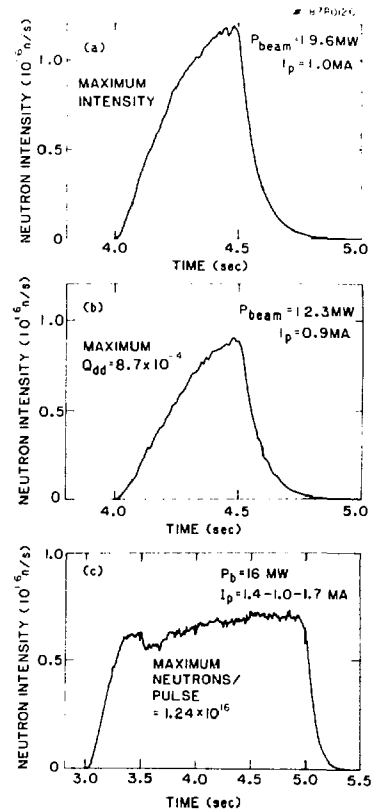


*Figure 35. The measured time behavior of deuterium-deuterium neutrons during a supershot.*

The neutron activation (NA) system is now fully operational and data were taken to deduce neutron spectra.[39] As and adjunct to the NA system a delayed neutron counting system was developed as another method to measure the TFTR total neutron fluence and yield. Fissionable materials which have high neutron fission threshold (i.e., $^{238}U \sim 1.2$ MeV, $^{232}Th \sim 1.1$ MeV) are irradiated by D-D or D-T neutrons. The neutron fluence and the total source yield can be determined from the number of delayed neutrons emitted from the material. The neutrons are counted using $BF_3$ counters in a moderator.[40]

Time-dependent measurements of 14-MeV neutron emission were made to study the "burnup" of the 1-MeV tritons produced in the d(d,p)t reaction. After the end of a neutral-beam injection pulse into a low-density TFTR plasma, once the beam-injected deuterons have thermalized, the neutron emission is dominated by the 14-MeV neutron production from burnup of tritons created in the D-D reaction. Ordinary fission detectors can measure the sum of the 14-MeV and 2.5 MeV emission rates, which in some cases can be extrapolated back in time to estimate the equilibrium triton burnup fraction. The fractional burnup determined by this method is in the range

of 0.3 to 1.5% for TFTR discharges to date, and is consistent with classical confinement and slowing down. A NE213 proton recoil spectrometer system, located in a large paraffin collimator on the TFTR Test Cell floor, could make energy sensitive measurements simultaneously of both the 2.5- and 14-MeV neutrons. Figure 36 shows data from this spectrometer compared with a theoretical calculation and with the fission detector system for a discharge with modest beam heating. Difficulties with discrimination again $\gamma$-ray background, and severe limitations in effective count rate limited the usefulness of this system. The NE213 results, however, were the first energy-dependent confirmation that the neutron emission from TFTR could become dominated after neutral-beam injection by 14-MeV neutrons from triton burnup. Surface barrier diode (SBD) detectors, originally installed to measure 15-MeV protons from $^3$He burnup, were found to be sensitive to 14-MeV neutrons through a $^{28}$Si(n,$\alpha$) reaction. The results from these detectors are similar to the NE213 measurements shown in Fig. 36.

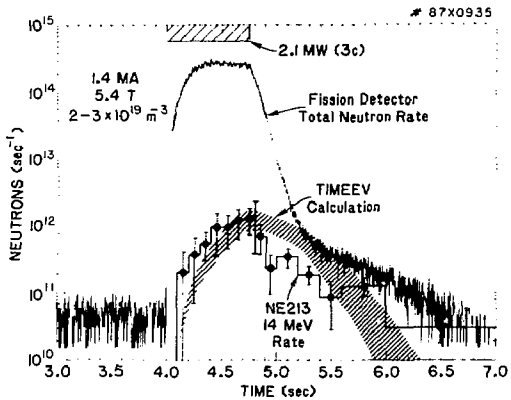


*Figure 36. Observed total and 14-MeV neutron rates, and classical calculation of expected 14-MeV emission. The 14-MeV neutrons originate from tritons produced by previous deuterium-deuterium reactions in the plasma and allow study of triton burnup physics.*

The escaping 1-MeV triton flux versus pitch angle was measured for the first time with a new imaging detector, with results as shown in Fig. 37. The success of this prototype allowed design and construction of an array of similar detectors to be installed inside the vessel in late 1987. These detectors will be able to measure both tritons in D-D plasmas and alpha particles in D-T plasmas, with the goal of understanding both the single-particle and collective alpha confinement properties of TFTR.

Gamma ray fluxes and energy spectra were measured[41] with deuterium and $^3$He plasmas in TFTR during injection of neutral beams for total neutron source rates up to $6 \times 10^{15}$ sec$^{-1}$. Using a NaI(Te) detector, the measured gamma background during $D^0 \rightarrow D^+$ discharges exhibited a broad energy spectrum extending to $\lesssim 13$ MeV. The first measurement was made of the 16.6 MeV prompt gamma ray emitted by the D($^3$He, $\alpha$)$^5$Li reaction during deuterium neutral-beam heating of $^3$He plasmas in TFTR, as shown in Fig. 38. The 16.6-MeV gamma ray is evident for energies between 15.8 and 17.0 MeV. This observation of the D-$^3$He fusion gamma ray encourages further development of fusion gamma ray spectrometry as a method for measurement of the fusion reaction source function.

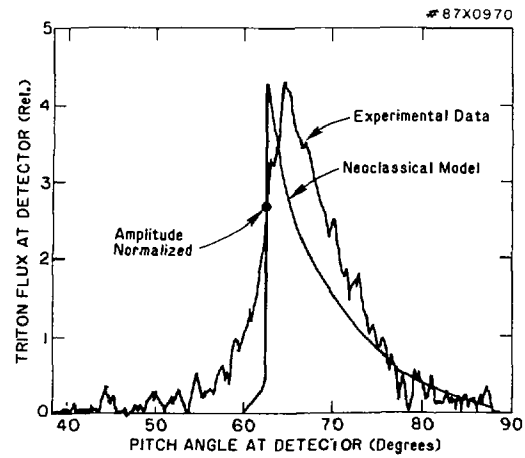


*Figure 37. Measured flux of escaping tritons versus pitch angle at the detector located below the TFTR plasma. The agreement with the neoclassical model curve is good (note that the instrumental resolution of approximately ±5° has not been folded into the model curve). The absolute flux also agrees to within the joint uncertainties of experiment and model.*

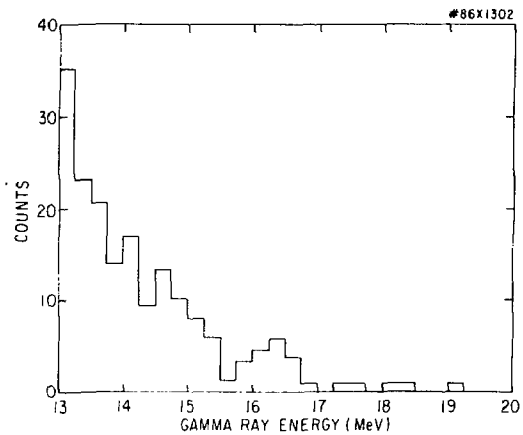


*Figure 38. Measurement of the 16.6-MeV gamma ray produced by the D-$^3$He reaction during $D^0 \rightarrow {}^3He^{++}$ plasma operation.*

## Probes

The most marked progress in edge probe diagnostics this year was in the operation of the midplane fast probe and improved data analysis techniques. The fast probe routinely collected Langmuir and calorimeter radial profiles of the scrape-off layer in a single discharge, by moving ±30 cm at an arbitrary time during the shot. These measurements revealed deviations from a simple exponential decay in the falloff of the electron density and ion flux in ohmic plasmas, as shown in Fig. 39. For this discharge, the exponential decay length varies from 3 to 11 cm in the plasma scrape-off layer.

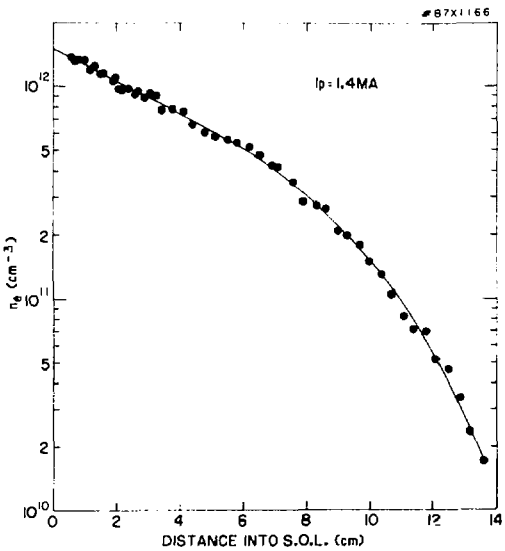


*Figure 39. Electron density observed in the scrape-off region of a 1.4-MA ohmic plasma, obtained from a Langmuir probe. The distance d is measured from the last closed flux surface.*

The vertical long probe system collected data in a dc triple Langmuir probe configuration, with good agreement with the fast probe measurements. It was also employed for machine conditioning studies with rotatable sample collection probe heads. The other midplane probe was deployed at the vessel wall to measure low-energy charge-exhange neutrals by a resistance probe technique previously used on PLT.[42]

A new diagnostic was installed during the last run period to investigate radio-frequency emission from the TFTR plasma and assess the possible relation of the spectrum to fusion product populations. A balanced magnetic loop probe, located near the outer midplane of the tokamak, allowed study of emission over the range of 1 to 500 MHz. General phenomena observed included a harmonic series of large amplitude spectral peaks during neutral-beam injection (corresponding to cyclotronic emission from the injected species at the outer plasma edge), weak emission from high-density ohmic plasmas, and a low-frequency (<10 MHz) continuum (see Fig. 40). Current work is focused on understanding the origin of these spectral components.

During the 1987 opening, an array of seven 2-axis radio-frequency probes was installed. These probes will be used both for characterizing radio-frequency waves generated during ICRF heating experiments and for further radio-frequency emission studies. Each probe allows measurement of the wave polarization, and the array includes toroidally and poloidally separated probes for determination of wave phase relationships.

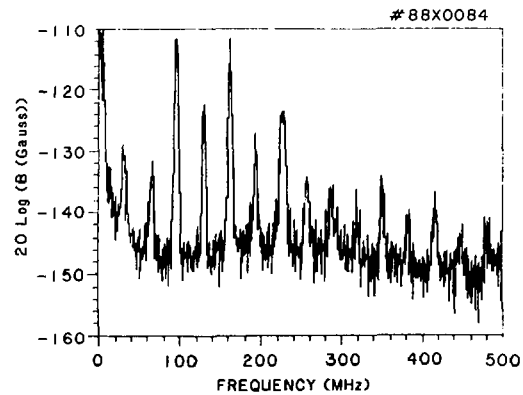


*Figure 40. Radio-frequency emission observed with the magnetic loop probe in a plasma with modest neutral-beam-injection power.*

## X-Ray Pulse-Height Analyzer

Two vertical X-ray pulse-height-analyzer (PHA) channels at major radii 1.94 m and 2.7 m, were added to the existing horizontal PHA, enabling measurement of three-point profiles of $Z_{eff}$, and metal concentrations, and $T_e$. Initial analysis showed $Z_{eff}$ and metal concentrations to be constant with radius in ohmic plasmas and with low-power neutral-beam injection. With high-power injection background noise from neutrons and gamma rays frustrated vertical PHA measurements because of inadequate shielding. This shielding has recently been improved.

A comparison of $Z_{eff}$ measurements by the horizontal PHA with values from visible bremsstrahlung for a large number of the supershots during the 1986 run showed good agreement on the average.

## Pellet Spectroscopy

The flash of light from pellets injected into TFTR has been studied in order to determine the time dependence of the electron density (by Stark broadening of atomic hydrogen lines) and temperature (by the line-to-continuum ratio) in the luminous cloud surrounding the ablating pellets.[43] The detection system is an eight-channel polychromator with

photomultiplier detectors which covers the spectrum from the line center to 250 Å off center and allows analysis of the Stark broadened spectra for electron densities of $10^{16}$ -$10^{18}$ $cm^{-3}$ (Ref. 44). The first measurements on TFTR indicate that the electron density in the luminous region of the cloud is within the range 1-7 × $10^{17}$ $cm^{-3}$, and the temperature is approximately 1.5 eV through most of the pellet lifetime. (An example of the density measurements is shown in Fig. 41). Detailed analysis of the emission line shapes will provide an estimate of the dimensions of the emitting region (from which H-alpha emission powers of 1-60 kW are observed by the absolutely calibrated detectors) and aid in evaluating the relationship between the luminosity of a pellet and the rate of ablation of particles from it as it penetrates the discharge. The polychromator system was modified for the next TFTR run by adding faster amplifiers and increasing the spectral resolution of the channels.

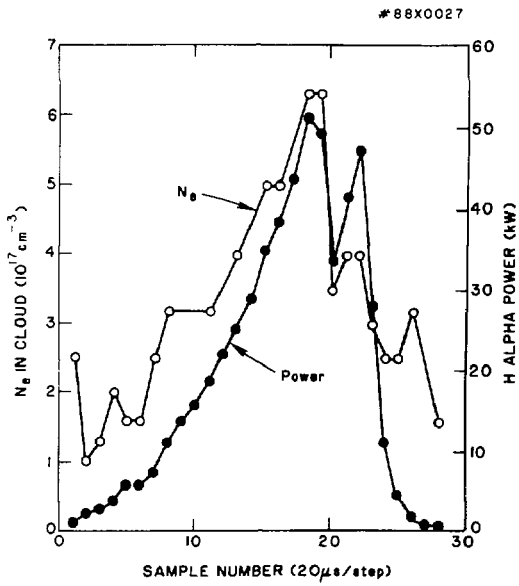


*Figure 41. Observed electron density and a lower bound of the $H_\alpha$ radiated power originating from pellet ablation.*

## Microwave Scattering

An apparatus for measuring density fluctuations by microwave scattering was installed on TFTR[45] and will be used in its next operational period on TFTR. The incident wavelength is 0.5 cm, which propagates in the extraordinary mode in the poloidal plane of the tokamak. The apparatus uses four antennae which view the plasma through fused quartz windows and can be aimed at various positions in the discharge.[46] A set of switches allows any of the antennae to be used as the transmitter, leaving the remaining three as receivers. Conventional heterodyne receivers will be used to resolve the direction of the frequency shift and spectrum associated with ambient or radio-frequency driven waves.[47]

## TOKAMAK OPERATONS

The engineers and technicians of this division operated TFTR on a two shifts per day, five days per week schedule during high-power pulsing (HPP) periods, with a third shift dedicated to routine preventive maintenance and calibration. During scheduled maintenance and shutdown periods, personnel performed more complex modification and repair tasks, notably removing the movable limiter, surface pumping system elements, and interior vacuum vessel protective tiles.

Scheduled shutdown periods to install the neutral-beam long-pulse ion sources and ICRF heating curtailed operating time, as shown in the summary of TFTR operations for FY87, Fig. 42. The available operating time limited the number of plasma attempts to 4,598, producing 3,851 successful experimental discharges. More detailed shot statistics are listed in Table II.

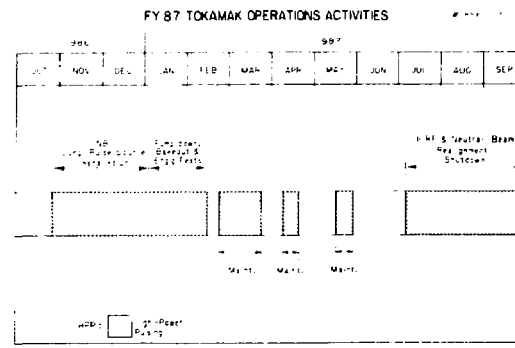


*Figure 42. Summary of Tokamak Fusion Test Reactor operations for FY87.*

**Table II. Fiscal Year 1987 Shot Statistics for TFTR.**

| | | |
|---|---|---|
| Attempts | | 4,598 |
| Plasma Discharges | | 3,851 |
| Ohmic Heating | 2,164 | |
| (Ohmic Heating with Pellet Injection—119) | | |
| Neutral-Beam Heating | 1,592 | |
| (Neutral-Beam Heating with Pellet Injection—57) | | |
| No Plasma Discharges | | 747 |
| Discharge Cleaning | | 9,685 |

Analyses of stresses in poloidal-field (PF) coils and supporting structures were completed. Stresses in PF Coil Stack No. 2 were recalculated using more realistic nonlinear boundary conditions. The analysis disclosed rotation of the stack causing maximum stress in the inboard turns of the OH-2 coil furthest from the midplane. The OH (ohmic-heating) operating current limit was reduced from 24 kA to 21 kA as a result of this analysis. This conclusion was confirmed by a group of independent reviewers from the fusion community. Consequently, the useful maximum plasma current is about 2 MA. The finite-element model used in this analysis of PF Coil Stack No. 2 is shown in Fig. 43.

Analysis of the umbrella structure, which supports the PF coils, disclosed several local areas requiring reinforcement to permit increased OH operating levels, consistent with the new coil-protection system. Reinforcements were designed and installation is in progress.

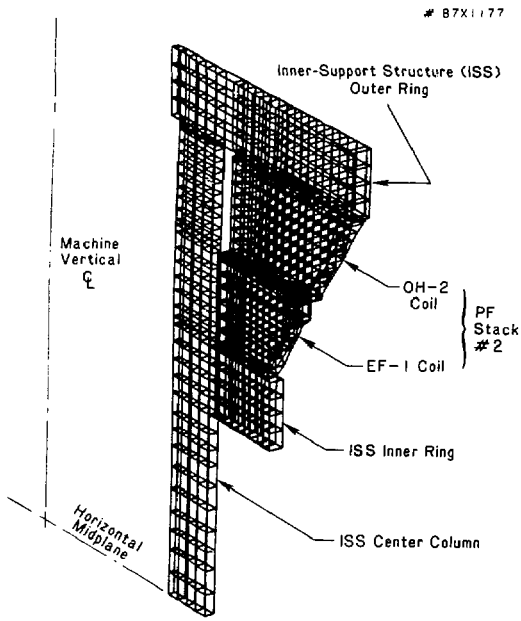


*Figure 43. Isometric of the nonlinear finite-element model used in analyzing the stresses in poloidal-field Coil Stack No. 2.*

A complex finite-element model of the center-plug, a reinforced concrete support for the umbrella structure, was subject to nonlinear stress analysis, including effects of possible concrete tension cracks. Results indicate that center-plug stresses would limit a proposed mode of operation which includes horizontal-field and vertical-curvature coils in the OH circuit to give a ten percent increase in volt-seconds (mode D). To achieve the full volt-second increase possible in this mode, several concepts were investigated to strengthen the center plug, but implementation is not planned due to the unacceptable impact on the schedule. Since center-plug stress is the limiting factor, efforts to reinforce the supports for the Stack No. 5 coil were discontinued.

Algorithms for stresses in PF coils and supporting structures were generated, checked, documented, and included in the systems code. As a result, a systems code to calculate stresses in various machine components for a given scenario is now available. The toroidal-field (TF) and PF algorithms are being incorporated in a new coil-protection system whose conceptual design underwent review early in FY87. A block diagram is shown in Fig. 44. The system performs real-time computation of coil thermal and electromechanical stresses and cuts off power to prevent exceeding specified limits.[48] When installed, the new coil-protection system will safely permit increased OH operating limits by removing conservative operating current margins required to cover approximations in the existing system.

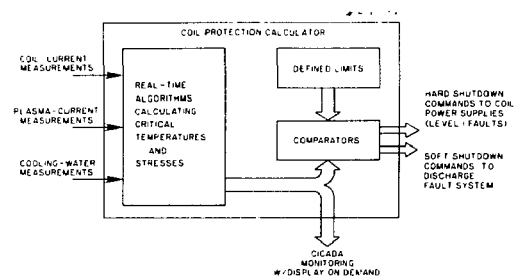


*Figure 44. Block diagram of the coil-protection system.*

Systems reliability improvements are planned in anticipation of operation with tritium. Irradiation by neutrons from deuterium-tritium (D-T) reactions will induce radioactivity in the machine, precluding normal hands-on maintenance. Reliability is, therefore, essential for D-T operation. A task force was established to examine the status of machine and personnel-safety interlocks and to recommend measures to improve reliability. An engineer experienced in reliability and fault-tree analysis is on loan from Idaho National Reactor Laboratory to lead the task force.

Other task forces studied TFTR preventive-maintenance practices and coil-cooling-water-flow interlocks. Reports were submitted describing the present status and recommending actions to improve operations in those areas. Following from the recommendations of the task forces, the manufacturer recalibrated cooling-water-flow switches and trained PPPL technicians to maintain and repair the interlocks. A programmable logic controller was installed to monitor flow switch status and to annunciate anomalies. A significant increase in availability is anticipated as a result.

To improve reliability and performance measurements, another task force is specifying a computerized system to acquire and process defined pertinent

reliability/availability data for each machine subsystem. The records produced by the system will clearly identify the areas for priority reliability improvement.

Low-level machine activation and contamination resulting from supershot operations required carefully planned and executed maintenance tasks. Special procedures were written and technicians trained to avoid contamination and unnecessary radiation exposure. For intensive work during the shutdown period, the radiation dose for individuals was minimized by rotating the assignments of the technicians, thus evenly dividing the exposure. Decontaminating facilities were set up and a storage facility for activated machine components was started. Shop facilities and procedures for safe machining of activated components were developed. The ability to maintain and repair activated components safely and efficiently proved essential to accomplishing tasks during the ICRF installation shutdown.

After the start of the shutdown in July, the highest activation gamma radiation level measured in the vacuum vessel after venting was 4.0 mR per hour on contact. An air sample indicated a concentration of tritiated water (HTO) and gas (HT) of 28 $\mu Ci/m^3$ and a HTO/HT ratio of 57/1. To reduce the HTO concentration, the vessel was purged twice with pumps exhausting through the stack. After the last venting, a gas sample measured less than 1 $\mu Ci/m^3$ which decreased to less than 0.1 $\mu Ci/m^3$ when vessel ventilation was installed. The USDOE guideline maximum for eight hours per day occupancy is 5 $\mu Ci/m^3$. Carbon dust was noted on vessel interior surfaces with smearable contamination levels measuring up to 36 k disintegrations per minute (dpm) per 100 $cm^2$. Since this level exceeded the USDOE and PPPL limit (1 k dpm/100 $cm^2$), personnel entering the vessel were required to wear anticontamination coveralls and appropriate personnel dosimeters with diligent checks for personnel contamination after exiting. By monitoring personnel exposure times and following written procedures, personnel doses have been limited to less than 20 percent of the PPPL quarterly allowable 600 mrem. In accordance with the "as low as reasonably achievable" (ALARA) principle, the PPPL quarterly allowable level is well below the USDOE level of 3 rem per quarter.

# D-T SYSTEMS

The D-T Systems Division provides a focus within the TFTR Project for the extensive preparations for deuterium-tritium (D-T) operation. Additionally, the Division is responsible for the tritium systems, shielding, and manipulators required for D-T operation.

The plan for the TFTR program has always included D-T operations as an important final part of the program, but due to changing programmatic and budgetary pressures, many of the D-T preparations have been delayed.

During FY87, a major project-wide effort was made to define the technical scope of the effort required to pursue D-T physics experiments on TFTR as vigorously as possible, given the various constraints which exist. The basic goal is to perform alpha-particle physics studies at Q values of approximately one, and a very important secondary goal is to gain experience in operating TFTR with tritium. Two basic plasma scenarios were delineated; one emphasized operating two neutral beams with deuterium and two with tritium, the other emphasized tritium pellet injection with deuterium neutral beams and ICRF heating. It was determined that the facility shielding should be compatible with production of $3 \times 10^{21}$ D-T neutrons. Code simulations gave roughly $10^{19}$ neutrons per discharge, so several hundred full-power discharges would be feasible in one year. Additional shielding would be needed, and the plan envisages approximately 30 inches of concrete in an igloo around the tokamak.

Since it is desired to perform alpha-particle physics experiments during these D-T runs, the plasma diagnostics have to be improved, new ones added, and all diagnostics have to be made compatible with the shielding. Initial scoping studies were performed during the year to define the needs.

A significant effort was initiated to determine the tritium gas-handling needs and the tritium inventory in the graphite tiles of the vacuum vessel. This work is being largely done by the Sandia National Laboratories and includes experimental work as well as modeling studies. Initial estimates of the tritium inventory were provided. They imply that the existing constraint of 50,000 curies on-site could imply very tight operational constraints.

Since the TFTR facility is needed for CIT construction, it was decided to limit the length of the TFTR D-T operational period to a few months. As a consequence, it is feasible to minimize the remote-handling considerations of TFTR if the parts of the machine which are inside the igloo can be made adequately reliable for this period of time. Work was initiated to investigate various aspects of this proposal. It was decided that two manipulators should be provided; one for inside the vacuum vessel, and one for outside the machine.

A draft "D-T Preparations" plan incorporating these ideas was produced in April 1987 (Ref. 1). Somewhat in parallel with this activity, the US Department of Energy requested the Magnetic Fusion Advisory Committee (MFAC) to review the proposed TFTR plans for D-T operation. The MFAC Panel XVII reviewed the plans, and issued a report[2] which was accepted by MFAC in September 1987. The MFAC recommendations to USDOE strongly supported the TFTR plans.

## Tritium Branch

The use of tritium as a fuel will be instrumental in the attainment of energy break-even conditions ($Q \sim 1$) expected for TFTR. A primary technical goal of D-T operation is to demonstrate tritium-handling capability in a tokamak environment. The demonstration of tritium handling in an operating confinement

experiment will provide invaluable experience for the design and operation of future D-T magnetic fusion devices. In addition, the issue of tritium inventory and control inside the tokamak is important for the ignition program.

The Tritium Branch is responsible for managing, modifying, and operating the tritium systems (including all ancillary tritium-related assemblies that will provide complete tritium handling), and radiation-monitoring capability for TFTR. A complete project schedule was made. It includes the design modifications, implementation of these modifications, commissioning, and operation of the system.

In 1985, the Burns and Roe Company was selected as the subcontractor to modify the design of the process systems for tritium storage, tritium cleanup, radwaste, monitoring, and HVAC (heating, ventilating, and air conditioning). This design work commenced in September 1985 and will continue through FY88. During FY87, the design effort was concentrated on modification of the tritium-process systems and the tritium-storage and tritium-delivery systems.

The tritium-delivery system was successfully tested with hydrogen, and the complete systems will be retested with hydrogen in the future.

New gas-injection valves are required for the tritium operation. The design of the piezoelectric valves was completed and two valves were ordered in FY87.

Design and procurement of the remote control and monitoring system for the tritium system has started. The system (called TRECAMS) is based on programmable logic controllers and will operate as a stand-alone system with interfaces to the Central Instrumentation, Control, and Data Acquisition (CICADA). The system will be delivered to PPPL in FY88. Installation and testing of the automated system will be completed during FY89.

### Tritium Pellet Injector

In 1987, a prototype tritium pellet injector was designed and built by Oak Ridge National Laboratory (ORNL). This prototype, shown in Fig. 45 and called "tritium-proof-of-principle" (TPOP), will be tested with tritium at the Tritium Systems Test Assembly (TSTA) at Los Alamos National Laboratory (LANL) early in FY88. The information derived from this prototype was to have been used in the design and manufacture of a tritium-pellet injector (TPI) to be installed and operated on TFTR.

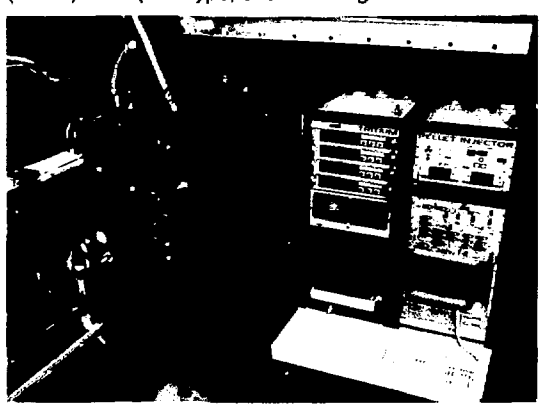

*Figure 45. Prototype tritium pellet injector and controls under test at the Oak Ridge National Laboratory. (ORNL 8860-87)*

The TPI requirements are similar to those of the existing deuterium pellet injector (DPI). The TPI would provide up to eight pellets of tritium for each TFTR pulse at velocities of up to 1.5 km/sec. Unfortunately, due to budget constraints, it is now expected that the TPI will be eliminated from the TFTR program plans.

## Manipulator and Shielding Branch

The Manipulator and Shielding Branch work during the year focused on several key areas:

- Radiation shielding required to provide biological and equipment protection for D-T experimental operations.
- Machine modifications to provide space for shielding.
- Engineering to follow the design, fabrication, and testing of the maintenance manipulator.
- Evolving the preconceptual requirements for an external manipulator to perform limited but important functions on TFTR.

### Radiation Shielding

The radiation shielding design evolved from analyses performed by the Engineering Analysis Division. The basis for the calculations was a total neutron yield of $3 \times 10^{21}$ and a design objective of limiting the dose equivalent at and beyond the site boundary to 10 mrem per year. The shielding (generally referred to as the "igloo") will be in the form of a cylinder around the tokamak and in the form of a box for equipment that is appended to the tokamak. Calculations show that 30 inches of borated concrete around the tokamak and approximately 24 inches sidewall and roof shielding around the appendages will provide effective shielding.[49] In addition to the biological exposure limit, the neutron and gamma-ray fluxes and resulting doses to equipment must be limited to insure the integrity of the equipment. This type of protection will be provided by a combination of the planned biological shielding and add-on local shielding.

The biological shielding is planned to be a 30-inch thick borated concrete closed cylinder on the 102-foot elevation. The cylinder will be approximately 40 feet in diameter and 30 feet high and enclose the tokamak. This configuration is shown in Fig. 46. Major hardware off the torus (such as the Bay C vacuum-pump duct, the four neutral beams, the diagnostic neutral beam, and the pellet injector) will have

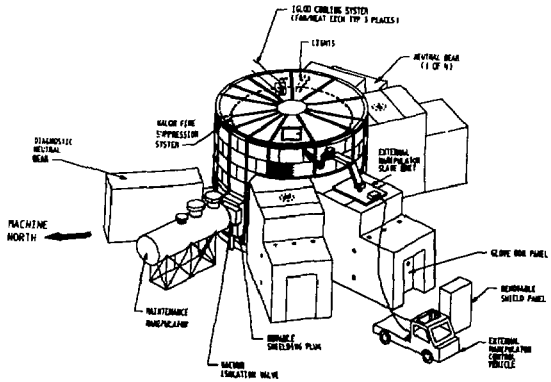


*Figure 46. Conceptual design configuration of radiation shielding for TFTR. (87E0507)*

separate enclosures or appendages that will butt up to the center cylinder of shielding.

The schedule is to have the Conceptual Design Review in January 1988 and the Final Design Review in May 1988 (Ref. 50). Installation will be carried out in two phases: Phase 1 (the January-July 1989 shutdown)—the upper-shielding structure and shielding in four or five lower bays will be installed; Phase 2 (the March-July 1990 shutdown)—the installation of the shielding in the remaining lower bays, the upper walls, roof, and appendages will be completed. After the 1990 shutdown, qualifying operations will occur, then D-T experiments will commence.

## Machine Shielding Modifications

In order to locate the 30-inch shielding around TFTR at the 102-foot elevation in the lower bays, existing hardware on the machine will have to be modified.

A Conceptual Design Review of the bays between the TF coil of TFTR was held. The hardware in the bays below the lintels between the vertical steel columns on the machine will be revised to move services such as electrical conduits and cables, TF cooling water lines, and pneumatic lines inboard. Any items that can be eliminated will be. Most items will move to allow the 30-inch shielding to fill the bays.

The upper part of the machine will be revised in that the bellows-cooling system will be eliminated, the vacuum-vessel heating and cooling system will be lowered, and the trays will be reduced in diameter to allow the shielding to encompass all the hardware and not be excessively high.

A conceptual design was made for the Bay C vacuum-pump duct modifications. This change will involve removing the four turbomolecular pumps and two valves. The remaining two valves will be repositioned under the duct and will service the two new cryo pumps to be installed. The residual gas analyzer will be moved north of its current position to allow the shielding to be positioned as required. This hardware arrangement will allow the appendage shielding at Bay C to be moderate in size.

## Maintenance Manipulator

The TFTR maintenance manipulator (MM), a six-link articulated arm, designed to allow one of several end-effectors to do inspection and maintenance in the torus, can be positioned at any location along the torus center line.[51] Figure 47 shows the maintenance manipulator and the general hardware arrangement. The maintenance manipulator is being designed, fabricated, and tested by KfK (Kernforschungszentrum-Karlsruhe, GmbH) Laboratory in

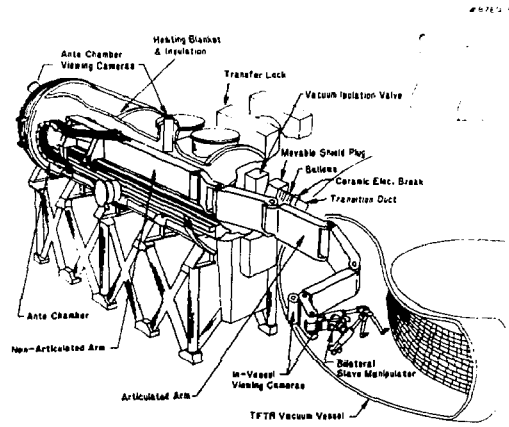


*Figure 47. Schematic of the maintenance manipulator with slave manipulator and general hardware arrangement.*

Karlsruhe, West Germany in a cost-sharing agreement. During the past year, the arm was fabricated by Noell GmbH of Wurzberg, West Germany, a subcontractor to KfK. The maintenance manipulator will be undergoing final assembly and test at KfK during the November 1987 to July 1988 period and is expected at PPPL in late July 1988. The general inspection arm (GIA), a vacuum-rated device that will be used for inspection and leak detection, was designed and built by KfK. A Teleoperator System (TOS) master/slave system, which is not vacuum rated, can be used for inspection, tile removal, and replacement or general tasks yet to be specified. The TOS, purchased by PPPL approximately ten years ago, is being refurbished at Los Alamos National Laboratory, Los Alamos, New Mexico.

The vision and lighting system for the maintenance manipulator was designed, fabricated and tested by Commissariat a l'Energie Atomique (CEA) at Fontenay-Aux-Roses, France in another cost-sharing agreement. The system consists of five cameras and associated lighting that provide the capability to view the maintenance manipulator as it maneuvers from its stowed position in the antechamber to any position in the torus, as well as the operation of either of the two end-effectors.

## External Manipulator

Preconceptual plans for an external manipulator evolve around either a vehicle that could maneuver about the Test Cell (a concept shown in Fig. 46) or a boom that could be mounted on the existing crane in the Test Cell. Either method would have a vision/lighting/audio system along with a master/slave manipulator that would provide inspection, crane assistance, and limited-maintenance capability for TFTR.

The vehicle would have the master in a shielded cab and the slave on an articulated boom to perform the above-noted tasks. The crane-mounted boom will require an additional bridge to allow the crane hooks to function as needed and the master might be in a control room located in the mock-up area.

Oak Ridge National Laboratories, Oak Ridge, Tennessee, have agreed to undertake the design, fabrication, and testing of the external manipulator.

## Radio-Frequency Limiters

A project was established in June 1986 to design, fabricate, and install two poloidal limiters of 240° extent to shield two rf antennae from plasma-heat loads. An edge-coupling distance between the plasma and the antennae of 2 cm is assumed. The design used a 2-D carbon-carbon composite with a staple-knit fiber. It was fabricated by the Super-Temp Operations of the BF Goodrich Company.[52] Each limiter is composed of 24 poloidally straight and toroidally curved segments. The limiters have a density greater than 1.70 gm/cc and are approximately 1-cm thick.

The limiters were designed for the supershot cases of 1-cm and 1.5-cm scrape-off length and are expected to reach temperatures in excess of 2300°C in localized areas along the surface. Calculated bulk temperatures of 600°C for a series of supershots required that water-cooling panels be installed between the limiter and vacuum vessel ±30° about the midplane.

The limiters are fixed directly to the vacuum-vessel wall with 718 Inconel flexible clips that permit both toroidal and poloidal differential expansion and provide isolation against toroidal electric current.

The installation of limiters is scheduled to be completed during November 1987.

## Lithium Blanket Module Program

The experimental program with the lithium blanket module (LBM) at the LOTUS facility at Ecole Polytechnique Fédéral de Lausanne (EPFL), Switzerland was terminated in October 1986. The LBM and all diagnostic equipment were shipped back to Princeton and are now in storage awaiting further disposition.

# SAFETY AND ENVIRONMENT

In anticipation of D-T operations in 1990, the TFTR Project increased its emphasis on environmental monitoring both on- and off-site to establish baseline data. This included monitoring for tritium and gamma emitters in surface water, groundwater, air, soil, and biota. Off-site monitors for air, air particulate, and tritium will be in place in late FY88. The U.S. Geological Service (USGS) groundwater study was completed and will be beneficial both to TFTR and CIT.[53] Samples taken by the USGS were split and supplied to the PPPL Health Physics Group and the University of Miami, Florida, for tritium analyses. The results from these two independent analyses agreed within counting statistics and indicated that the present level of HTO (tritiated water), in the wells located on the TFTR site, was approximately 3 Bq per liter (80 pCi per liter). Also, a third full year of meteorological data was collected and analyzed, providing the required baseline for future operation. The Health Physics Group received an "excellent" rating in their FY87 DOE/CH appraisal and it is felt that this group has one of the best capabilities in the U.S. in the detection of low levels of tritium in the environment.

The modifications of the TFTR tritium and heating, ventilating, and air conditioning systems proposed by Burns and Roe were extensively reviewed. The reviews will continue in FY88 in preparation for D-T operation. Project and Operational Safety (P&OS) participated as a member of the Seismic Task Force to develop revised seismic requirements for TFTR systems and components. An internal audit and review of TFTR safety-related documentation was made and a report issued to help TFTR improve its written documentation and procedures prior to D-T operation. The P&OS also participated in the D-T Interface Committee activities and led an effort to forge a consensus at PPPL on the appropriate methodology and parameters for calculating maximum accident doses at the D-Site control-area boundary due to ground-level releases of tritium. These dose levels are critical to development of the revised seismic criteria for TFTR systems and components.

The increased neutron production, especially after "supershots," elevated activation levels of the TFTR machine in FY86 (Ref. 54) and further verified the need for an active health physics program. From January to July 1987 approximately $3 \times 10^{18}$ D-D fusion neutrons were produced. These D-D reactions produced machine activation and approximately 5.4 GBq (145 mCi) of tritium, much of which was absorbed in the vessel graphite tile. The HTO concentration in the air in the vacuum vessel was six times the air-concentration guideline for personnel when the vessel was initially opened in July 1987. The HTO/HT measurement indicated a 57/1 ratio. The tritium contamination of the graphite, which was not unexpected, has been one of the first significant health physics considerations for any tokamak. There was

also an outgassing effect from the graphite during the subsequent activities within the vessel. Figure 48 shows that activation levels of the vessel decrease

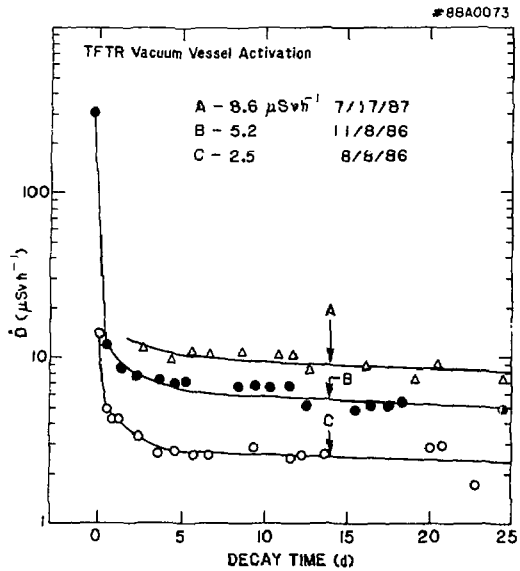


*Figure 48. A comparison of contact dose rate following two weeks of decay after Tokamak Fusion Test Reactor operation shows the gradual buildup of residual activation with time.*

rapidly after periods of machine operation to a level of long-lived radionuclides which increases predictably with operation. Figure 49 shows the decay of activation during the 1987 shutdown. The data are consistent with the code predictions of a 90-day

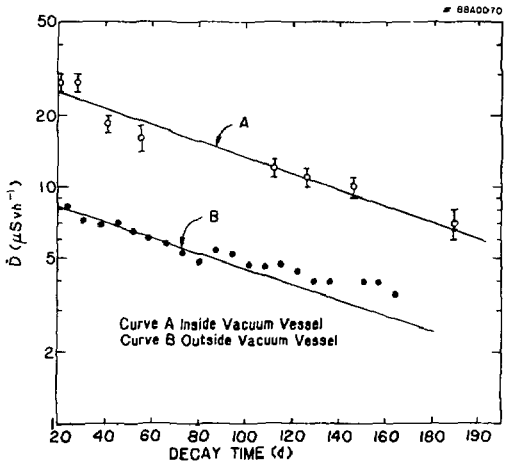


*Figure 49. Comparison of late 1987 survey data measured inside and outside the Tokamak Fusion Test Reactor vacuum vessel. Bars represent the range of readings for each in-vessel curve. The lines represent 90-day half-life decay.*

effective half-life.[55] The 90-day half-life is illustrated with the lines on this figure. Dose rates inside the vessel remained three times higher than outside the vessel. The health physics experience gained in FY87 was a good training exercise for upcoming D-T operations. Outside the shielding walls of the Test Cell, the radiation-monitoring system detector at the Test Cell walls and perimeter fence indicated insignificant levels at these locations. Personnel exposures were also insignificant.

A task force was set up to develop emergency-response procedures. This is expected to take two years, but the expected result is that safer responses will be made in case of fires or other emergencies, with proper shutdown of electrical power and implementation of other appropriate safety measures within the particular area of concern. Development of adequate written operating procedures has become a high priority. Extensive procedures were written for the Energy-Conversion Systems and now this effort is expanded into the Neutral-Beam area of the Heating Systems Division.

## References


[1]J. Alton, H.F. Dylla, J. Gilbert *et al.*, "D-T Plan," Princeton University Plasma Physics Laboratory Report DT5D-R-5 (Draft), April 1987, 231 pp.

[2]Magnetic Fusion Advisory Committee Panel XVII "Report on The Scientific and Technical Merit of Deuterium-Tritium Operation in TFTR," (September 1987).

[3]G.S. Lee and P.H. Diamond *et al.*, "Theory of Ion-Temperature-Gradient-Driven Turbulence in Tokamaks," *Phys. Fluids 29* (1986) 3291.

[4]J.D. Strachan, M. Bitter, A.T. Ramsey, *et al.*, "High-Temperature Plasmas in the Tokamak Fusion Test Reactor," Phys. Rev. Lett. *58* (1987) 1004.

[5]R.J. Hawryluk, V. Arunasalam, M.G. Bell, *et al.*, "TFTR Plasma Regimes," in *Plasma Physics and Controlled Nuclear Fusion Research 1986* (Proc. 11th Int. Conf., Kyoto, Japan, 1986) Vol. *I* (IAEA, Vienna, 1987) 51.

[6]R.J. Goldston, "Energy Confinement Scaling on Tokamaks: Some Implications of Recent Experiments with Ohmic and Strong Auxiliary Heating," in *Plasma Physics and Controlled Fusion 26* (Proc. 11th European Conf., Aachen, FRG, 1983), No. 1A (Great Britain, 1984) 87.

[7]K.M. McGuire, V. Arunasalam, M.G. Bell, *et al.*, "Coherent and Turbulent Fluctuations in TFTR," in *Plasma Physics and Controlled Nuclear Fusion Research 1986* (Proc. 11th Int. Conf., Kyoto, Japan, 1986) Vol. *I* (IAEA, Vienna, 1987) 421.

[8]A.W. Morris, E.D. Fredrickson, K.M. McGuire, *et al.*, "Beta Limits and MHD Activity in TFTR," in *Controlled Fusion and Plasma Physics* (Proc. 14th European Conf., Madrid, Spain, 1987) 189.

[9]F. Troyon, R. Gruber, H. Saurenmann *et al.*, "MHD-Limits to Plasma Confinement," in *Plasma Physics and Controlled Fusion 26* (Proc. 11th European Conf., Aachen, FRG, 1983), No. 1A (Great Britain, 1984) 209.

[10]M. Bitter, V. Arunasalam, M.G. Bell, *et al.*, "High Power Neutral Beam Heating Experiments on TFTR with Balanced and Unbalanced Momentum Input," in *Controlled Fusion*

*and Plasma Physics 29* (Proc. 14th European Conf., Madrid, Spain, 1987) No. 10A (Great Britain, 1987) 1235.

[11]R.J. Goldston, "Topics in Confinement Analysis of Tokamaks with Auxiliary Heating," in Course and Workshop on Basic Physical Processes of Toroidal Fusion Plasmas (Varenna, Italy, 1985) Vol *I* (Euratom, 1986) 165.

[12]R.J. Groebner, W. Pfeiffer, F.P. Blau, *et al.*, "Experimentally Inferred Ion Thermal Diffusivity Profiles in the Doublet III Tokamak: Comparisons with Neoclassical Theory," Nucl. Fusion *26* (1986) 543.

[13]K.L. Wong, C.Z. Cheng, B.C. Stratton, and A. Ramsey, *et al.*, "Impurity Penetration into a Rotating Plasma—Theory and Experiment," in *Controlled Fusion and Plasma Physics* (Proc. 14th European Conf., Madrid, Spain, 1987), Vol *II*, 121.

[14]H.F. Dylla, P.H. LaMarche, M. Ulrickson, *et al.*, "Conditioning of the Graphite Bumper Limiter for Enhanced Confinement Discharges in TFTR," Nucl. Fusion *27* (1987) 1221.

[15]H.F. Dylla, D.B. Heifetz, M.A. Ulrickson, *et al.*, "Wall Pumping and Particle Balance in TFTR," in *Controlled Fusion and Plasma Physics* (Proc. 14th European Conf., Madrid, Spain, 1987) Vol. *II*, 698.

[16]M.A. Ulrickson, H.F. Dylla, P.H. LaMarche, *et al.*, "Particle Balance in TFTR," Proc. 34th Symp. AVS J. Vac. Sci. Technol., in press.

[17]W.R. Wampler, B.L. Doyle, S.R. Lee, *et al.*, "Deposition of Carbon, Deuterium, and Metals on the Wall and Limiter of TFTR," Proc. 34th Symp. AVS J. Vac. Sci. Technol., in press.

[18]A.B. Rechester, M.N. Rosenbluth, *et al.*, "Electron Heat Transport in a Tokamak with Destroyed Surfaces," Phys. Rev. Lett. *40* (1978) 38.

[19]S.D. Scott, M. Bitter, H. Hsuan, *et al.*, "Measurements of Toroidal Rotation on TFTR," in *Controlled and Plasma Physics* (Proc. 14th European Conf., Madrid, Spain, 1987), Vol. *II*, 65.

[20]R.J. Goldston, Y. Takase, D.C. McCune, *et al.*, "Edge and Center Heating Experiments on TFTR," in *Controlled Fusion and Plasma Physics* (Proc. 14th European Conf., Madrid, Spain, 1987), Vol. *II*, 140.

[21]G.L. Schmidt, S.L. Milora, V. Arunasalam, *et al.*, "Pellet Injection Results During TFTR Ohmic and Neutral Beam Heating Experiments," in *Plasma Physics and Controlled Nuclear Fusion Research 1986* (Proc. 11th Int. Conf., Kyoto, Japan, 1986) Vol. *I* (IAEA, Vienna, 1987) 171.

[22]S. Sengoku, A. Funahashi, M. Hasegawa, *et al.*, "Regime of Improved Confinement in Neutral-Beam-Heated Limiter Discharges of a Tokamak," Phys. Rev. Lett. *59* (1987) 450.

[23]P.C. Efthimion, D.W. Johnson, N.L. Bretz, *et al.*, "Recent Confinment Studies of Ohmically-Heated Helium Plasmas," in *Controlled Fusion and Plasma Physics* (Proc. 14th European Conf., Madrid, 1987), Vol. *II*, 136.

[24]D.K. Mansfield, P.C. Efthimion, R.A. Hulse, *et al.*, "Particle Confinement Studies on Ohmically-Heated Plasmas in TFTR Using Gas Modulation Techniques," in *Controlled Fusion and Plasma Physics* (Proc. 14th European Conf., Madrid, Spain, 1987) Vol. *II*, 314.

[25]J.D. Strachan and A. Chan *et al.*, "Helium Transport in TFTR," Nucl. Fusion *27* (1987) 1025.

[26]E.S. Marmar, J.E. Rice, J.L. Terry, and F.H. Seguin *et al.*, "Impurity Injection Experiments on the Alcator C Tokamak," Nucl. Fusion *22* (1982) 1567.

[27]G. Schilling, T.A. Kozub, S.S. Medley, K.M. Young, "TFTR Diagnostic Neutral Beam," Rev. Sci. Instrum. *57* (1986) 2060.

[28]A.L. Roquemore, S.S. Medley, "Design Concepts for Compact Mass/Energy Charge Exchange Analyzers," Rev. Sci. Instrum. *57* (1986) 1797.

[29]C.L. Fiore, S.S. Medley, G.W. Hammett, *et al.*, "Ion Temperature from Tangential Charge Exchange Neutral Analysis of the Tokamak Fusion Test Reactor," Princeton University Plasma Physics Report PPPL-2476 (September 1987) 48 pp; submitted to Nucl. Fusion.

[30]M. Bitter, K.W. Hill, S. Cohen, *et al.*, "Vertical High-Resolution Bragg X-ray Spectrometer for the Tokamak Fusion Test Reactor," Rev. Sci. Instrum. *57* (1986) 2145.

[31]H. Hsuan, M. Bitter, K.W. Hill, *et al.*, "Satellite Spectra of Heliumlike Nickel," Phys. Rev. A *35* (1987) 4280.

[32]D. Mansfield, H.K. Park, L.C. Johnson, *et al.*, "MIRI: A Multichannel Far-Infrared Laser Interferometer for Electron Density Measurements on TFTR," Appl. Optics *26* (1987) 4469.

[33]C.H. Ma, D.P. Hutchinson, K.L. Vander Sluis, *et al.*, "Measurement of Faraday Rotation in TFTR Plasmas," Rev. Sci. Instrum. *57* (1986) 1994.

[34]A. Brizard, B. Grek, B. LeBlanc, and D. Johnson, "Feasibility Study of Using the TFTR Thomson Scattering System for q Profile Measurements," Rev. Sci. Instrum. *57* (1986) 1813.

[35]A Cavallo, M.P. McCarthy, R.C. Cutler, "A Twenty Channel Grating Polychrometer for Millimeter Wave Plasma Emissions," in *Infrared and Millimeter Waves* (Proc. 11th Int. Conf., Tirrenia-Pisa, Italy, 1986), published by ETS Editrice, Pisa, Italy (1986) 317.

[36]B.C. Stratton, A.T. Ramsey, F.P. Boody *et al.*, "A Spectroscopic Study of Impurity Behavior in Neutral Beam and Ohmically Heated TFTR Discharges," Nucl. Fusion *27* (1987) 1147.

[37]J. Schivell and C.E. Bush, "Analysis of Highly Asymmetric Radiation Loss Profiles in TFTR," Rev. Sci. Instrum. *57* (1986) 2081.

[38]E.B. Nieschmidt, "Analysis Programs and Standardization of the Neutron Activation System at TFTR," Rev. Sci. Instrum. *57* (1986) 1757.

[39]D.L. Jassby, H.W. Hendel, C.W. Barnes, *et al.*, "Fission-Detector Determination of D-D Triton Burnup Fraction in Beam-Heated TFTR Plasmas," Princeton University Plasma Physics Laboratory Report PPPL-2454 (June 1987) 8 pp.

[40]F.E. Cecil and S.S. Medley, "Gamma Ray Measurements During Deuterium and $^3$He Discharges on TFTR," Princeton University Plasma Physics Report PPPL-2444 (May 1987) 35 pp; accepted for publication in Nucl. Instrum. Methods (A).

[41]W.R. Wampler and D.M. Manos, "Plasma Edge Studies Using Carbon Resistance Probes," J. Vac. Sci. Technol. *A1* (1983) 827.

[42]D.H. McNeill, G.J. Greene, and D.D. Schuresko, "Parameters of the Luminous Region Surrounding Deuterium Pellets in the Princeton Large Torus Tokamak," Phys. Rev. Lett. *55* (1985) 1398-1401.

[43]D.H. McNeill, G.J. Greene, J.D. Newburger, *et al.*, "Measurements of Plasma Parameters in the Luminous Regions of Pellets Injected into Tokamaks," in *Controlled Fusion and Plasma Physics* (14th European Conf., Madrid, Spain, June 1987), Vol. *11D*, 209-212.

[44]N. Bretz, P. Efthimion, J. Doane, and A. Kritz, "A Microwave Scattering Apparatus for TFTR," in *Laser-Aided Plasma*

*Diagnostics* (Proc. 3rd Int. Sym., Los Angeles, CA, 1987) 5 pp.

[45]N. Bretz, "Geometrical Effects in X-Mode Scattering," Princeton University Plasma Physics Laboratory Report PPPL-2396 (October 1986) 14 pp; accepted for publication in J. Plasma Phys.

[46]N. Bretz, "Scattering Below the Electron Cyclotron Frequency," in *Laser-Aided Plasma-Diagnostics* (Proc. 3rd Int. Sym., Los Angeles, CA, 1987) 5 pp.

[47]R.J. Marsala, E.D. Woolley, *et al.*, "Coil Protection Calculator for TFTR," in *Progress in Fusion Engineering* (Proc. 12th Symp., Monterey, CA., 1987), to be published by IEEE.

[48]S. Raftopoulos. P. Heitzenroeder, and E. Kaminsky, "TFTR D-T Shielding," in *Progress in Fusion Engineering* (Proc. 12th Symp., Monterey, CA., 1987), to be published by IEEE.

[49]D. Kungl, "TFTR D-T Plan," in *Progress in Fusion Engineering* (Proc. 12th Symp., Monterey, CA, 1987), to be published by IEEE.

[50]G. Loesser, P. Heitzenroder, "Design of the TFTR Maintenance Manipulator," in *Progress in Fusion Engineering* (Proc. 12th Symp., Monterey, CA, 1987), to be published by IEEE.

[51]G. Labik, J. Bialek, R. Ritter, and M. Ulrickson, "TFTR Carbon-Carbon Composite RF Limiters, Design, Selection, Fabrication and Installation," in *Progress in Fusion Engineering* (Proc. 12th Symp., Monterey, CA., 1987), to be published by IEEE.

[52]J.C. Lewis, F.J. Spitz, *et al.*, "Hydrogeology, Ground-Water Quality, and the Possible Effects of a Hypothetical Radioactive-Water Spill, Plainsboro Township, New Jersey." USGS Water Resources Investigations Report 87-4092. Trenton, NJ. (1987) 45 pp.

[53]J.D. Gilbert, J.R. Stencel, J.G. Couch, and J.J. Fennimore, "Activation Measurements on the Tokamak Fusion Test Reactor (TFTR)," (Proceeding of the Twentieth Midyear Topical Symposium of the Health Physics Society, February 8-12, 1987. Reno, NV) pp. 365-69.

[54]L-P Ku, "Radioactivation Characteristics for the Tokamak Fusion Test Reactor," Nucl. Tech./Fusion *4* (1983) 586.

# PRINCETON BETA EXPERIMENT-MODIFICATION

## INTRODUCTION

Modification of the Princeton Beta Experiment (PBX) to Princeton Beta Experiment-Modification (PBX-M) was completed in FY87 and the first plasma milestone was reached at the end of October 1987. As previously described[1] and as shown in Fig. 1, PBX-M differs from PBX in three major respects: the major plasma radius was increased from 145 cm to 165 cm; the conducting shell was extended to hug the plasma over most of its perimeter; and the poloidal field was made much more articulated and responsive.[2] The larger major radius provides space for a true divertor; the extended shell provides stability against long wavelength kink modes[3] and, in addition, improves stability to the n=0 vertical displacement mode, thereby strengthening the indentation capability of PBX-M relative to PBX; and the new poloidal-field system meets the higher requirements for control of the plasma shape and of the X-point location that are implied by the tightly fitting shell.

To complement construction activities, PBX-M research efforts in FY87 were devoted to planning for experimental operation in FY88. The most important actions were (1) a loan by the Massachusetts Institute of Technology (MIT) to PPPL of half of its 4.6-GHz lower-hybrid system (2 MW) to implement lower-hybrid current drive (LHCD) on PBX-M; (2) an agreement with the Oak Ridge National Laboratory (ORNL) to design and build an eight-shot deuterium pellet injector; and (3) a contractual agreement with the Culham Laboratory in England to build an 80-kV neutral probe beam (NPB) for PBX-M, to be used to measure—at a minimum—the safety factor q in the plasma center. The year's activities were rounded off by diagnostics development, a considerable upgrading of the neutral-beam heating system, and preparation of a prototype low-power ion-Bernstein wave heating (IBWH) antenna.

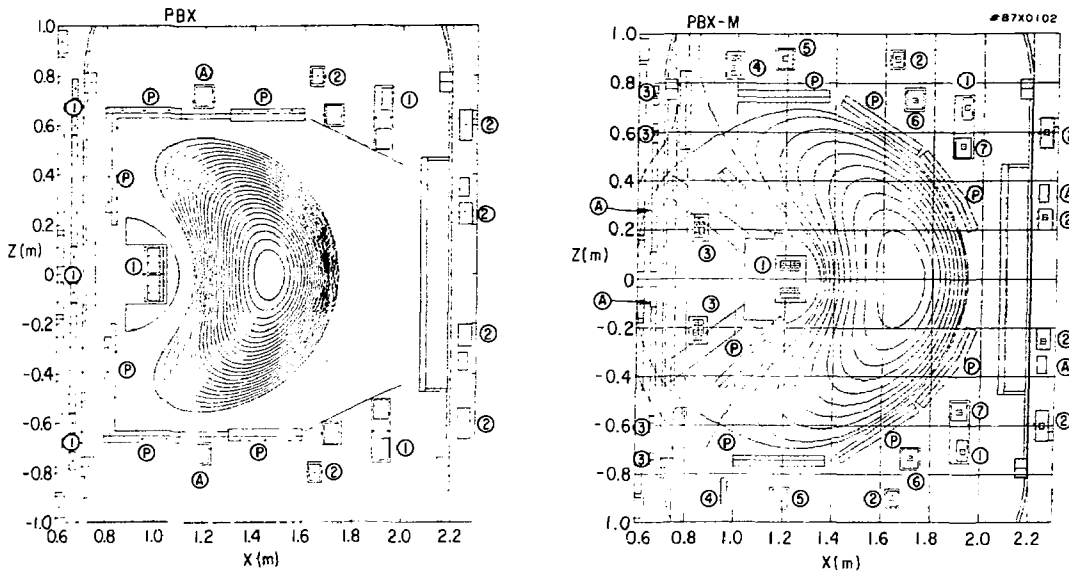


*Figure 1. Comparison of PBX and PBX-M. (a) PBX: [1] indentation field coils; [2] equilibrium-field dipole field; [P] passive stabilizer plates; [A] active feedback coil for vertical position control. (b) PBX-M: [1] indentation field coils; [2] equilibrium-field dipole field; [3] divertor field coils; [4-7] trimming coil; [P] passive stabilizer plates; [A] active feedback coil for vertical position control.*

The basis for these ambitious plans is rooted both in results obtained with PBX and in the PBX-M program plan, which is built on them. In brief, PBX results and theoretical work of recent years have made it clear that to operate successfully in the second MHD stability region it is not enough to fix the shape of the plasma cross section, it is equally important to control the pressure and current profiles which are closely linked in high-beta plasmas. With broad, optimized profiles the shape requirements are much relaxed and, conversely, with very peaked profiles no amount of shaping gives access to the second stability region.

Second stability is intrinsically an effect of high poloidal beta, $\beta_p$, and to a lesser degree of high safety factor, q. Bean shaping is a way of securing by geometry the same changes in magnetic configuration that result from high $\beta_p$, and the higher the $\beta_p$ the less strenuous the required shaping. Likewise, the more external control over the plasma shaping, the less strenuous requirements on specific plasma pressure and current profiles. The role of q is more ambiguous. At low q (less than 4), the second stability region easily disappears while kinks and modes become more violent. But at high q, where high $\beta_p$ is most accessible, the profile of the inductively driven current is much too peaked for second stability and, as an important and practical aside, for proper cross-section shaping as well.

Thus, in PBX the most deeply indented plasmas were low-q discharges in which an already broad current profile was widened still more, though transiently, by ramping the plasma current up at rates of 1-2 MA per sec. The higher-q, higher $\beta_p$ discharges with their more peaked current profiles could not be as fully indented as their lower-q counterparts. The observed disappearance of m=1 activity in the interior of the highly shaped discharges, as compared to its highly visible presence in the weakly shaped high-q ones, is quite consistent with theoretical anticipation, but proof awaits a q(r) measurement.

In view of the foregoing, it is clear that progress toward quasi-steady-state second stability operation in PBX-M requires active pressure profile control and noninductive plasma current drive. Tools for active control of the pressure profile include directed neutral-beam injection, pellet injection, and radially localized radio-frequency (rf) heating. Two sources of noninductive current, i.e., the neutral beams and the pressure gradient ("bootstrap" current), either exist or are inherent in the experiment; the plan is to supplement them with rf driven current. Clearly, the task is easiest when the supplemental current requirement is least, so that there is a natural convergence between a second stability experiment at high q and $\beta_p$ and rf current drive: high q implies low absolute values of current and high $\beta_p$ implies a strong source term for bootstrap current.

Since budget constraints are forcing a delay in the installation of the 4.6-GHz lower-hybrid current-drive system, the PBX-M program during its initial phase will continue with the techniques used with PBX. The high-$\beta$ plasma attained in PBX at low q in fact demonstrated the onset of a reversed gradient in |B| as well as the near expulsion from the plasma of the zero local shear surface (Fig. 2). If the PBX-M configuration does, as expected, permit the achievement of significantly higher betas than in PBX, then the reaching of a new confinement regime, even at low q and however transiently, is a real possibility. Similarly, if the deeper indentation made possible by the shell allows a sufficiently high $\beta_p$ at high q to

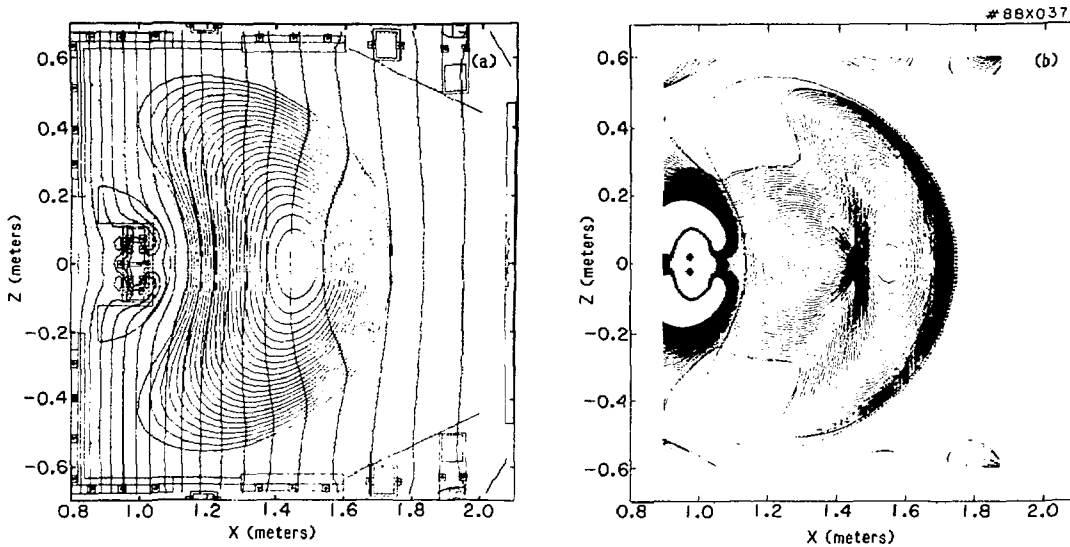


*Figure 2. The MHD stability properties for a PBX high-β shot (β = 5.3%). (a) mod-B contours superimposed on the plasma equilibrium surfaces and (b) local magnetic shear contours (solid lines are for greater than 0 and dash lines are for less than 0).*

generate appreciable bootstrap current, then interesting possibilities may open in that operating regime as well, even without rf current drive.

Ion-Bernstein wave heating is a major element in the PBX-M program for control of the pressure profile and as a source of additional heating power to aid in accessing the second stability regime. The ultimate purpose is to provide up to 7 MW of additional heating by utilizing the Tokamak Fusion Test Reactor (TFTR) radio-frequency power supplies, with a measure of control over the deposition profile. However, the possibility for good coupling to H-mode (High-mode) plasmas, the beneficent effects on particle confinement observed on the Princeton Large Torus (PLT), and even the possibility of using IBWH for stabilizing surface modes[4] make the IBWH program a particularly exciting one, with applications of great potential importance to future devices.

The role of the pellet injector under construction by ORNL is a bit more speculative in its direct application to second stability access. Experience with pellets on PBX and elsewhere suggests improved confinement as a result of a peaked density profile (PBX profiles typically were extremely flat). The pressure profile is also observed to be more peaked after the plasma reheats than before the injection of the pellet, thus modifying the MHD equilibrium as well. Finally, it serves as a primary means of centrally fueling diverted discharges, which have in the past exhibited low fueling efficiencies and very broad density profiles when fueled by gas puffing at the plasma edge.

More detailed discussion of these and other topics follows.

# HEATING SYSTEMS DEVELOPMENT

## Neutral-Beam-Injection System Upgrade

Extensive maintenance and upgrading of the PBX-M neutral-beam-injection system took place during tokamak modification activities. The goal of this work was to maximize beam heating performance by focusing on reliability, efficiency, physics capability, and safety. Some of what was done to improve the efficiency of operation and the physics capability is of general interest and is described below.

For efficiency of operation with only two operators and to achieve and maintain optimum beam performance at high powers and long-pulse lengths, a reliable and automatic computer control system is essential. For this reason the original computer system, which was based on a DEC PDP 11/34 with a CAMAC interface to the beam system, was replaced with a DEC MicroVAX II system including 142 Mbytes of disc storage and new CAMAC highway drivers. The applications software is also new, except for the basic automatic control logic which was translated from Fortran into C. The automatic control functions were expanded so that they now include complete automation of all timing and sequencing operations. This will allow efficient pulse width and pulse timing changes for optimizing plasma conditions during heating experiments. The new system will also allow the implementation of more advanced control functions.

Work to expand the injection options by developing long pulse, power modulation, and diagnostic capabilities is in progress. A principal requirement for PBX-M neutral-beam heating is to extend the injection pulse length from 300 msec to 500 msec. The original Poloidal Divertor Experiment (PDX) neutral-beam development at ORNL was directed mainly toward qualifying the ion sources for 300-msec operation. An attempt was made at ORNL, with one of the ion sources (No. 4), to achieve 50-keV, 500 msec, 1.5-MW $H^0$ pulses. During this work, it was found that the decel current increased precipitously at pulse lengths greater than 400 msec, and exceeded interlock levels for 50-keV, 80-A 0-msec pulses. Preliminary investigations determ that this increase in decel current with pulse length was attributable, in part, to electrons backstreaming into the ion source from excessive beam-induced outgassing in the neutralizer. The effect could be ameliorated somewhat by reducing the programmed gas input to the neutralizer. This kept the net gas load at the ion source nearly constant, despite the increased outgassing. Using this method, 50-keV, 500-msec, 1.5-MW $H^0$ pulses were achieved, but with still relatively high decel currents. However, the observed behavior under these conditions was not entirely consistent with the neutralizer outgassing hypothesis, and grid thermal loading and deformation, as suggested by computational evidents, were not eliminated as possible contributing factors.

At PPPL, towards the end of PBX beam operations, 500-msec-pulse length operation was investigated and achieved with each ion source separately, with 40-keV, 1-MW $D^0$ pulses. At this power level, it was found that the 500-msec-pulse length operation exhibited no rise in decel current, and it was not necessary to reduce the gas input to the neutralizer during the pulse. This difference in the behavior of the present injection system relative to the ORNL development test stand results with $H^0$ beams was possibly due to the lower power levels, the benefits of $D^0$ operation, and the conditioning that has occurred in the neutralizers as a result of many years of neutral-beam operation with the PDX and PBX tokamaks. These results demonstrated that operating with 500-msec-pulse lengths is possible with total injected powers of at least 4-MW of $D^0$, and that higher injected powers may be achievable. This will be tested when experimental operation is resumed.

In order to prepare for safe and reliable operation with 500-msec-pulse lengths, additional tasks specific to longer pulse operation were undertaken. These included installing additional beamline thermal sensors, as well as optical diagnostics to measure beam position and profiles. The optical diagnostics will allow beam alignment to be monitored at the input to the transition duct, in order to minimize beam-

induced outgassing and impurity generation. The same optical diagnostics will be used to measure beam profiles to optimize focusing of the injected beams. In addition, the new automatic timing control was configured to allow automatic switching from short conditioning pulses to longer injection pulses. This will minimize system duty during long-pulse operation, thereby reducing beam-induced erosion of beamline components and cyclic thermal stress in the electrical and mechanical subsystems.

In addition to long-pulse operation, the physics experimental options of the neutral-beam system were increased by providing the ability to modulate the beams every 50 msec during injection. This was accomplished using the automatic timing computer control system discussed above. Magnetic, spectroscopic, charge-exchange, and neutral diagnostic measurements, for example, will benefit from the ability to study background and relaxation effects during brief interruptions (e.g., 2 msec) in neutral-beam injection during high-power, high-temperature plasma conditions.

The neutral-beam system has, of course, been central to the high-beta experiments in PDX and PBX. With the improvements that have been made and those still to come, the neutral beams can be counted on to support the PBX-M experiment at the high level of reliability and sophistication that the experiment requires.

## Ion-Bernstein Wave Heating Experiments

In FY87, after termination of PLT, the IBWH experiment was moved to PBX-M. The main aim of IBWH in the PBX-M long-range research effort is to provide extra heating power and to modify the heating power profile in order for PBX-M plasmas to attain the region of second stability. In the case of heating off axis (where high-energy ions are not well confined), the localized bulk ion heating property of IBWH can be particularly useful.

The present plan for IBWH on PBX-M is to test antenna loading in FY88 and start IBWH experiments in earnest in FY89. A total power of 4 MW will be made available to this effort in a very cost effective way, by tapping into the TFTR ICRF power supplies. With this additional power (together with the neutral-beam heating power), the PBX-M auxiliary heating power will be increased to over 10 MW, which should greatly aid in pushing the plasma beta value well into the second stability regime. At the 4-MW power level, IBWH can actively control the heating profile of the plasma, which may be crucial for high-beta plasma stability. This power level should also be sufficient for IBWH alone to induce the H-mode, which would be relevant for the Compact Ignition Tokamak (CIT). Although somewhat more speculative, recent theoretical work suggests an interesting possibility for high-power IBWH to actively stabilize the ballooning and kink instabilities and thus provide an additional capability for reaching the second stability regime.[4]

On PLT, the application of more than 0.5 MW of IBWH power resulted in an improved particle confinement (as much as 300%) with an accompanying reduction of low-frequency turbulence in the plasma. The H-mode-like improved confinement property of IBWH offers an interesting prospect for the initial PBX-M ion-Bernstein wave heating experiments in FY89 where neutral-beam heating will be used to maximize the plasma beta. Since the plasma confinement during neutral-beam heating generally goes down with the heating power, any improvement in the confinement would be significant. Another important area of investigation for the early experiments is the identification of good heating regimes in PBX-M. Since the PBX-M experiment will span a wide range of magnetic field (8-12 kG for the high-beta regime and 16-20 kG for the high-poloidal-beta regime), various heating scenarios such as an H-minority, $n\Omega_D$, and $m\Omega_{3He}$ ($n$ = 2-5, $m$ = 2-4) regimes must be investigated.

In FY88 ion-Bernstein wave heating antenna loading measurements on PBX-M plasmas will be performed utilizing much of the PLT ion-Bernstein wave heating/ion-cyclotron radio-frequency (ICRF) hardware. To that end, a 1-MW PBX-M ion-Bernstein wave heating antenna was designed and has been largely fabricated for machine installation. This IBWH antenna, which extends in the toroidal direction and fits nicely in the midplane gap of the PBX-M stabilizing plates, will be used for rf coupling studies, and it is expected to provide important physics information for the 4-MW experiment planned for FY90. For example, it is important to check how well the IBWH antenna can couple power to a diverted discharge. During H-mode discharges, in particular, the rf plasma coupling can be significantly reduced due to a sharp density gradient created near the plasma edge. This has been observed for fast-wave ICRF antennas in the JET (Joint European Torus), ASDEX (Axially Symmetric Divertor Experiment), and JFTII-M devices. For IBWH, since the WKB condition is satisfied even for a very steep edge density gradient ($\partial n_e/\partial r \approx 4 \times 10^{13}$ cm$^{-4}$), the coupling can be expected to be reasonable even during the H-mode.

In preparation for these experiments, an IBWH ray tracing code was developed for the PBX-M configuration. In Fig. 3(a), the poloidal projection of the various IBWH rays (the power flow paths) released from the antenna is shown. The power flows approximately in a horizontal path, depositing the power mostly into the ions near the ion cyclotron resonance layer, in this case, $\omega = 2\Omega_{3He}$. As shown in Fig. 3(b), localization of heating is excellent, which is very important for control of the heating profile. The density profile used in this calculation is an H-mode-like profile with a steep edge density gradient.

# DIAGNOSTICS DEVELOPMENT

A moderate level of diagnostic planning and development took place during the past year to prepare for measurements of the high-beta plasmas

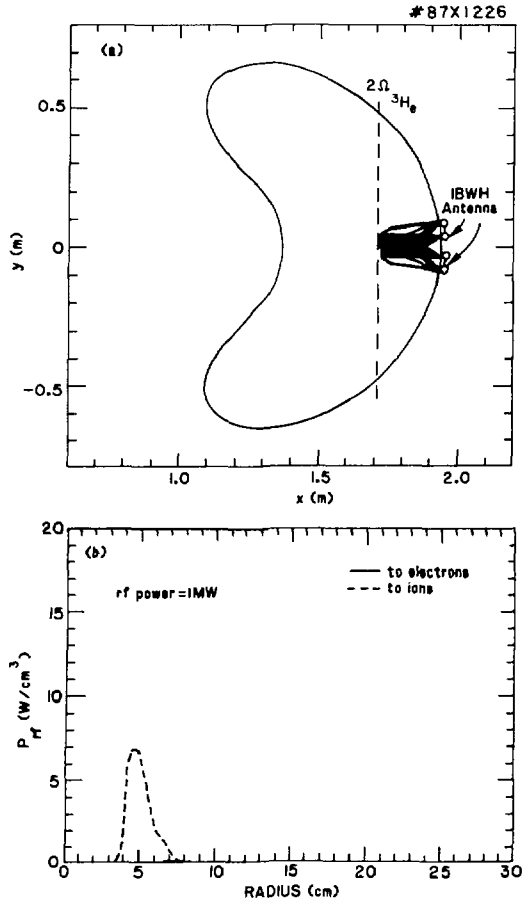


*Figure 3. (a) The 2Ω(³He) ion-Bernstein wave heating (IBWH) configuration. Lines are IBWH ray trajectories for $n_{//} = \pm 1, \pm 3, \pm 5$ released from the antenna current maxima. N(D):N(³He) = 0.95:0.05, f = 30 MHz, $\bar{n}_e \simeq 5.0 \times 10^{13}$ cm$^{-3}$, $T_T(0) = 1.5$ T and $T_e(0) \approx T_i(0) \approx 2.0$ keV. (b) Corresponding power deposition profiles. $P_{rf} = 1.0$ MW.*

expected in PBX-M. The goal of the diagnostic efforts for PBX-M is to provide sufficiently detailed measurements to guide the approach to the second stability regime while minimizing the size of the diagnostic set. In pursuit of that goal, most standard plasma parameters will be measured with a single diagnostic; diagnostic redundancy will be provided only for those parameters which are crucial to understanding the plasma behavior and for which reliable techniques have not been readily available in the past. An overview of the diagnostics planned for the first year of operation on PBX-M is shown in Fig. 4. The new diagnostic systems developed for the PBX-M high-beta experiments are discussed below.

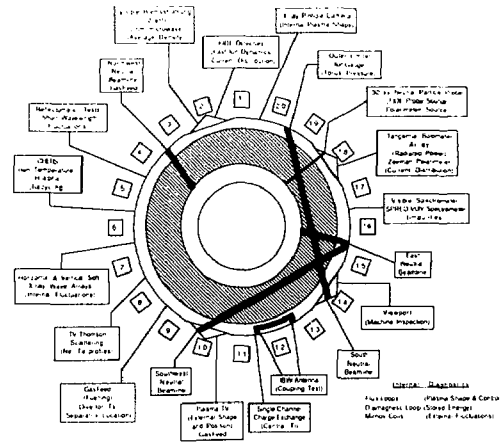

*Figure 4. Plan view of the PBX-M tokamak facility with the location and primary purpose of each major diagnostic system on the device for the first year of experimental operation. (88X3046)*

## High-Beta, Equilibrium, and Confinement

The study of high-beta stability in shaped plasmas requires a detailed knowledge of the equilibrium plasma for any comparison to theoretical expectations. In practice, the radial profiles of the plasma pressure, both thermal and fast ion, the plasma current density, and the shape of the exterior and internal flux surfaces are all needed. The electron temperature and density profiles will be measured by the multipoint TV Thomson scattering system, while the ion temperature profiles will be provided by charge-exchange recombination spectroscopy measurements. Standard spectroscopic and bolometric measurements will allow impurity densities to be evaluated. As with PBX, knowledge of the fast-ion distribution in the plasma will be derived from comparisons of beam-particle orbit calculations combined with spatially and angularly resolved particle charge-exchange measurements. All of these capabilities are available either through moderate modifications of the old PBX diagnostic systems or emulation of technology developed for TFTR diagnostics.

The measurements of the plasma shape rely on magnetics and an equilibrium code to analyze the external plasma surface. The measurement of the internal plasma shape will be performed by a tangentially viewing soft X-ray pinhole camera. The prototype of this diagnostic was tested in the final months of PBX operation, and proved capable of measuring internal plasma shape,[5] which in turn can be used to infer the central current distribution. During the past year, a completely new pinhole camera was

designed and fabricated for PBX-M, as was an automated data acquisition system for the very high data flows from the video system. The camera itself consists of a scintillator at the focal plane of a pinhole camera, which is fiber optically coupled to an intensified high-speed ($\Delta t$ = 3 msec) video camera. Data acquisition is performed on a standalone image-processing system, and data archiving takes place on an optical disk video recorder (Fig. 5). In support of this camera development, a series of modeling equilibrium calculations were performed for PBX and PBX-M plasmas to show that the central safety factor q(0) may be inferred from accurate measurements of the elongation of the inner plasma flux surfaces.

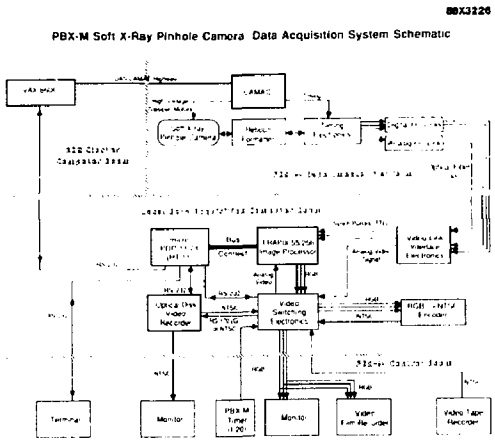


*Figure 5. Block diagram of the control and data acquisition system for the X-ray pinhole camera diagnostic on PBX-M. All video data (up to 4 mbytes per shot) is acquired and archived via the standalone system controlled by the local micro PDP 11/73 computer. Permanent archival of data is on the local optical disk video recorder.*

## Current Profile Measurements

Since the plasma high-beta equilibrium depends sensitively on the current distribution in the plasma, several diagnostic techniques were considered for providing the plasma current density, j(R,t), on PBX-M. Following an international workshop on current density profile measurements in tokamaks held this past year at PPPL, three candidates for current density profile measurements were chosen for installation on PBX-M. The first, already mentioned above, is based on measurements of the inner plasma flux surface shape (inferred from soft X-ray emissions from the plasma core) and in principle allows a direct determination of the plasma current density distribution. In practice, combining these shape measurements with external magnetic measurements to determine a plasma equilibrium should provide a reasonable determination of the central plasma current density.

A second current density profile measurement planned for PBX-M employs Zeeman polarimetry of a helium diagnostic beam injected into the plasma to measure the local magnetic field orientation, and hence the local rotational transform. The theory behind this measurement has been extensively studied and developed by staff at Jaycor Corporation of San Diego, California,[6] and a diagnostic system for such measurements will be installed and operated by Jaycor staff on PBX-M in 1988. The 30-keV diagnostic neutral beam (DNB) already on PBX will be operated with helium to provide the helium neutral beam. Initial evaluation of obtainable line intensities and fabrication of the polarimeter optics will take place in 1988.

Finally, a major diagnostic development effort has been initiated on PBX-M to provide current profile measurements by determining the shift of orbits of fast ions injecting into the plasma by a highly collimated diagnostic neutral beam.

This technique, used for the Fast Ion Diagnostic Experiment (FIDE), and demonstrated on two previous tokamak experiments,[7,8] avoids most of the difficulties of other methods used in determining j(R). Some of these methods are complex, exhibit an unfavorable signal-to-noise ratio, cannot be applied conveniently to noncircular plasmas, or involve relatively large uncertainties from deconvoluting the plasma current density from the measured quantities. The previous work on the FIDE technique has shown that radial profiles of the rotational transform, q(R), can be measured directly by detecting the orbital displacement of injected circulating fast ions from magnetic surfaces (Fig. 6). A tightly collimated neutral probe beam (NPB) can be aimed to inject tangent to a magnetic surface at a chosen plasma minor radius on the midplane, and the resultant ion orbit shifts, due to conservation of canonical toroidal angular momentum, can be determined with a multi-sightline charge-exchange analyzer. In addition, since the NPB has three energy components, each

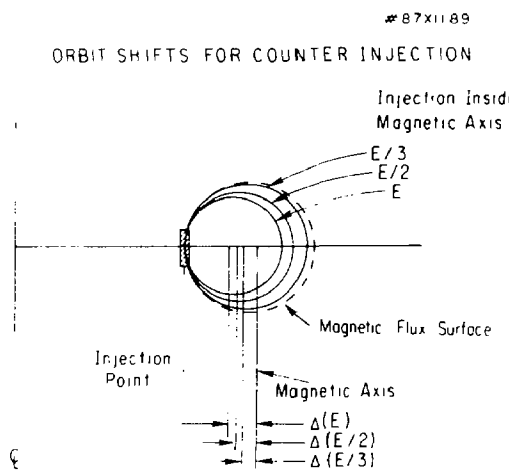


*Figure 6. Orbits for particles with $V_{\parallel}/V \approx 1$ born inside the magnetic axis in major radius at three diagnostic neutral-beam energies.*

injection pulse at a particular major radius yields three independent measurements and eliminates the need to know the location of the magnetic axis. Using these three NPB energy components, the measured fast-ion orbital shifts yield a direct measurement of flux surface inner and outer edges, the radial position of the magnetic axis and magnetic flux profiles, and hence the current density profile and the q profiles for circular and near-circular flux surfaces.

In the case of highly noncircular plasmas, the generalized definition of the rotational transform, q(R), must be employed. Since this involves a line-integral of the ratio of the toroidal and poloidal fields taken over the applicable flux surface, both local and line-averaged q measurement methods require a detailed knowledge of the shape of the flux surface in order to derive q from their measured signals. However, the relative simplicity, directness, and precision of the FIDE method should allow it to be used in conjunction with magnetic diagnostic loop data to yield a measurement of radial q profiles, or relative changes in central q, for highly indented, highly loped, or rapidly changing plasmas, and to place rigorous constraints on the analysis of plasma conditions presently derived solely from plasma edge magnetic measurements.

Recently, an extensive reanalysis of the experimental conditions and uncertainties in earlier circular plasma PDX measurements has been undertaken, with a view toward upgrading this technique for application to PBX-M plasmas. Fokker-Planck simulations of the observed NPB fast-ion spectra were performed and used to simulate the expected NPB signals for dense [$n_e(0) = 1.0 \times 10^{14}$ cm$^3$] PBX-M plasmas heated with 6 MW of 50-keV $D^0$. The results showed that for these PBX-M plasma conditions, the expected signal-to-noise ratio, using the previous methodology, was about 4:1 at 23 keV (comparable to the signal-to-noise ratio at 30-keV in the PDX q measurements), and 11:1 at 35 keV. There was no observable background predicted at 70 keV. These results supported empirical conclusions from the PDX experiments regarding the need for higher NPB injection energies in order to avoid the limitations described above.

Various experimental uncertainties encountered in the previous work have been analyzed and include systematic effects involving background corrections, energy bandwidth, stray fields, finite spatial resolution, and toroidal field uncertainty. This work and the analyses described above have suggested methods for reducing the relative and absolute experimental uncertainties in similar measurements to be performed on PBX-M. For example, the use of an 80-keV NPB will allow the study of highly indented, neutral-beam-heated, high-temperature plasmas by providing injected probe ions with energies well above those of the fast-ion distribution from the Maxwellian distribution and the heating beams. This will permit the detection, during high-power neutral-beam heating, of much stronger signals with only a few amperes of injected beam current and yield larger ion orbit shifts due to the increased beam momentum. Additional improvements in experimental precision should accrue from improvements in alignment, spatial resolution, background correction, and magnetic shielding. In general, the results of this work indicate that with higher NPB energies, an experimental precision of about 20% should be achievable for measurements of $q \sim 1$ in very dense high-power neutral-beam-heated plasmas, and that with the improvements discussed above, experimental precisions of about 10% may be possible. In addition, actual operating experience with an improved NPB system may suggest additional ways to further reduce residual experimental uncertainties.

Based upon this extensive analysis and given the crucial need to measure j(R) in high-beta plasmas in PBX-M, a contract was let to Culham Laboratory in Great Britain to construct an 80-keV, 2.7-A neutral probe beam source and beamline for installation on PBX-M in FY89. Until that time, the older 30-keV NPB from PDX will be employed on PBX-M to pursue an upgrading of the detection and data analysis techniques for these measurements.

## Stability and Fluctuations

Since the experimental goal of the PBX-M program in 1988 is the careful study of the effect of the close-fitting conductive shell on the high-beta disruptions commonly observed near the first stability limit, the initial emphasis in the fluctuations diagnostic program is on the ability to diagnose low-frequency, long-wavelength perturbations in the plasma. In addition to the usual extensive arrays of Mirnov coils to measure the perturbed magnetic fields at the plasma periphery and a set of two one-dimensional diode soft X-ray wave detectors, two further measurement techniques will be applied to PBX-M in the first year of operation. First, a complete set of small Rogowski loops were installed on the current return buswork which electrically connect the upper and lower passive plates. These loops will provide a direct measurement of the current induced in the outermost passive plates, which in turn will provide crucial information on the effectiveness of the plates in stabilizing long-wavelength modes. Second, a maximum entropy reconstruction algorithm has been formulated to allow the plasma images from the soft X-ray diode arrays to be inverted to provide a measurement of the distorted inner plasma flux surfaces in the presence of instabilities. A unique feature of the PBX-M approach is the use of the low time-resolution soft X-ray images from the tangentially viewing pinhole camera system to provide a time-averaged first-order solution to the inversion of the two diode fan arrays. Given this time-averaged emission profile, the higher-frequency diode array images are used to produce a perturbed solution to provide a complete high time-resolution image of the perturbed flux surfaces (Fig. 7). This use of X-ray images from both the relatively slow tangentially viewing pinhole camera and the two fast-time response X-ray wave arrays allows a reasonable tomographic reconstruction of the perturbations

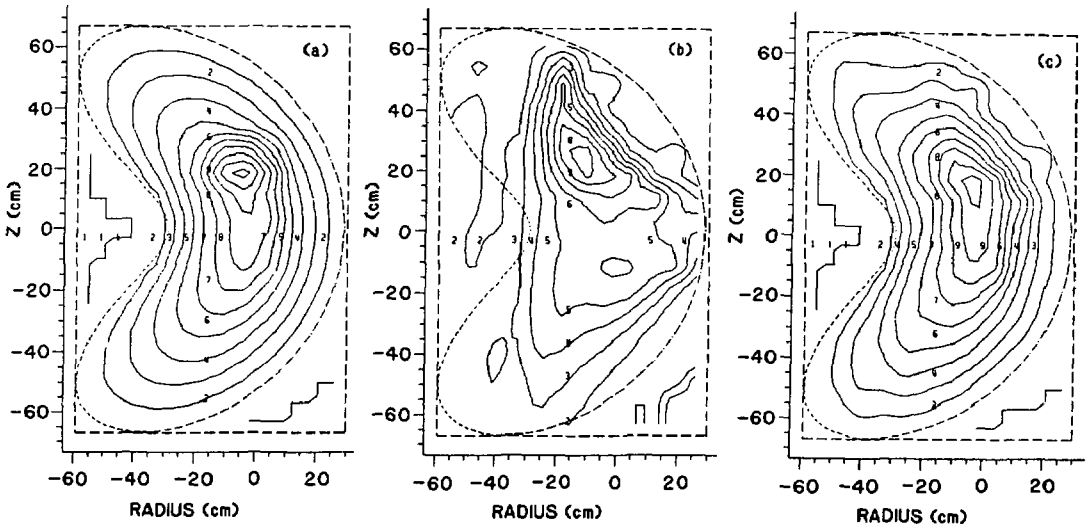


*Figure 7. Effect of using the low-time resolution image of the plasma obtained with the tangentially viewing X-ray camera as a zero-order solution to the tomographic inversion of the images from the two soft X-ray diode arrays on PBX-M. (a) Assumed emission profiles containing a bean-shaped plasma with a local hot spot at R = 5 cm and Z = 20 cm; (b) Reconstructed image of the bean-shaped plasma distribution containing the hot spot using two diode arrays with no prior constraints; (c) Reconstructed image of the bean-shaped plasma distribution containing the hot spot using two diode arrays with a background image from the pinhole camera used as a prior constraint on the reconstruction.*

without requiring several more soft X-ray diode arrays to simultaneously view the plasma.

Efforts to define the diagnostics for high-frequency, short-wavelength perturbations were started during FY87. Preliminary indications are that a densely paced set of Mirnov coils on the outer plasma midplane, a multichannel microwave reflectometer system, and detailed tomography using soft X-ray diodes with access to the outer plasma region are all reasonable candidates for implementation on PBX-M in the future as ballooning mode diagnostics. Further studies will continue through 1988 with the goal of installing these or other ballooning mode diagnostics in 1989.

## H-Mode, Divertor, and Plasma Wall Interactions

The divertor on PBX-M has a closed geometry, compared to the open divertor on PBX. That is, mechanical baffles are used to restrict the backflow of recycled neutral particles from the divertor region so that these particles pass through scrape-off plasma before reentering the main vacuum chamber. Since the closure of the divertor region is expected to allow routine operation in the high-confinement (H-mode) regime observed on most divertor machines, optimization of plasma performance with the new closed divertor on PBX-M is a high priority in the PBX-M program. A minimal diagnostic set of $H_\alpha$ monitors, bolometers, and a divertor microwave interferometer is planned to allow monitoring of the divertor plasma density and recycling. Beyond that, the major concern for the PBX-M program in the first year is the exact location and behavior of the plasma separatrix in the divertor region as the main plasma body changes shape and beta.

Earlier studies on PBX showed that observations of the divertor plasma region near the separatrix X-point via a spectrally filtered video camera provide an economical means of observing the plasma X-point during operation. The technique relies on the sharp gradients in the electron temperature near the separatrix, which in turn results in sharp spatial gradients in the density and emissivity of low ionization states of hydrogen, carbon, and oxygen. Thus, application of simple image processing to pictures of the edge plasma region can produce a measure of the location of the plasma edge, especially near the critical X-point region. This technique will be routinely applied on PBX-M to allow shot-to-shot monitoring of the separatrix.

## PROFILE MODIFICATION CAPABILITIES ON PBX-M

Given the central role of plasma current and pressure profiles in gaining access to the second stability regime, two other major tools are planned for PBX-M. As mentioned earlier, the high-power IBWH system may provide a means of directly controlling the ion-heating profile. While neutral-

beam injection, transient plasma current ramps, H-mode-induced profile changes, and the possibility of significant bootstrap currents all provide some means, usually indirect, of altering the current profile and hence q(0), noninductive current drive via lower-hybrid rf heating provides a possible means of controlling j(r) and q(0) in a quasisteady state manner. Likewise, frozen deuterium pellet injection provides a potential means of altering plasma fueling and density profiles in a controlled manner. Since the NBI and IBWH systems have already been described, we discuss here the lower-hybrid current-drive (LHCD) and pellet injection systems planned to aid in PBX-M profile control experiments. Eventually, the simultaneous application of all, or a significant subset, of these profile modification techniques should pave the path towards a viable design concept of a fusion reactor based on second stability operation.

## Lower-Hybrid Current-Drive for PBX-M

During FY87, preparations for a lower-hybrid current-drive experiment on PBX-M with a specific goal to modify the current density profile were started. In order to reach the second stability regime in PBX-M, it is necessary to obtain a current density profile which is somewhat broader than the one that can be achieved with the ohmic system alone in a quasisteady mode. In fact, broader profiles were obtained in PBX by using fast current ramping, but this limited the duration of the stable discharge. Despite the proven ability of lower-hybrid (LH) waves to drive current and maintain it, this experiment will be largely novel in that, instead of stressing the accessibility of the waves into the core of the plasma, it will be necessary to trap them in the outer region of the plasma and dump them into fast electrons. Ray tracing calculations show that this "trapping" can be achieved by launching an appropriate $n_{\parallel}$ spectrum, where $n_{\parallel}$ is the parallel index of refractions, and is materially aided by the relatively high density and low magnetic field in the preferred regime of operation. An important question remaining is the efficiency that can be achieved.

Because of the PBX-M plasma parameters (e.g., low $B_T$, high $n_e$), we will use a higher frequency than was used for the PLT experiment. As mentioned earlier, half (2 MW) of the MIT 4.6-GHz lower-hybrid system was moved to PPPL for this effort. Budget constraints have pushed significant lower-hybrid current-drive experiments on PBX-M to late FY89, when a 1-MW test will be performed, followed quickly thereafter by an upgrade to 2 MW total power.

Some simple calculations which include Fisch's efficiency normalized to the PLT results, the confinement time of fast electrons, and the electron thermal conductivity as measured for PLT and calculated for PBX in L-mode, show that it should be possible to drive up to 150 kA near the edge of the plasma with the available power of 2 MW. This is shown in Fig. 8, where the shaded areas are the

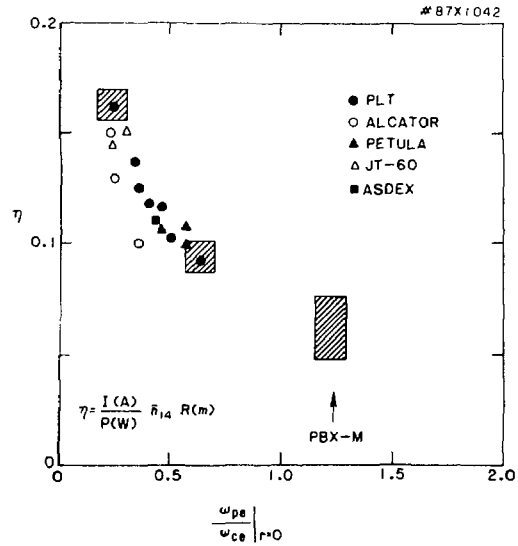


*Figure 8. Current drive figure of merit $\eta = I(A)/(W)\ \bar{n}(10^{14}\ cm^{-3})\ R(m)$ versus $\omega_{pe}/\omega_{ce}$ calculated in the center of the discharge.*

results of the calculation normalized to the highest efficiency in PLT. In Fig. 8, the data points are for steady-state current drive in various machines. To launch the waves, it is planned to use two couplers with 32 waveguides each, arranged in two banks of 16 each. This feature combined with the requisite power splitters and phase shifters will give the needed control of the $n_{\parallel}$ spectrum.

## Pellet Injection in PBX-M

As described in earlier sections, strong bean shaping in PBX was intended to enhance the MHD stability that is naturally strengthened as a consequence of high $\beta_p$. Both strong shaping and high $\beta_p$ are needed elements in finding a path to the second stability regime. The MHD stability depends mainly on properties of the current profile in relation to those of the pressure profile. These profiles in high-$\beta_p$ discharges are intertwined through, for example, currents driven by the pressure gradient. In the absence of a direct means of controlling the profiles in PBX, strong shaping was achievable only at modest $\beta_p$, and high $\beta_p$ was obtained only at the expense of shaping. A different combination of tools may thus be needed in different plasma regimes: direct means to modify the current profile, such as LHCD, could be primary tools in the high-$\beta_p$ regime, while means to raise $\beta_p$, such as additional heating by IBWH, could be important in the strongly shaped plasma regime. Indirect current profile modification, such as through altered distributions of the bootstrap and beam-driven currents, could also be important. In this respect, roles that could be played by pellet injection, either used alone or in combination with other tools, would also

vary in different regimes. Another element needed to reach the second stability regime is good confinement, which allows production of high-$\beta_p$ plasmas with limited heating power.

Pellet injection can produce large changes in plasma density and its profile, and is a tool useful in its own right and in combination with other available tools to PBX-M in its effort to reach the second stability regime.

Discharges that would take PBX-M plasmas into the second stability regime are likely to be H-mode diverter discharges heated mainly by neutral-beam injection (NBI) and perhaps by ion-Bernstein waves (IBW). Needed pressure and current profile changes may be accomplished directly by localized IBW heating and lower-hybrid current drive, respectively. Pellet injection, used alone or in combination with NBI, IBWH or LHCD, could help raise $\beta_p$, change the MHD stability, enhancement, and confinement, and fuel divertor discharges without degrading the confinement. The plasma environment into which pellets are injected is, however, quite hostile to pellet penetration requirements: high edge $T_e$ of an H-mode discharge, fast ions generated by NBI, and suprathermal electrons produced by LHCD are all efficient agents to ablate pellets before they reach the plasma interior. Thus, it is necessary to devise clever experimental procedures to take advantage of synergic effects, if any, of pellet injection and other tools available to PBX-M.

Strong experimental evidence obtained in many tokamaks indicates that a peaked $n_e$ profile leads to better confinnement than a flat profile. Possible connections between the density profile and confinement are theoretically predicted based upon the so-called $\eta_i$ mode. Beam-heated, edge-fueled discharges in PBX invariably had a flat, nearly trapezoidal $\eta_e$ profile, as shown in Fig. 9. The profile would become peaked if the discharge is fueled from the core by a pellet, rather than from the edge by gas puffing, provided that the pellet penetrates into the plasma center. Under conditions in which the q = 1 surface exists within the plasma, pellets may only need to reach the surface inside which large transport associated with the sawtooth is expected to carry

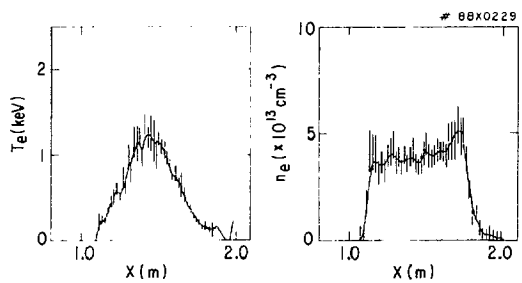


*Figure 9. Temperature (left) and density (right) profiles of a typical PBX plasma heated by neutral-beam injection. The density profile is very flat, nearly trapezoidal, and is suspected to be a cause for poor confinement. Pellet injection is able to produce a more peaked profile.*

the particles into the center. This will not be the case if the current profile is broadened sufficiently by LHCD to raise q above unity everywhere inside the plasma. Pellet penetration will be addressed later in this section.

The confinement quality of the H-mode is an important issue for PBX-M because the second stability regime cannot be accessed with L-mode confinement. Inclusion of closed divertor chambers in the PBX-M design, was in fact motivated from such considerations. It is generally known that excessive gas puffing, especially through the main vacuum chamber, compromises good confinement. In the face of a poor fueling efficiency in divertor discharges, strong gas puffing is, however, often required to build up the density before NBI heating. Strong gas puffing is also often needed to prevent disruptions in H-mode plasmas. The ability of a pellet to fuel the discharge from the core offers a solution to the density build-up problem in divertor discharges. Core fueling may also help prevent disruptions in H-mode discharges by keeping the impurity concentration in the plasma interior down through dilution by the working gas element.

Pellet injection can radically alter the density profile, through which both the pressure and current profiles could also be modified. A direct way in which pellet injection alters the current distribution is by lowering $T_e$ in the plasma interior, thus forcing $q_0$ to rise above unity. Many effects of pellets on the MHD stability, however, appear to come about in more indirect and subtle ways. There is much experimental evidence that pellet injection can change the MHD stability properties, and these may possibly involve altered distributions of bootstrap and beam-driven currents. In TFTR, sawteeth were suppressed over a period following pellet injection into a sawtoothing discharge. In other experiments such as PDX and Alcator-C, a period of generally altered MHD activity was observed following pellet injection. Future experimental results will show whether the changed MHD properties are beneficial to achieving the second regime of stability. The plasma response to pellet injection is initially adiabatic: the density rises and temperature falls in such a way to conserve the stored energy. The density relaxes toward the preinjection level in a characteristic time comparable to the particle confinement time. During this period the plasma reheats under the action of ohmic and supplementally heating at a rate generally faster than the density decay rate. The disparity in the time scales can be exploited to produce a plasma with a higher stored energy than in the absence of pellet injection. Repeated injection and reheating leads to a higher beta plasma on a time-averaged basis. In this regard, experimentally observed enhancement of the particle confinement by IBWH suggests a possible synergic effect with pellet injection.

Finally the issue of pellet penetration is addressed. The rate of ablation increases and hence the penetration depth decreases significantly as $T_e$ rises. Fast ions and suprathermal electrons also ablate the pellet rapidly. High density, high temperature, NBI-

heated H-mode divertor discharges driven by LHCD would represent a hostile environment for pellets. Even before their entry into the main body of the plasma, injected pellets would encounter divertor scrape-off plasma and fast ions making excursions outside the main plasma. They would be ablated by a high-$T_e$, high-$n_e$ plasma near the plasma edge, which is characteristic of an H-mode discharge, and would continue to encounter a high-$T_e$ dense plasma as well as fast ions and suprathermal electrons in the interior of the plasma. In this respect, IBWH may offer a friendlier environment to pellets because of its bulk heating properties without producing a significant amount of energetic ions or electrons. The generally severe environment of non-ohmically heated discharges driven by noninductive means is ameliorated to some extent in PBX-M because the pellet passes through the smallest cross-sectional dimension of the plasma (i.e., in the horizontal midplane from the outboard side). In low-q discharges, the distance from the plasma edge to the q = 1 surface is also expected to be a small fraction (say, one half) of the midplane half-width. A capability to modulate NBI, introduced in the PBX-M system, should also help in reducing beam-induced ablation.

Pellet penetration was studied using the Houlberg-Attenberger code developed at ORNL and a PBX-M model plasma with H-mode like profiles. Plasmas with IBWH or LHCD were not considered. The fixed-thickness neutral shield and collisionless self-limiting model were chosen in the computations. Five sets of plasma parameters were considered: ohmically heated plasma and four beam-heated plasma conditions with a successively larger beam power incremented by 1.5 MW. The $T_e$ ranged from 1 keV for the ohmic plasma to 5 keV for the 6-MW beam-heated plasma. The central $n_e$ was assumed to be $5 \times 10^{13}$ cm$^{-3}$ and the ion temperature, which is less important in ablation, was taken to be 4 keV for all cases. A total of five pellets of different sizes was considered. The smallest pellet was a spherical pellet of diameter 1.3 mm containing $0.7 \times 10^{20}$ deutrons and would cause a density rise of $16 \times 10^{13}$ cm$^{-3}$ in PBX-M. The pellet speed was taken to be 1.5 km per sec. The results of the pellet penetration calculations are summarized in matrix form in Fig. 10. As can be seen from the figure, the largest two pellets must be employed in the ohmic stage if central penetration is required. The requirements are relaxed considerably if only the q = 1 penetration is needed in low-q discharges.

The deposition pattern of the pellet atoms along its trajectory in the midplane was studied with the TRANSP code, using an ablation model which is simpler than the Houlberg-Attenberger code. The results are shown in Fig. 11(a) and (b) for two different pellet speeds, 1.5 km per sec and 0.75 km per sec, respectively. Clearly, the faster pellet speed is required to deposit the bulk of the atoms in the plasma center.

An eight-barreled pipe gun injector is being constructed by the Oak Ridge National Laboratory for use in the PBX-M Project. It is capable of injecting,

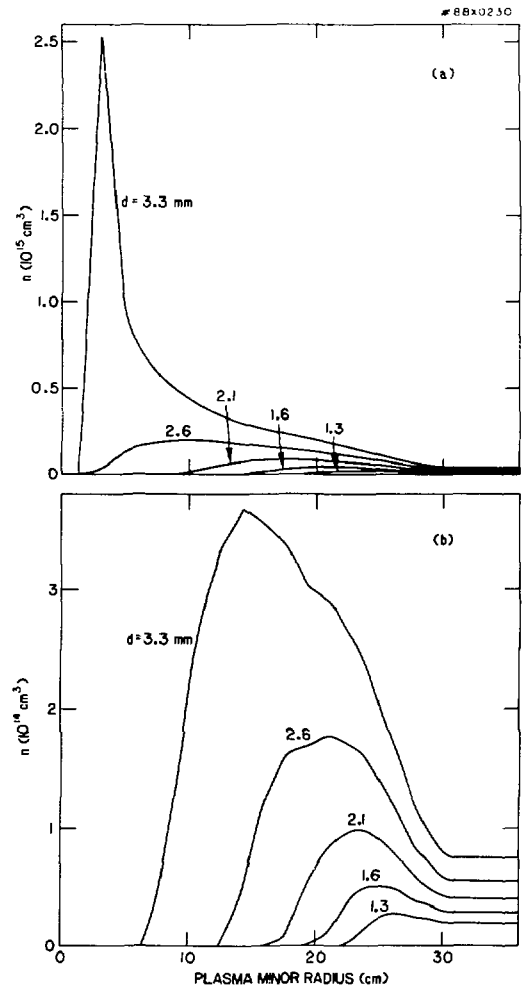


*Figure 10. The rows of the above matrix refer to five different pellet sizes, representing progressively larger sizes from top to bottom. The columns refer to five different plasma parameter combinations, representing progressively more severe sets of conditions from left to right. Each circle in the matrix represents a pellet and the diameter of the circle is proportional to the pellet diameter. The number in percent underneath each circle represents the fraction of the midplane half-width penetrated by the pellet before complete ablation. The circles are separated into three groups by a solid line and a broken line. Circles to the left of the solid line represent pellet penetrated to the plasma center, and those to the left of the broken line penetrated to the q = 1 surface (here, assumed to be at the half way to the plasma center).*

at arbitrary intervals within the course of a PBX-M discharge, a combination of up to eight pellets of varying size, roughly covering the range discussed in the above calculations. The expected speed is 1.5 km per sec for deuterium pellets. The injector

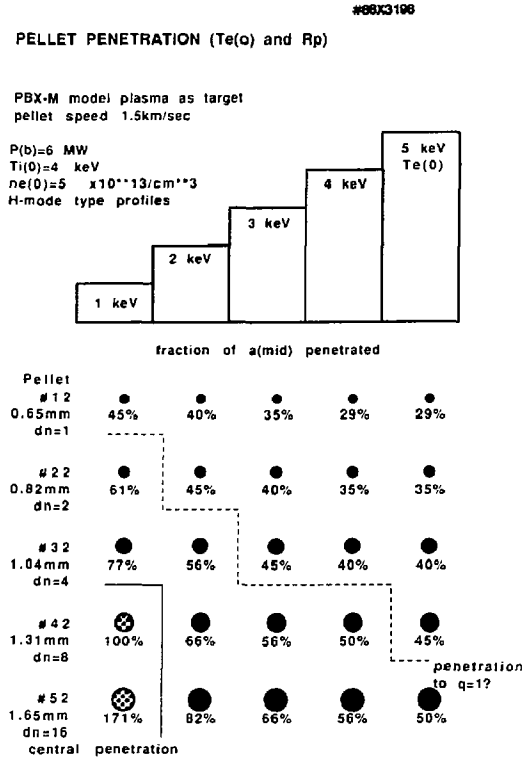


*Figure 11. Particle deposition for pellet injection with pellet speeds of (a) 1.5 km/sec and (b) 0.75 km/sec. The vertical axis of each figure is the number density of pellet atoms deposited at a point along its trajectory after they are distributed on the pertinent flux surface. The horizontal axis is the distance from the center of the plasma. The half-width is 36 cm.*

will be used alone or in various combinations with other tools to search for accessible paths to the second stability regime.

## References


[1]Princeton University Plasma Physics Laboratory Annual Report PPPL-Q-44 (October 1, 1985-September 30, 1986) *48-57.*

[2]*Ibid*, 104-121.

[3]*Ibid*, 74-85.

[4]D.A. D'Ippolito, J.R. Myra, and G.L. Francis, "RF Stabilization of Ballooning Modes in Tokamaks," Phys. Rev. Lett. *58* (1987) 2216.

[5]R.J. Fonck, M. Reusch, K.P. Jaehnig, R. Huls . and P. Roney, "Soft X-Ray Imaging System for Meas . ment of Noncircular Tokamak Plasmas," in *Proceedings of SPIE—The International Society for Optical Engineering*, Vol. *691*, SPIE, Bellingham, Washington, 21-22 August 1986, 111.

[6]F.M. Levinton, "Plasma Diagnostics using Injected Neutral Helium Beam," Rev. Sci. Instrum. *57* (1986) 1834.

[7]R.J. Goldston, *et al.*, "Radially Resolved Measurements of 'q' on the Adiabatic Toroidal Compressor Tokamak," in Phys. Fluids *21* (1978) 2346.

[8]D.D. Meyerhofer, *et al.*, "Measurement of Current Penetration During PDX Discharge Start-up," Nucl. Fusion *25* (1985) 321.

# S-1 SPHEROMAK

The spheromak is a toroidal magnetic confinement configuration for plasmas of the "compact toroid" type. The toroidal field in the plasma is sustained entirely by poloidal plasma currents, eliminating the need for coils that link the plasma. This topology allows for a simply connected first wall and blanket and also allows for translation so that the plasma can be created in one place and then moved to a separate burn region. In addition, adiabatic compression can be conveniently applied to the spheromak. The very low aspect ratio of the spheromak permits a small volume for a given characteristic confinement scale length, which makes possible a small-sized reactor core. The objectives of the S-1 experiment are to investigate the formation, equilibrium, stability, and confinement characteristics of hot plasmas; the scaling of confinement quality with various parameters; and the physics of sustainment of spheromak plasmas. Spheromak plasmas produced in the S-1 device have major radii in the range 0.4 to 0.65 m and minor radii of 0.25 to 0.45 m.

One interesting feature which distinguishes spheromak plasmas from, for example, tokamak plasmas is the strong tendency to self-adjust, or "relax," to a "Taylor state." Taylor proposed that a force-free ($j = \mu B$) plasma in which the resistivity is small but finite will relax with the aid of some type of turbulence to a minimum-energy state through reconnection of field lines, the only constraint being the conservation of global magnetic helicity. (Helicity can be thought of as the linkage of magnetic field lines.) This relaxation is viewed as a convenient phenomenon to both access stable equilibria (e.g., spheromak formation) and maintain stable equilibria against diffusive forces.

The main features distinguishing S-1 from other spheromak schemes are (1) the plasma formation technique, which is based on an inductive transfer of toroidal and poloidal magnetic flux from a toroidal "flux core" to the plasma, and (2) the stabilization of the plasma against dangerous rigid-body tilt and shift instabilities by use of loose-fitting conductors and coils.

## SUMMARY

The potential of the spheromak magnetic configuration as the core of a fusion reactor depends in part on its basic energy and particle confinement properties. Assessment of the confinement and its scaling needs to be done in a parameter regime in which the relevant transport mechanisms are active. One important requirement is high temperature. Significant progress has been made in improving plasma parameters over the past several years. Recently, the plasma parameters have been improved to the extent that a preliminary assessment of confinement scaling is possible.[1,2] Operations into regimes of high current and high current density in S-1 has shown promising results for spheromaks in comparison to other toroidal magnetic confinement schemes. In particular, electron plasma pressure $n_eT_e$ is found to scale as $j^2$, indicating constant beta ($\beta$) scaling similar to Reversed-Field Pinch (RFP) devices. This scaling, in part, motivates the study of higher-current spheromak plasmas.

Since MHD activity can in some cases influence the obtainable parameters and confinement, research has emphasized, among other things, identifying, understanding and controlling the MHD instabilities in the experiments and assessing their impact on confinement.[3-5] Relaxation itself occurs in conjunction with instabilities and fluctuations, which in turn can affect confinement. The relaxation event sometimes observed during the decay phase has been characterized in detail. The evolution of a decaying spheromak which exhibits these relaxation events displays many similarities with the numerical simulation, using the three-dimensional (3-D) resistive MHD equations, of a decaying spheromak of moderate magnetic Reynolds number S [A.G. Sgro *et al.*, Phys. of Fluids *30* (1987) 3219]. Comparison of the simulation with experimental observations has afforded an opportunity to better understand this relaxation process: It appears that transport modifies the basic Taylor equilibrium during the decaying portion of a spheromak lifetime so that the plasma evolves to one unstable to low-toroidal number (n=2) ideal MHD modes. This 3-D equilibrium in turn becomes unstable to a reconnection event which returns the configuration to a Taylor state. An instability such as this has important consequences to the transport as it may sometimes destroy good confinement, as has been demonstrated.

The S-1 device was operated intensively for much of the year (October 1986 to July 1987) with the newly installed (August 1986) upgraded flux core. The new core was more reliable than the original one; more "research-grade" discharges were fired during this year than in all previous years combined. Also it could operate at higher coil currents than the original core and, hence, allow higher plasma currents.

Concurrent with the S-1 operation, compression coils (Fig. 1) were being designed and fabricated. Compression of the spheromak plasma is a conve-

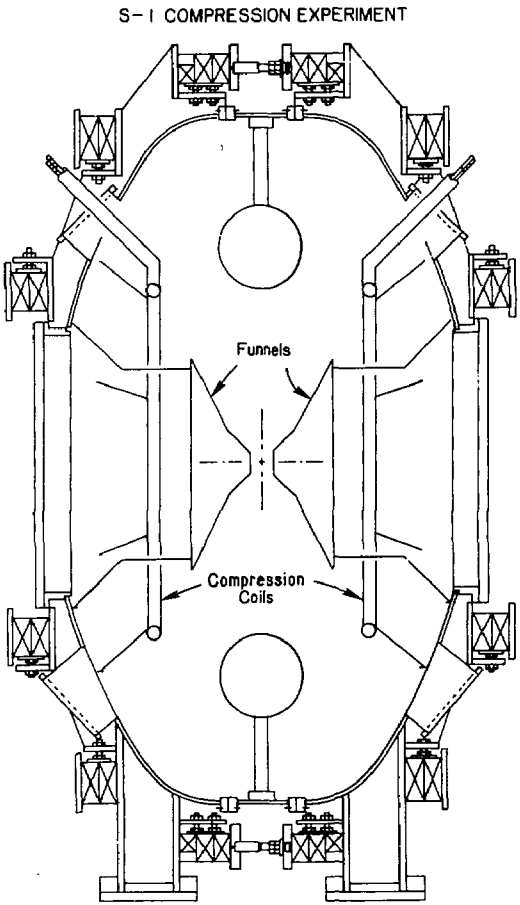


*Figure 1. Diagram of S-1 device showing funnel-shaped stabilizers and compression coils.*

nient method to obtain high current density discharges, thus improving the ohmic heating density and the possibility of increasing the temperature.[6,7] Self-similar compression would increase the current density without forcing relaxation phenomena to occur which might possibly degrade parameters and confinement. High compression ratios are possible in these compact toroids in contrast to other magnetic confinement configurations (e.g., tokamaks, RFP's). The S-1 operation was halted during the July to September period for installation and testing of a compression coil system which would allow a compression in major radius of $R/R_0 = 2$. [The compression coils were originally the pulsed equilibrium field coils designed for use with the poloidal flux transformer ohmic heating system proposed for S-1]. The plasma will be stabilized against n=1, and higher n modes, by use of passive conducting "funnel-shaped" plates (Fig. 1). Physics results on compression will be forthcoming in the beginning of FY88.

# EVOLUTION OF A DECAYING SPHEROMAK

A relation between transport and relaxation events in S-1 has recently been demonstrated.[3,4] More generally, a consistent picture has been unfolding about the evolution of a decaying spheromak configuration, this picture, supported by both 3-D numerical simulations of resistive MHD equations and experimental results from several spheromak devices, is as follows.

A spheromak initially in a Taylor state is a stable two-dimensional (2-D) equilibrium. Since it is stable, it will at first resistively evolve through a sequence of stable equilibria. In experiments, one expects a resistivity profile with higher resistivity at the edge compared to the center. Such a profile is consistent with a temperature profile peaked at the center where the ohmic-heating power is highest. Resistive diffusion based on such a profile will cause q to decrease everywhere. When q drops below 1/2, the spheromak becomes ideal MHD unstable to an n=2 mode.

In 3-D numerical simulations of the resistive MHD equations, this n=2 mode saturates. Then, the spheromak resistively evolves through a sequence of now 3-D equilibria until it reaches another unstable configuration, after which it undergoes reconnection and relaxes back to a (2-D) Taylor state.

In the S-1 experiment, the entire sequence of events leading up to, during, and after a relaxation event was documented (Fig. 2). The above simulation provides a useful framework from which to interpret the experimental results since many of the observed phenomena agree with the simulation. The time evolution of the electron temperature $T_e$ shows an increasingly peaked profile in minor radius (Fig. 3) due to the rise in temperature near the magnetic axis. Such a profile is consistent with a resistivity profile peaked near the edge of the plasma. From t = 300 to t = 375 $\mu$sec, the poloidal field profile shows a steepening near the magnetic axis, indicating a peaking of the toroidal current density, while the toroidal field profile also shows a peaking (Fig. 4). By directly measuring the poloidal and toroidal fluxes with magnetic probe arrays, one can see (Fig. 5) how the ratio of poloidal flux to toroidal flux ($\psi/\phi$) initially at a Taylor state value after formation, starts to increase (t = 300 to 370 $\mu$sec), indicating the development of a poloidal-flux-rich configuration due to the preferential decay of toroidal flux over poloidal flux.

This preferential decay can be seen in Fig. 6 which shows the evolution of poloidal current $I_{pol}$ versus poloidal flux $\psi$ for a different set of discharges ($\psi = 0$ is symmetry axis of configuration, $\psi = \psi_{max}$ is magnetic axis). At first, $I_{pol}(\psi)$ is linear in $\psi$, with $I_{pol}/\psi$ = constant representing the $\mu$ value for a Taylor state. As time evolves, $I_{pol}$ near the edge ($\psi = 0$) falls below the

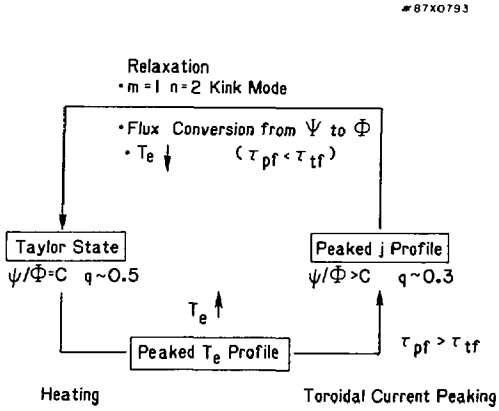


*Figure 2. Sequence of events through a relaxation cycle in S-1.*

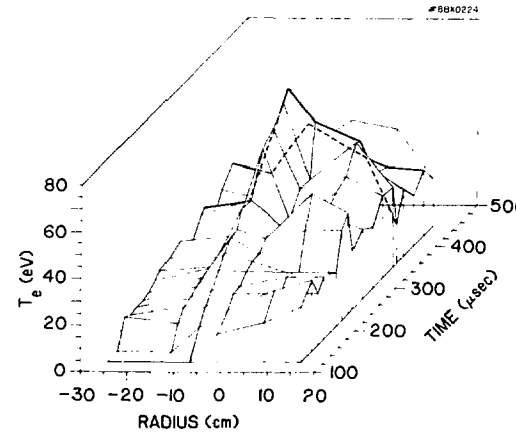


*Figure 3. Time evolution of $T_e$ profile showing peaking prior to a relaxation event.*

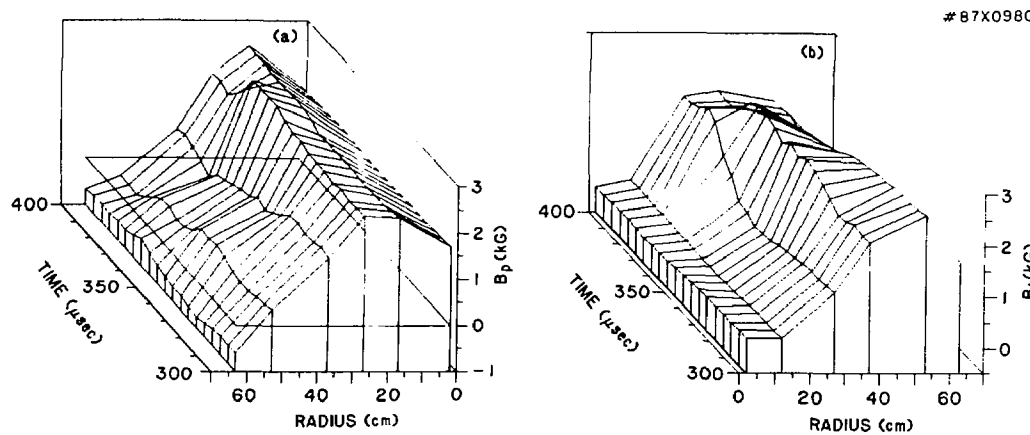


*Figure 4. Radial profiles of poloidal ($B_p$) and toroidal ($B_t$) magnetic fields as a function of time, showing toroidal current peaking prior to a relaxation event. Note time directions are reversed.*

Taylor value, and a peaking occurs near the magnetic axis ($\psi_{max}$). A relaxation event occurs after t = 500 μsec and the discharge is restored to nearly the same state as the initial Taylor state.

For the set of discharges shown in Fig. 5, this preferential decay is emphasized by the plot of $\dot{\psi}/\psi - \dot{\phi}/\phi$, which is essentially the difference in decay rates between the poloidal flux and the toroidal flux. During this time period, $q_o$ is falling below 0.5. An n=2 mode is observed to suddenly develop (t = 350 μsec) and increase the amplitude.

Around t = 370 μsec, the polarity of $\dot{\psi}/\psi - \dot{\phi}/\phi$ reverses, indicating a conversion of poloidal flux to toroidal flux. During this flux conversion period, $\psi/\phi$ is restored to the Taylor state value and $q_o$ rises above 0.5 again. Also, magnetic field profiles broaden now. Just after the relaxation event, $T_e$ is observed to have collapsed. This is consistent with the simulation of Sgro *et al.* which suggests that during the relaxation, the hot plasma near the original magnetic axis is expelled while a new magnetic axis, which is formed near the edge, brings in cold plasma.

In principle, the cycle described above can be repeated. In fact, multiple relaxation events are sometimes observed in S-1, giving the appearance of "sawtooth"-like phenomena, although usually only one event occurs per discharge. The behavior of the decaying spheromak depends on the magnetic Reynolds number S and the resistivity profile. If S is too low (less than 500), there is little resistivity gradient between the plasma's center and its edge so the configuration decays self-similarly and no instability is encountered. For high S (greater than 2000), the time between relaxations is predicted to become comparable to the configuration lifetime, so one expects to be able to observe only one or two relaxations, if any. For intermediate S, one predicts multiple relaxations. In practice, however, a relaxation reduces S so that, again, only one or two relaxations at most may be expected.

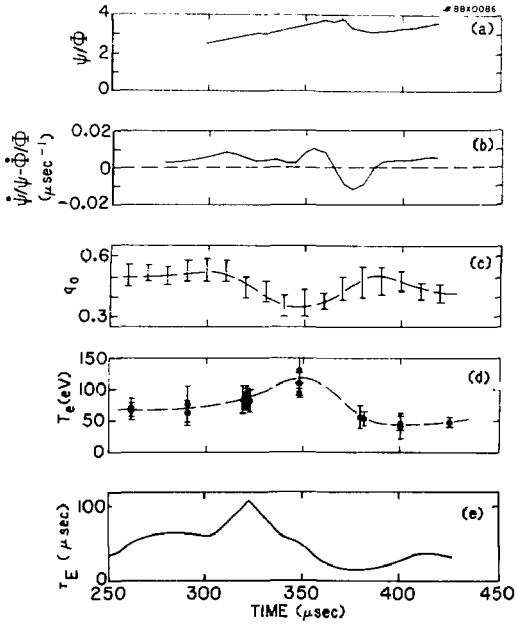


*Figure 5. Time evolution of $\psi/\phi$, $\dot{\psi}/\psi - \dot{\phi}/\phi$, $q_o$, n=2 mode amplitude, $T_e$, and $\tau_E$ through a relaxation cycle during decay phase.*

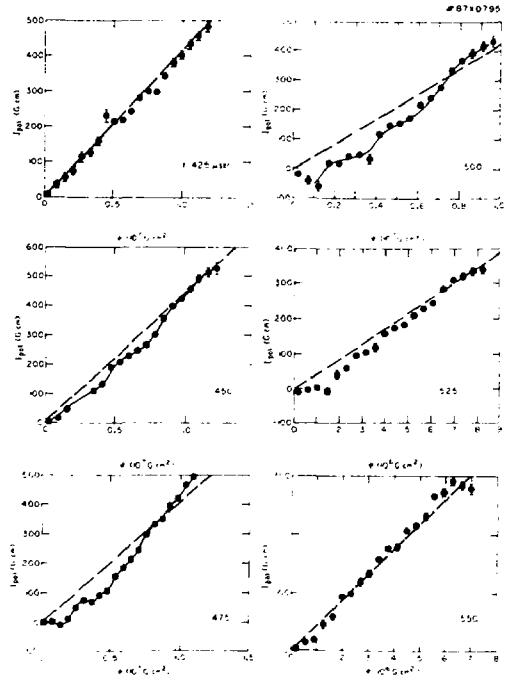


*Figure 6. Evolution of poloidal current $I_{pol}(\psi)$ in S-1 during decay, showing an initial Taylor-like profile, followed by peaking until a relaxation event occurs around 500 μsec.*

# TURBULENCE

In addition to the low-n number global modes, there exists a background of high-frequency, broadband magnetic-field fluctuations, or turbulence, in spheromaks. These fluctuations were studied near the edge but outside of the spheromak plasma, a region which has been well characterized in other confinement devices (e.g., high temperature tokamaks). The fluctuation level is usually higher during formation or after a relaxation event (t = 0.5 - 0.7 msec in Fig. 7) than during the decay phases before a relaxation event (quiescent period) or during the decay phase in a discharge without relaxations. The frequency range is typically between 10 and 100 kHz.

Several interesting facts emerge when one compares the turbulence outside (but near) the edge measured in spheromaks to that of tokamaks. The $\tilde{B}/B$ in spheromaks is typically 0.1-1.0% or greater; this is much larger (about 100 times) than that in tokamaks. Also, $\tilde{B}/B$ displays a frequency (f) dependence of $f^{-1}$, or turbulent spectrtum (Fig. 7); this is also observed in tokamak plasmas such as the Tokamak Fusion Test Reactor.

The study of turbulence in spheromaks has just begun and much remains to be done.

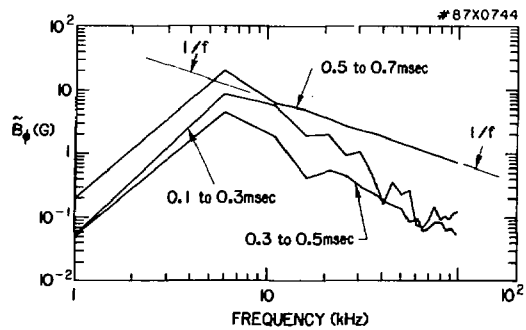


*Figure 7. Frequency spectrum of high-frequency, broadband magnetic field fluctuations outside of and near the edge of spheromak plasmas during formation (0.1 - 0.3 msec), during decay but before relaxation event (0.3 - 0.5 msec), during decay but after relaxation event (0.5 - 0.7 msec).*

# CONFINEMENT AND SCALING

The multipoint (10 spatial channel) Thomson scattering system continued to be a crucial diagnostic in this study of confinement and scaling. Scaling studies of n, T, and nT as a function of toroidal current density j were performed over the range j = 0.6 to 1.9 MA/m$^2$, corresponding to toroidal plasma currents below 300 kA levels.[2]

The scaling of the electron pressure (Fig. 8) was found to be $n_e T_e \propto j^2$, where the parameters are taken to be averages from inside the core region. This implies that beta $\beta_o$ is independent of plasma current density, similar to results for RFP's. These results

can be compared to data from RFP devices. Since there is a dependence of $n_eT_e$ on size (proportional to $a^2$) for fixed j, assuming constant $\beta$ scaling, there would be quantitative differences between the various devices. If the size dependence is removed by plotting $n_{eo}T_{eo}$ versus magnetic field strength, then the data from various devices follow a universal curve (Fig. 9). The central beta

$$\beta_o = (2n_eT_e)/[B_{\phi o}^2/(2\mu_o)]$$

is typically 9% in S-1, with the assumption $T_e = T_i$.

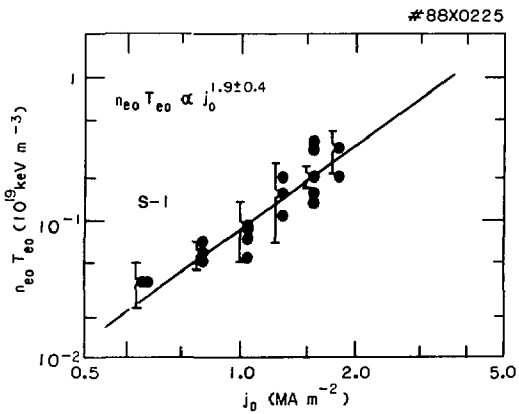


*Figure 8. Dependence of plasma electron pressure $p_{eo} = n_{eo}T_{eo}$ on peak current density j.*

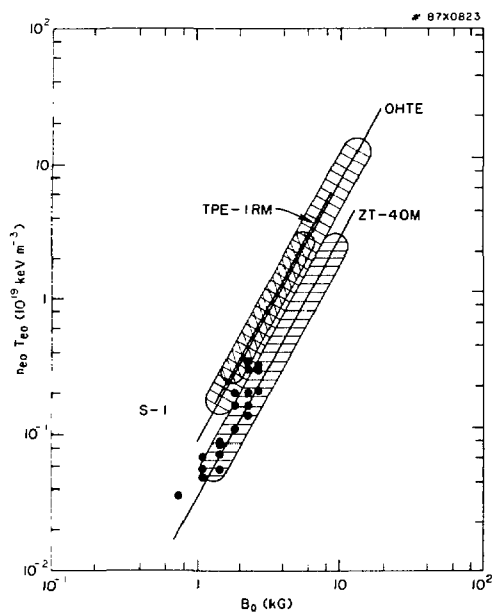


*Figure 9. Scaling of $p_{eo} = n_{eo}T_{eo}$ versus magnetic field strength $B_o$. $n_{eo}T_{eo} \propto B_\phi^2$.*

Individually, the scalings of $T_e$ and $n_e$ versus j are different from that of RFP's. The electron temperature increases roughly as $j^2$ (see FY87 Annual Report), from 10 eV to over 100 eV over the above range in j, as opposed to $j^1$ for RFP's, while the electron density increases much more slowly [Fig. 10(b)]. This is presently the subject of further investigation.

The energy confinement time is given by

$$\tau_E = \frac{3/2 < n_eT_e + n_iT_i >}{\eta(T_e) < j^2 > - (3/2)(\partial/\partial t) < n_eT_e + n_iT_i >}$$

where the averages are over $r/a < 0.7$ and $(T_e)$ is the plasma resistivity assuming $Z_{eff} = 3$. If $T_e = T_i$ is assumed, $\tau_E$ exceeds 100 $\mu$sec.

These confinement studies were conducted with funnel-shaped passive conductors (Fig. 1) providing for the n=1, and higher n, stability of the discharges. Whereas stabilization with the Figure-8 coil system decreases as the plasma decays and effectively moves further away from the coils, stabilization was maintained with the funnels as the plasma decayed or was compressed, allowing further studies of the confinement issues in the near term.

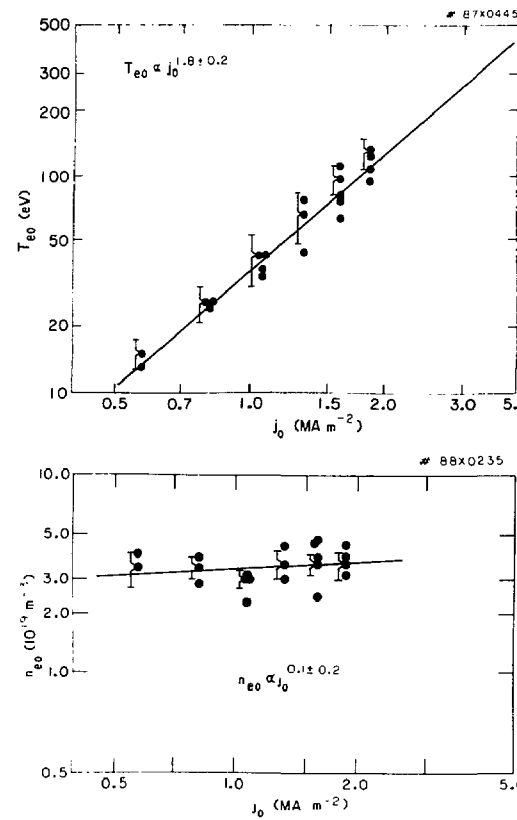


*Figure 10. Dependence of (a) $T_e$ and (b) $n_e$ on peak j.*

## References


[1]Y. Ueda, T.K. Chu, R.A. Ellis, Jr., A.C. Janos, F.M. Levinton, R.M. Mayo, R.W. Motley, Y. Ono, and M. Yamada, "Review of the Recent S-1 Experimental Results," to be published in a supplement to the *Proceedings of the 8th U.S. Compact Toroid Symposium and the 9th U.S.-Japan Workshop on Compact Toroids* (College Park, Maryland, 1987).

[2]F.M. Levinton, D.D. Meyerhofer, Y. Ono, Y. Ueda, and M. Yamada, "Power Balance and Temperature Scaling in the S-1 Spheromak," in *Proceedings of the 8th U.S. Compact Toroid Symposium and 9th U.S.-Japan Workshop on Compact Toroids* (College Park, Maryland, 1987), edited by A.W. DeSilva and G.C. Goldenbaum (Laboratory for Plasma and Fusion Energy Studies, University of Maryland, College Park, Maryland, 1988) 62-65.

[3]A.C. Janos, "MHD Stability and Confinement of Spheromaks," in *Physics of Mirrors, Reversed-Field Pinches and Compact Tori*, (Proc. of Course and Workshop, Varenna, Italy, 1987) to be published by International School of Plasma Physics, Varenna, Italy (1988).

[4]Y. Ono, T.K, Chu, A.C. Janos, F.M. Levinton, Y. Ueda, and M. Yamada, "MHD Feature of the High $T_e$ S-1 Spheromak," in *Proceedings of the 8th U.S. Compact Toroid Symposium and 9th U.S.-Japan Workshop on Compact Toroids* (College Park, Maryland, 1987), edited by A.W. DeSilva and G.C. Goldenbaum (Laboratory for Plasma and Fusion Energy Studies, University of Maryland, College Park, Maryland, 1988) 85-88.

[5]A.C. Janos, J. Cuthbertson, R.M. Mayo, and D.D. Meyerhofer, "Nonlinear Resistive Evolution of Global MHD Modes and 3-D Mode Structure in Spheromaks-Experimental," in *Proceedings of the 8th U.S. Compact Toroid Symposium and 9th U.S.-Japan Workshop on Compact Toroids* (College Park, Maryland, 1987), edited by A.W. DeSilva and G.C. Goldenbaum (Laboratory for Plasma and Fusion Energy Studies, University of Maryland, College Park, Maryland, 1988) 45-48.

[6]R.W. Motley and F.M. Levinton, "Simulation of the S-1 Compression Experiment," in *Proceedings of the 8th U.S. Compact Toroid Symposium and 9th U.S.-Japan Workshop on Compact Toroids* (College Park, Maryland, 1987), edited by A.W. DeSilva and G.C. Goldenbaum (Laboratory for Plasma and Fusion Energy Studies, University of Maryland, College Park, Maryland, 1988) 77-80.

[7]D.D. Meyerhofer, R.A. Hulse, and E.G. Zweibel, "Zero-Dimensional Study of the Compression of Low Temperature Spheromaks," Nucl. Fusion *26* (1986) 235.

[8]R.M. Mayo, F.M. Levinton, D.D. Meyerhofer, S. Paul, and Y. Ueda, "Spatial and Temporal Behavior of Some Low-Z Impurities in the S-1 Spheromak," in *Proceedings of the 8th U.S. Compact Toroid Symposium and 9th U.S.-Japan Workshop on Compact Toroids* (College Park, Maryland, 1987), edited by A.W. DeSilva and G.C. Goldenbaum (Laboratory for Plasma and Fusion Energy Studies, University of Maryland, College Park, Maryland, 1988) 69-72.

# CURRENT-DRIVE EXPERIMENT

The Current-Drive Experiment (CDX) is used to test new ideas for nonclassical radial diffusion of toroidal current that may lead to more efficient tokamak current drive and current profile control, both crucial for an economical reactor. Inductive ohmic current drive and radio-frequency current drive are the methods presently employed to drive tokamak currents. However, the former method is inherently not steady-state and the efficiency of the latter may not be high enough for reactor application. The principal approach on CDX, termed dc-helicity injection, utilizes steady-state injection of an electron beam at the plasma edge and the subsequent inward penetration of this current to maintain the plasma current. A strong inward current diffusion could lead to high-current-drive efficiency. This, coupled with its simple technology, would make dc-helicity injection an attractive candidate for tokamak reactor current drive.

In FY87, through detailed measurements of the dc-helicity-injected plasma, a direct confirmation of the tokamak-like state was obtained. Through successive improvements, the driven current was increased to the 1-kA level. This amount of driven current represents a threefold increase from the previous level, and corresponds to q = 5 at the plasma edge, which is in the operating range of a typical ohmic-driven tokamak.

The CDX experimental facility utilizes the former Advanced Concepts Torus-I (ACT-I) device, a steady-state, 5-kG toroidal device with minor and major vacuum chamber radii of 10 cm and 59 cm, respectively. In FY87, new diagnostics were added, including magnetic and plasma potential probes and a scanning Fabry-Perot interferometer system. The CDX data acquisition system was fully implemented on most of the CDX diagnostics.

One of the important parameters in the helicity-injection experiment is the plasma current profile. Since helicity or current is injected from the plasma edge, the current profile measurement provides essential information on radial current diffusion, as well as on the plasma's internal magnetic structure. To measure the generated poloidal magnetic field in CDX, a special water-cooled, radially-scanning magnetic probe was developed. Figure 1(a) shows the measured poloidal magnetic field through the plasma mid-plane. As expected, this field reverses sign near the center of the discharge. The current density and the q profile obtained from this measurement, $q = (B_t/B_p)(r/R)$, are shown in the inset of Fig. 1(a). The q(r) increases monotonically with plasma radius from q ≈ 4 at the center to q = 10 at the edge.

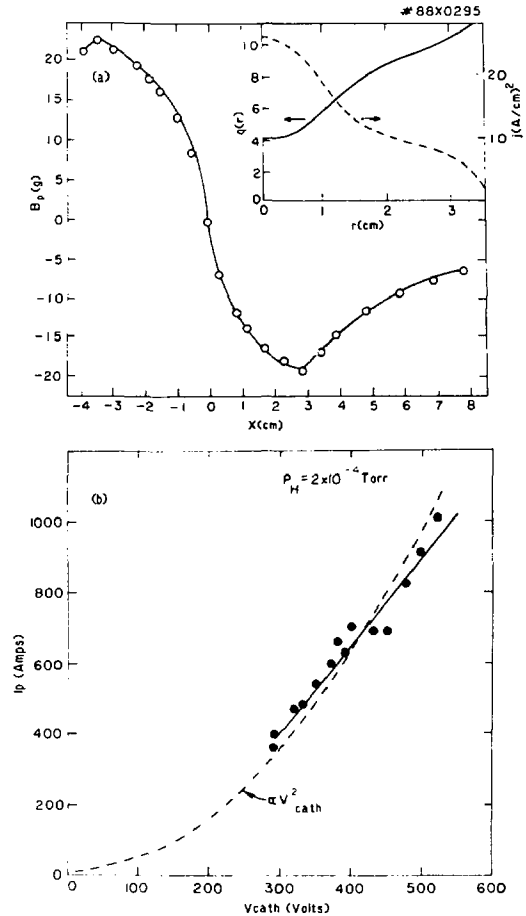


*Figure 1. (a) The poloidal field on the plasma mid-plane, measured by a magnetic probe in a discharge of 330 amperes. The q and j profiles computed from the poloidal-field measurement are shown in the inset. (b) Applied cathode voltage and measured plasma current in CDX discharges, showing the increase of plasma current with cathode voltage. The solid line is a linear fit to the points; the dashed line is a quadratic fit.*

This measurement shows that the current is strongly-peaked at the plasma center, a consequence of strong inward current pinching in the experiment. Indeed, a comparison of the experimental results with a

modeling code shows the presence of very strong current diffusion and an inward current pinch, $D_j \approx 1.6 \times 10^5$ cm$^2$/sec and $V_j \approx 1.2 \times 10^5$ cm/sec, respectively. Evidently, the toroidal current system tends strongly to relax toward a tokamak-like state, a very encouraging result.

From the point of view of helicity-injection efficiency as applied to current drive, cathode voltage with respect to the plasma is a critical quantity. A theoretical model of helicity injection suggests that the driven current increases with cathode voltage and also increases with the average plasma conductivity. In Fig. 1(b), the observed plasma current is seen to increase nearly as the square of the cathode voltage, consistent with plasma conductivity ($\sim T_e^{3/2}$) increasing with current. About 50% of the beam helicity is transferred to the plasma.

Significant efforts during this period were also applied to the study of plasma fluctuations in dc-helicity-injected CDX plasmas. Frequency spectra of probe floating potential, of magnetic field fluctuations, and of far-infrared scattering signals reveal several coherent oscillations superimposed upon a broad band, incoherent background. A coherent mode appears regularly at 17 kHz in helium plasmas, and this drift-wave type mode exhibits an m=1 dependence, its largest amplitude occurring near the plasma edge where the density gradient is large, as expected.

A more unusual fluctuation occurs at higher frequencies, typically at 62 kHz in helium plasmas and at 135 kHz in hydrogen plasmas. This mode appears only when the plasma beta is sufficiently large and when the onset beta condition corresponds roughly to the Troyon-Sykes limit for ballooning instability [i.e., $\beta_c(\%) = 2.2\ \mu_o I_p / a\ B_T$ and is 0.1% for typical CDX parameters]. Moreover, the mode is observed predominantly on the large-major-radius side of the discharge (a region of unfavorable curvature) as shown in Fig. 2(a). The sharp density threshold, at which the mode becomes unstable, is clearly seen in Fig. 2(b). Since plasma density and temperature increase together (and much faster than the plasma current) in these discharges, Fig. 2(b) can be interpreted in terms of an onset condition based upon the plasma beta. From these observations and from the parametric dependence of its frequency, this mode appears to be a pressure-driven ballooning mode. It is generally believed that such ballooning instabilities inhibit reaching the second stability regime, and experimental studies on CDX aimed at the stabilization of this mode could be of great significance to the fusion program.

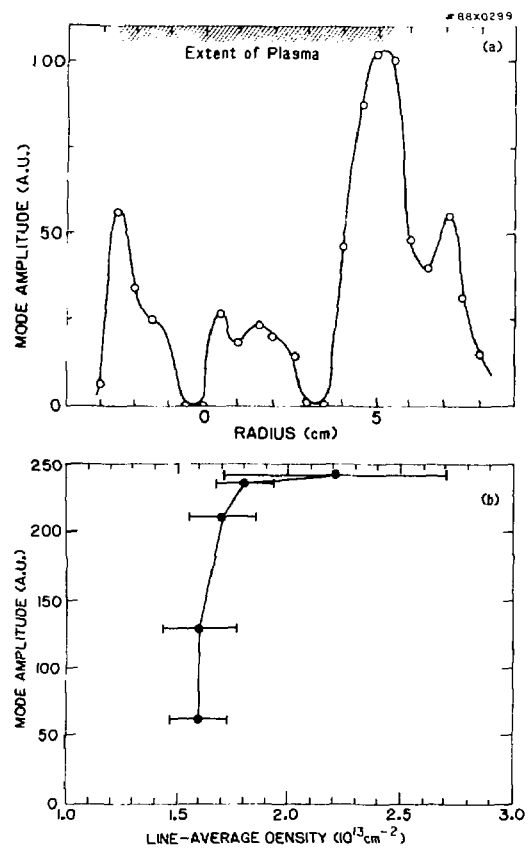


*Figure 2. (a) Amplitude of the pressure-driven mode versus minor radius, measured with an emissive probe. (b) Plasma current scan plotted as the pressure-driven mode amplitude versus line-averaged density.*

# X-RAY LASER STUDIES

## INTRODUCTION

During FY87, X-ray laser research at the Princeton Plasma Physics Laboratory (PPPL) continued to show significant progress in several directions. During this period, work continued on the system that has yielded stimulated emission with enhancement up to 500 at 182 Å, as reported in previous annual reports,[1,2] and in the literature. Not only improvements to this system and, in particular, methods to reach shorter wavelengths were explored, but the research has started to include applications of the 100 kW X-ray beam. At the same time, steady progress continued on the new X-ray laser development facility which will use the powerful picosecond laser to study multiphoton processes. This progress included the design and installation of a new magnet, new lasers, new lens systems and new diagnostics, culminating in the preparation and successful completion of the first integrated test of the system.

These facilities serve to study methods of obtaining a gain medium for amplification of radiation in the soft X-ray range of wavelength: If a large amount of energy is concentrated in a very short time on a small plasma, for instance by a powerful commercial laser in the infrared, visible or ultraviolet, the resulting deviation from equilibrium may create population inversions from which energy can be extracted by stimulated emission of radiation. A difficulty is the need to translate the small energy of each photon in the visible or infrared from the first "pump" laser to the more than $10^2$-$10^3$ times larger energy gap of the soft X-rays where the gain is wanted. Another difficulty results from the absence of efficient optical elements in the soft X-ray wavelength region. The X-ray Laser Project is primarily devoted to the study of two different approaches for obtaining such a gain medium that can generate lasing action in the X-ray wavelength range.

In the first "Recombining Plasma" approach, the lasing medium is a rapidly recombining carbon plasma column, which is produced and heated to an almost completely stripped state by a 0.3-0.5 kJ $CO_2$ laser and which is held to a specific diameter by a strong magnetic field. In this plasma, which cools rapidly through intense radiation losses, free electrons recombine rapidly with the stripped nuclei producing highly excited hydrogen-like ions. The cascading decay through the lower energy levels of these ions produces population inversions and gain at 182 Å. This approach has already resulted in an intense, narrow, soft X-ray laser beam for which applications, particularly holographic and contact imaging of living cells, are being explored at PPPL. Other improvements being explored for this approach are the use of various elements (N, Mg, Al, or Si) to reach shorter wavelengths, and there are attempts to increase the intensity of the beam by changing the geometry or increasing the path length through the gain medium by the use of multilayer soft X-ray mirrors or the generation of multiple plasmas.

The second approach explores the possibility that at the very high power density which can be reached with new picosecond laser systems, "multiphoton processes" occur, wherein a number of photons of low energy acting together efficiently populate higher energy levels and generate gain at wavelengths shorter than 100 Å. A power density in excess of $10^{15}$ W/cm$^2$, where efficient multiphoton processes are expected, can be reached by using extremely short pulses in the picosecond range: otherwise, the necessary stored energy becomes prohibitively expensive. The target plasma must then be generated and brought to the correct ionization state by a separate laser. This picosecond laser, a separate $CO_2$ laser, and associated facilities (magnet, spectroscopic diagnostics) have had a successful first integrated test. Preliminary spectroscopy work on the picosecond laser-target interaction had already started.

An additional supporting experiment with two lasers [a 10-J $CO_2$ TEA (Transverse Electrical excitation at Atmospheric pressure) and a 1-J XeCl eximer] allows spectroscopic investigations of laser-generated plasmas and has produced interesting new measurements of radiative decay coefficients.

The interest of the academic and research communities in these experiments has stimulated the start of several collaborative ventures. There are five graduate students currently associated with the project, with several preparing doctoral theses. Some of the insights obtained during the period covered by this report, both in experiment and theory, will shape future studies and point to a close relationship between X-ray laser research and basic problems of current interest in physics, i.e., ionization balance modeling, the structure of ions in extremely large fields, and a possible coupling of radiative decay rates to plasma characteristics.

In order to coherently present this varied array of achievements, we will follow a progression from a description of the new facilities with their attendant capabilities, to an explanation of the current experimental efforts and their results, and conclude with selected experimental observations and theo-

retical interpretations that indicate promising future research directions.

## NEW EXPERIMENTAL FACILITIES

The period of this report was marked by the development of new experimental facilities (Exp. II) in the new 1,000-square foot laboratory which was built adjacent to the original facility in FY85 and which will be used to study the two laser (multiphoton processes) approach to soft X-ray laser development (Fig. 1).

A target chamber with its vacuum pumping system, diagnostics and inspection ports, and laser focusing lens assembly was installed in an enclosed experimental area (Fig. 2). To avoid vibrations of the target which impede alignment (important due to the small area of the gain medium and small divergence of the beam), the magnet structure that surrounds the vacuum chamber is kept mechanically separate, and special care was taken to insulate structural members so that no electrical closed loop can carry eddy currents. The magnet, composed of two coils placed in a configuration similar to Helmhotz coils, is powered by a 375-kJ capacitor bank located on the third floor of the RF Building. Power is fed to the laboratory through long coaxial cables. This magnet system has successfully produced fields of up to 100 kG (we expect 120 kG in the near future) with a time scale of milliseconds, much longer than the plasma duration.

The target chamber is open in both axial directions, and is connected to two vacuum pumping systems to allow, if needed, differential pumping. It has four small transverse ports for inspection or fiber-optic access in addition to the three large ones for the lasers and diagnostics. Currently, a transverse port is used by the target holder, a second is connected to a large vacuum chamber holding a 12-inch diameter salt lens system for focusing the $CO_2$ laser beam, and the third port will be used for a second laser beam (see Fig. 3).

Beams from three different laser systems, each suitable to generate various plasma regimes, will be available at this new facility. The first system is the 1-kJ $CO_2$ Lumonics laser used in the old facility: copper mirrors in holders with capability for precise steering were installed to divert the beam and direct it to the focusing optics on the target chamber. This laser system will soon be upgraded to have a shorter and better controlled temporal pulse shape using the master oscillator and preamplifier system from the

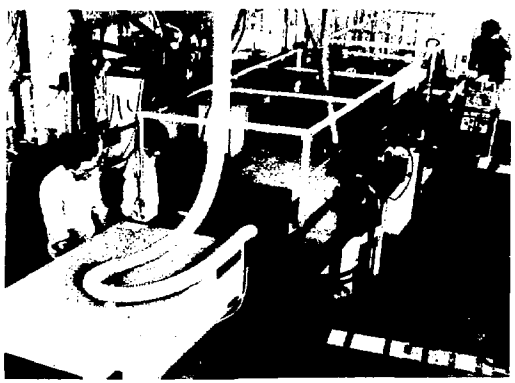

*Figure 1. A view of the picosecond laser located in the new X-ray laser facility: Exp. II. (87E0344)*

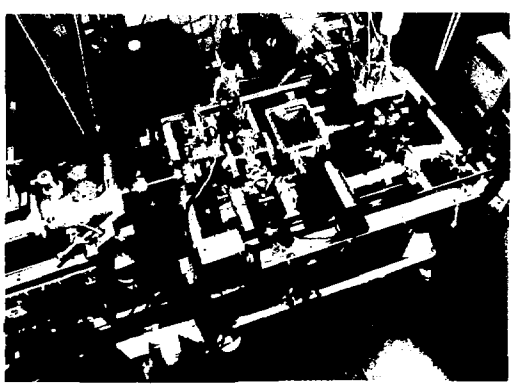

*Figure 2. The experimental area showing the magnet surrounding the target chamber (toward the right), the large chamber containing the optics for the $CO_2$ laser (top), and diagnostics and alignment chambers on the axial direction (center and left). (88E0770)*

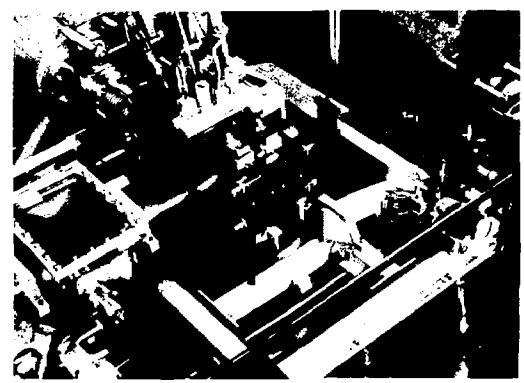

*Figure 3. Closer view of the magnet around the target chamber. The magnet is supported on a table, whose top is visible, and is connected to the large coaxial cable and cooling water lines on top. The target chamber, optics, and diagnostics are attached to the independent aluminum framework: upper left, the chamber for the $CO_2$ laser optics and above it a boroscope using a small inspection port. In the axial direction (lower left), the empty alignment chamber which will contain a cavity mirror. The target is supported from the bottom port (not visible). To the right one sees the opening of a port for an additional laser. (88E0771)*

large-scale $CO_2$ laser HELIOS, which were transferred to PPPL from the Los Alamos National Laboratory in FY86.

The second laser system is the new Nd-Yag laser which was received and tested recently; optics to steer and focus the beam are presently being installed. This modern commercial laser, QUANTEL PG-770, will produce up to 100 joules of 1053 nm radiation in 2 to 3 nsec with a very small divergence. These characteristics allow the sharpest and best concentration of energy in a time scale suitable to obtain a seed plasma of specific ionization state. Due to its shorter wavelength, a higher density can also be reached than with the $CO_2$ laser.

The third laser system is the picosecond laser, developed in FY85-87, which is central to multiphoton schemes for generation of gain. It is composed of a chain of nine individual laser components including KrF eximer amplifiers at 248 nm and was described in the FY86 annual report.[2] A more complete description together with the first spectroscopic results is given in Refs. 3 and 4.

The first stage of the picosecond laser is complete and power levels of 20-30 GW in 1-1.5 psec pulses have been achieved.[4] An extensive experimental effort was made during FY87 to design, build, and test at PPPL, in cooperation with the University of Maryland (Prof. J. Goldhar), the large final KrF amplifier that will increase the pulse power to the order of 0.5-1.0 TW and allow studies of laser interactions at power densities in excess of $10^{18}$ W/cm$^2$. The electric field created by such a beam will be in excess of $10^{11}$ V/cm.

These three different laser systems, each with a unique capability for X-ray laser research, are now available. Currently, the various beam steering and focusing optics (including line foci and high F-number optics for better focusing) are being installed, and the complex safety interlock system required to allow safe use of any combination of these lasers is being set up. The multichannel soft X-ray spectrometer SOXMOS, previously used for spectroscopic studies on the Princeton Large Torus Tokamak (PLT),[5-7] was installed on an axial port of this experimental facility; its vacuum pumping systems and electronic control were rebuilt. A complete data acquisition system was built in a special Faraday cage with extensive use of fiber-optics links to avoid radio-frequency noise problems generated by the powerful laser systems. Since the precise timing of the magnet, lasers, and diagnostics is of great importance in each experimental configuration, a timing system of a new design[8] was built and installed.

The installation of this new facility was an extensive undertaking, and although a number of initial experiments were started during the summer, it was late at night on October 15th when the first successful integrated test of the whole system was achieved. Correct timing of the picosecond laser, the $CO_2$ laser, the magnet and diagnostics, as verified by the obtainment of spectra and signals from fast diodes, was documented. Since then, this system has been used to produce carbon and aluminum plasmas shaped by line focus optics and confined with large magnetic fields.

The design and upgrade work was not limited to the new facility: during the installation effort, the option of steering the beams of the new laser systems towards the old facility was retained and new experiments with line foci and the 1053 nm laser beam have begun. Several of these multilaser experiments are planned for the near future.

# EXPERIMENTAL RESULTS

During the past year, part of the experimental efforts with the recombination approach were devoted to reaching shorter wavelengths by using targets of other elements while still retaining the physical principle and experimental design of soft X-ray laser in 182 Å. The logical choice was replacing the carbon ($Z = 6$) with heavier elements to take advantage of the overall increase in transition energy with increasing Z. Some data was collected with a nitrogen plasma ($Z = 7$; obtained with $Si_3N_4$ targets), with a potential lasing transition at 133.8 Å. This approach appeared to require a larger pump energy than was easily available and further efforts were mostly devoted to studies of the lithium-like ions that are more efficient in this respect.

These lithium-like ions have three electrons remaining around the nucleus, but since usually two electrons stay in a closed shell ($1s^2$) with few interactions, the energy spectrum and physical interactions associated with the third electron have a similarity with the corresponding quantities in the hydrogen-like (one electron) spectrum. By analogy with the CVI recombination laser, inversion and gain between 4f and 3d levels of the lithium-like ion was expected during recombination from the helium-like state. This concept was supported by our observations of a few years ago of population inversions in lithium-like OVI and NeVII and by the observation in France by Jaeglé and his colleagues of gain in the 5f-3d transitions of lithium-like ions. The wavelengths at which gain could be expected are 187 Å for MgX, 154 Å for AlXI, and 130 Å for SiXII.

Targets were made from these materials and plasmas of the correct state of ionization generated and confined by the magnetic field. The observed intensity variations indicated gain, especially when a blade containing iron (or titanium) was added to the target to stabilize the plasma and increase radiation cooling, as shown in Fig. 4. With these encouraging results,[9,10] a model combining hydrodynamic code to compute the plasma evolution and an atomic code to compute the population levels, including recombination effects, was developed and the model predictions compared with observation.[11] The ability of this code to compute synthetic spectra corresponding to the spectrometer observation region and time integration allowed a preliminary estimate of a gain length product between 4 and 3 AlXI, as seen in Fig. 5. Similar results but with a lower gain-length between 1 and 2 were obtained for SiXII at 130 Å.

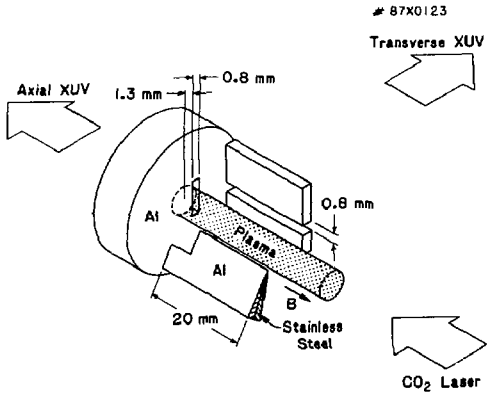


*Figure 4. An aluminum disc target geometry with 0.8 × 2 mm vertical slot and with an aluminum/stainless steel composite blade attached normal to the target surface.*

Concomitant with these experiments, a separate effort was launched to utilize the strong X-ray beam obtained with the recombining carbon plasma column. As discussed in the FY86 Annual Report,[2] this soft X-ray beam has a very low divergence of 5 mrad and corresponds to an enhancement of 500 times the spontaneous emission expected for an equilibrium plasma. It has a peak power around 100 kW for about 10-30 nsec. These characteristics attracted a lot of interest, and the X-Ray Laser Group was awarded the coveted I.R. 100 Award from R&D Magazine for this achievement.

Biological applications including medical diagnostics are probably the first and most straightforward application of the soft X-ray laser. This is because practical soft X-ray microscopy would bridge the gap between the high-fidelity light microscopy with resolution too low for observing the finer details of cellular structure and the high-resolution electron micorscopy with lower fidelity (due to the requirement for extensive specimen preparation that may disrupt the original structure of the living cell). The observation of details as yet unknown about living cells may result from an instrument where the specimen, still living, is contained in an environmental cell isolated from the X-ray laser vacuum system by a 1200-Å-thick silicon nitride window. Flash illumination by the X-ray laser pulse causes a high-resolution image to be recorded on a photoresist which is later viewed by an electron microscope.

With a X-ray sensitive substrate, usually a photoresist plastic for good resolution or special photographic emulsions, there are two possible methods for imaging. The simplest is contact printing, consisting of nearly parallel ray illumination of the object with the substrate kept as close as possible. With the more difficult but powerful holographic techniques, the coherent diffraction patterns on the substrate are decoded to furnish a high-resolution three-dimensional image.

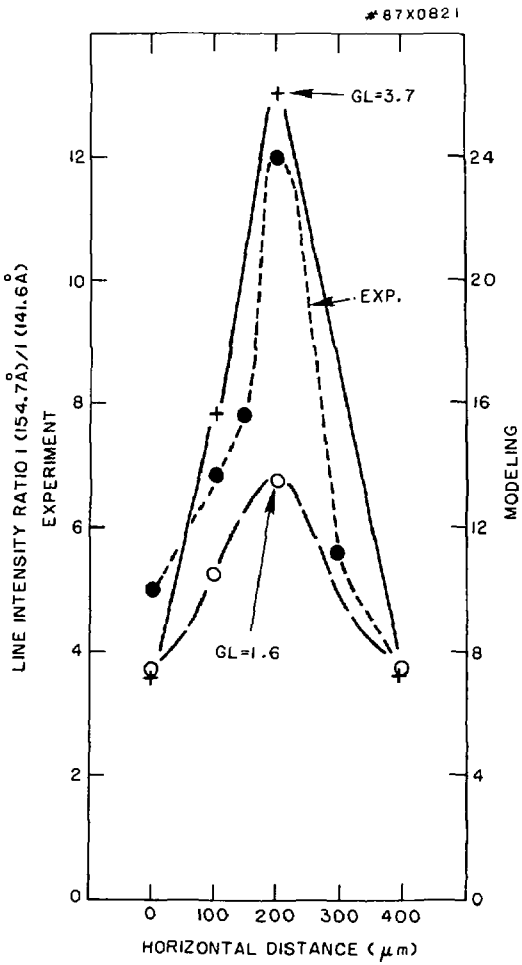


*Figure 5. Observed and predicted line intensity ratio showing the rise in relative intensity of the A1XI 3d-4f transition at 154.7 Å in the region of the plasma with gain. Experimental data, filled circles; modeling with peak gain-length product GL = 3.7, pluses; modeling with peak-gain length product GL = 1.6, open circles.*

During FY87 investigation of the different options for soft X-ray microscopy[12,13] began, and preparations for new experiments with the aim of imaging living cells were started. Figure 6 illustrates the results from tests with a metallic mesh. Both images were taken with a single laser shot. In the photographic one (a), the beam intensity was greatly reduced by the window needed for imaging an object at atmospheric pressure, as required in the case of living cells. The second image (b), which shows the higher resolution available with polymer photoresists, was taken inside the vacuum chamber to use the maximum intensity while testing resolution. Because of the good exposure obtained with the photoresists (the same type used in soft X-ray lithography), there is also the

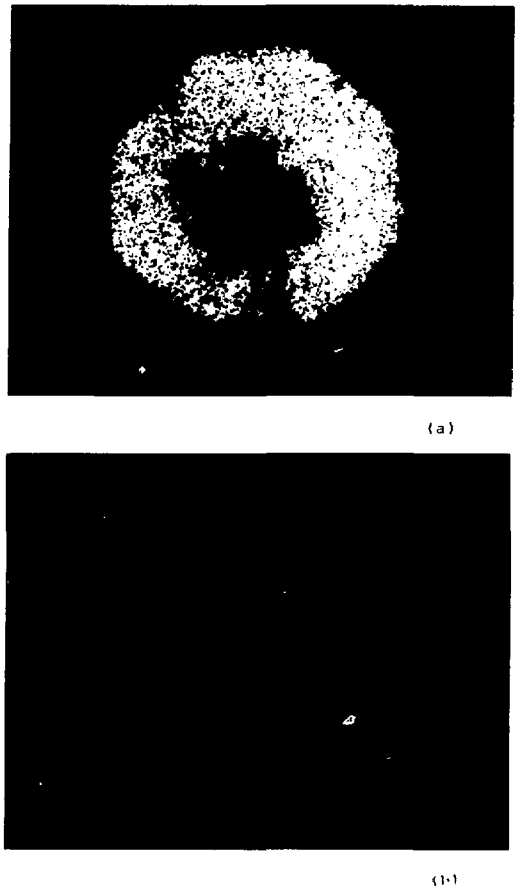

*Figure 6. (a) Image of mesh on Kodak 101 with $Si_3N_4$ window and aluminum filter (one laser shot). (b) Image of mesh on Poly (methylmetaacrylate-metaacrylic acid) co-polymer (one laser shot). (88X3030)*

possibility of using PPPL's soft X-ray laser for microlithography.

During FY87, the building of the new facility also offered a splendid opportunity to attempt to increase the intensity of the beam either by changing the geometry, thus increasing the path length through the gain medium by the use of soft X-ray mirrors or generation of multiple plasmas, or by using a second laser to change and improve some characteristics of the plasma. In the new facility (Exp. II), experiments were started to study the recombining gain medium produced by a different geometry, i.e., with a line focus transverse to the laser, and also with a cavity formed with soft X-ray mirrors. These experiments are progressing in concert with the testing of the magnet. Many spectra from the $CO_2$ laser-produced plasmas have been recorded with magnetic fields up to 100 kG. The use of a second laser to influence some characteristics of the plasma is also being actively pursued in the first facility (Exp. I).

Spectroscopic studies of the interaction of a powerful picosecond laser pulse with solid targets began in FY87. After the first extensive measurements of the pulse width and focal spot size, which required development and installation of special diagnostics in order to confirm a power density around $10^{16}$ W/cm$^2$ could be attained, the beam was focused on various targets and spectra were recorded, first in the visible, then in the ultraviolet and soft X-ray wavelength range.[3,4] These first spectra show significant line broadening and a high state of ionization of the target elements. This data, from targets composed of elements with atomic numbers in the range Z = 3 to Z = 26, as taken with a pulse duration of 1.2 psec and an intensity of $10^{16}$ W/cm$^2$. The spectra in the range of 6 Å to 370 Å were recorded by a 3-meter photographic grazing incidence spectrograph[4] (work done in collaboration with Naval Research Laboratory) and by the 2-meter multichannel spectrometer "SOXMOS" installed on the system.

Analysis of the spectra of highly charged ions is still in progress. Figure 7 shows that high ionization states (up to FeXVI, ionization potential = 489 eV) are reached by these very high power density but low-energy laser pulses. Figure 8 shows the experimental spectra of FVII and FVI from a teflon target, with broadening from Stark effect and enhancement of forbidden components, both due to the extremely high electron density ($10^{22}$ cm$^{-3}$, close to solid density) preserved during such short pulses. This data is being analyzed for possible additional effects from the high electric fields generated by the laser light, and new experiments are planned to elucidate the large variations in the spectrum that are observed when the laser is modified so that small amounts of ASE (amplified spontaneous emission) are present as a prepulse.

This intensive experimental effort is supported by theoretical efforts. An one-dimensional code was adapted for modeling spectrum in the lithium-like sequence, and continued modeling of recombination laser is in progress. Much effort is devoted to the

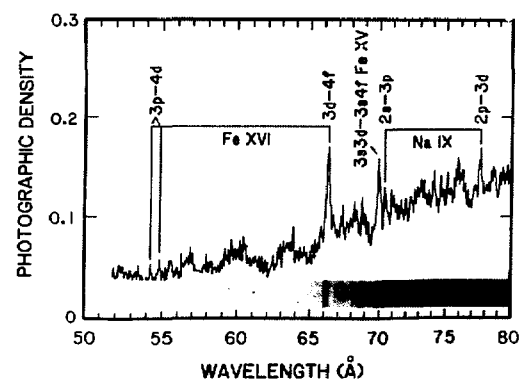


*Figure 7. Densitometer trace of the spectrum from an iron target with surface contamination of sodium. Identified are transitions in lithium-like NaIX, sodium-like FeXVI, and magnesium-like FeXV. (88X3047)*

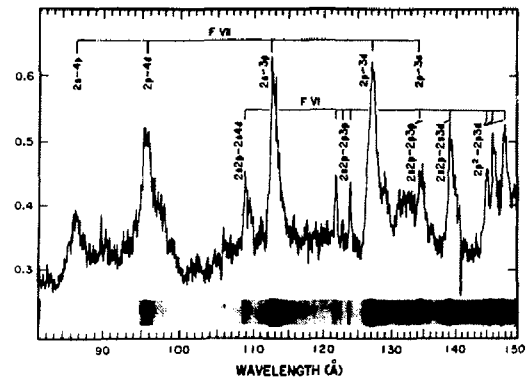


*Figure 8. Densitometer trace of the spectrum from a teflon target showing transitions in lithium-like FVII and beryllium-like FVI. (88X3048)*

theoretical study of multiphoton processes for Exp. II and, for instance, asymptotic techniques previously developed to analyze a two-level system have been used to model multiphoton transitions between Rydberg states of an atomic system subjected simultaneously to low-frequency ac and dc electric fields.[14] The theoretically computed excitation rates agree well with those observed experimentally and work is in progress to model the competition between multiphoton excitation and ionization. A promising approach will be discussed in the next section.

Similarly, the contribution from the supporting experiment were substantial and useful. For instance, these experiments first showed the possibilities and intricacies of generating a plasma with two lasers at different wavelengths. Now, a collaborative effort with Princeton University's Mechanical and Aerospace Engineering Department will study quenching of transitions due to high fields present inside a laser cavity. It is, however, the recent results about radiative decay coefficients that are most interesting and they will be discussed below.

# DEVELOPMENTS

X-ray laser research has been closely associated with fundamental problems of astrophysics and atomic plasma physics. The efforts to determine the level populations and the recombination rates that lead to gain and X-ray lasing action generated a strong interest in a number of problems that currently attract significant attention from the physics community, for example, ionization balance, resonances in excitation rates, ionic spectroscopy including *ab initio* computations, and quantum electrodynamic effects. In this section two developments in our area of research that contribute to these fields will be discussed.

In the supporting experiment, an interesting phenomenon was observed related to Einstein emission coefficients. Emission and absorption of radiation by ions is usually treated by a set of radiative decay, absorption, and stimulated emission coefficients characteristic of the ions. These coefficients, due to Einstein, are the foundations on which discussions of interaction of atoms with radiation are built: in the case of thermodynamic equilibrium, one can recover the Planck emission law when the levels are populated according to Boltzmann law. In general, the population of a level can be deduced from a line intensity in an optically thin plasma. By equating two measures of the population of the same level from two lines originating from it, calibrations at widely differing wavelengths can be related. This is the well-known "branching ratio" method of spectrometer calibrations. In practice, indications of discrepancies forced us to verify, very carefully, the consistency of this method at different densities. The results, Fig. 9, showed a very large change (up to a factor of 10) in Einstein's emission coefficient ratio for densities larger than $10^{18}$ cm$^{-3}$. This observation[15] was carefully verified with new spectrometers (a specially built set of visible and soft X-ray spectrometers sharing the same entrance slit). The experiment not only indicated the need for more care that was thought necessary in spectroscopic calibrations, but also the need for an urgent theoretical effort to search for an explanation, because it may invalidate the results of some methods of level population measurements. Moreover, as the effect of opacity is expected to be

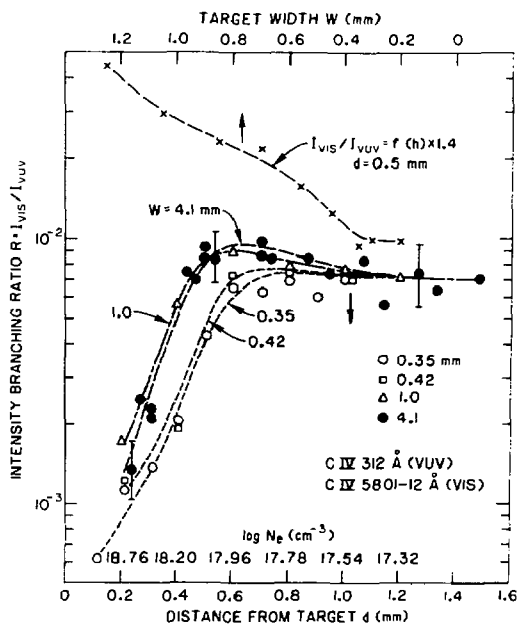


*Figure 9. Branching ratio $I_{VIS}/I_{VUV}$ for CIV 5801-5812 Å and 312 Å lines as a function of distance d from the target (corresponding to indicated electron density) for various target widths W. The dashed curve (same ratio × 1.4) shows the effect of opacity by changing this width at a constant distance (0.5 mm) from the target. (87X33132)*

in the opposite direction, as shown by the experimental data in the upper part of Fig. 9, the theoretical implications become very important. The observational data indicate a quenching of the radiation emission coefficient which may be due to collisions, but that requires the introduction into the theory of some new interaction.

In the multiphoton approach, we are greatly interested in studying, theoretically, the behavior of atoms and ions in the very strong fields produced by the laser. As the laser fields will be larger than the intraionic fields at the maximum power density of the picosecond laser, we may expect new phenomena that cannot be studied as a small perturbation to a simple ion. A previously developed nonperturbative analysis of the two-level atom, with the rates appearing as a result of solving the time evolution of the system by the Hamiltonian of an atom in the varying field due to the laser light, was applied to problems of multiphoton excitation of interest to X-ray laser research[14] and generated theoretically computed excitation rates that agree well with available experimental data. Both excitation and ionization rates by multiphoton processes are needed in X-ray laser research and a study of these rates is being currently performed for a new model system with a short range binding potential, idealized as a set of Dirac functions. This analysis, using both numerical and analytic methods, will extend previous treatments of such a model system (which examined multiphoton ionization only) to allow an examination of the competition between multiphoton excitation and ionization. Current investigation of this exciting development centers on the generality of the method. The approach was developed and clearly will be useful for modeling and gaining a conceptual understanding of the various processes of importance in plasmas influenced by fields from high power laser pulses, and the extension to multiple levels can of course expand tremendously its usefulness. There is also the intriguing possibility that a way can be found to model specific ions and thus develop a new method of computing level populations and rates for special applications when strong fields are present.

## References


[1]Princeton University Plasma Physics Laboratory Annual Report PPPL-Q-43 (October 1, 1984 to September 30, 1985) p. 61.

[2]Princeton University Plasma Physics Laboratory Annual Report PPPL-Q-44 (October 1, 1985 to September 30, 1986) p. 67.

[3]W. Tighe, C.H. Nam, J. Robinson, and S. Suckewer, "High Power Picosecond Laser System at 248 nm," Princeton University Plasma Physics Laboratory Report PPPL-2516 (May 1988) 21 pp.

[4]C.H. Nam, W. Tighe, S. Suckewer, J.F. Seely, U. Feldman, and L.A. Woltz, "Observation of Asymmetric Stark Profiles from Plasmas Created by a Picosecond KrF Laser," Princeton University Plasma Physics Laboratory Report PPPL-2484 (October 1987) 14 pp; Phys. Rev. Lett. *59* (1987) 2427.

[5]J.L. Schwob, A.W. Wouters, S. Suckewer, and M. Finkenthal, "High-Resolution Duo-Multichannel Soft X-Ray Spectrometer for Tokamak Plasma Diagnostics," Rev. Sci. Instrum. *58* (1987) 1601.

[6]J.H. Davé, U. Feldman, J.F. Seely, A.W. Wouters, S. Suckewer, E. Hinnov, and J.L. Schwob, "Time-Resolved Spectra in the 80-340 Å Wavelength Region from Princeton Large Torus Tokamak Plasmas," J. Opt. Soc. Am. B *4* (1987) 635.

[7]A.W. Wouters, J.L. Schwob, S. Suckewer, J.F. Seely, U. Feldman, and J.H. Davé, "Spectra in the 60 Å - 345 Å Wavelength Region of Elements Injected into the PLT Tokamak," Princeton University Plasma Physics Laboratory Report PPPL-2504 (March 1988) 32 pp; to be published in J. Opt. Soc. Am. B.

[8]L. Meixler, K. Ilcisin, J. Robinson, W. Tighe, and L. Guttadora, "Picosecond Delay Timer," patent disclosure, April 1986.

[9]D. Kim, C.H. Skinner, A.W. Wouters, E. Valeo, D. Voorhees, and S. Suckewer, "Toward Shorter Wavelengths for Soft X-Ray Lasers Based on Li-like Ions," Proceedings of SPIE's O-E/LASE '88 Symposium on Innovative Science and Technology, Los Angeles, CA, 10-15 January (1988).

[10]C.H. Skinner, D. Kim, A.W. Wouters, D. Voorhees, and S. Suckewer, "Progress With Gain Measurements in Li-like Ions at 15.4 nm (AlXI) and 12.9 nm (SiXII)," Proceedings of SPIE Conference in San Diego, CA, (1987).

[11]D. Kim, C.H. Skinner, A.W. Wouters, E. Valeo, D. Voorhees, and S. Suckewer, "Soft X-Ray Amplification in Lithium-like AlXI (154 Å) and SiXII (12.9 Å)," Princeton University Plasma Physics Laboratory Report PPPL-2502 (March 1988) 37 pp.; submitted to J. Opt. Soc. Am. B.

[12]C.H. Skinner, D.E. Kim, A.W. Wouters, D. Voorhees, and S. Suckewer, "X-Ray Laser Sources for Microscopy," Invited Talk at Int. Symposium on X-Ray Microscopy, Brookhaven, NY, August (1987), to be published by Springer-Verlag.

[13]D.DiCicco, L. Meixler, C.H. Skinner, S. Suckewer, J. Hirschberg, and E. Kohen, "Soft X-Ray Laser Microscopy," Contributed Talk at Int. Symposium on X-ray Microscopy, Brookhaven, NY, August (1987), to be published by Springer-Verlag.

[14]R.E.Duvall, E.J. Valeo, and C.R. Oberman, "Nonperturbative Analysis of the Two-Level Atom—Applications to Multiphoton Excitation," Princeton University Plasma Physics Laboratory Report PPPL-2464 (August 1987) 31 pp; to be published in Phys. Rev. A.

[15]Y. Chung, P. Lemaire, and S. Suckewer, "Quenching of Spontaneous Emission Coefficients in Plasmas," Princeton University Plasma Physics Laboratory Report PPPL-2472 (September 1987) 14 pp; Phys. Rev. Lett. *60* (1988) 1122.

# THEORETICAL DIVISION

The Theoretical Division is engaged in a broad spectrum of state-of-the-art research on the physics of hot plasmas; both analytic theories and computational tools are developed. The primary activities focus on both short- and long-term goals of the magnetic confinement fusion program of the Laboratory; a small portion of the work is devoted to topics in related areas such as space plasma physics. Theoretical research is also done in support of the X-Ray Laser Program.

There were several significant trends in the work of the Division. In particular, there was an increased level of activity on physics and design issues associated with the Compact Ignition Tokamak (CIT), and on the consequences of the significant alpha-particle population in such devices. Several new theoretical approaches to plasma diagnostics were pursued. In theories of turbulent transport, attention began to turn from the quasilinear-like "estimates" of transport due to known fluctuations to methods capable of actually "predicting" quantitatively the self-consistent spectra and associated transport. Both the analytic and computational methods became substantially more sophisticated in their abilities to handle three-dimensional (3-D) effects. In general, the work of the Division reflected a continuing trend toward a very detailed quantitative, rather than simply qualitative, understanding of the plasma state both in the laboratory and in space.

The following detailed discussion is divided into five parts: (1) magnetohydrodynamics (MHD), (2) kinetic microinstability theory; (3) diagnostics and data analysis, (4) turbulence and transport, and (5) space plasma physics. However, in some cases there is considerable overlap between these topics.

## MAJOR ACTIVITIES

### Magnetohydrodynamics

Arguably the most significant success of plasma theory in general has been the use of the MHD description to explain and predict many details of the macroscopic behavior of tokamak plasmas, and important contributions have been made by the Theoretical Division. For example, the Division continues to maintain and develop a variety of large, complex computer programs useful for the analysis and design of tokamak experiments. These codes—as examples, the Princeton Equilibrium, Stability, and Transport code (PEST) and the Tokamak Simulation Code (TSC)—have been used for the design of a large number of tokamaks throughout the world: in the U.S., at Cal Tech, Columbia, GA Technologies, Inc., Los Alamos National Laboratory (LANL), Lawrence Livermore National Laboratory (LLNL), and Massachusetts Institute of Technology (MIT), among other places; internationally, in Canada (IREQ), Germany (Garching), Japan (Nagoya), and Switzerland (Lausanne). Recently, these tools have been used extensively to answer design questions associated with the CIT; the detailed accomplishments will be reported below, as will new analytical insights into the linear and nonlinear behavior of tokamak plasmas in the MHD approximation.

#### Applications of the Tokamak Simulation Code: CIT Simulations and Feedback Stabilization

The TSC[1] was used to simulate the current ramp-up, current flattop with burn phase, and the current ramp-down phase of a nominal CIT discharge. Of particular interest for machine design is an inverse problem: Given a predetermined evolution of the plasma current, shape, and position, determine the required time histories of the current in the poloidal-field (PF) coils. This is nontrivial because each coil has a dual role; it contributes to providing both the required inductive flux linkage to the plasma and the equilibrium fields, which determine the plasma shape and position. In principle, static free-boundary equilibrium solvers could be used to determine the necessary PF coil currents at any instant of time. However, such codes require a guess for the plasma profiles at each time, so the equilibrium states thus obtained may well not be dynamically connected to each other. The TSC, on the other hand, includes a two-dimensional (2-D) transport description. This transport model, which includes both neoclassical resistivity and a model of anomalous thermal conductivity, has been successfully calibrated against existing experiments,[2,3] so the ambiguity of the profiles obtained in a TSC simulation of CIT is replaced by the issue of whether the particular transport model used is applicable to the CIT device.

An important requirement for the PF system is the control of the divertor strikepoint location: during the burn phase of operation, the strikepoint will be swept across approximately 18 cm of the divertor plates to alleviate the severe heat loads experienced by the plates. The predicted evolution of plasma shape during a discharge is shown in Fig. 1, in which snapshots of the plasma-vacuum interface are shown at various times. For the simulations, the plasma

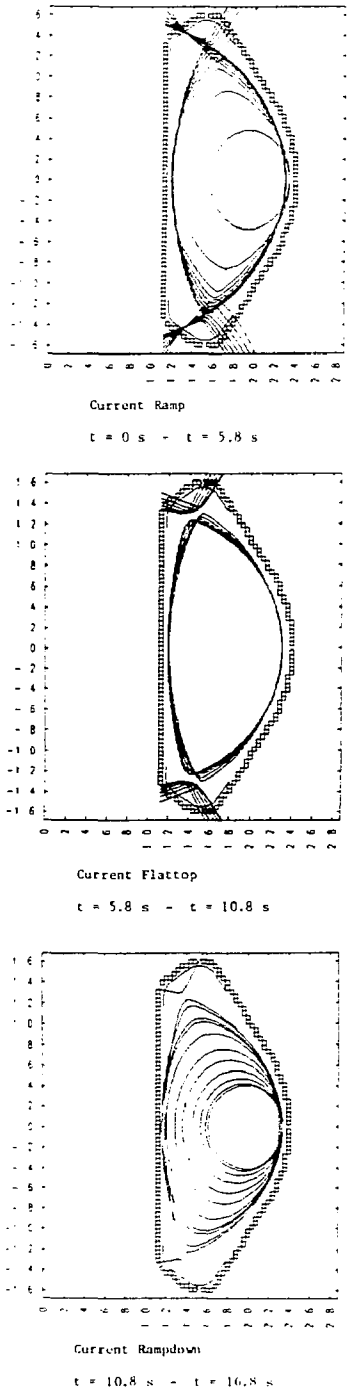


*Figure 1. Snapshots of plasma-vacuum interface at several times during Compact Ignition Tokamak nominal discharge. (88T1021)*

current $I_p$ and toroidal field $B_t$ were chosen to ramp piecewise linearly with time. The plasma is seen to grow from the outboard limiter and becomes divertor-limited at t = 2.0 sec. During the current flattop phase the divertor is swept in the direction of increasing triangularity. The calculated time histories of the PF coil currents during the simulation are shown in Fig. 2. Poloidal flux is increased in the plasma by PF coil currents swinging from positive to negative values. During the flattop phase, PF2 and PF3 are adjusted to provide the triangularity needed for the divertor sweep. Since the current in PF2 increases in this phase (in order to pull on the plasma), the current in PF1 must decrease to compensate for this loss of flux as well as to make up for resistive losses in the plasma.

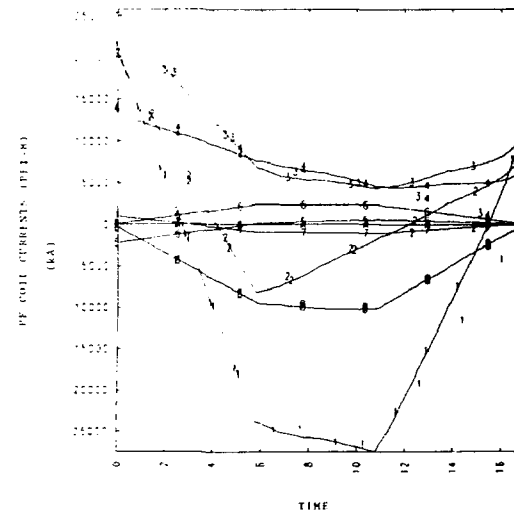


*Figure 2. Coil currents versus time in each of the eight poloidal-field coils for a Compact Ignition Tokamak nominal discharge. Flattop portion is for 5.8 sec < t < 10.8 sec. (88T1020)*

The TSC was also used to study feedback stabilization of tokamak plasmas. It is well known that elongated cross-section tokamak plasmas are subject to a pernicious axisymmetric MHD instability and must be stabilized both by the placement of nearby passive conductors as well as by an active feedback system which responds on the resistive time of those plates. Though it is clear that the placement of the feedback coils is important for the successful design of a feedback system, it was found that the careful placement of the flux pick-up loops for sensing the instability is equally important: in some cases, it is possible to place loops in locations which are intuitively sensible but which turn out to be completely inappropriate for use in a successful control system. As an example, the TSC was used[4] to analyze vertical position control issues for the modified Princeton Beta Experiment (PBX-M).

In Fig. 3 is given a schematic of the plasma, showing contours of poloidal flux and the poloidal-field coil system used for equilibrium, shaping, and feedback control. In addition, two pairs of up-down symmetric observation points are shown—one inboard with respect to the plasma, one outboard—at which the poloidal flux is monitored by the code. Surprisingly, the results of the numerical experiments with TSC showed that although the outboard observation pair can be used successfully in the feedback scheme to stabilize the plasma, the use of the inboard pair can never lead to a stabilized plasma.

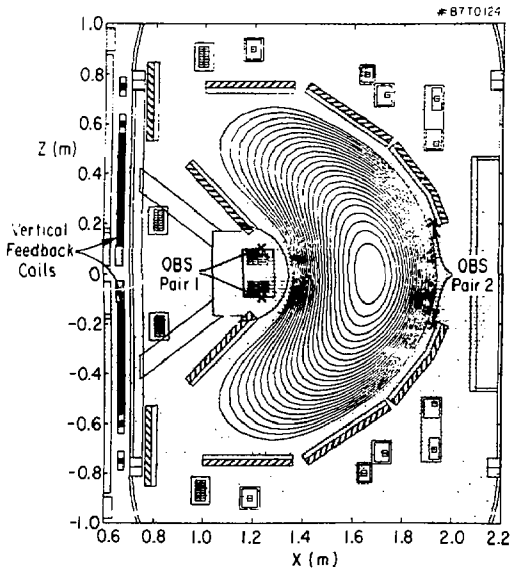


*Figure 3. Schematic of modified Princeton Beta Experiment (PBX-M). For the numerical simulations, observation (obs) pairs 1 and 2 are separately used for feedback control.*

To investigate the nature of the behavior, Rosen's $\delta W$ analysis[5] was generalized to include active control coils in the vacuum region and a simple feedback system analogous to the one used on the TSC simulations. The results of the analytical model suggest that the failure of certain flux observation positions to respond to the plasma motion results from the deformable nature of the plasma cross section. As part of the plasma instability, a perturbed magnetic field is produced in the vacuum region. However, if the plasma is sufficiently unstable it can modify its eigenfunction to deform its cross section so that a null in the perturbed vacuum magnetic field appears in the position of the observation loops. Since these loops will then be unable to detect the plasma instability, the feedback system will be rendered inoperative.

## 3-D MHD Equilibrium

Although the basic equations describing MHD equilibrium are well known, considerable physics remains unclear and must probably be elucidated by numerical solution of the equilibrium equations, which is nontrivial. This is particularly true for the non-axisymmetric, 3-D situations which arise because of the presence of magnetic field ripple (due to the discreteness of the toroidal-field coils) and because of nonaxisymmetric instabilities such as tearing modes. In such situations, not only islands but also stochastic regions can arise, and these complicate significantly both the physics and numerics of the solution.

Thus, a 3-D equilibrium code is essential for realistic modeling of equilibria. In addition, such a code, if coupled to equations describing the evolution of the pressure and current profiles, also describes the fully 3-D evolution of the plasma on the resistive and transport time scales, where the effects of inertia can be neglected. An example of physics on this time scale is the nonlinear evolution of tearing modes having poloidal mode number $m > 1$ (and sometimes $m = 1$). The quasi-equilibrium solution for these modes corresponds to the solution of the time-dependent equations in the limit of large Lundquist number (or magnetic Reynolds number) S. In this limit, a quasi-equilibrium code provides information complementary to that available from inertial time-dependent codes, which are typically limited to values of S much smaller than those encountered experimentally.

A new algorithm for obtaining 3-D equilibria was developed[6,7] which is quite different from the variational algorithms used by conventional codes that assume the existence of good flux surfaces. The magnetic field is updated at each step by first calculating the pressure-driven currents, then solving Ampere's law in the presence of those currents. Extensive convergence studies for 3-D equilibria with good flux surfaces demonstrate that the algorithm converges rapidly. Several numerical advances were needed to implement the algorithm: (1) an efficient method for solving 3-D magnetic differential equations to a specified accuracy, even in the presence of low-order rational surfaces; (2) an efficient Ampere's law solver in 3-D, which uses a general, numerically specified coordinate system; and (3) a numerical diagnostic for distinguishing islands and stochastic regions from good flux surfaces.

With the new code, work on equilibrium islands has focused on the application to tearing modes. In principle, one could follow the quasi-equilibrium growth of tearing modes until they saturate. However, it was found that the new code gives the solution for the nonlinearly saturated tearing mode directly, with no need to follow the evolution. Having found one such solution, one uses that as the initial guess

for the next run, varies the parameters slightly, and sees how the solution changes. This gives the dependence of the island width on such parameters as aspect ratio, current profile, and shape of the cross section. If one considers a set of parameters for which the tearing mode is stable, it is found that the island width vanishes. Instead of the familiar plot of growth rate as a function of parameters that one gets from a linear stability code, the present code gives a plot of the island width as a function of the parameters. In that mode of operation, it can be regarded as a nonlinear stability code.

The code was also used to study the effects of self-consistent plasma currents on the magnitude of the magnetic field ripple in tokamaks.[8] To do that, tokamak equilibria in which a ripple is imposed at the plasma boundary were calculated. By normalizing the calculated ripple to the local vacuum field, the effect of flux surfaces shifting into a region of larger ripple was separated out; that effect is included in the conventional model that superimposes a vacuum ripple on an axisymmetric equilibrium solution. It was found that the self-consistent effects always increase the magnitude of the magnetic ripple. This can lead to significant deleterious effects on the confinement of fusion alpha particles.

## MHD Stability

For fusion, an important goal of both experiment and theory is to optimize the plasma pressure ($\beta$). Above all else, this requires a detailed understanding of MHD stability. The Theoretical Division has particular expertise in this area, and a wide variety of calculations were performed.

The stabilization[9] and mechanisms[10] of sawtooth oscillation were studied in detail. The basic stabilizing effect comes from the pressure inside the magnetic island. This pressure prevents the angle of the separatrix at the x point from reaching zero. Thus, a singular current sheet does not form and the reconnection rate is drastically reduced. The anomalously fast crash of a sawtooth was modeled in two ways: (1) when the driving free energy is large while the shear is small, the usual Sweet-Parker reconnection rate gives a fast crash; (2) when microinstabilities inside the current sheet give rise to an anomalous resistivity, the reconnection rate increases accordingly [for some Tokamak Fusion Test Reactor (TFTR) data, this mechanism fits well]. These studies utilized the compressible nonlinear helical MHD code MH2D. (Since the sawtooth mechanism involves high-order terms in the inverse aspect ratio, the reduced equations cannot be used. For finite pressure cases the compressibility is critically important.) What is still neglected in these studies are the toroidal effects. This will not be a serious defect in the stabilization study, where the main effect depends on the local curvature of the magnetic field near the x point. In other studies where the global magnetic field curvature is important, one must use a fully 3-D code. Such a code, MH3D, was written and is currently being used to study sawtooth mechanism.

Recently it has been noted that there is an n=m=1 ideal instability in a plasma with $q > 1$ everywhere, but where $q - 1$ is small in some region. The nonlinear saturated behavior of these modes was calculated.[11] This mode is a possible candidate for the observed m=1, n=1 activity in nonsawtoothing discharges, which occur when there is lower-hybrid current drive stabilizing the sawtooth.

By using the PEST code, a detailed analysis was performed[12] of the ideal MHD stability of selected "supershots" close to the experimental $\beta$ limit. First, free-boundary MHD equilibria were obtained using the known poloidal-field coil currents. Then, the plasma profiles were varied until good agreement was found with the current and pressure profiles inferred from the Thomson scattering data. The plasma position was varied by adjusting the central plasma pressure to give good agreement between observed and calculated magnetics data. The results indicate that the plasmas may be unstable for n=1, but are stable for n=2 for all cases tried. Theoretically, n=1 stability depends on both the position of the conducting wall surrounding the plasma and the precise value of q(0); both internal and external kinks can appear, but not for the same discharge. The mode structure predicted with PEST is close to that observed on TFTR for the m=1, n=1 modes, but does not match the form of the 3/2 and 2/1 fluctuations associated with the degraded confinement.

A very convenient way to study the properties of ballooning modes in realistic toroidal systems is based upon the procedure developed by Greene and Chance,[13] who show how to solve the ballooning equation for equilibria consistent with the Grad-Shafranov equation but obtained as short-scale perturbations upon arbitrary, numerically calculated equilibria. The perturbative technique is such that the results obtained are well within the range of validity of the expansion. Since the zeroth-order equilibria can be quite arbitrary, this provides a convenient tool for understanding the effect of the equilibrium parameters on the stability of the mode. In particular, one can generalize the familiar S-$\alpha$ plot of Connor, Hastie, and Taylor[14] to a $(q_\psi, p_\psi, \psi)$ space. An example of this is seen in Fig. 4 for a bean-shaped tokamak plasma in the second stable region. There the space curve for the equilibrium threads itself beyond the ballooning unstable barrier into the second region. This technique enables one to determine how robust the unstable region is, how to optimize for the first stable region, and how accessibility to the second stable region can be obtained.

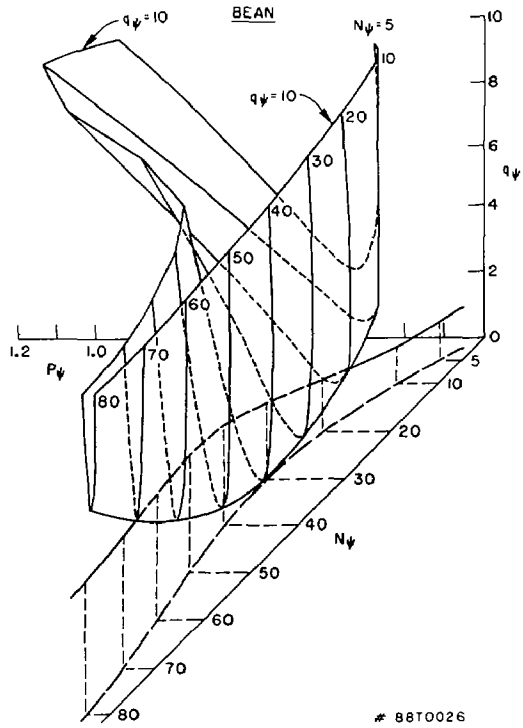


*Figure 4. Generalization of the S-α plot to $(q_\psi, p_\psi, \psi)$ space, for a bean-shaped tokamak plasma in the second stable region.*

One way to facilitate access to the second region of stability to ballooning modes in the Princeton Beta Experiment-Modification (PBX-M) is by broadening the usual peaked, ohmically driven current profile by noninductive means such as lower hybrid current drive (LHCD). For efficient operation, the parameters of the available LHCD system and the PBX-M configuration demand operation at higher magnetic fields and hence higher q. Numerical estimates for the MHD requirements for accessibility have shown that, for $q_{lim} \sim 6.3$, q(0) must be kept above about 1.5 and the decrement of current needed from the LHCD system is about 30% of the total plasma current. These estimates, done for a relatively broad pressure profile, are within the capabilities of the LHCD system.

Low shear at a rational surface was shown to be stabilizing to resistive tearing modes. The effect is quite strong for higher n and can also stabilize the n=m=1 mode, which is expected to play a role in sawtooth oscillations [a result corroborated by data from the TEXTOR (Tokamak Experiment for Technologically Oriented Research) experiment]. The dependence of the stability criterion on aspect ratio and q' was determined. Based on this model a low-q ($q_{axis} \approx 0.6$) tokamak was proposed.

In the design of CIT, an important issue is the stability properties of configurations with elongations up to 2, a new regime for tokamaks. The parameter range for safe operation was established. This essentially requires an adequate triangularity, in the range of 0.1 to 0.5, and a current limitation which maintains $q_{edge} \gtrsim 3.2$. The role of the plasma profiles is critical, and a range of allowed profiles was studied.

Further investigations were made into the properties of tearing modes in toroidal geometry. In particular, the influences of diamagnetic drift and beam-driven rotation were studied.[15] Since a toroidal tearing mode has many poloidal harmonics, it can interact with many rational surfaces. Also, reconnection and the formation of magnetic islands cannot take place unless the mode is nearly stationary in a frame moving with the plasma. It therefore follows that for a mode with, say, two rational surfaces, reconnection takes place at only one rational surface if the two surfaces have different rotation rates. If the two surfaces have the same rotation speed, reconnection takes place at both surfaces and the mode is considerably more unstable than in the unmatched rotation case. The Mirnov coils can measure the harmonic content of the toroidal mode, which depends strongly on whether reconnection takes place at one or both rational surfaces.

An understanding of MHD modes in the presence of energetic particles is important to the theory of confinement in thermonuclear regimes. In particular, bursts of large-amplitude, m=n=1 MHD fluctuations (fishbones) have been observed in tokamak experiments with high-power neutral-beam injection. These fishbone bursts are found to be correlated with significant losses of energetic beam ions and thus play an important role in limiting the beta values of tokamak devices. In order to study these low-n MHD modes for realistic toroidal equilibria with arbitrary cross sections and hot particle distributions, the NOVA-K code was developed.[16] This code is an extension of the previously developed nonvariational ideal-MHD stability code NOVA.[17] The new code solves a set of non-Hermitean integro-differential eigenmode equations in a general flux coordinate $(\psi, \theta, \zeta)$ system by employing Fourier expansion in the poloidal and toroidal variables $\theta$ and $\zeta$, and cubic-B spline finite elements in the radial ($\psi$) direction. The code was applied to the study of energetic particle effects on the internal kink modes, as well as to excitation of new trapped-particle-induced internal kink modes due to bounce-averaged magnetic drift resonances. For a circular cross-section numerical equilibrium, it was demonstrated that for $\omega \gtrsim (\omega_d)_h$, where $(\omega_d)_h$ is the average diamagnetic drift frequency of the hot component, the growth rate of the n=1 internal kink mode is reduced for small $\beta_h$, but turns around at $\beta_h/\beta_c \sim 3\%$, and increases with $\beta_h$ values. For $\omega \lesssim (\omega_d)_h$, though the internal kink is stabilized for $\beta_h/\beta_c > 3\%$, a new trapped-particle-induced internal kink mode is excited. For $\beta_h \to 0$, the trapped-particle induced mode evolves into a discrete shear-Alfvén wave with frequency below the shear-Alfvén continuous spectrum. Studies of energetic particle (including alpha particle) effects on MHD modes for

more realistic tokamak equilibria are in progress.

Analytic and numerical MHD stability calculations are important not only for tokamaks but also for stellarators, which are intrinsically three-dimensional and nonaxisymmetric. Thus, the effects on MHD stability of varying the width of the pressure profile were studied[18] in the Heliotron-E configuration. The calculation employed free-boundary stellarator expansion MHD equilibrium and stability codes, using a model for the Heliotron-E vacuum magnetic field which was constructed by means of a Biot-Savart integration of the exact coil configuration. The calculated critical beta values were in the same range as those observed in the Heliotron-E experiments.

## Kinetic Microinstability Theory

Even when MHD stability is achieved so that the plasma is grossly confined, microinstabilities can exist which limit the particle and energy confinement times and thus hinder or preclude ignition. In this section several detailed linear analyses which were performed are described. Nonlinear calculations are discussed under the heading Turbulence and Transport.

### Physics of the H-Mode

In magnetically diverted plasmas, the presence of a separatrix may influence in an important way the nature of microinstabilities, and this, in turn, may bear on the physics of the high (H) confinement mode. A prominent feature of auxiliary-heated discharges in the H mode is that, with the exception of the edge region, their density profiles tend to be relatively flat. Even though there can be a factor of 2 to 4 improvement in the energy confinement time $\tau_E$ for such plasmas, the electron thermal transport nevertheless remains anomalously large by at least two orders of magnitude. During the last year, analytic and numerical studies demonstrated that, even in the limit of zero density gradient, low-frequency microinstabilities can persist because of the nonzero temperature gradient.[19] The weaker overall pressure gradients in the interior region of H-mode plasmas do lead to correspondingly smaller values of the electron thermal diffusivity $\chi_e$ which is, in turn, consistent with the observed improvement in $\tau_E$ (Refs. 19 and 20). However, in order to be consistent with the thermal flux coming from the interior, the local $\chi_e$ in the very steep gradient edge region must be small. To demonstrate that the drift-type microinstabilities are indeed either very weak or absent here, a study was made of electrostatic instabilities in the very steep gradient region near the plasma edge just inside the separatrix for H-mode, neutral-beam-heated, diverted tokamak plasmas. To do this, a comprehensive kinetic stability code[21] was interfaced with a model tokamak MHD equilibrium[22] which incorporated both a separatrix and an x point, thus taking into account the strong local shear effects in the vicinity of the separatrix. Edge data obtained from H- and Low-(L) mode PDX (Poloidal Divertor Experiment) discharges were used as input. The results indicate that the proximity of the separatrix has a significant stabilizing influence. In particular, the finite-$\beta$-modified drift modes are expected to be "stable" over a region extending several centimeters inside the separatrix for H-mode profiles. These enhance local stability properties near the separatrix thus support the notion that the observed thermal transport in H-mode plasmas can be reconciled with the microinstability picture.[20]

In order to address the question of what physical processes could be responsible for actually triggering the transition from the L-mode to the H-mode type of equilibrium, studies were carried out[23] extending previous work of Hinton. He had proposed that the onset of a large ion temperature gradient near the separatrix could be the mechanism triggering this transition and that the development of such a gradient could be explained by ion neoclassical effects in the highly collisional (Pfirsch-Schlüter) regime. Specifically, if the ion $\nabla B$ drift is toward the x point, a very steep gradient is predicted to occur for a sufficiently large ion thermal flux. However, for the same ion heat flux, the gradient is predicted to be significantly weaker if the ion $\nabla B$ drift is away from the x point. This picture has been supported by experimental results from H-mode discharges in the ASDEX and D-III-D tokamaks—i.e., the L- to H-mode transition has been observed to occur at significantly lower power when the $\nabla B$ drift is toward the stagnation point. Recently, it was demonstrated[23] that the basic qualitative conclusions drawn from the strongly collisional neoclassical model can persist in the physically more relevant lower collisionality (plateau and banana) regimes and even when enhanced cross-field ion thermal losses are taken into account.

### Alpha-Particle Effects

Although for the present-day machines the effects of alpha particles are essentially negligible, the physics of alpha particles is of crucial interest for CIT and future machines. Theoretical work on this issue was begun by performing a comprehensive electromagnetic kinetic stability calculation on the effects of hot alpha and thermalized helium ash particles in tokamaks. For modes that can be unstable even without the alpha particles, such as the trapped-electron drift mode or the kinetically-calculated MHD ballooning mode, the effects of the alpha and the helium ash particles can be either destabilizing or stabilizing, depending on the parameters involved. For a CIT case, the trapped-electron drift mode interacts only very weakly with the alphas, but causes significant quasilinear transport of the helium ash, while the MHD ballooning mode is strongly destabilized by the alphas and transports them with a flux comparable to that of the background ions and electrons.

# Diagnostics and Data Analysis

Often attempts to understand the fundamental physics of confined plasmas leads to new ideas about experimental diagnostics and data analysis, and vice versa. Such is the case with the next two topics.

## Plasma Rotation

A possible global diagnostic for alpha-particle confinement in ignited plasmas such as CIT is plasma rotation; however, neoclassical effects make the analysis nontrivial. Rotation can be related to the process of electrically charging the plasma. For example, neutral-beam injection onto a trapped orbit whose initial velocity is in the same direction as the plasma current constitutes an effective inward radial current because the ions' position, averaged over a banana orbit, lies at a smaller minor radius than its birth radius. Banana-tip diffusion of alpha particles in a reactor, arising from small deviations from axisymmetry, produces an outward radial current. The question is then: How does a tokamak generate a compensating radial current to maintain overall charge neutrality? Calculations were performed using an axisymmetric neoclassical model of the bulk plasma ions and allowing for a net toroidal torque to be exerted. (In the absence of torque, no radial ion current can arise.) It was found that the plasma develops a small radial electric field $E_r' = E_r - \nu_\phi B_\theta / c$ in a frame moving with the local rotation velocity $\nu_\phi$. Mathematically, the calculations reduce to a standard neclassical equation whose solution gives the orthogonal conductivity, defined by the relation $\sigma_\perp = j_r / E_r'$. In practice, $\sigma_\perp$ turns out to be sufficiently large that a potential drop $e\phi' < T$ can easily drive bulk-plasma ion neoclassical radial currents equal and opposite to the forcing currents in the examples cited above. Of more interest is the $J_r B_\theta / c$ torque necessarily associated with the bulk-plasma ion current. Thus, a reactor plasma losing alpha particles by banana-tip diffusion will spontaneously start to rotate. The time $\tau_S$ required to spin up to a rotation velocity comparable to the ion thermal speed is $\tau_S \approx 2\tau_E / \Delta$ where $\tau_E$ is the energy confinement time and $\Delta$ is the fraction of alpha particles lost.

## Synchrotron Radiation

Synchrotron radiation provides another possible diagnostic tool. One way in which this radiation might be used would be to infer the electron distribution function $f_e$ from the 2-D radiation pattern $R(\omega, \theta)$, i.e., the radiation as a function of frequency and observation angle. This approach is limited by poor theta resolution due to the small number of detectors, so there may be advantages to a rather different approach.[24] Here, radio-frequency (rf) power is introduced into the plasma to create an instantaneous perturbation that decays in time. The problem one then poses is to deduce the velocity-space details of this perturbation, given the time-dependent radiation pattern $R(\omega, t)$; these details of the source function can provide useful information on the rf power absorption of high-energy electrons. In this method only one detector is needed, and one can exploit the separation in time scales between the decay of radiation associated with the perturbation and the fast time response of the detectors. Moreover, if the perturbation can be made in a narrow range in velocity space, it may be possible to infer plasma parameters such as the ion charge state or the current profile.

A different use of synchrotron radiation was made by analyzing synchrotron data from lower hybrid current drive runs on the Princeton Large Torus (PLT). By transforming the radiation measurements to moments of the electron distribution at each energy, constraints were obtained on $f_e$ that enable one to picture the velocity-space dynamics of the energetic electrons.

# Turbulence and Transport

In this section are described a variety of nonlinear calculations directed at improving one's understanding of the anomalously short confinement times in tokamaks.

## Ion Cyclotron Radio-Frequency

Both quasilinear theory and a single-particle model were applied to calculate the radial flux of energetic trapped ions induced by ICRF waves in tokamaks. It was shown that the flux consists of both classical and neoclassical contributions, each composed of convective and diffusive terms. The convective term may become significant if the wave spectrum is asymmetric in the toroidal wave number. The results[25] indicate that ICRF-induced radial transport should be unimportant for present experiments.

## Relativistic Collision Operator

Collisional effects are known to be important in a variety of processes which depend strongly on a population of fast electrons, such as synchrotron radiation or absorption of rf waves. Now that machines which operate at temperatures as high as 40 keV are contemplated, it becomes necessary to use a relativistic collision operator. Although the nonrelativistic, Fokker-Planck formulation of collisions in a plasma has long been known, it has usually been used in the Landau integral form; however, for numerical work a differential representation is preferred. Recently such a representation was found for the relativistic collision operator[26]: it is expressible in terms of five scalar potentials, each of which satisfies an elliptic differential equation. Work is underway to incorporate this collision operator into a multigrid Fokker-Planck code.

## Supplementary Heating

Recent experimental results in tokamaks with powerful supplementary plasma heating via neutral injection and radio waves have shown confinement deterioration associated with such heating. Both theoretical and numerical investigations were made on the effects of such heating on plasma confinement.

As the neutral particles ionize along the injection path, a polarization electric field is generated at the boundaries of the beam, creating an E × B drift of the beam and ambient particles across the magnetic field. In the absence of a rotational transform ($k_{\|} = 0$), numerical simulation confirms that such plasma convection leads to anomalous plasma diffusion associated with either neutral injection or rf plasma heating.[27] In the presence of a rotation transform ($k_{\|} \neq 0$) such polarization charges are quickly dissipated by the electron flow along the magnetic field. With steady-state injection of neutral beams, however, there exists a steady-state electric field arising from the residual charges associated with the balance of dissipation and source. Numerical simulation in slab geometry confirms such an electric field, and hence predicts plasma diffusion in the presence of steady-state neutral injection with a rotational transform. Preliminary results of two-dimensional plasma simulations in toroidal geometry indicate that neutral injection can be responsible for generating an up-down electric field as well as a turbulent convective electric field via neutral injection.

## Current Drive

Both ACT-I and CDX experiments have shown that a steady-state electron beam can be successfully injected into a toroidal magnetic field, raising the possibility of steady-state current drive in a tokamak. One of the key processes associated with the scheme is diffusion of the electron beam toward the center of the torus. It was determined[28] that even in the electrostatic, low-$\beta$ limit, beam electrons can diffuse across the magnetic field at an anomalously fast rate. This occurs because the electrons in the beam are in resonance with the waves generated by the beam-plasma instability, so that they experience a nearly dc electric field, causing large E × B excursions. Numerical simulations confirm both the existence and the scaling of such anomalous beam diffusion.

## Alpha-Particle Losses

One of the key transport issues in reactor-grade tokamaks concerns the rate of loss of the alpha-particle fusion products. To study the possible loss mechanisms, a Hamiltonian guiding-center formalism[29] was employed. It was learned that on some devices severe restrictions must be imposed on ripple magnitude in order to prevent depletion of the trapped-particle population due to stochastic ripple-induced loss. Previous calculations for the International Tokamak Reactor (INTOR) arrived at significantly different results, indicating the need for an independent calculation. The present results for INTOR indicate fairly low fusion alpha power loss, primarily due to stochastic diffusion, amounting to about 3%, in agreement with earlier work.[30] However, the results are strongly dependent on the plasma density profile assumed and on the magnitude and profile of the plasma current. In addition, the presence of low-mode-number MHD modes, such as the sawtooth, can significantly accelerate alpha-particle loss. It was found that the original, smaller CIT design was marginal for alpha-particle confinement, and this result led to a redesign which substantially reduced the ripple magnitude.

The alpha-particle distribution due to stochastic ripple loss leads to a distribution in the outer regions of the CIT which is both inverted in energy space and anisotropic. It is possible for such a distribution to drive magnetosonic waves unstable, which would modify the alpha-particle distribution function so as to recover some of the alpha-particle energy that would otherwise be lost. This situation was analyzed by postulating that a sawtooth mode would bring all the alpha particles existing inside the $q = 1$ surface at the time of the sawtooth to a region just beyond the $q = 1$ surface. Further, it was assumed that the ripple variation in the field strength was large enough to lead to rapid loss of the alpha particles, so that immediately following the sawtooth there would be a flux of 3.5-MeV alpha particles through the outer parts of the CIT. It was then shown that those particles would interact resonantly with a magnetosonic mode whose frequency was a large mutliple of the doubly charged alpha-particle gyrofrequency. The mode was shown to be trapped at a radius of order 0.7a by refraction due to the decrease in density. It was also shown that the mode propagated in a manner that kept $k_{\|}$ small enough that transit-time damping by the electrons was smaller than the growth produced by the alpha particles. A quasilinear analysis showed that the mode quickly saturates in a time short compared to the length of the pulse of the outgoing alpha particles. Saturation occurs by a flattening of the alpha-particle distribution in energy until growth is just balanced by the electron damping of the wave. Under these conditions a significant fraction of the alpha-particle power goes to the wave and is immediately converted to heating the electrons.

## Self-Consistency Effects on Turbulent Transport

"Anomalous" transport (of either particles or heat) has often been estimated in the "passive" approximation, in which the perturbing fluctuations are assumed to be given rather than determined self-consistently. Although such a description is justifiable when the perturbations are extrinsic (due to coil asymmetries, say), it is dubious when they are produced by turbulence. Several analyses were done which bear on this issue.

First, a generalization of the standard Balescu-Lenard operator (for binary scattering due to electrostatic fluctuations in spatially uniform, unmagnetized plasma) was developed[31] which unifies a number of previously disparate formalisms. The generalized operator, constructed using an action-angle formalism, is valid for electromagnetic fluctuations and for any geometry for which the unperturbed motion is integrable. It thus applies to either toroidal, cylindrical, or slab geometry. Furthermore, it describes the effects of fluctuations of all wavelengths, so one can treat on the same footing both the effects of short-wavelengths perturbations, which give rise to axisymmetric collisional transport, as well as the effects of longer wavelength turbulent and ripple fluctuations. The unification makes it clear that these three transport mechanisms share, under appropriate conditions, important properties such as intrinsic ambipolarity. Along with the turbulent "anomalous diffusion coefficient" D calculated for tokamaks in previous works (cf. Ref. 32), the generalized operator also implies an anomalous pinch term F of closely related structure and scaling, so that the particle confinement times for one species computed from this self-consistent theory are much longer than they would be from a theory involving D alone, analogous to the situation in standard neoclassical theory.

The theory of self-consistent turbulent transport which has been most commonly used for plasmas is the so-called "clump" theory. Because some of the predictions of that theory are dramatic and counterintuitive, it was deemed important to analyze the foundations of the scheme in view of the many well-understood facets of the general theory of turbulence.[33] The results of that analysis revealed substantial logical inconsistencies in current implementations of the clump theories, and vitiate certain general conclusions. For example, whereas the old theory led to the conclusion that the effects of self-consistent magnetic fluctuations on electron thermal transport should be very small,[34] the new analysis[35] concluded the opposite: namely, that self-consistent electron heat transport should be of the same order as the test particle transport.

### Gyrokinetic Particle Simulation

A viable method for numerically studying the physics of low-frequency plasma turbulence is the technique of gyrokinetic particle simulation. Investigations into the physics of gradient-driven microinstabilities continued with a study of ion-temperature-gradient-driven drift modes. It was found that n=0 radial eigenmodes dominate the saturated stage of the instability. The steady-state thermal conductivity tends to be lower than its quasilinear value and depends strongly on the dissipation properties of the system. In a related study of particle flux, it was found that the bulk of the observed cross-field diffusion comes from the resonant electrons which are E × B trapped, and that electron-ion collisions can enhance the diffusion by repopulating the resonant region.

The formalism was extended nontrivially by deriving various sets of self-consistent, energy-conserving, nonlinear, gyrokinetic equations—electromagnetic, in slab geometry; electrostatic, in toroidal geometry—from the gyrophase-averaged Vlasov-Maxwell system. The method is based on a systematic Lagrangian variational principle in phase space, followed by Lie transformation. The resulting formulation[36] is valid for arbitrary values of $k_\perp \rho_i$, and is thereful suitable for studying both the linear and, especially, nonlinear evolution of microinstabilities in finite-$\beta$ tokamak plasmas. Since the underlying conservation laws of the original Vlasov-Maxwell equations are preserved in the present formulation, the equations can be used directly for gyrokinetic particle simulation studies, and such simulations are pressently being designed.

### Rigorous Bounds on Transport

Finally, the theory of rigorous bounds on anomalous transport was extended in several directions. In particular, it was shown[37] that a two-point constraint, additional to the global energy balance, is crucial if one wants to obtain a bound which predicts both the quasilinear as well as the strong turbulence scalings, and the first calculations using such a constraint were performed. Rigorous upper bounds were obtained for a variety of regimes for particle and heat transport in specified stochastic magnetic fields.[37,38] The general theory of two-point constrants has applications to problems of fluid dynamics as well as to plasma physics, and appears to figure importantly in modern attempts to derive practical statistical closures by marrying statistical decimation and realizability constraints.[39]

## Space Plasma Physics

The Theoretical Division also devotes some attention to linear and nonlinear problems which arise in space plasma physics. The theoretical aspects of these problems have much in common with those which arise in tokamak physics: tools developed for tokamaks may be usefully applied to the space problems, and successful analysis of the space plasma problems provides important checks on the theoretical methods which may stimulate further analysis of the tokamak data. Much of this research is supported by the National Science Foundation. Several topics were considered in detail.

### Applications of Particle Simulation

The first two topics employ the numerical technique of particle simulation, which was developed and continues to be extended at Princeton. First, the injection and propagation into space of an electron beam from a satellite was studied via two-dimensional particle simulation.[40] It was found that the injection current can exceed the thermal return current carried by the ambient electrons as long as the beam density

is smaller than the ambient density.[41,42] Second, the formation and stability of the magnetopause current layer at the boundary of the solar wind and the earth's magnetic field was considered. Two-dimensional electromagnetic numerical simulations showed that such a current layer is unstable with respect to Kelvin-Helmholtz instability: This results in a broad boundary layer, in agreement with satellite observations.

## Waves in the Magnetosphere

A general theory was developed for the excitations of hydromagnetic waves within the earth's magnetosphere by the storm-time energetic ring current particles. The theory employed the low-frequency gyrokinetic equations, and assumed that the energetic particles are injected adiabatically. It was found[43] that the dominant destabilization mechanism is due to the magnetic drift-bounce resonances of energetic protons. The predicted instability features are also shown to be consistent with satellite observations.

Finally, a study was made of the ultra-low-frequency compressional Pc5 magnetic perturbations (Pc5 means wave periods in the range of 150-600 sec) which have long been observed around the earth's magnetic equator by satellites near geosynchronous orbit ($L \approx 6R_E$). These highly compressional magnetic perturbations are usually observed during the recovery phase of substorms; they are considered to be drift-mirror instabilities driven by high-$\beta$ anisotropic plasmas produced by the substorms. Multiple-satellite observations of compressional Pc5 waves during November 14-15, 1979 indicated[44] that the field-aligned mode structure of the compressional magnetic field $\delta B_{\parallel}$ is antisymmetric with respect to the earth's magnetic equator with a full latitudinal range of about 20°. The transverse magnetic components $\delta B_{\perp}$ have a symmetric parity. These observations were explained[45] by a comprehensive eigenmode analysis of compressional Alfvén waves for a two-component (hot and cold) anisotropic plasma in a dipole magnetic field. The eigenmode equations were derived from the gyrokinetic equations, including the hot trapped-particle effects. Though the latter are strongly stabilizing for $\delta B_{\perp}$ with symmetric parity, their effect is small for antisymmetric and one finds that the drift-mirror mode is unstable with a threshold condition $1 + 4\pi\partial P_{\perp}/B\partial B \leq 0$. Coupling to the transverse magnetic field reduces the instability threshold to a value[45] which is generally satisfied during the recovery phases of substorms. The theoretical results are in close agreement with the satellite observations of the mode structures, and suggest that the westward propagation of the Pc5 waves with respect to the ground occurs on the outer edge of the ring current plasma.

## X-Ray Laser

A previously developed nonperturbative theory of multiphoton transitions in two-level systems[46] was applied to transitions between adjacent Rydberg levels in an atom subjected simultaneously to static and slowly time-varying external electric fields. Resonance conditions, transition thresholds, and ionization thresholds (due to amplitude mixing between the upper state in the model and states of higher energy) were found which are in close agreement with experimental observations. Further developments in X-ray laser theory are reported in X-Ray Laser Studies.

### References


[1]S.C. Jardin, N. Pomphrey, and J. DeLucia, "Dynamic Modeling of Transport and Positional Control of Tokamaks," J. Comput. Phys. *66* (1986) 481.

[2]S.C. Jardin, J. DeLucia, M. Okabayashi *et al.*, "Modeling of Post-Disruptive Plasma Loss in the Princeton Beta Experiment," Nucl. Fusion *27* (1987) 569.

[3]M.H. Redi, W.M. Tang, P.C. Efthimion, D.R. Mikkelsen, and G.L. Schmidt, "Transport Simulations of Ohmic TFTR Experiments with Profile-Consistent Microinstability-Based Models for $\chi_e$ and $\chi_i$," Princeton University Plasma Physics Laboratory Report PPPL-2368 (March 1987) 53 pp; Nucl. Fusion (in press).

[4]N. Pomphrey and S.C. Jardin, "Feedback Stabilization of the Axisymmetric Instability of Tokamak Plasmas," Princeton University Plasma Physics Laboratory Report PPPL-2468 (September 1987) 21 pp; submitted to Nucl. Fusion.

[5]M.D. Rosen, "Infinite Wavelength Kink Instabilities in Uniform Current Cylindrical Plasmas with Rectangular Cross Sections," Phys. Fluids *18* (1975) 482.

[6]A.H. Reiman and H.S. Greenside, "Numerical Solution of Three-Dimensional Magnetic Differential Equations," J. Comput. Phys. (in press).

[7]H.S. Greenside, A.H. Reiman, and A. Salas, "A Nonvariational Code for Calculating 3-D MHD Equilibria," Princeton University Plasma Physics Laboratory Report PPPL-2469 (September 1987) 64 pp.

[8]J.L. Johnson and A.H. Reiman, "Self-Consistent, Three-Dimensional Equilibrium Effects on Tokamak Magnetic Field Ripple," Princeton University Plasma Physics Laboratory Report PPPL-2483 (October 1987) 18 pp.

[9]W. Park, D.A. Monticello, and T.K. Chu, "Sawtooth Stabilization Through Island Pressure Enhancement," Phys. Fluids *30* (1987) 285.

[10]W. Park, K. McGuire, D. Monticello, and W. Morris, "Sawtooth Oscillation: Mechanisms and Stabilization," in *Controlled Fusion and Plasma Physics* (Proc. 14th European Conf., Madrid, Spain, 1987) Vol. *I* (1987) 85.

[11]Avinash, J.B. Taylor, R.J. Hastie, and S.C. Cowley, "Nonlinear m=n=1 Modes with Hollow 'q' Profiles," Phys. Rev. Lett. (in press).

[12]J. Manickam and N. Pomphrey, "Ideal MHD Stability Properties of Pressure-Driven Modes in Low Shear Tokamaks," Nucl. Fusion *27* (1987) 1461.

[13]J.M. Greene and M.S. Chance, "The Second Region of Stability Against Ballooning Modes," Nucl. Fusion *21* (1981) 453.

[14]J.W. Conner, R.J. Hastie, and J.B. Taylor, "Shear, Periodicity, and Plasma Ballooning Modes," Phys. Rev. Lett. *40* (1978) 396.

[15]S.C. Cowley and R.J. Hastie, "Electron Diamagnetism and Toroidal Coupling of Tearing Modes," Princeton University Plasma Physics Laboratory Report PPPL-2478 (October 1987) 12 pp.

[16]C.Z. Cheng, "Kinetic-MHD Stability Calculations for Toroidal Plasmas using the NOVA-K Code," submitted to Workshop on Theory of Fusion Plasmas (Varenna, Italy, 1987).

[17]C.Z. Cheng and M.S. Chance, "NOVA: A Nonvariational Code for Solving MHD Stability of Axisymmetric Toroidal Plasma," J. Comput. Phys. *71* (1987) 124.

[18]G. Rewoldt, M. Wakatani, and J.L. Johnson, "Studies of Pressure Profile Effects on MHD Stability in Heliotron-E," Kyoto University Plasma Physics Laboratory Report No. PPLK-R-14 (April 1987); Plasma Phys. (in press).

[19]W.M. Tang, G. Rewoldt, and L. Chen, "Microinstabilities in Weak Density Gradient Tokamak Systems," Phys. Fluids *29* (1986) 3715.

[20]W.M. Tang, C.M. Bishop, B. Coppi, S.M. Kaye, F.W. Perkins, M.H. Redi, and G. Rewoldt, "Microinstability-Based Models for Confinement Properties and Ignition Criteria in Tokamaks," in *Plasma Physics and Controlled Nuclear Fusion Research 1986* (Proc. 11th Int. Conf., Kyoto, Japan, 1986), Vol. *I* (IAEA, Vienna, 1987) 337.

[21]G. Rewoldt, W.M. Tang, and R.J. Hastie, "Collisional Effects on Kinetic Electromagnetic Modes and Associated Quasilinear Transport," Phys. Fluids *30* (1987) 807.

[22]C.M. Bishop, "Stability of Localized MHD Modes in Divertor Tokamaks—A Picture of the H-Mode," Nucl. Fusion *26* (1986) 1063.

[23]W.M. Tang and F.L. Hinton, "Anomalous Transport Effects on the Neoclassical Model for the H-Mode Transition," GA Technologies, Inc. Report No. GA-A18885, 1987; Nucl. Fusion (in press).

[24]N.J. Fisch, "Inverse Problem for Incremental Synchrotron Radiation," Princeton University Plasma Physics Laboratory Report PPPL-2457 (June 1987) 8 pp.

[25]L. Chen, J. Vaclavik, and G.W. Hammett, "Ion Radial Transport Induced by ICRF Waves in Tokamaks," Princeton University Plasma Physics Laboratory Report PPPL-2441 (May 1987) 17 pp; Nucl. Fusion (in press).

[26]B.J. Braams and C.F.F. Karney, "Differential Form of the Collision Integral for a Relativistic Plasma," Phys. Rev. Lett. *59* (1987) 1817.

[27]H. Okuda and S. Hiroe, "Diffusion of a Plasma Subject to Neutral Beam Injection," Phys. Fluids *30* (1987) 1160.

[28]H. Okuda, M. Ono, and R.J. Armstrong, "Anomalous Electron Diffusion Across a Magnetic Field in a Beam-Plasma System," Princeton University Plasma Physics Laboratory Report PPPL-2486 (October 1987) 13 pp; submitted to Phys. Fluids.

[29]R.B. White and M.S. Chance, "Hamiltonian Guiding Center Drift Orbit Calculation for Plasmas of Arbitrary Cross Section," Phys. Fluids *27* (1984) 2455.

[30]L.M. Hively, "TF-Ripple Losses from a Non-Circular Tokamak," Nucl. Fusion *24* (1984) 779.

[31]H.E. Mynick, "The Generalized Balescu-Lenard Collision Operator: A Unifying Concept for Tokamak Transport," Princeton University Plasma Physics Laboratory Report PPPL-2458 (August 1987) 29 pp; J. Plasma Phys. (in press).

[32]A.B. Rechester and M.N. Rosenbluth, "Electron Heat Transport in a Tokamak with Destroyed Magnetic Surfaces," Phys. Rev. Lett. *40* (1978) 38.

[33]J.A. Krommes, "Statistical Descriptions and Plasma Physics," in *Basic Plasma Physics II*, edited by A.A. Galeev and R.N. Sudan (North-Holland, Amsterdam, 1984), Chap. 5.5.

[34]P.W. Terry, P.H. Diamond, and T.S. Hahm, "Self-Consistency Constraints on Turbulent Magnetic Transport and Relaxation in a Collisionless Plasma," Phys. Rev. Lett. 57 (1986) 1899.

[35]J.A. Krommes and C.B. Kim, "Magnetic Fluctuations CAN Contribute to Plasma Transport, 'Self-Consistency Constraints' Notwithstanding," Princeton University Plasma Physics Laboratory Report PPPL-2473 (September 1987) 41 pp; Phys. Fluids (in press).

[36]T.S. Hahm, W.W. Lee, and A. Brizard, "Nonlinear Gyrokinetic Theory for Finite-$\beta$ Plasmas," Princeton University Plasma Physics Laboratory Report PPPL-2498 (December 1987) 27 pp.

[37]J.A. Krommes and R.A. Smith, "Rigorous Upper Bounds for Transport Due to Passive Advection by Inhomogeneous Turbulence," Ann. Phys. *177* (1987) 246.

[38]J.A. Krommes, R.A. Smith, and C.B. Kim, "Rigorous Upper Bounds for Fluid and Plasma Transport Due to Passive Advection," in *Plasma Physics* (Proc. Int. Conf., Kiev, USSR, 1987), World Scientific Publishing Co., Singapore, in press.

[39]R.H. Kraichnan, "Decimated Amplitude Equations in Turbulence Dynamics," in *Theoretical Approaches to Turbulence*, edited by D.L. Dwayer, M.Y. Hussaini, and R.G. Voight (Springer, New York, 1983) 91.

[40]H. Okuda and J. Berchem, "Injection and Propagation of a Nonrelativistic Electron Beam and Spacecraft Charging," Princeton University Plasma Physics Laboratory Report PPPL-2438 (May 1987) 48 pp; J. Geophys. Res. 93 (1988) 175-195.

[41]H. Okuda, R. Horton, M. Ono, and M. Ashour-Abdalla, "Propagation of a Non-Relativistic ELectron Beam in a Plasma in a Magnetic Field," Phys. Fluids *30* (1987) 200.

[42]H. Okuda and J.R. Kan, "Injection of an Electron Beam into a Plasma and Spacecraft Charging," Phys. Fluids *30* (1987) 209.

[43]L. Chen and A. Hasegawa, "Theory of Magnetospheric Hydromagnetic Waves Excited by Energetic Ring-Current Protons," Princeton University Plasma Physics Laboratory Report PPPL-2456 (June 1987) 19 pp; Geophys. Res. Lett. (in press).

[44]K.J. Takahashi *et al.*, "Field-Aligned Structure of the Storm Time Pc5 Wave of November 14-15, 1979," J. Geophys. Res. *92* (1987) 5857.

[45]C.Z. Cheng and C.S. Lin, "Eigenmode Analysis of Compressional Waves in the Magnetosphere," Geophys. Res. Lett. *14* (1987) 884.

[46]R.E. Duvall, E.J. Valeo, and C.R. Oberman, "Nonperturbative Analysis of the Two-Level Atom—Applications to Multiphoton Excitation," Princeton University Plasma Physics Laboratory Report PPPL-2464 (August 1987) 31 pp; submitted to Phys. Rev. A.

## Additional Material Published in FY87 by Theoretical Division Personnel:


J.M. Albert and A.H. Boozer, "A Bounce-Averaged Monte Carlo Collision Operator and Ripple Transport in a Tokamak," Princeton University Plasma Physics Laboratory Report No. PPPL-2376 (September 1986) 20 pp.

M. Ashour-Abdalla and H. Okuda, "Transverse Ion Heating in Multicomponent Plasmas," Geophys. Res. Lett. *14* (1987) 375.

H. Biglari, L. Chen, and R.B. White, "Theory of Resistive Magnetohydrodynamic Instabilities Excited by Energetic Trapped Particles in Large-Size Tokamaks," Princeton University Plasma Physics Laboratory Report No. PPPL-2412 (February 1987) 9 pp.

A.H. Boozer, "Ohm's Law for Mean Magnetic Fields," J. Plasma Phys. *35* (1986) 133.

L. Chen, A. Bondeson, and M.S. Chance, "Asymptotic Stability Boundaries of Ballooning Modes in Circular Tokamaks," Princeton University Plasma Physics Laboratory Report No. PPPL-2445 (June 1987) 14 pp; Nucl. Fusion *27* (1987) 1917-1922.

C.Z. Cheng, H.P. Furth, and A.H. Boozer, "MHD Stable Regime of the Tokamak," Plasma Phys. Cont. Fusion *29* (1987) 351.

S.C. Cowley, R.M. Kulsrud, and T.S. Hahm, "Linear Stability of Tearing Modes," Phys. Fluids *29* (1986) 3230.

N.J. Fisch, "Theory of Current-Drive in Plasmas," Rev. Mod. Phys. *59* (1987) 175.

E.D. Fredrickson. J.D. Callen, K. McGuire *et al.*, "Heat Pulse Propagation Studies in TFTR," Nucl. Fusion *26* (1986) 849.

H.P. Furth and S.C. Jardin, "The Speromak as a Prototype for Ultra-High Field Superconducting Magnets," Princeton University Plasma Physics Laboratory Report No. PPPL-2465 (August 1987) 11 pp.

H.P. Furth, S.C. Jardin, and D.B. Montgomery, "Force-Free Coil Principles Applied to High-Temperature Superconducting Materials," Princeton University Plasma Physics Laboratory Report No. PPPL-2485 (November 1987) 11 pp.

R.J. Goldston, V. Arunasalam, M.G. Bell, *et al.*, "Energy Confinement and Profile Consistency in TFTR," Princeton University Plasma Physics Laboratory Report No. PPPL-2425 (April 1987) 16 pp.

R.J. Hawryluk, V. Arunasalam, M.G. Bell, *et al.*, "TFTR Plasma Regimes," in *Plasma Physics and Controlled Nuclear Fusion Research 1986* (Proc. 11th Int. Conf., Kyoto, Japan, 1986), Vol. *I* (IAEA, Vienna, 1987) 51.

K.W. Hill, V. Arunasalam, M.G. Bell, *et al.*, "Impurity and Particle Transport and Control in TFTR," Princeton University Plasma Physics Laboratory Report No. PPPL-2421 (April 1987) 17 pp.

W.N.G. Hitchon and H.E. Mynick, "Ripple in 'Transport-Optimized' Stellarators," J. Plasma Phys. *37* (1987) 383.

R.M. Kulsrud, "Course/Workshop on Muon-Catalyzed Fusion and Fusion with Polarized Nuclei," Princeton University Plasma Physics Laboratory Report No. PPPL-2461 (August 1987) 27 pp.

R.M. Kulsrud, "Polarized Advanced Fuel Reactors," Princeton University Physics Laboratory Report No. PPPL-2446 (July 1987) 15 pp.

K. McGuire, V. Arunasalam, M.G. Bell, *et al.*, "Coherent and Turbulent Fluctuations in TFTR," Princeton University Plasma Physics Laboratory Report No. PPPL-2435 (April 1987) 19 pp.

H.E. Mynick, "Alpha Particle Effects as a Test Domain for PAP, a Plasma Apprentice Program," Physica Scripta *T16* (1987) 133.

H. Okuda and M. Ashour-Abdella, "Ion Acoustic Instabilities Excited by Injection of Electron Beam in Space," J. Geophys. Res. (in press).

D. Post *et al.*, "Physics Aspects of the Compact Ignition Tokamak," Physica Scripta *T16* (1987) 89.

M.F. Reusch, L. Ratzan, N. Pomphrey, and W. Park, "Diagonal Padé Approximations for Initial Value Problems," Princeton University Plasma Physics Laboratory Report No. PPPL-2451 (June 1987) 17 pp.

E.R. Salberta, R.C. Grimm, J.L. Johnson, J. Manickam, and W.M. Tang, "Anisotropic Pressure Tokamak Equilibrium and Stability Considerations," Phys. Fluids *30* (1987) 2796.

B.L. Smith and H. Okuda, "Particle Simulation of Auroral Double Layers," Lasers and Particle Beams *5* (1987) 367.

R.B. White, "Transport in Systems with Destroyed Magnetic Flux Surfaces," in *Turbulence and Anomalous Transport in Magnetized Plasmas*, edited by D. Gresillion and M.A. Dubois (Editions de Physique, Orsay, 1987) 155.

K.L. Wong and C.Z. Cheng, "Neoclassical Diffusion of Heavy Impurities in a Rotating Tokamak Plasma," Phys. Rev. Lett. *59* (1987) 2643.

# TOKAMAK MODELING

A variety of computer codes are being utilized and developed by the Tokamak Modeling Group at the Princeton Plasma Physics Laboratory (PPPL). The codes are used to interpret tokamak experiments at PPPL and at other laboratories and to assist in the design of future machines [Compact Ignition Tokamak (CIT), International Tokamak Reactor (INTOR), Tokamak Ignition/Burn Experiment (TIBER)] as well as in the operations planning of experiments on present machines [Tokamak Fusion Test Reactor (TFTR), Princeton Beta Experimental Modification (PBX-M)].

The BALDUR plasma transport code, in both one-dimensional (1-D) and one and one-half dimensional ($1\frac{1}{2}$-D) versions, models the widest range of physical processes affecting plasma transport for two hydrogen species and up to four impurities. The PLANET code simulates two-dimensional (2-D) transport in the plasma scrape-off layer, and the DEGAS code calculates the transport of neutral atomic and molecular hydrogen through plasmas in complex magnetic geometries. The transport of impurities is modeled by the MIST code. The WHIST/ICRF code [(developed with W. Houlberg at the Oak Ridge National Laboratory (ORNL)] is also used for $1\frac{1}{2}$-D plasma transport simulations, particularly for radio-frequency (rf) heating scenarios. The SURVEY and TRIUMPH codes are used to compare a wide range of plasma parameters for $Q \sim 1$ scenarios and to evaluate a wide range of particle transport models for particular experiments, respectively.

## ONE-DIMENSIONAL PLASMA TRANSPORT

The one-dimensional BALDUR code was used for continued testing of theoretically based confinement models for anomalous electron and ion losses, as well as for predictive simulations of future TFTR performance near $Q = 1$.

The transport model study concerned gas and pellet-fueled discharges on TFTR, Alcator-C, and ASDEX (Axially Symmetric Divertor Experiment). In simulating experiments on the three different tokamaks, the models, which were calibrated on TFTR alone,[1] were found to predict confinement and electron temperatures to within about 20%. Simulation of the ASDEX multipellet-fueled discharges served as an important validation of the model predictions, since the quasi-steady-state peaked density profiles permitted a clear signature of improved confinement from reduced $\eta_i$ transport. This improved confinement is due to suppression of anomalous ion losses when $\eta_i = (\partial \ln T_i)/(\partial \ln n_i)$ is below a critical value, 1.5.

As part of a study of TFTR $Q \sim 1$ performance, the alpha storage mode concept of S.J. Zweben was investigated in a series of BALDUR runs and was found to be of potential interest even in $Q < 1$ situations. The simulations were used to find the expected regimes of $n_\alpha/n_e$ and $\beta_a$ so that theorists could study potential alpha-particle-driven instabilities. In addition, these modeling efforts sought ways to observe strong alpha-heating effects despite $P_\alpha/P_{tot} = 20\%$ at $Q = 1$. The code results verified simpler preliminary estimates of the feasibility for TFTR of a significant alpha-particle build-up, during neutral-beam heating at low density as well as the consequent appearance of an alpha heating pulse following densification by pellet fueling. The time-independent SURVEY code was also used in this study. Results were in agreement with the BALDUR simulations of alpha-particle densities and heating.

A well-documented version of the BALDUR transport code[2] and the set of fourteen standard test cases[3] have been accepted for publication in the Computer Physics Communications Journal and program library and will now be available to the wider fusion community. More recent versions of the code include the calculation of the Shafranov shift and improved beams packages. The beam simulation package was extended to simulate two beam species and beam-beam fusion reactions were added.

## $1\frac{1}{2}$-DIMENSIONAL BALDUR CODE TRANSPORT SIMULATIONS

The $1\frac{1}{2}$-D BALDUR transport code was upgraded to include more detailed interactions with MHD instabilities,[4] more realistic models for pedestal boundary conditions, the L-mode transport model developed by Tang and Redi,[1] an improved treatment of impurity influx, the bootstrap current, and a new algorithm for mapping from an equilibrium computed on a rectangular grid to flux coordinates.[5]

Three types of MHD instabilities are now included in the $1\frac{1}{2}$-D BALDUR code—sawtooth oscillations, ballooning modes, and tearing modes.[4] Sawtooth oscillations are simulated using a differential reconnection model, with simpler options available for periodic central profile flattening or steady-state enhanced transport. The ballooning mode stability condition is computed for short wavelength ideal

modes on each flux surface, and the plasma transport can be enhanced where these modes are unstable. Saturated tearing-mode magnetic-island widths are computed and the plasma profiles are flattened in the neighborhood of each island. It is found that sawtooth oscillations and ballooning modes can have a substantial effect on ignition, mainly because they flatten the density and temperature profiles over a broad region across the center of the plasma, in elongated high-current tokamak reactor designs such as CIT,[6-8] INTOR, and TIBER.[9] It is much easier to reach ignition in simulations with peaked profiles (particularly density).[8,10]

New models were developed for BALDUR to simulate the density and temperature pedestals that are observed just inside the separatrix during the H-mode transition and in high-density tokamaks.[11] This is an essential step needed to simulate the effect of H-modes on the shape of the profiles as well as on the confinement times.

The BALDUR simulations of complete, reference discharges of CIT were updated to match the present machine design, and now they include such effects as plasma growth onto the divertor during current ramp,[7] as shown in Figs. 1 and 2. These simulations provide plasma parameters for other groups doing diagnostic design for CIT and detailed stability calculations of CIT equilibria.

In the process of developing these simulations, several aspects of the physics of CIT discharges were studied.[12] For instance, the impact of the time evolution of the edge safety factor on the plasma current profile and the sawtooth mixing radius was examined and the ramp scenario optimized accordingly. The inclusion of bootstrap current also led to improved predictions for the performance of CIT by reducing, slightly, the size of the sawtooth mixing radius. On the other hand, it was noted that when the electron density was held constant in time without helium ash removal, the burn-up of deuterium and tritium in fusion reactions constituted an effective means of burn control.

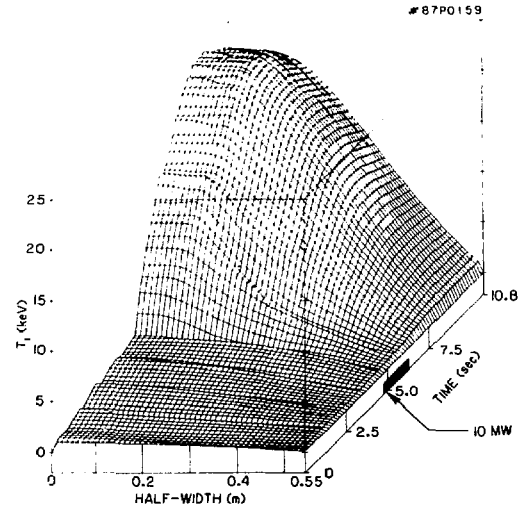


*Figure 2. Ion temperature as a function of half-width and time for a Compact Ignition Tokamak simulation with 10 MW of auxiliary heating applied between 4.8 and 6.3 sec. The plasma is ignited by 6 sec.*

Previous studies of CIT pointed out the deleterious effects of profile flattening by broad sawtooth oscillations on the chances for ignition[6] and on plasma stability. Recently, these same arguments were found to hold true for several of the present designs for engineering reactors, most notably INTOR and TIBER.[9]

An in-depth investigation of the tokamak density limit is now in progress. The presently accepted cause of this limit is excessive radiation by impurities.

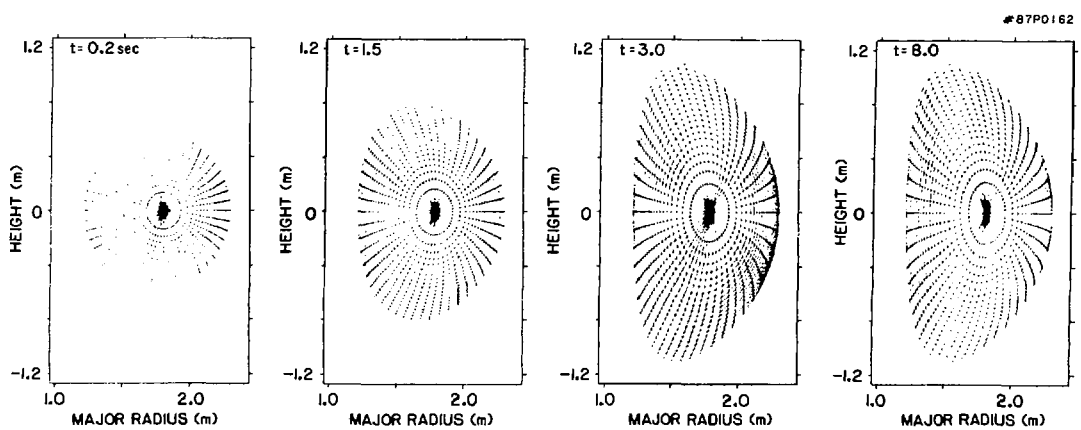


*Figure 1. Plasma cross sections for a selection of times during the start-up and burn phase of the Compact Ignition Tokamak. In the last frame on the right, the plasma beta is about 3.8% and it is producing about 300 MW of fusion power (alpha plus neutron power).*

One preliminary result of this study is that the dependence of the Murakami-Hugill limit on plasma current can be reproduced in BALDUR simulations with a relatively simple physical model.

## WHIST/ICRF PLASMA TRANSPORT MODELING

The WHIST/ICRF integrated code package,[13] which has been developed jointly by ORNL and PPPL over the past few years to simulate ICRF-heated tokamaks, was used to assess the conditions under which Q = 1 can be attained in TFTR plasmas. The package consists of the WHIST two-dimensional MHD equilibrium, one-dimensional flux-surface-averaged transport code, and the ICRF two-dimensional wave propagation and power deposition code. Tritium-pellet-fueled discharges in TFTR, which are heated by an additional 20 MW of neutral-beam injection (NBI) and 7 MW of ion-cyclotron radio frequency (ICRF) power, were simulated using an empirical transport model based on L-mode confinement scaling. The value of $\chi_e$ was adjusted dynamically so that the global value of $\tau_e$ remained consistent with scalings of the form $(\tau_E^{-2} = (\tau_o^H)^{-2} + (\alpha\tau_{aux})^{-2}$, where $\tau_o^H$ is the neo-Alcator formula, $\tau_{aux}$ is Goldston's formula, and $\alpha$ is an adjustable constant multiplier. Calculations indicate that the NBI power penetrates reasonably well to the plasma core and that the ICRF power will be deposited within the a/3 radius. For $\tau_E$'s of 250-300 msec, the results indicate that Q = 1 can be attained at central electron densities of $1.5 \times 10^{14}$ cm$^{-3}$, with $T_i \sim 20$ keV and $T_e \sim 10$ keV. This value of the confinement time represents a factor of 1.7 to 2 increase beyond the Goldston L-mode level. Some of this increase may be expected to arise from isotope effects, which have not been included in the current model. Furthermore, preliminary studies of the supershot regime using the Tang-Redi[1] transport model are in rough agreement with the experimental observation that confinement can be enhanced above the L-mode level, at least in this regime of operation.

## PLASMA REQUIREMENTS FOR Q ~ 1 IN TFTR

The plasma optimization code SURVEY, first described in last year's annual report, was extended to generate sequences of model plasmas with a given Q or $\tau_E$. The plasma characteristics of these model plasmas were compared with those of plasmas which have already been produced in TFTR to find routes to higher Q performance. They have also been used to evaluate the TFTR's potential for producing "interesting" alpha-particle effects and define the conditions under which these effects (see the discussion of the "alpha storage mode" in the TFTR Physics Program section) could be produced.

A new feature of Q contours in the Lawson diagram of $T_{eo}$ versus $\bar{n}_e\tau_E$ is a broad local minimum in $T_{eo}$. This arises from the determination of the ion temperature by a power balance—in contrast to previous work of this kind, in which $T_i \propto T_e$. The $T_e$ levels out as the density rises along a Q contour because the $T_i$ needed to produce the given level of fusion power could not be supported against electron-ion temperature equilibration losses with a lower $T_e$. As a result, we find both a minimum $\tau_E$ and $T_{eo}$ for a given Q.

The plasma requirements for Q = 0.5 and 1 in full power D-T (deuterium-tritium) plasmas for both supershot and L-mode density and temperature profile shapes are given in Table I. The plasmas described have the minimum $\tau_E$ (and $T_e$ is near the minimum) for the desired Q. The present supershot energy confinement and $T_{eo}$ are sufficient for Q = 0.5 if this regime can be extended to higher power, density, and plasma current while lowering the $Z_{eff}$. Similarly, the anticipated L-mode $\tau_E$ with $I_p$ = 3 MA is sufficient for Q = 0.5 if $Z_{eff}$ and the plasma density can be held down to the desired level. This year's preliminary experimental results on ion-thermal transport (see TFTR Physics Program section) could change these results (which assume neoclassical ion thermal transport) by raising the requirement for $T_{eo}$ by 3-4 keV and for $T_{io}$ by 5 keV. In this event the

**Table I. Deuterium-Tritium Plasma Requirements.**

| | Units | Supershot | | L-Mode | |
|---|---|---|---|---|---|
| | | Q=0.50 | Q=1.00 | Q=0.50 | Q=1.00 |
| $\tau_E(a)$ | sec | 0.129 | 0.215 | 0.152 | 0.258 |
| $\bar{n}_e$ | $10^{19}$/m$^3$ | 5.2 | 7.3 | 4.4 | 6.5 |
| $n_{eo}$ | $10^{19}$/m$^3$ | 11.9 | 16.5 | 6.0 | 8.9 |
| $T_{eo}$ | keV | 6.8 | 10.4 | 7.3 | 11.3 |
| $T_{io}$ | keV | 19.1 | 21.2 | 23.7 | 24.1 |
| $<\beta_{tot}>$ | % | 1.2 | 1.6 | 1.3 | 1.9 |

optimal density (minimum $\tau_E$ for fixed Q for Q = 0.5) is below the range of validity for SURVEY, and effects such as beam-beam fusion reactions and Coulomb collisions between fast ions should be added to the simulations.

## PLASMA TRANSPORT IN THE SCRAPE-OFF REGION

In the scrape-off region the magnetic field lines are open in the sense that they intersect a solid object (limiter or wall) which completely changes the nature of transport compared to the closed field lines region of the main plasma. In particular, the very high parallel heat conductivity transports the heat very quickly down the field lines accounting for the very rapid temperature fall-off with the (minor) radius. Another scrape-off feature is the often very strong interaction (ionization) of the surrounding neutral gas with the plasma leading to plasma recycling at the places of contact with solid objects. The two-dimensional transport code PLANET predicts the scrape-off plasma behavior, which includes the plasma temperature, density, and the mass flow patterns important for impurity transport.

The task for FY87 was to develop an impurity transport code, to be coupled to PLANET, and to obtain more accurate hydrogen flow patterns to be used by the impurity code. A time-dependent impurity transport code was written, employing the alternate direction implicit (ADI) solution method. Only the implicit solver in the parallel direction has been tested so far.

In a separate development, the PLANET equations were supplemented by the particle drift terms, which were expected to modify the hydrogen flow patterns in the highly subsonic region surrounding the main plasma. (The flows are fast in the recycling region near the plate). Applied to the D-III-D geometry, the drifts (unexpectedly) resulted in near-sonic toroidal flows which, coupled to poloidal flows, produced large density and pressure variations. In particular, following the separatrix from the plate, it was found that the plasma pressure and the related electrostatic potential, increase abruptly at the x point (by about a factor of 2). The related radial flows near the x point were found to result in substantial (unidirectional) poloidal flows around the main plasma.

These findings have opened up a whole new field of phenomena which will take considerable time to investigate. For the first time, features have been seen, such as potential barriers at the x point, which could be related to the triggering of the H-mode. The unidirectional flows could also be important in reducing poloidal asymmetries, and so effect the transport across the separatrix. Finally, the newly found flow patterns are bound to impact on the impurity transport.

## ACTIVITIES IN NEUTRAL TRANSPORT

A useful indicator of hydrogen ionization is $H_\alpha$ emission, since the energy required to excite hydrogen to the n = 3 level is approximately the same as to ionize the hydrogen atom. Other aspects of recycling, such as plasma scrape-off parameters, wall particle fluxes, and wall retention rates can be inferred from spatial distributions of $H_\alpha$ emission.

There are two $H_\alpha$ diagnostics on TFTR observing the inner limiter: a relatively calibrated wide-angle TV camera, and the absolutely calibrated HAIFA (Hydrogen Alpha Interference Filter Array) diagnostic, both viewing the inner limiter. Observations of $H_\alpha$ by these instruments were analyzed using the DEGAS neutral transport code. The core recycling rate, and ion and neutral particle limiter fluxes, have been deduced from the calculations. The results are very sensitive to the ion flux distribution, and therefore also provide information on the plasma scrape-off conditions.

A survey was made of over 500 consecutive TFTR discharges, from which two tentative conclusions can be drawn: (1) $H_\alpha$ emission varies roughly as the square of the plasma density, not linearly, as has been previously thought, and (2) the ratio of total $H_\alpha$ brightness to core fueling is roughly constant. This is a refinement over the traditional application of the Johnson-Hinnov theory to a simplified geometry.

Tokamak device components can retain particles for varying lengths of time. Particles embedded in the first few angstroms of a wall or limiter may desorb almost instantly. High-energy incident particles, however, may become embedded at depths of hundreds of angstroms, diffuse further into the structure if it is heated, and remain in it for long periods of times.

A strong pumping effect has recently been observed with the operation of the toroidal graphite bumper limiter on TFTR. The pumping effect was induced by conditioning the limiter with a short series of low-density deuterium or helium discharges. Coincident with the low recycling conditions, low current neutral-beam-fueled discharges show global energy confinement times which are enhanced a factor of two over results with an unconditioned limiter.

It would be extremely useful to understand the physical processes of both the conditioning process, during which the limiter was depleted of hydrogen, and the pumping during the discharges. Knowledge of the amount of hydrogen and its isotopes retained in the wall and limiters over many discharges may explain isotope exchange rates. It is also critical that accurate predictions of tritium wall inventory be made before TFTR enters into D-T operations in 1990, in order to optimize those operations.

A joint program between Sandia National Laboratories and PPPL has resulted in the combination of a suite of computer codes capable of predicting the fuel recycling rates, as well as the permeation and inventory of hydrogen in vessel components. An emphasis has been placed on including an accurate description of the device geometry in the model. The ion limiter particle and heat fluxes are calculated with the FLATLI code, and the subsequent neutral particle transport with the DEGAS code. The resultant implant profile of hydrogen in the walls and limiters is calculated using Sandia's version of the Monte Carlo binary collision code TRIM. The temperature and particle distributions are then used as inputs to Sandia's hydrogen-solid interaction codes, the Local Mixing Model, which calculates near-surface retention, and DIFFUSE, which computes bulk hydrogen isotope diffusion and trapping. The entire model is still under development, and new physical data and processes, in particular carbon-hydrogen code position and ion-impact desorption, are presently being added.

A number of collaborations were started or continued during the last year. These include: (1) analysis of recyling in the D-III-D divertor using $H_\alpha$ emission, as done for TMX-U (Tandem Mirror Experiment-Upgrade) and TFTR, (2) study of recycling and diagnostic beam penetration in TEXT (Texas Experimental Tokamak), (3) Injection Studies Experiment (ISX) pump limiter analysis, TORE-SUPRA (tokamak at Cadarache, France) pump limiter design, and Advanced Limiter Test-II (ALT-II) $H_\alpha$ behavior, (4) preliminary recycling predictions for the W-VIIAS stellarator (Wendelstein VII Stellarator Modified, West Germany), and (5) divertor impurity transport in ASDEX.

An International Atomic Energy Agency (IAEA) sponsored meeting was held at PPPL on hydrogen retention in tokamaks in July, and a review article on the subject is in preparation.

The INTOR/TIBER-II/ITER International Tokamak Experimental Reactor test reactor design studies were supported during the year, primarily the impurity control design effort. A significant contribution was the modification of the original TIBER-II divertor region design, based on the experience gained from modeling work done as part of the INTOR design work. We expect our participation to increase as TIBER-II evolves into a new design for ITER.

## MODELING HYDROCARBON AND CARBON TRANSPORT IN THE SCRAPE-OFF REGION

It is important to understand the mechanisms for carbon entering tokamaks and other plasma devices for impurity control, transport models, hydrogen and carbon recycling, carbonization, fueling, and erosion. Plasma wall interactions with graphite release hydrocarbons and carbon by chemical and physical erosion, respectively. To study hydrocarbon transport at the edge we have, in the past year, assembled a data base for hydrocarbon interactions with a hydrogen plasma[14] and begun development of a transport program based on the neutral transport DEGAS code. The main problem in this modeling is the need to follow the impurities as both neutrals and as ions since the plasma reactions which break down these species convert one into the other.

The report "Collisional Processes of Hydrocarbons in Hydrogen Plasmas"[14] provides quantitative information on the most significant reactions of methane and methane fragments with electrons and protons over the temperature range from 0.1 eV to 2 keV. It reviews reaction properties and provides cross sections, reaction rate coefficients, estimates of energy lost and gained, and graphs and analytic fits to these. The data base is derived from a survey of the most up-to-date literature. This report is currently being distributed to laboratories and research facilities engaged in fusion and plasma work for their use in modeling and interpreting experiments. We developed the code SIGMAV, which is an updated version of the Ken Evans' (Argonne National Laboratory) program MODIFY, to compute the carbon and methane reaction cross sections. To allow convenient use for future set of reactions, publication-quality graphics were added and documentation written to cover setting up input, running the code, and obtaining plots of $\sigma$ and $\langle\sigma v\rangle$, as well as making the analytic fits.

To model transport of hydrocarbons at the edge we have modified the DEGAS neutral transport code to follow the multiple reaction paths that occur in the breakdown of hydrocarbons by reactions with the plasma. Presently, we launch methane from the wall or from a limiter and follow it with Monte Carlo techniques as it moves through and reacts with the plasma. Once it is ionized it is assumed to be fixed to the field lines and remains within a computational cell until reactions produce a neutral, which, being unattached to the field lines, can move freely in the plasma. The original particle is followed until a carbon ion is produced. A large number of sample flights are made until good statistics are available. At present, we have only incorporated the energy and momentum changes due to the reaction dynamics into the models, but plan to include the ion transport in the near future. The DEGAS user's manual was updated to include use of the extended carbon and methane subroutines. The examples were expanded to include a three-dimensional (3-D) case, and many sections were added to explain how to use the various capabilities.

We have used the modified DEGAS code to make preliminary model calculations of hydrocarbon and carbon profiles at the edge of TFTR and for comparison with recent carbon probe experiments on DITE (Divertor and Injection Tokamak Experiment).[15] The models should be useful to interpret if methane release (chemical erosion) is a function of plasma temperature and density. The DITE measurements, for example, show more CD emission in the outer part of the plasma. Figure 3 provides the model density profiles for methane, CH, and $CH^+$ as a

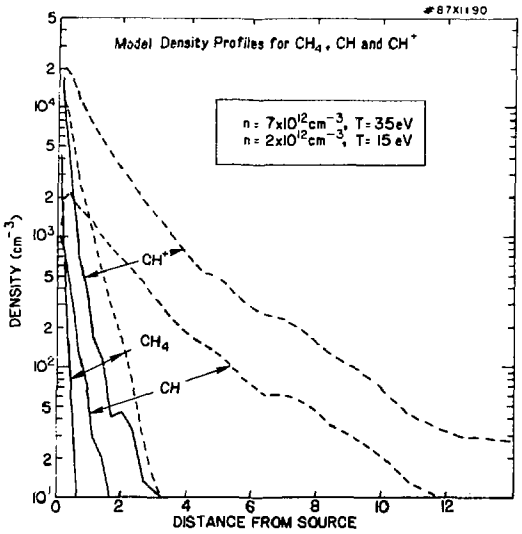


*Figure 3. Model density profiles for methane, CH, and $CH^+$ as a function of distance from a unit source, for a constant plasma with n = 7.0 × $10^{12}$ $cm^{-3}$, T = 35 eV, and a constant plasma with n = 2.0 × $10^{12}$ $cm^{-3}$, T = 15 eV.*

function of distance for two probe positions. It can be seen that even though methane is ionized very close to the edge its daughter species penetrate much further into the plasma. Furthermore the CD/$CD^+$ ratio is smaller further into the plasma because the primary daughter product is $CD^+$, rather than CD. Thus the plasma reactions may explain the failure to detect CD when the DITE carbon probe is in a hotter part of the plasma. Such models and comparison with experiments will allow us to study carbon transport in the edge of TFTR and its penetration past the scrape-off and into the plasma.

# IMPURITY AND PARTICLE TRANSPORT MODELING

The MIST multi-species impurity transport code serves as the principal tool for impurity transport modeling and analysis of spectroscopic and other impurity-related diagnostic data on TFTR and other PPPL tokamak experiments. Beginning this year, the MIST code also provides similar modeling support for experiments on the D-III-D tokamak at GA Technologies, Inc. MIST modeling for ZT-40M (Los Alamos National Laboratory) has also been added to the other continuing MIST applications outside of PPPL. Code development work has included the addition of time-dependent profile data input to MIST. This allows detailed modeling of impurity behavior to be carried out in strongly time-varying plasma conditions, such as during TFTR "supershot" and pellet-injection experiments.

A new effort towards comprehensive analysis and modeling of electron and ion-particle transport in tokamak plasmas has been undertaken beginning this year. To carry out this work, a new one-dimensional particle transport code, TRIUMPH, was developed to provide detailed modeling of time-dependent electron density profile data. An important feature of TRIUMPH is that it calculates the electron-density profile evolution for up to 32 model cases simultaneously, in direct comparison with the experimental data. This allows the effect of multiple parameter variations in the transport models to be tested and compared in a single code run. Particle transport in TFTR pellet-fueled ohmic plasmas[16] was the initial focus for TRIUMPH analysis this year. An example of experimental and modeled electron density behavior after pellet injection is shown in Fig. 4. MIST modeling was used to complete the particle transport picture in these same discharges by analysis of the transport of intrinsic and injected impurity ions.

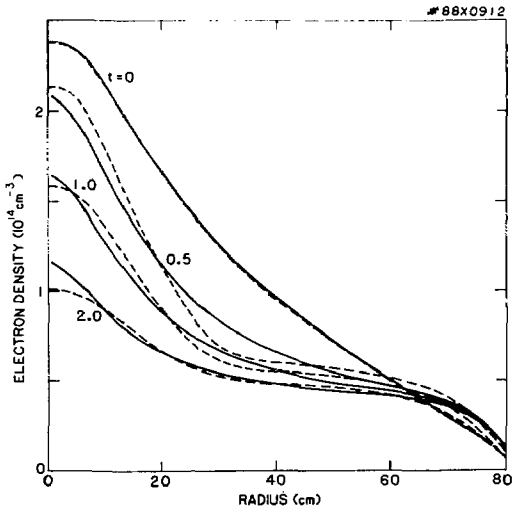


*Figure 4. Experimental (dashed) and model (solid) electron density profiles at t = 0, 0.5, 1.0, and 2.0 sec after pellet deposition. Model has D = 50 + 3950 $(r/a)^2$ $cm^2$/sec plus the neoclassical flux.*

### References

[1]M.H. Redi, W.M. Tang, P.C. Efthimion, D.R. Mikkelsen, and G.L. Schmidt, "Transport Simulations of Ohmic TFTR Experiments with Profile-Consistent Microinstability Based Models for $\chi_e$ and $\chi_i$," Princeton University Plasma Physics Laboratory Report PPPL-2368 (March 1987) 53 pp; Nuclear Fusion 27 (1987) 2001.

[2]C.E. Singer, D.E. Post, D.R. Mikkelsen, M.H. Redi, A. McKenney, *et al.*, "BALDUR: A One-Dimensional Plasma Transport Code," Princeton University Plasma Physics Laboratory Report PPPL-2073 (July 1986) 237 pp; to be published in Computer Physics Communications (1988).

[3]M.H. Redi, "Standard Test Cases for the BALDUR Transport Code," to be published in Computer Physics Communications (1988).

[4]G. Bateman, "Simulation of Transport in Tokamaks," in *1987 IEEE Minicourse on Computer Applications in Plasma Science* (Springer-Verlag, New York, 1989) in press.

[5]W. Schneider and G. Bateman, "Mapping from Rectangular to Harmonic Representation," J. Comp. Phys. *71* (1987) 169.

[6]G. Bateman, "Delaying Sawtooth Oscillations in the Compact Ignition Tokamak," Princeton University Plasma Physics Laboratory Report PPPL-2373 (September 1986) 23 pp; to be published in Fusion Technology.

[7]D. Stotler and G. Bateman, "Simulation of a Compact Ignition Tokamak Discharge (CIT-2L)," Princeton University Plasma Physics Laboratory Report PPPL-2415 (February 1987) 25 pp.

[8]D. Post, W. Houlberg, G. Bateman, L. Bromberg, D. Cohn, *et al*, "Physics Aspects of the Compact Ignition Tokamak," Physica Scripta *T16* (1987) 89.

[9]D. Stotler, D. Post, and G. Bateman, "Sawtooth Effects in Elongated, High Current Tokamak Reactors," Princeton University Plasma Physics Laboratory Report PPPL-2463 (August 1987) 18 pp; Fusion Technology (in press).

[10]M.H. Redi, S.J. Zweben, and G. Bateman, "Tokamak Fusion Test Reactor Central Ignition Scenarios," Fusion Technology *13* (1988) 57.

[11]C.E. Singer, G. Bateman, and D. Stotler, "Boundary Conditions for OH, L, and H-mode Simulations," Princeton University Plasma Physics Laboratory Report PPPL-2527 (June 1987) 29 pp.

[12]C. Singer, L. Ku, and G. Bateman, "Plasma Transport in a Compact Ignition Tokamak," Princeton University Plasma Physics Laboratory Report PPPL-2414 (February 1987) 33 pp; Fusion Technology (in press).

[13]D.G. Swanson, S. Cho, C.K. Phillips, D.Q. Hwang, W. Houlberg, and L. Hively, "Recent Advances in the Theory and Modeling of RF Heating in Inhomogeneous Plasmas," in *Plasma Physics and Controlled Nuclear Fusion Research 1986* (Proc. 11th Int. Conf., Kyoto, Japan, November 1986), Vol. *I*, (IAEA, Vienna, 1987) 653.

[14]A.B. Ehrhardt and W.D. Langer, "Collisional Processes of Hydrocarbons in Hydrogen Plasmas," Princeton University Plasma Physics Laboratory Report PPPL-2477 (September 1987) 94 pp.

[15]C.S. Pitcher, G.M. McCracken, D.H.J. Goodall, A.A. Haasz, G.F. Matthews, and P.C. Stangeby, "An Experimental Investigation of Chemical Sputtering of Carbon in a Tokamak Discharge," Nucl. Fusion *26* (1986) 1641.

[16]R.A. Hulse, P. Efthimion, B. Grek, *et al.*, "Particle Transport in TFTR Ohmic Pellet Injection Experiments," in *Controlled Fusion and Plasma Physics* (Proc. 14th Conf., Madrid, Spain, 1987) Vol. *11D*, Part 1 (European Physical Society, 1987) 318.

# COMPACT IGNITION TOKAMAK

## INTRODUCTION

Discussions within the international fusion research community over the last few years have focused on a collaborative program designed to maximize the overall cost-effectiveness of fusion research during the coming decades. The U.S. has proposed to take the lead in a Compact Ignition Tokamak (CIT) Project that could begin construction as early as 1989. The Princeton Plasma Physics Laboratory (PPPL) has been designated to lead the CIT effort.

The programmatic role of the CIT is to bridge the gap between the realization of transient, subignited deuterium-tritium (D-T) operation on the Tokamak Fusion Test Reactor (TFTR) and the Joint European Torus (JET) and the need for a stable equilibrium burn regime in a future Engineering Test Reactor (ETR). As defined by the Department of Energy (DOE), Office of Fusion Energy (OFE),

> "The mission of the Compact Ignition Tokamak will be to realize, study, and optimize fully ignited plasma discharges."

A set of detailed physics parameters and operational requirements has been developed to satisfy the basic CIT mission. The most important "figures of merit" are plasma current and toroidal magnetic field strength. Because ignition is the primary mission of CIT, assurance must be provided that this goal can be achieved even in the face of empirical transport scalings that are on the pessimistic side of the present-day range of projections. This assurance is provided by requiring large magnetic fields (approximately 10 T) and large plasma currents (approximately 9 MA). The CIT design is also capable of accommodating substantial auxiliary heating (about 20 MW) to insure passage through the ignition temperature threshold. To meet its scientific research objectives, the CIT is designed to operate in dimensionless parameter ranges and areas of the Lawson diagram that will be directly relevant to the ETR and to future toroidal power reactors.

Achieving ignition has long been viewed as one of the major steps—and the single most important step—in the effort to harness practical fusion power. The existing fusion program, both U.S. and international, is producing individual elements of the total physics basis for a tokamak fusion reactor (e.g., techniques for the control of plasma heating, purity, and stability), which will be required to achieve fully ignited discharges. The CIT will be the first experiment where these elements are assembled in a single device, so as to achieve equilibrium burn conditions.

The CIT Project is based on a strategy of minimizing cost and construction time by specifying a relatively small physical size. A favorable potential for achieving ignition is made possible by a number of special techniques developed during the past decade of fusion research: the use of very strong magnetic fields, first proposed by B. Coppi and demonstrated by the ALCATOR experiments at the Massachusetts Institute of Technology (MIT); the development of tokamak plasma-shaping techniques at GA Technologies, Inc. (GAT), PPPL, and elsewhere; the demonstration of the effectiveness of ion cyclotron range of frequencies (ICRF) plasma heating at PPPL; and the development of highly successful pellet injectors by Oak Ridge National Laboratory (ORNL). Experimental results from the present generation of large tokamak devices, which will be reaching their maximum productivity during the next several years, are serving to provide timely confirmation for the CIT design and operating plans.

## SITING OF CIT

In FY87, it was decided by the DOE that the Compact Ignition Tokamak would be sited at PPPL, next to TFTR, to take maximum advantage of the facilities and infrastructure that are presently in use on TFTR. This strategy will minimize construction time and will save between $200-million and $300-million, as opposed to beginning CIT construction at a "greenfield" site. The largest savings will be seen in buildings, electrical power supplies, water cooling systems, and tritium storage and handling facilities. Figure 1 shows the location of CIT at PPPL.

The assembly of the CIT device itself is planned to be outside the exclusion boundary fence of TFTR, to minimize interference with TFTR operations. The CIT test cell construction will be adjacent to the TFTR test cell, with the CIT construction schedule being dovetailed with the TFTR schedule to allow maximum experimental run times on TFTR. In 1991 TFTR will have performed its tritium breakeven experiments, after which the utilities will be disconnected from TFTR, modified, and reconnected to the CIT facility.

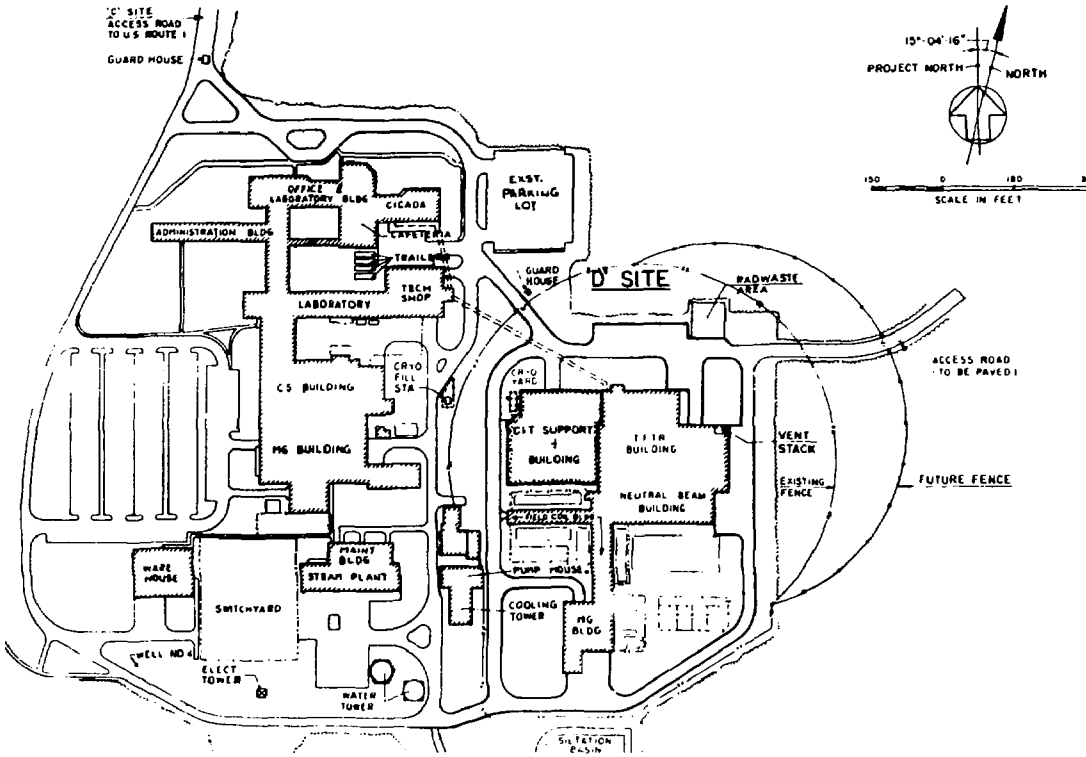


CIT FACILITIES SITE PLAN

*Figure 1. Siting of Compact Ignition Tokamak at PPPL. (86P1056)*

# PROJECT ORGANIZATION

In FY87, the CIT Project organization continued to develop under DOE guidance. The organization chart representing the project near the end of FY87 is shown in Fig. 2. As can be seen from this chart, PPPL has not only a major share of technical responsibility on CIT but has been assigned the role of project management as well. In partnership with PPPL are a number of Principal Participants, making the CIT the first U.S. fusion project to be a truly national effort.

The CIT Principal Participants are as follows:

Idaho National Engineering Laboratory (INEL)

Los Alamos National Laboratory (LANL)

Lawrence Livermore National Laboratory (LLNL)

Massachusetts Institute of Technology (MIT)

Oak Ridge National Laboratory (ORNL)

Princeton Plasma Physics Laboratory (PPPL)

Industrial Subcontractor (to be determined by competitive bidding)

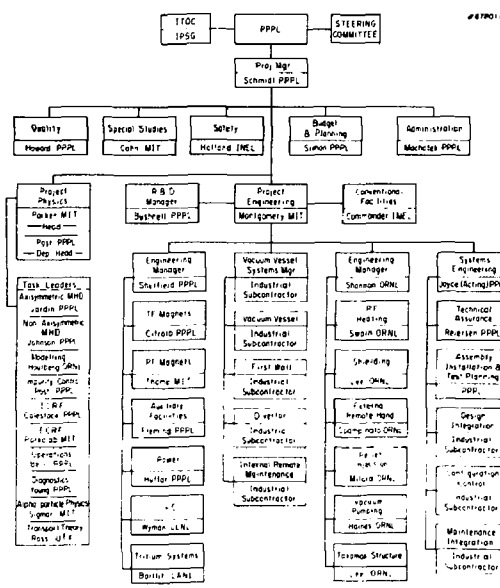


*Figure 2. Compact Ignition Tokamak FY87 organization chart.*

# DESIGN EVOLUTION

Preliminary studies aimed at the development of an optimal CIT design were initiated in the U.S. in 1984. A national design team was established involving leading fusion engineers and physicists, and the Ignition Technical Oversight Committee (ITOC) was formed to oversee the design studies. Taking as its starting point the earlier IGNITOR (IGNIted TORus) studies, the national design team investigated a broad range of engineering approaches. In January 1986 a consensus was reached within the design team and ITOC concerning the most appropriate engineering approach and detailed physics characteristics for the CIT proposal.

A Conceptual Design Report was published in June 1986, and this report was used by the DOE to determine whether to propose the project for inclusion in the President's FY88 budget. With this basis, the DOE decided to recommend proceeding with the project.

Since the original proposal was submitted, the design has undergone considerable development. In FY87:

- The divertor region was expanded to improve divertor operation.
- A control coil configuration contiguous to the vacuum vessel was developed to provide control of the divertor with varying plasma conditions and diverted flux sweeping to reduce average heat loads.
- The edge safety factor (q) of the plasma was increased to improve plasma operation.
- Stresses were reduced in the magnets.
- The flux produced by the poloidal-field coils was increased relative to the level needed for plasma current production and maintenance.
- The external structure (press) was relegated to an upgrade and the internal magnet structure was increased to react the magnetic forces.

The evolution of the CIT design in 1987 is shown in Table I, which lists selected machine parameters as they appeared in the 1986 Annual Report, and as they are today. The most obvious change has been an increase in major radius by 43% over its earlier value.

# R&D PROGRAM

The design of the toroidal-field coils, and some of the poloidal-field coils, is based upon the use of an explosion-bonded laminate of steel-copper-steel. This "quasi-alloy" will provide optimum electrical conductivity, with mechanical strength needed to accommodate the very high currents and very high field stresses in CIT. The development of the laminate is at the center of a vigorous CIT research and development (R&D) program which, within the constraints of a limited budget, was quite active in FY87. A summary of R&D activities during this time is shown in Table II (see next page).

**Table I. Important Parameters of the CIT Design.**

| Parameter (Units) | 1986 Value | 1987 Value |
|---|---|---|
| Major Radius (m) | 1.22 | 1.75 |
| Minor Radius (m) | 0.45 | 0.55 |
| Elongation ($\kappa$) | 1.80 | 2.0 |
| Plasma Current, Limiter (MA) | 10 | 9 |
| Plasma Current, Divertor (MA) | 9 | 9 |
| Toroidal Field (T): | | |
| Baseline | 10.4 | 10.0 |
| Upgrade | — | 12.0 |
| Toroidal Field Flattop (sec) | 3.7 | 5.0 |
| Plasma Burn Time (sec) | 3.1 | 5 |
| Radio-Frequency Heating, Initial (MW) | 10 | 10 |
| Radio-Frequency Heating, Full Complement (MW) | 20 | 20 |
| Number of Full-Field Pulses | 3,000 | 3,000 |
| Number of Half-Power Pulses (70% Field) | 50,000 | 30,000 |
| Fusion Power (MW) | 300 | 300 |

### References

#### Project Documents


[1]"CIT Research and Development Plan," FY87, Rev. 3, Doc. No. AA-870901-PPL-01.

[2]"CIT Research and Development Plan," FY88, Rev. 0, Doc. No. AA-870901-PPL-06.

[3]"Project Management Plan," (Draft), FY88, Doc. No. AA-870902-PPL-01.

[4]"CIT QA Requirements Document," Doc. No. AC-871026-PPL-01.


#### Laboratory Reports


[5]G. Bateman, "Delaying Sawtooth Oscillations in the Compact Ignition Tokamak," Princeton University Plasma Physics Laboratory Report PPPL-2373 (September 1986) 23 pp; to appear in Fusion Technology.

[6]D. Stotler and G. Bateman, "Simulation of a Compact Ignition Tokamak Discharge (CIT-2L)," Princeton University Plasma Physics Laboratory Report PPPL-2415 (February 1987) 25 pp.

[7]C. Singer, L. Ku, and G. Bateman, "Plasma Transport in a Compact Ignition Tokamak," Princeton University Plasma Physics Laboratory Report PPPL-2414 (February 1987) 33 pp; to appear in Fusion Technology.

[8]D. Post, W. Houlberg, G. Bateman, *et al.*, "Physics Aspects of the Compact Ignition Tokamak," Physica Scripta *T16* (1987) 89-106.

**Table II. Compact Ignition Tokamak R&D Activities in FY87.**

| *Area of Activity* | *Scope of Activity in FY87* |
|---|---|
| First Wall Tiles and Tile Attachment | Bulk carbons screen-tested thermally. Tiles/tile mounting schemes fabricated and tested thermally and mechanically. |
| Vacuum Vessel Joint Development | Automatic welding techniques reviewed and compared with analytical efforts. |
| Development of In-Vessel Equipment | Automatic sector welder specified and put out for bid on trial unit. Conceptual design for device to inject and remove tiles developed. Leak telescope concept developed and tested. |
| Poloidal-Field Coil Materials and Methods | Copper and Inconel ordered, characterized, and bonded for ohmic-heating solenoid. Shear, shear compression biaxial tension/compression and fatigue tests conducted. Liquid nitrogen cooling test setup fabricated. Water jet cutting developed. |
| Ohmic-Heating Solenoid Joint Evaluation | Joint samples designed and fabricated. Testing started. |
| Toroidal-Field Coil Copper/Nickel Alloy Material Development | 12,000 lbs Copper and Inconel purchased and characterized. Three explosion-bonded samples for test (100-foot square). Machining methods investigated. Compression tests including cyclic Jenes were run and basic material parameters were defined. |
| Toroidal-Field Coil Insulation Development | Conducted material search, began fabrication of samples for screening tests. |
| Press Concept Development | Hydraulic jacks investigated, along with construction schemes. |
| External Remote Maintenance Equipment and Procedures | Remote Maintenance Designers Guide drafted. Training courses for designers held. Work on mock-ups to simulate basic tasks was undertaken to establish manipulator functional requirements. |

# ENGINEERING DEPARTMENT

## COMPUTER DIVISION

Computer Division activity in FY87 supported the Tokamak Fusion Test Reactor (TFTR), Experimental Projects [PBX-M, S-1, and the last months of the Princeton Large Torus (PLT)], the Compact Ignition Tokamak (CIT), and the General Purpose Users [User Service Center, Computer-Aided Design and Drafting (CADD), Data Communications for remote sites, and a conversion of PPLnet to new hardware].

The TFTR program emphasized both (1) increases in reliability in preparation for TFTR tritium operations and (2) increases in functionality. Specifications for the tritium remote control and monitoring system (TRECAMS) were completed and the equipment was ordered for installation in FY88. A MicroVAX for the ion cyclotron radio-frequency (ICRF) heating system was installed. The DEC VAX 8600 was replaced by a VAX 8700 for the high-level data analysis system.

Experimental Projects support emphasized the preparations for Princeton Beta Experiment-Modification (PBX-M). The VAX 8600 was transferred from TFTR to Experimental Projects as a replacement for the obsolete DEC KL-10 data acquisition system.

The Division began preliminary specification and design work for the instrumentation and control system for CIT.

General Purpose Users were supported by enhancements of the User Service Center, an expansion of the CADD system, and the extension of data communications to the new site at 307 College Road East, supporting the Engineering Department and CIT.

A diagram of the current Princeton Plasma Physics Laboratory (PPPL) computing system is shown in Fig. 1. A listing of publications by Computer Division personnel is given in the references.

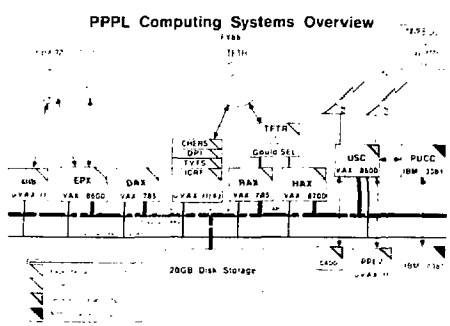


*Figure 1. Overview of Princeton Plasma Physics Laboratory computing systems. (88E0477)*

## TFTR Computer System

The TFTR computer system[1-5] is composed of a network of eleven on-line Gould/SEL computers, two DEC VAX superminicomputers, and four DEC MicroVAX minicomputers. Tokamak Fusion Test Reactor data acquisition has been enhanced and now acquires 20 Mbytes in approximately 3 min on the Gould/SEL System and stores compressed data on the VAX Cluster. Data acquisition on the MicroVAXs is on a per-shot basis: 256 kbytes on TV Thomson scattering (TVTS); 2.0 Mbytes on the charge-exchange recombination spectrometer (CHERS); 0.5 Mbytes on the deuterium pellet injector (DPI); and 2.5 Mbytes on ICRF. Figure 2 shows the growth of data accumulation per shot on TFTR. Figure 3 shows a representative distribution of TFTR acquired data (from Shot #30938 on 5 June 87). The TFTR Gould/SEL Control Room is shown in Fig. 4.

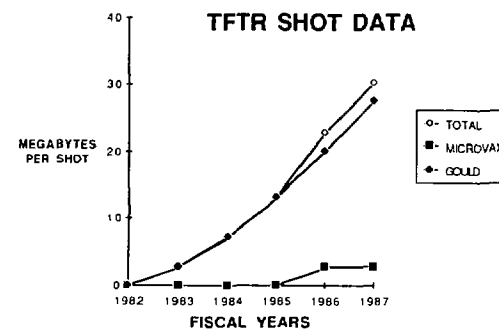


*Figure 2. Growth of data accumulation per shot on TFTR from FY82 through FY87. (88E0478)*

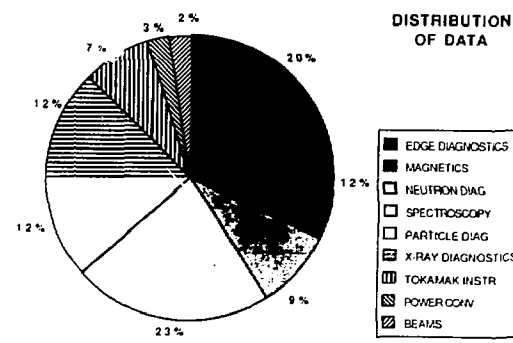


*Figure 3. Representative distribution of TFTR acquired data (Shot #30938, 5 Jun 87). (88E0476)*

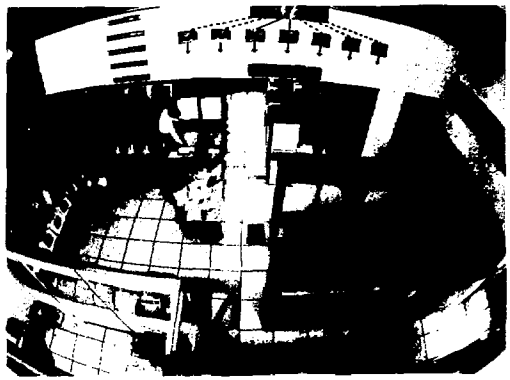

*Figure 4. The TFTR Gould/SEL Control Room as seen from the Gallery. (87A0220)*

## TFTR Reliability Enhancements

The Gould/SEL real-time systems were enhanced to increase reliability. Software to support multiple computer-automated measurement and control (CAMAC)[6] links on a subsystem computer were installed. This installation made it possible to merge the tokamak subsystem (TOK) into a single computer and the diagnostic subsystem (DIAG) into another single computer, thus decreasing the number of computers by two. The merger improves reliability of the overall system and, by decreasing the number of computers, lowers hardware and software maintenance costs. Kinetics System 2070 CAMAC interfaces were installed on all Gould subsystems to improve reliability and maintainability. The device control system was redesigned to support the new Kinetic System 2070 interface in order to improve reliability. The latest real-time operating system, MPX 3.3, was installed on the Central Facility on-line computers. The prepulse checking system, to abort shots in case of a subsystem failure, is ready for operation. Reliability and security enhancements were made to both the MicroVAXs and the VAX Cluster.

## TFTR Performance and Functionality Enhancements

Gould/SEL computers were upgraded to improve performance and functionality. A 16-Mbyte memory upgrade was installed on the Central Facility computers to improve maintainability, coding efficiency, and performance. A second CAMAC link was installed on the Console Computer to double the maximum throughput of the graphics system. The device control subsystem data-base capacity was expanded to allow twice the previous number of CAMAC devices. Programmable controllers were integrated into the Device control support package. These controllers will include I/O (input/output) monitoring in the 2-sec data-base and set-point control. These upgrades should provide sufficient capacity through the end of the TFTR operations.

Performance and functionality enhancements were also made on the VAX computers. The VAX Event System was installed, making it possible to analyze TFTR shot data as soon as the necessary data are available. Raw data compression prior to archival on the VAXs was implemented, resulting in a 3-to-1 reduction in raw data storage requirements.

## TFTR New Systems

Hardware and software support for new applications included the microwave scattering system, the radio-frequency (rf) probe, the grating polychromator, the charge-exchange mini-analyzer, and the disruption trigger system. Software enhancements included power conversion and motor generator (MG) control interfaces to the master control system, and redesign of the X-ray crystal analysis to provide confirmation of supershot temperatures.

The TRECAMS (tritium remote control and monitoring system) was specified and ordered.[7] This distributed control system will support automated and remote control and, through continuous monitoring, will provide the necessary high reliability for tritium-handling equipment. The system will be based on several microprocessor-based controllers, will interface to approximately 2,000 I/O points, and will contain several operator control stations.

A MicroVAX was installed on the TFTR ion cyclotron radio-frequency[8] heating system and the access control interface was developed.

## Experimental Projects

The PBX-M control system was upgraded with distributed programmable logic controllers.[9] Increased processing support, provided by the addition of the VAX 8600 and 5 RA81s to the DAS[10] configuration, is expected to meet all Experimental Projects requirements through FY88. The data acquisition system was redesigned to incorporate the VAX 8600 for raw data acquisition and displays. Preliminary studies indicate that 10 Mbytes of data can be processed in three minutes, thereby meeting the PBX-M requirement for a 3-min shot cycle. Half of the Princeton Beta Experiment CAMAC system was converted to the VAX link from the PDP-11s. Code was developed, converted, and upgraded to support the 12 diagnostics needed for initial PBX-M operations. The PBX-M CAMAC highway was converted from a bit to a byte serial highway. The neutral-beam control and data acquisition system [11] was converted from a PDP-11 to a MicroVAX in order to support more functions and to provide greater reliability.

Analysis programs were developed for numerous S-1 diagnostics. A new control system for the equilibrium field-pulse (EF-P) coil was designed to support S-1. (S-1 was closed down in December 1987.)

DECserver 200s were installed. They allow up to four concurrent process contexts, thereby eliminating the need to login and logout when switching contexts.

The queue control system (QCS) was developed to permit asynchronous data analysis with any experimental shot cycle. Stand-alone systems in support of CHERS and X-ray pinhole camera diagnostics were developed.

## Compact Ignition Tokamak

Specifications and system descriptions concentrated on the definition of requirements, interfaces,[13] and the development of schedules and budgets. A preliminary data handling system specification was developed. A conceptual design for the process control system and a preliminary analysis of data structure were created.

## General Purpose Systems

An on-site training program was instituted for basic CADD applications and additional workstations were provided. One of these workstations is shown in Fig. 5. The training of additional people in CADD, and the new workstations, will enable PPPL's draftspeople not only to support current TFTR, PBX-M design and drafting but to handle CIT work as it develops. The CADD system files may now be transferred automatically through the VAX Cluster to other Department of Energy (DOE) sites.

A data communications link between C-Site and 307 College Road, where PPPL's Engineering Department is now based, was accomplished with the installation of a high-speed digital service, a 1.544 Mbytes T1 carrier that uses time division multiplexers. The multiplexer channels were used for: one synchronous channel for DECnet communications between the User Service Center (USC) and the MicroVAX at 307 College Road; two synchronous channels for sixteen-channel statistical multiplexers into PPLnet; one synchronous channel for Fastlink communications between USC and CADD; and eight asynchronous channels into PPLnet. The system, currently using 10% of the T1 link's capacity, can be expanded with the addition of terminations.

*Figure 5. A typical computer-aided design and drafting (CADD) workstation in use. (85A0421)*

# ELECTRONIC AND ELECTRICAL ENGINEERING DIVISION

Fiscal year 1987 was one in which the Electronic and Electrical Engineering Division had responsibility for the design, development, maintenance, and operation of electrical and electronic equipment associated with all of the major Laboratory programs. Highlighted among the more than 200 diverse jobs undertaken during this fiscal period are the TFTR Ion Cyclotron Radio-Frequency (ICRF) Program, the PBX-M Upgrade, the Diode and Coil Protection Programs, and the Compact Ignition Tokamak (CIT) Power System Design.

The Division took significant steps to insure continued improvement in technology and staff development by promoting several growth areas. Technician training was furthered through the sponsorship of courses in circuit design and associated mathematics. Engineering courses focused on digital signal processing, computer languages, power engineering technology, and selected topics of Division interest. General training included safety meetings, computer usage courses, and Laboratory-sponsored management and professional seminars. As a result of these endeavors, the level of engineering performance and applied technology registered a notable advancement during the report period.

While the Division continued to support the Laboratory's programs, a major facility relocation effort was undertaken. As part of the overall Laboratory move out of A- and B-Sites, the Division moved its engineering offices to 307 College Road East and its heavy shops to the CAS building. This move has enabled the collocation of all three electrical branches at one site and will allow for greater interaction and sharing of resources between the branches.

## Radio-Frequency Branch

### Radio-Frequency Operations Section

During the last weeks of PLT operations, two of its 30-MHz sources were used up to peak power levels of 3.0 MW into a dummy load for short pulses. This use verified the higher power capability of these amplifiers for future TFTR upgrades. Princeton Large Torus operation of these sources continued at 30 MHz until machine shutdown in December 1986.

A major redesign of the PLT amplifiers for TFTR was undertaken to shift the frequency from 30 MHz to 47 MHz and to increase the peak power and pulse width capability. Included in this redesign was the addition of an amplifier stage before the intermediate power amplifier (IPA). This stage will provide an

additional margin of drive power capability to conservatively meet the higher power requirements of TFTR. An instability problem in the IPA, evident on PLT operations, will no longer exist since the additional stage allows the IPA to be reconfigured as a grounded grid amplifier with considerably lower stage gain. The new design will provide 3.0 MW of power at 47 MHz from each of the two sources. Two other amplifiers used on PLT, built by Continental Electronics Manufacturing Corp. (CEMC), will be upgraded by CEMC and reinstalled at C-Site to provide an additional 4 MW of power over the frequency range of 40 MHz to 80 MHz.

The RF (Radio-Frequency) Operations Section designed and built the transmission and matching system which carries the power from the four sources across the field between C- and D-Sites and couples it to the dual strap TFTR ion cyclotron radio-frequency antennas. The matching system consists of high-power coaxial line stretchers and stub tuners located in the mock-up area at D-Site. Four nine-inch transmission lines couple the sources at C-Site to the matching system.

In preparation for the CIT machine and the major effort anticipated to provide ICRF heating power to this device, RF Operations' specialists in high-power tubes and cavity design investigated options and approaches to enable the meeting of system requirements in a cost-effective manner. A course of action was outlined and a proposal written to design and develop a prototype source at PPPL using as much of the original Fusion Material Irradiation Test (FMIT) hardware as applicable. The system will use the newly developed Eimac X2242 tetrode tube, a redesigned cavity and driver, and a modified FMIT power supply. After the prototype is evaluated and documented, a competitive production contract will be awarded to fabricate all subassemblies of the new system.

## Radio-Frequency Projects Section

Throughout the fiscal year the RF Projects Section was responsible for engineering management of the TFTR ICRF Project. (See RF Operations Section above for details.)

Experiments with the 2.45-GHz lower hybrid system continued on PLT using the new sixteen-waveguide launcher until the machine was closed down at the end of 1986. The three system 2.45-GHz, 500-kW klystrons will be sent to the Max Planck Institut für Plasmaphysik, Garching, West Germany for experiments on the Axially Symmetric Divertor Experiment (ASDEX).

The Grumman coupler (see Fig. 6) was fitted on PLT for the 800-MHz fast-wave experiment. It was powered up to a level of 400 kW. Run time was limited by the short PLT schedule. The coupler had arcing problems that limited power levels. Despite these constraints, useful experimental results were achieved. The system was then dismantled. One of the transmitters was sent to the Lawrence Livermore National Laboratories (LLNL) on loan. The remaining five sources and associated equipment will be sent to the Massachusetts Institute of Technology (MIT) on loan.

The closing of PLT made available the modulator/regulator previously shared between the 2.45-GHz lower hybrid current drive and 60-GHz electron cyclotron resonance heating systems. This unit is being converted for use on PBX-M on the diagnostic neutral-beam power supply. This involves a reversal of polarity and the addition of a capacitor charging supply. Forty percent of this task was completed in FY87. The remaining work is to be completed by the summer of 1988.

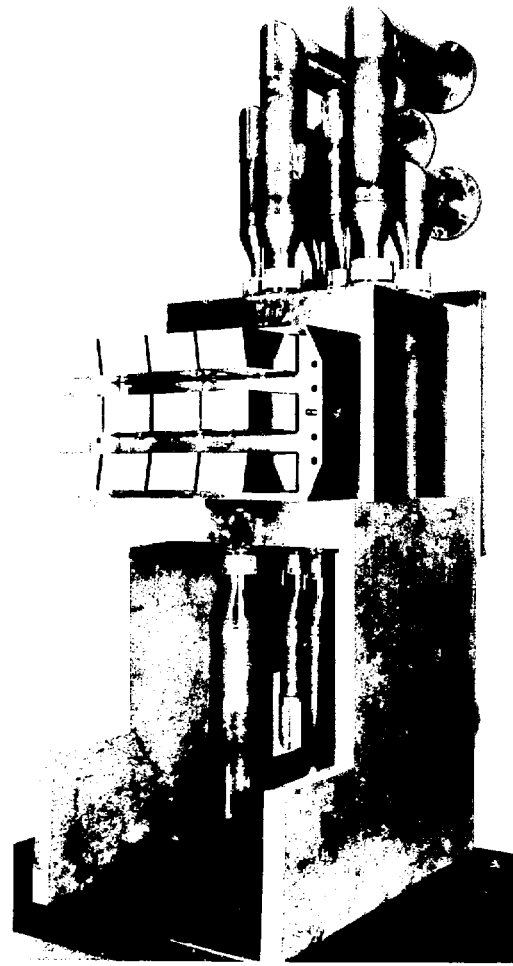

*Figure 6. The Grumman coupler used on the PLT 800-MHz fast-wave experiment. (86X3282)*

Continued support for microwave diagnostics on TFTR and PLT was supplied. The electronics, antennas, and transmission line components (see Fig. 7) for a 60-GHz microwave scattering system

for TFTR were constructed. This system is now ready for installation and test and will be commissioned in early 1988. The Section contributed to work on the move of radio-frequency shops from B-Site to C-Site.

Two papers written in FY87 on microwave techniques described work accomplished in FY86: J.L. Doane, "Low Loss Propagation in Corrugated Rectangular Waveguide at 1 mm Wavelength," International Journal of Infrared and Millimeter Waves, Vol. *8*, (1987) and J.L. Doane, "Polarization Converters for Circular Waveguide Modes," International Journal Electronics, Vol. *61*, (1986) 1109-1133.

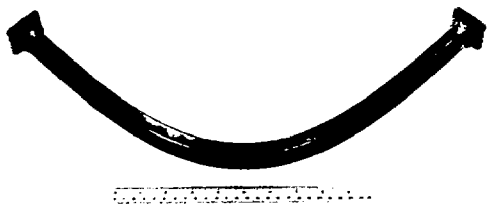

*Figure 7. Ultrawide band E-plane bend for the TFTR 60-GHz microwave scattering system. (87X3207)*

# Electronics Branch

## Electro-Optics Section

The Electro-Optics Section was engaged primarily in upgrading and maintaining a variety of instruments for TFTR, plus the definition of diagnostic concepts for CIT.

### Compact Ignition Tokamak

The ignited plasmas of CIT will create a neutron and gamma ray environment that makes instrumenting the machine especially challenging. The neutron flux corresponding to 300-MW fusion power is about 2 $\times 10^{15}$ neutrons $sec^{-1}$ $cm^{-2}$ at the vacuum vessel wall. The lifetime output of the CIT is approximately $10^{24}$ neutrons corresponding to a silicon Kerma of about $10^{10}$ Rad for components inside the vacuum vessel and on port covers. This extraordinary nuclear fusion radiation environment has a major influence on the conceptual design of CIT and the instrumentation needed for plasma diagnostics and machine operation. The CIT concept encloses the fusion machine in an igloo 1.8 meters thick. (The igloo provides about $10^6$ attenuation of the radiation and, equally important, makes possible personnel access to the Test Cell when the CIT is not operating.) CIT access requires removing igloo sections and the use of remote manipulators inside and outside the vacuum vessel. Plasma diagnostic instrument designs must be amenable to using remote manipulators for maintenance and replacement.

### Tokamak Fusion Test Reactor

A method was devised for inspecting the inner support structure/toroidal field (ISS/TF) shim blocks under the tokamak. Conduits under various bays guide a flexible 20-foot long, 5/8-inch diameter video probe/illumination system through the maze of coils under the machine to the ISS/TF shim block region. The two-axis articulation of the probe tip allows viewing of two to three shim blocks per conduit.

A system was designed for the lost alpha diagnostic that employs a solid-state video acquisition system to buffer the high bandwidth video going to the low bandwidth host computer processing and archival tasks. The system can acquire 360 video fields (32 Mbytes) at 60 fields per sec during a TFTR shot cycle. After the TFTR shot cycle a local microprocessor clips and windows the regions of interest to reduce the data set from 32 Mbytes to approximately 2 Mbytes, which is then transmitted to the host computer system (VAX Cluster) via an Ethernet link.

A color charge-coupled device (CCD) video camera was added to the TFTR plasma TV system mounted on the Bay H periscope. The existing monochrome CCD video cameras were adjusted (using gamma and white clip) to provide a logarithmic response. The cameras were characterized for quantitative illumination measurements. A low cost, all solid-state (RAM) color video acquisition and playback system was designed for integration in FY88.

## Instrumentation Section

A number of electronic equipments (new and existing designs) were provided as part of the PBX-Modification (PBX-M) program. Units in use since the beginning of PBX operation, were refurbished and redesigned to bring them up to current standards. Newly designed and constructed devices include the plasma current computer, the plasma position control summer, the analog computer-timer interface, the coil current measurement analog buffer, and the coil current measurement digital display. The refurbished units include the optically-isolated coil current monitoring system and the remote digital display system.

A major effort during 1987's TFTR opening was the relocation of neutral beamline No. 3 to position No. 1. This entailed a new instrumentation cable tray system that allowed use of existing cables. Instrumentation cables and support facilities had to be installed to complement the new positions of the neutral beamline and high-voltage enclosure. Ongoing improvements and modifications were made to the neutral-beam system electronics, including the gas valve driver and controller upgrades and a new vacuum gauge signal linearizer. As a result of the calorimeter interlock failure, an evaluation of the neutral-beam instrumentation and control was performed; the calorimeter position switches were redesigned; and the new calorimeter interlocks were included in the overall interlock logic.

The deuterium pellet injector (DPI), installed on TFTR last summer (1986), was commissioned and is being operated by the Instrumentation Section. Due to the accelerated installation schedule, much of the initial testing and system integration were performed at PPPL. The design was fine tuned, and complex operating procedures were developed to get the required performance from the DPI. By the later part of the run period, the equipment's reliability had been greatly improved. Under the direction of a well-trained operating staff, the DPI had many successful run days. During this summer's opening the mezzanine control electronics were relocated to make room for installation of the neutral beamline No. 1 power supplies. The DPI is now recommissioned.

The TFTR diagnostic vacuum system was upgraded with improved controller firmware, reworked ion gauge cabling, and fail-safe additions to vacuum sensor electronics. The torus interface valve (TIV) controller system was expanded. It now consists of four crate controllers, each with a new lock-out feature. It will allow control of new TIVs being added to TFTR, including electro-mechanical interlocked TIV controls for probe diagnostics. Torus interface valve interlocks were added to the gas handling system.

A dual sixteen-channel analog multiplexer was designed and built. It will monitor density and Faraday rotation signals from the ten-channel TFTR multichannel infrared interferometer (MIRI), and transmit its two outputs to the control room via dc-to-10 MHz analog fiber-optic links. A backup high-voltage laser power supply was upgraded to provide remote control and to reduce its magnetic field susceptibility.

### Analog Engineering Section

As an integral part of the TFTR Ohmic Heating (OH) Upgrade Program, a new coil protection system is being designed. The concept of a microprocessor-based system, providing more accurate stress simulation of the field coils on TFTR, was presented at a Conceptual Design Review. A preliminary design of the coil protection calculator has been prepared based upon the information gathered at the Conceptual Design Review and stress algorithms prepared jointly by the Engineering Analysis Division and the Tokamak Operations Division staff.

A life test was performed on a vacuum vessel illumination probe to determine failure modes. Modifications will be made to prevent these possible failures. The TFTR bolometer arrays were relocated, and a new tangential bolometer array was installed. Patch panels were installed so that the limited number of signal processing boards could be shared by the bolometer sensors.

A phase and amplitude feedback control system was installed in the radio-frequency control room for use with the ICRF program on TFTR. The four rf sources can be pulsed with independently adjusted rise and fall times and pulse lengths. The relative phases of the four sources can be preset for antenna phasing; because of the feedback, the desired phase relationship will be maintained regardless of power level or system drifts. The amplitude control loop has modulation provisions for future experiments. The voltage standing wave ratio (VSWR) of each source load is monitored, and if a preset level is exceeded, the rf is blanked for a short time to extinguish the arc. If the number of arcs exceed a preset maximum during one shot, the rf is shut down.

Microprocessor-based protection systems for the TFTR power diode assemblies were designed and are under construction. Each system is able to calculate the diode junction temperature in real time and shut down the input current if safe limits are exceeded. A major task during the year was to experimentally validate the heat flow model that is used.

A unique circuit was developed to monitor low current (1 A) flowing in a conductor at very high voltage. With a dead band of only ±2 milliamperes, this new circuit derives high power from the conductor being measured and couples information to ground potential through fiber optics.

## Power Branch

### AC Power Section

During FY87, the AC Power Section continued to provide installation and operational support to TFTR, a major effort that resulted in improved ac power system reliability and availability. The Section also fully supported the move of numerous Laboratory shops and engineering offices from A- and B-Sites to College Road East. Power demands of newly developing uses at C-Site required significant expansion of the Laboratory's electrical transmission and distribution system.

As a direct outgrowth of this move, the Section provided engineering review and management for a combined PPPL/consultant design of a new 26-kV six-transformer substation for the C-Site southeast quadrant area (see Fig. 8). Related tasks included equipment relocation, preparation, and procurement; installation, contractor review and selection, and considerable construction management. The 26-kV six-transformer substation is nearing successful completion and will shortly be available to supply its initial major load—the Research Equipment Storage and Assembly (RESA) Building.

The design of the RESA Building's electrical distribution system, along with procurement of the equipment, represented a significant task. Design is essentially complete, procurement is nearing completion, and start of installation is imminent.

The Section's broad range of Laboratory support tasks included continuing supervision and management of an ongoing electrical preventive maintenance subcontract program. This program contributes to reliability and availability of the Laboratory's overall electrical system by identifying inoperative, fault-prone components, leading to early identification and repair.

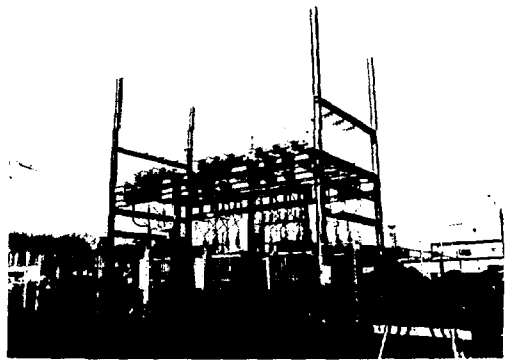

*Figure 8. New 26-kV six-transformer substation for the C-Site southeast quadrant area. (87E1585)*

Following design completion, transformer procurement awards were made for three major General Plant Projects, including: replacement of two PCB transformers and the upgrade of the TFTR ring bus emergency power system. Fabrication of the PCB replacement transformers is complete, and factory witness testing is imminent, with installation planned for early FY88. Transformer procurement for upgrade of the TFTR emergency power system is on schedule.

Additional tasks performed by the Section included: support, review, and engineering commentary for consultant-originated studies and recommendations for the TFTR tritium system; preparation, relocation, and installation of a second dc control power battery bank at C-Site; investigation, coordination, removal, repair, and reinstallation of several failed medium voltage 990 HP TFTR chiller motors; support implementation of the PSE&G/PPPL interruptible power contract (reducing Laboratory power costs); and maintenance, operation, and load testing of various mobile and stationary emergency generators.

## Power Conversion Section

The Power Conversion Section provided technical support to all sections of the Laboratory in repair and maintenance of power equipment. In addition to daily support, significant technical effort was applied to TFTR and PBX neutral-beam activities, PBX-M, and CIT power systems.

For neutral-beam activities, the Power Conversion Section continued to furnish manpower to TFTR and PBX neutral-beam operations and maintenance efforts: approximately one-half of the Section staff remains on extended temporary assignment. The Section provided engineering support and design drafting services for the relocation of neutral beamline No. 3 on TFTR to location No. 1 (Bay Q). This effort was undertaken to obtain a more equal injection power balance from the four tangentially positioned beamlines. Prior to this modification, the configuration on TFTR had three co-injected beamlines and one counter-injected beamline (as defined by the usual direction of plasma current). This imbalance causes the plasma to rotate in the direction of the greater injection power, at speeds up to $8 \times 10^5$ meters per second with resultant reduction in stored energy and heating efficiency.[14] The relocation effort included the disassembly and reinstallation of the associated flexible transmission lines, installation of new high-voltage triaxial and coaxial cables, and extension of existing electrical power cables and raceways.

Six new shaping-field power supplies were delivered by Robicon Corporation and installed in the basement of the Experimental Systems Assembly and Test Building (see Fig. 9), along with associated cabling, disconnect switches, circuit breakers, reactors, and instrumentation. All power supplies were tested, operated individually and as a group into the PBX-M machine coils. Each facet of the control system, annunciation, and self-protection was tested and demonstrated to be satisfactory.[15] Additional PBX-M activities included installation of an Electronic Associates Inc. (EAI) computer in the control signal feedback loop. This system is used for real-time processing of signals required to control the six shaping-field power supplies and the equilibrium-field power supply used for plasma positioning. Five new high-current disconnect switches were designed, built, and installed in the dc power system to support the new power supplies.

Work commenced on CIT power system studies to investigate various power system configurations and control techniques for the CIT Project.

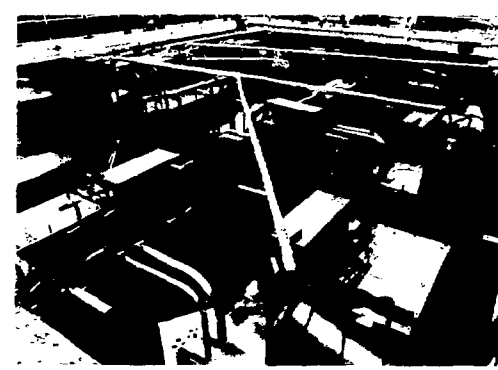

*Figure 9. New PBX-M shaping-field power supplies. (87E0602)*

## Motor Generator Section

During FY87 operation, maintenance, and upgrade of the TFTR motor generator (MG) system was transferred to the Electronic and Electrical Engineering Division's MG Section. With consolidation of TFTR and C-Site operating personnel, greater flexibility was achieved. Cross training of personnel for both systems is ongoing. In FY87, the MG Section accomplished the following tasks:

**C-Site MG System.** Seven high-speed dc circuit breakers were remanufactured and acceptance

tested, bringing the number of refurbished breakers to ten. The remaining six breakers are scheduled to be refurbished during FY88 and FY89. The trip setting control for the high-speed breakers was upgraded by using a constant current regulator which has the flexibility to transfer to the old scheme (rheostat control) if a problem arises. The computer program for C-Site MG simulation was upgraded and a SPITBOL program was converted to spreadsheet format in order to calculate PPPL's power bill. Detailed electrical demand and energy charges can now be provided to the individual projects. Support was provided for PBX-M, S-1, and the Radio-Frequency Test Facility. The power interruption procedure was executed successfully upon PSE&G's request. Two preventive maintenance subcontracts for the C-Site MG system and water system were monitored and supervised. The MG Section responded efficiently to many emergency situations, thus minimizing downtime.

**D-Site MG System.** Projected TFTR power requirements are as high as 140% of the rated power of the MG system. PPPL and Canadian General Electric (CGE) completed a mechanical study of end turns of the generator stator windings. Forces measured as part of the study on the upper and lower end turn heads of the stator windings were small, even under the projected 140% of rated power. The electrical evaluation, including exciter capability, CCV, protection and control, is in progress. Additional items accomplished included updating MG spares; installing a $CO_2$ alarm in MG basement; providing level monitor for MG emergency cooling water; continuing measurement and analysis of the ground currents around the generator reactor; continuing improvement in TFTR motor generator availability to nearly 99% for the last three run months of FY87 (see Fig. 10); monitoring and supervision of D-Site MG maintenance subcontract; updating of maintenance procedures.

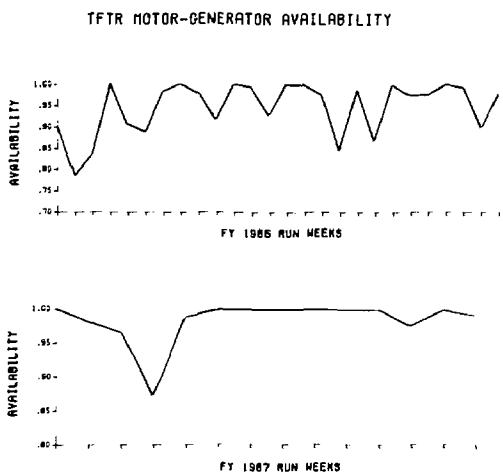


*Figure 10. Comparison of TFTR motor generator availability for FY86 and FY87. (88E0755)*

During the FY87 annual motor generator inspection, three major problem areas were uncovered:

(1) The babbitts of the thrust bearing segments in both MG No. 1 and No. 2 have depressions where the cooling water pipes run inside the segments. The depressions are deeper in Unit No. 1. This may explain why the thrust bearing's temperature ran unusually high during hot summer days, causing the motor generator to trip. Figure 11 shows the thrust bearing segments of MG No. 2. Engineering analysis is presently under way and is scheduled to be completed in FY88.

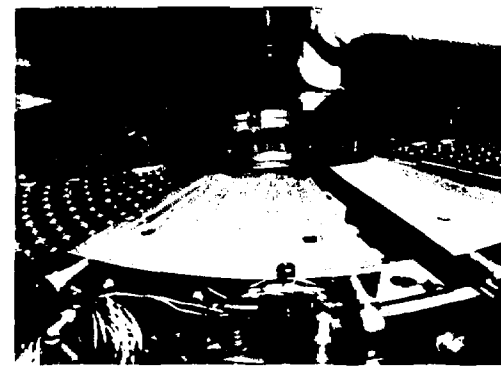

*Figure 11. Motor generator No. 2 thrust bearing segments. (87E1037)*

(2) In MG No. 2, the lower bore plug (generator shaft) became dislodged. As a result, rusted metal chips from inside the shaft were found in the oil of the lower guide bearing, which caused pitting on the thrust bearing surface. The bore plug was removed and replaced with a blank cover, the oil was cleaned and the manufacturer was asked to assess the significance of the bearing pitting.

(3) Cracked welds were found between four motor rotor gussets and the motor coupling flange (see Fig. 12). A decision was made to repair

*Figure 12. Weld crack between motor gusset and flange. (87E1030)*

the cracked welds in place. A sample of the cracked weld was cut from gusset No. 4. It was found to be a poor weld. Cracked welds were discovered on Motor Generator No. 2 in the same area. The cause for these cracks is as yet unknown. Stress analysis is in progress and scheduled to be completed by December 1987.

The MG Section and the Laboratory suffered a major loss during FY87 with the death of Henry Chandler, who had served as MG Section Head since 1980. Henry will be fondly remembered by all for his dedication, personal warmth, skill, and leadership.

# ENGINEERING ANALYSIS DIVISION

The role of the Engineering Analysis Division (EAD) is to support the physics programs of the Laboratory and the national fusion effort by providing evaluation and planning of new and upgraded experiments, conceptual and preliminary engineering design services, and systems engineering services. The EAD also develops and maintains computer programs for design and analysis and performs engineering and scientific analyses in specialized areas of technology such as radiation, solid and fluid mechanics, heat transfer, vacuum and cryogenics, superconductivity, electromagnetics, and field design. This year, the division performed analysis on the Joint European Torus (JET) under a contract. There are two technical units in the division: the Thermomechanical Branch and the Plasma Engineering Branch.

## Thermomechanical Branch

The Thermomechanical Branch provides a broad spectrum of capabilities in engineering mechanics, finite element analysis, thermal analysis, and mechanical design. Most of the activity for this year was divided between the Tokamak Fusion Test Reactor (TFTR) and the Compact Ignition Tokamak (CIT) projects. The Branch also performed analysis in support of the JET contract. In addition, the Branch supported the ongoing effort to enhance the analytical capabilities of the EAD.

### TFTR/Operations System Engineering Support

The Branch supported many areas of the TFTR Project. Analyses of the poloidal-field (PF) coils, which were begun under the Operations System Engineering Support (OSES) contract, were concluded, and the matrix of stress coefficients for the PF coil system was finalized. These coefficients, which allow prediction of critical stresses in a coil given the radial, vertical, and thermal loads, are used in the TFTR systems codes and coil protection calculator (CPC).

A nonlinear finite element analysis was performed on PF stack No. 2 of TFTR. Modified versions of the OSES models of the coils in the stack were run with the internal loads from OSES analyses and boundary forces on the coils obtained from a model of the coil stack and internal support structure (ISS) which contained the nonlinearities. This work represented the state-of-the-art in finite element analysis of copper-epoxy composite coils. Linear approximations to the behavior of the coil stack were found for several different operating modes, and stress coefficients for the coils in this stack were determined and used for the CPC.

### TFTR Radio-Frequency Heating

The ion cyclotron radio-frequency (ICRF) antenna and radio-frequency (rf) limiter were extensively analyzed in order to verify the designs. Heat transfer and stress analyses were performed. Eddy current and thermal loads due to plasma disruptions were simulated as were thermal loads for normal operation. A series of SPARK and NASTRAN models were developed and used to examine the rf antenna under static and dynamic eddy current loadings (Fig. 13 and Fig. 14). The rf limiters, which shield the rf antenna from the plasma, are unique in that the carbon composite is the structural material of the limiter. This results in a simple design with substantially lower eddy current forces than would be present in a conventional graphite-on-metal design. Thermal analysis predicted high temperatures in the limiter which would produce excessive thermal loads on the TFTR vacuum vessel bellows. A cooling shield was designed to alleviate this effect.

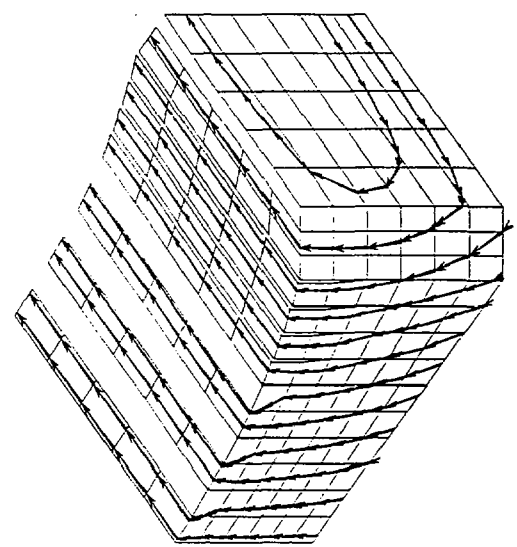

*Figure 13. SPARK-code model of radio-frequency limiter showing eddy currents. (88E0684)*

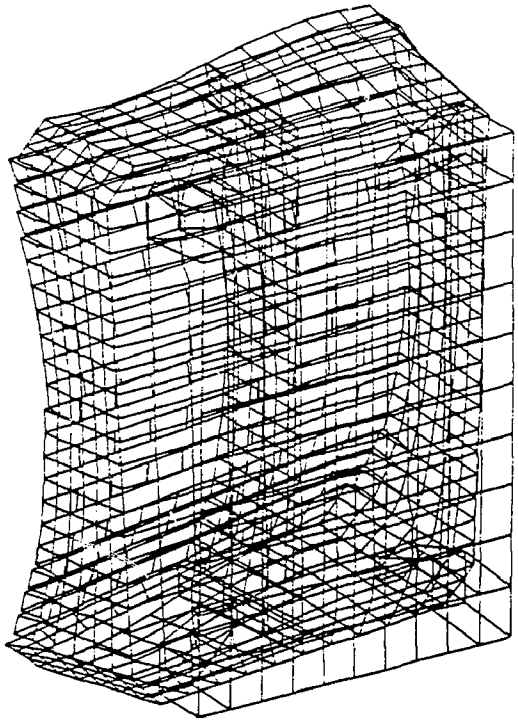

*Figure 14. NASTRAN-code model of radio-frequency limiter under load. (88E0683)*

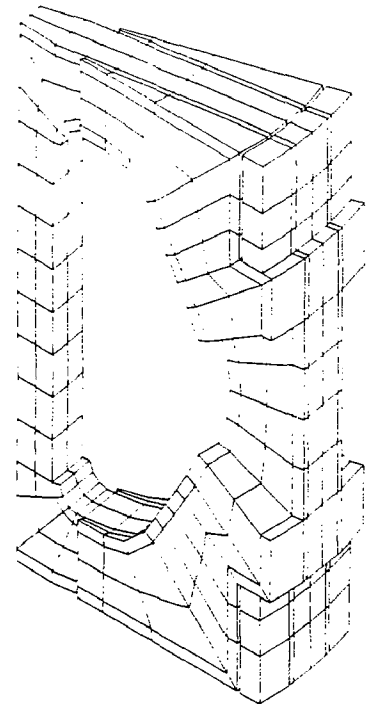

*Figure 15. NASTRAN-code model of the Compact Ignition Tokamak coil and case. (88E0682)*

## TFTR Engineering Support

A nonlinear finite element analysis was performed on the center plug of TFTR.

Studies of the General Electric (GE) turn-around conductors on the motor generator stator, which analyzed enhanced performance conditions, were completed. A review of the GE conversion transformers was also performed.

## Compact Ignition Tokamak

An integrated toroidal-field (TF) coil analysis capability was developed. This enabled the generation of a finite element model and the associated loads given a set of machine parameters (Figs. 15-17). Linear and nonlinear analyses of the TF coil and case were performed. The integrated coil analysis enabled a faster turnaround in response to changing machine parameters, and was used extensively in design studies. The effects of dewedging the inner corner of the TF coil and of unbonded turns were investigated in various sensitivity studies.

A detailed nonlinear analysis of the inner leg of the TF coil at the midplane was performed. This model used separate elements for the copper, Inconel, and insulation and yielded a detailed understanding of the behavior of the inner leg.

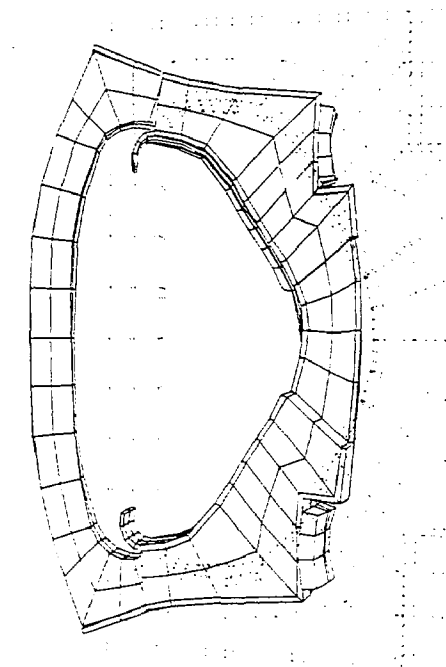

*Figure 16. In-plane deformation of the Compact Ignition Tokamak toroidal-field coil. (88E0685)*

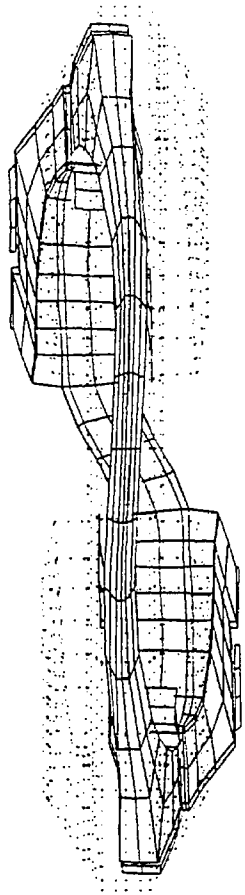

*Figure 17. Out-of-plane deformation of the Compact Ignition Tokamak toroidal-field coil. (88E0681)*

The laminated copper/Inconel conductor proposed for the CIT toroidal-field coils has never been used at the stress levels of CIT. A test program was initiated in order to verify the performance of the laminate at high stresses. The program consisted of compression tests of differently sized specimens at the National Bureau of Standards. Nonlinear finite element analysis was performed on the specimens, and the predicted displacements matched the test results. These tests verified the modeling techniques as well as the laminate performance.

The conceptual design of the supports and cases for the external poloidal-field coils and the internal control coils was initiated.

### Joint European Torus

The Thermomechanical Branch initiated finite element thermal and stress analyses of the poloidal-field coils on the Joint European Torus (JET) under a contract. This work will result in detailed turn-by-turn models of the JET poloidal-field coils, similar in scope to the Operations System Engineering Support models developed for TFTR.

Figure 18 shows the results of thermal analysis of a poloidal-field coil. The first picture is an elevation view of the model of the coil, without thermal loads. The second picture shows the model with its elements displaced vertically in proportion to their change in temperature.

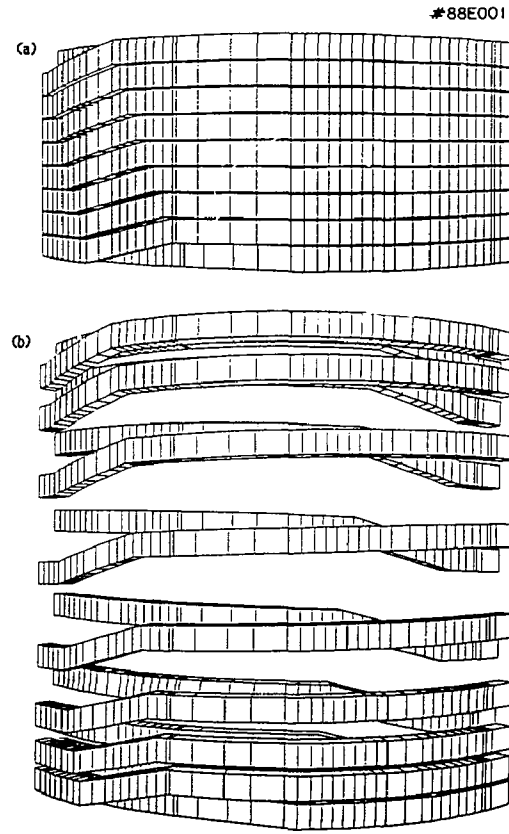


*Figure 18. Postprocessed results of Joint European Torus poloidal-field coil model. (a) Before thermal loads have been applied. (b) Elements are displaced in proportion to their temperature.*

## Plasma Engineering Branch

The Plasma Engineering Branch provides services in the areas of systems engineering, electromagnetic analysis and design, and radiation analysis. Systems support for large experiments is provided from the preconceptual design phase to the start of operation. Design and analysis of magnetic field systems and their interaction with the associated electrical and mechanical systems are performed. The Branch also performs radiological and radiation-related analyses and assessments for the design, operation, and instrumentation of experimental devices at the

Princeton Plasma Physics Laboratory (PPPL). This year, the activities of the Branch were primarily divided between CIT and TFTR. Some work was performed in support of the JET contract and the Princeton Beta Experiment-Modification (PBX-M).

## CIT Systems Engineering

The General Requirements Document (GRD) and Systems Requirements Document (SRD) were developed for CIT. These documents define the top level and system level requirements that CIT must meet. Systems Description Document inputs from the Work Breakdown Structure (WBS) managers were compiled and released.

The effects of varying machine parameters and envelopes were investigated in a series of scoping studies, which led to the evolution of a more optimal and feasible design.

Various analyses, which were performed at the WBS level, were validated during the technical assurance program. The areas addressed included the vacuum vessel, plasma initiation, and poloidal-field stress and temperature histories. Development of a global tokamak simulation model was also initiated.

Several major analysis tasks were performed in support of the CIT Project. Static and dynamic analyses were performed on the CIT vacuum vessel. Software that translates SPARK geometry to NASTRAN geometry was modified and expanded to provide full transient eddy current load capabilities and options for interactive modeling of boundary conditions.

Analysis of the CIT power systems was performed. The proposed design utilizes the TFTR power supplies. Poloidal-field coil designs were analyzed in order to determine compatibility with the power supplies. A plan to minimize the cost impact of the upgrades, by optimal exploration of existing resources and staged implementation of the expanded facility, was developed. The projected expansion is modest; the existing 138-kV power line along with an upgraded 138-kV substation will be adequate.

An equivalent axisymmetric modeling technique that electrically matched the response of a nonaxisymmetric vacuum vessel was developed. Moving plasma scenarios were investigated in conjunction with the TSC plasma modeling code.

Work on the manufacture of laminated conductors progressed during the fiscal year. Several vendors produced increasingly larger explosion bonded samples of the conductor. Copper-Inconel conductors of adequate size for the toroidal-field coils have been successfully fabricated.

## Radiation Analysis on CIT

Neutronics analysis of CIT was initiated. A three-dimensional calculational model was developed, and it is the basis for predicting the radiation environment around the CIT facility. The building wall and device shielding thicknesses required to meet the radiological design objectives were defined, and the effects of using different shielding materials were studied. Induced radioactivities in the Test Cell air, nitrogen cryopanels, and structural materials were derived. These data were used to assess the environmental impact of CIT operation under normal and abnormal conditions. An assessment of radiation damage potential was also made, and the results will aid the selection and placement of materials and instruments

The effects of radiation streaming through diagnostic penetrations in the device shielding were studied. Results were incorporated into a data base which permits the choice of an optimal location and arrangement for diagnostic components and detectors in order to minimize damage and radiation-induced noise. A more detailed study was made for the epithermal neutron detector system to define the expected operating range and for the bolometer diagnostics to estimate the amount of gamma-ray heating.

## Joint European Torus

A cylindrically symmetric magnetic materials program was developed and applied successfully to JET. The code, IRONRZ, produced results that were in excellent agreement with measurements for several test cases.

SPARK Version 1.1 was installed on the computers at JET in England.

## PBX-M

Several Poincare plots were generated for PBX-M. This work helped to determine the sensitivity of the machine's field to coil perturbations.

## TFTR Power Supply Upgrade

The ac (alternating-current) distribution for the ohmic-heating supply was studied extensively, with the objective of obtaining ohmic-heating drive for plasma currents of up to 4 MA. An increase in the number of ohmic-heating feeders was recommended along with decreased impedance for the current limiting reactors and replacement of the ohmic-heating feeder breakers.

The high-voltage power line and associated 138-kV substation were studied with the objective of obtaining higher energy. Alternatives included better utilization of existing equipment, regrouping voltage sensitive loads, and minor expansion of the high-voltage substation.

The operating limits of the motor generator sets were studied extensively. A "permissible operating envelope" for the motor generators, as a function of frequency, power factor, real power, exciter capability, voltage overshoot, and other variables, was developed.

A protective system that permits operation within the full envelope, but prevents a transgression, was developed. Such a system will permit better exploitation of the motor generator sets than existing operating limits that are based on MVA (megavolt amperes) or megawatt ratings.

The overvoltage protection of the TFTR coils was reviewed. Replacement of overvoltage protectors by more up-to-date devices was recommended.

### TFTR Diagnostics

Field perturbation and magnetic force calculations were performed for diagnostics prior to and during the machine opening. The results of these calculations were used to define mounting structure requirements and permissible locations for diagnostic components.

### Radiation Analysis for TFTR

The Branch actively participated in the planning of deuterium-tritium (D-T) operations. The additional radiation shielding required to satisfy the radiological design objectives was defined. An "igloo" concept was chosen because of its effectiveness. Shielding design requirements for penetrations, such as the neutral-beam injectors, were defined and will be included as part of the igloo design.

Design and analysis support for shielding of diagnostics continued during the fiscal year. The objective is to analyze the detector noise induced by neutrons and secondary gamma-rays and to find ways to reduce their contributions to detector readings. Major activities were shielding for the X-ray crystal spectrometer, streaming and scattering studies for the multichannel neutron collimator, and energy deposition studies for the escaping alpha detector system. Measurements have shown that the neutronics analysis yields accurate predictions and can be used as the basis for a design.

On-site meteorology data have been continuously processed, and their relation to the dispersion of radioactive effluents released from the Laboratory site was analyzed. A comprehensive sensitivity study examined the effects of various assumptions and parameter values on the results of dispersion calculations. Based on this study, a reference dispersion calculational model and procedure were established. They will be used to estimate doses due to the release of radioactive air and tritium from TFTR and CIT.

Modeling of the gas transport in the TFTR torus and neutral-beam vacuum system was initiated. The objective is to provide a model for estimating the tritium inventory anywhere in the vacuum system. A data base that includes all of the essential elements of the as-built geometry of the torus vacuum system was established, and a transient simulation model was created. Work on a carbon outgassing and absorption model is in progress.

## MECHANICAL ENGINEERING DIVISION

The Mechanical Engineering Division (MED) provides engineering and technical services to the many projects and programs at the Laboratory. The Division consists of three branches: the Mechanical Technology Branch, the Vacuum and Cryogenics Branch, and the Coil Systems Branch. In addition to the branches, there is an independent Engineering Services Group. The Division's major efforts and activities during FY87 were for TFTR, however, significant resources were applied to the PBX-M and S-1 projects. The needs of the remaining research programs were met as required.

The Engineering Services Group provides skilled technicians to perform maintenance, fabrication, and installation work for the various MED branches and for any other groups within the Laboratory. This group is organized into several shops according to skill. The electrical shop pulls heavy cable and performs electrical work up to 200 kV, both for the major experimental devices and smaller individual laboratories at PPPL. The electrical shop also installs control wiring, interconnecting computer cabling, and some instrumentation wiring. The plumbing shop maintains water systems for the experimental devices and fabricates new systems. The carpenters' shop builds wooden structures, platforms, and enclosures. It also fabricates special molds and forms for coil winding, models for developmental studies, and shielding for diagnostic devices. The metal and weld shops design, fabricate, modify and install various mechanical structures throughout the Lab. Work ranges from electronic enclosures to very large structural weldments in metals ranging from 0.010-inch to 1.5-inches thick. The electrical design group designs control and power cable installations including the required conduit and tray work. These design services are mainly in support of the TFTR device. The Engineering Services Group also hired, trained, and provided daily supervision and administration for the over 150 subcontract technicians used by the various MED and TFTR divisions during the FY87 TFTR shutdown.

## Coil Systems Branch

During FY87, the Coil Systems Branch participated in work for PBX-M, S-1, TFTR, CIT and the Los Alamos National Laboratory (LANL) ZT-H program. A major effort involved the completion of tasks for PBX-M. In this catergory was the design, fabrication, and installation of nine separate poloidal-coil bus systems connecting the poloidal-field coils to the switching panels. Figure 19 is a view of the buswork behind the switching panels. The passive stabilization coils for PBX-M were finish machined and installed during the fiscal year. The passive coil system contains five pair of single-turn coils fabricated from an explosively

*Figure 19. The PBX-M buswork configuration behind the PBX-M switching panels. (86E0887)*

bonded stainless steel, aluminum composite. A total of seventy coil segments and fourteen pairs of interconnecting bus comprise the passive coil system, Fig. 20.

Two new equilibrium-field pinch coils were fabricated and installed in the S-1 device, Fig. 21. Each coil consists of four turns, with series-parallel connectors providing flexibility in operating as a one, two, three, or four turn-coil. Each of the four turn-coils are potted in stainless steel bellows as shown in Fig. 22.

Two programs in preparation for D-T operations on TFTR were initiated during FY87. A study of the modifications required for D-T shielding was started. Each bay of the TFTR was surveyed for electrical, pneumatic, and cooling lines which interfere with the proposed igloo shielding and which will have to be accommodated in the shielding design. This job will continue in FY88. A preliminary study was also started on an external manipulator for D-T operations. The basic design that evolved consists of a mobile unit with the capability of performing simple inspection and maintenance tasks which will reduce the radiation exposure time of operating personnel.

Coil Branch engineering assisted the Los Alamos National Laboratory in generating design specifications for the poloidal-field and toroidal-field coils for their ZT-H program. In addition, studies began and will continue on the selection of a suitable insulation for the CIT toroidal-field coils. This scope of work includes existing insulation screening, development, and testing.

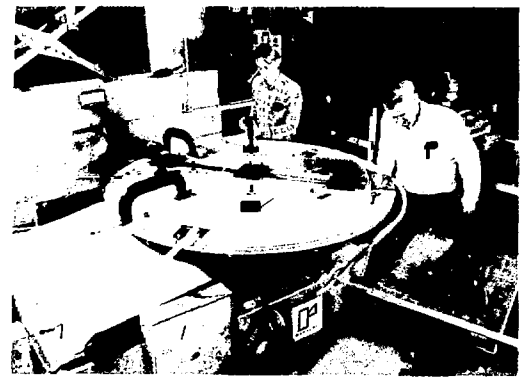

*Figure 20. Trial assembly of a PBX-M outer cone passive coil segment. (87E0373)*

*Figure 21. Fabrication of a S-1 equilibrium-field pinch coil. (87E0554)*

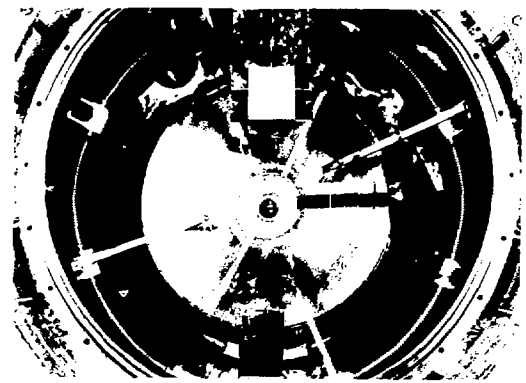

*Figure 22. Assembly of S-1 equilibrium-field pinch coil. (87E1324)*

# Mechanical Technology Branch

The Mechanical Technology Branch consists of two engineering sections: the Diagnostics and General Fabrication Section and the Materials Test and Machine Design Section. In addition, the Branch includes the Mechanical Drafting Group and the Machine Shop Services Group.

## Diagnostics and General Fabrication Section

Two fixed poloidal limiters were designed, fabricated, and installed in TFTR to protect the rf antennas from plasma thermal loads. The 24-segment limiter, Fig. 23, is constructed of a carbon-carbon composite material and will replace the movable limiter previously used. Installation will be completed in November 1987.

Neutron shielding was designed and fabricated for protecting the vertical X-ray pulse-height analyzer and the vertical X-ray crystal spectrometer. Over 80 tons of lead are involved in the construction of the shielding in the TFTR Test Cell Basement. Installation is approximately 75% complete.

A heating and cooling system for the S-1 vacuum vessel wall was designed and installed during FY87. The heat of compression of air is utilized for the heating cycle and liquid nitrogen injected into an air stream provides the necessary cooling. Design specifications were achieved during system tests.

Two new tangential bolometers were added to the TFTR. One bolometer is a single module viewing in the co-direction of injected neutral beam, the other is an array of eight modules viewing in the counter-direction of injected neutral beam. In addition to the presently installed vertical and horizontal arrays and the six wide-angle bolometers, the new assemblies will allow a more complete evaluation of radiated power distribution and energy losses due to charge-exchange of fast ions in TFTR.

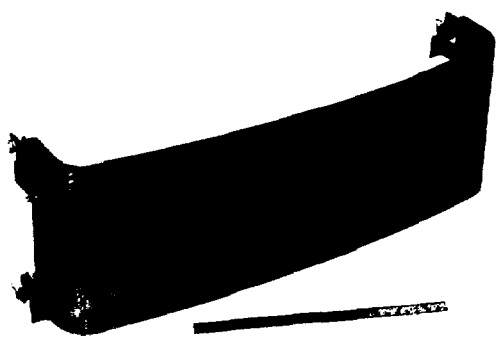

*Figure 23. The TFTR carbon-carbon composite of a radio-frequency limiter segment. (87E1579)*

A plasma current-measuring diagnostic, a diamagnetic loop, was designed and fabricated for PBX-M. A unique approach involves the use of seven subassemblies, fabricated from rectangular cross sections of stainless steel tubing. These subassemblies are then mechanically attached to form a rigid frame inside of the PBX-M vacuum vessel.

During the FY87 TFTR shutdown, a neutral-beam was relocated from Bay K to Bay Q to improve plasma characteristics. This effort required considerable coordination between the Mechanical and Electrical Engineering Divisions and the TFTR Heating Systems Division. The job included the design and fabrication of a new beam duct and duct support. The resulting design will be the prototype for modifying the remaining neutral-beam ducts for D-T shielding.

## Materials Test and Machine Design Section

In FY87, the Materials Test Laboratory (MTL) performed a total of 85 tasks; approximately 50% were for CIT and 40% for TFTR. Work projects for CIT involved tension/compression tests on copper, beryllium copper, and Inconel. Shear and compression tests were run on a special composite material for CIT consisting of polyimide/glass insulation sandwiched between layers of Inconel. In addition to tests at PPPL, larger pieces of a copper-Inconel composite underwent compression testing at the National Bureau of Standards Laboratory in Gaithersburg, Maryland, utilizing their 12 million pounds compression capability. Additional tests on this composite material were performed in the MTL.

A variety of tasks were performed for TFTR including thermocouple fabrication and installation on long-pulse stripper assemblies, gauge calibration, and repairs for the MG section, and fatigue testing of carbon laminate bars. Other tasks involved the measurement of temperatures generated by arc welding and its potential damaging effect on G10 insulating material. Tests were also run on cast aluminum safety aid fixtures identifying a possible safety hazard.

A number of ongoing tasks are performed in the MTL, including the testing of lifting fixtures and the testing of sample welds for welders certification.

Machine design activities by the section include a number of seismic analyses. The ICRF transmission line and its support towers in the TFTR Test Cell were qualified for the most probable earthquake (MPE). A major effort involved the seismic analysis of various TFTR igloo shielding concepts in support of D-T preparations for TFTR. A study of the seismic as well as pressure and static loading was completed for the new duct and neutral-beam enclosure supports for neutral-beam No. 1 in its relocated position.

Miscellaneous design activities include the design of a new concrete foundation for the line backer circuit switcher tower in the 137-kVA enclosure at C-Site and a study of the adequacy of the third floor of the RF building for water tanks and dummy loads

associated with the 40 MHz/40-80 MHz transfer switch and dummy loads.

# Vacuum and Cryogenics Branch

## Vacuum Section

During FY87, the majority of the Vacuum Section's activities were in support of the TFTR device.

The maintenance manipulator program, undertaken last year, is proceeding well. The manipulator, shown in Fig. 24, will provide limited service in the interior of TFTR's vacuum torus during its D-T phase of operation, when high levels of activation make manned servicing prohibitive. The Vacuum Section provides the technical management for the program and is fabricating the vacuum antechamber in which the manipulator will be installed on TFTR. This chamber, which is now 90% complete, is shown in Fig. 25. The Laboratory is also procuring an in-vessel leak detector to permit vacuum leaks to be located from inside the torus using the manipulator as a positioning device. During this year, a commercially available ion-gauge type of leak detector was purchased from Seiko and tested in the test stand shown in Fig. 26.

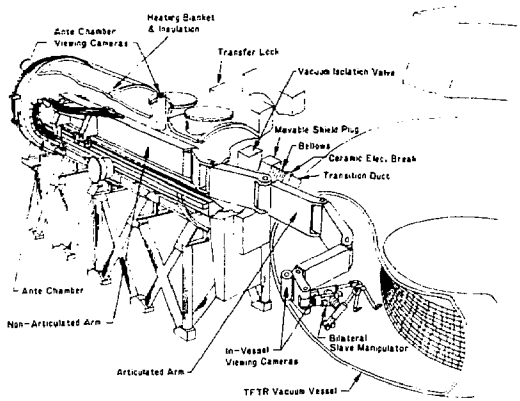


*Figure 24. The TFTR maintenance manipulator. (87E0103)*

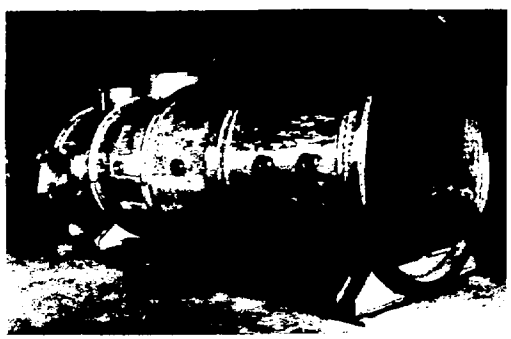

*Figure 25. The TFTR maintenance manipulator antechamber. (87E0592)*

The manipulator itself is being designed, assembled, and tested by Kernforschungszentrum-Karlsruhe (KfK) of Karlsruhe, W. Germany, under a cost-sharing agreement with PPPL. The mechanical components of the manipulator are being fabricated by Noell, GmbH of Wurzburg, W. Germany under subcontract to KfK. The controls system is being designed and fabricated by KfK. The vision and lighting system is being supplied by Centre Energie Atomique (CEA) of Paris, France, under a cost-sharing agreement with PPPL. The cameras were manufactured by their subcontractor, Hytec Hydro-Technologie of Marseilles, France. By the end of FY87, approximately 95% of the components of the manipulator, its control system, and vision and lighting system were fabricated and were being assembled. Figure 27 shows the manipulator during its initial assembly at Noell. The completed manipulator system will be shipped to TFTR during the first half of 1988 and will be tested on the M-3 Mock-Up in preparation for installation on TFTR in 1989.

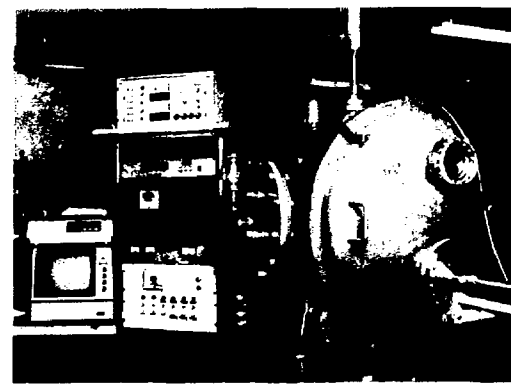

*Figure 26. In-vessel leak test stand. (87E0483)*

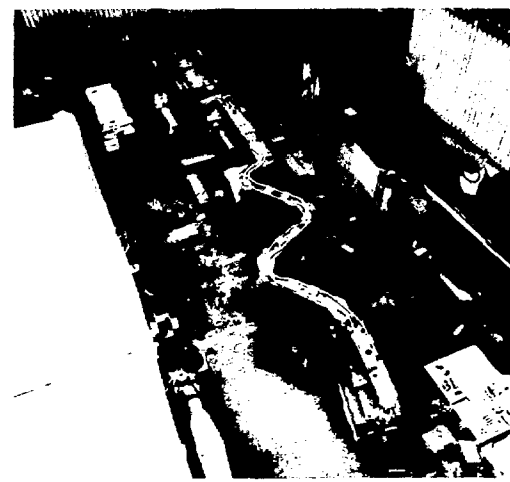

*Figure 27. The TFTR maintenance manipulator during initial assembly. (87E1633)*

The Vacuum Section undertook the TFTR deuterium-tritium shielding program in early CY87. A preconceptual design was proposed in the Draft TFTR D-T Plan in March, 1987. The shielding configuration proposed, shown in Fig. 28, adds a 30-inch thick concrete "igloo" around the TFTR device and encloses the neutral beams, diagnostics neutral beam, and pellet injector in concrete blockhouses to minimize the effect of radiation streaming through the nozzles connecting these devices to TFTR's vacuum vessel. Although similar to the configuration originally planned for TFTR, it has several significant differences. Whereas the original igloo design supported the igloo roof directly on the machine structure (the poloidal-field coil "umbrella structure"), the new configuration adds an independent support structure. This increases the overall height enclosed by the igloo and makes it possible to completely enclose the top of TFTR with its myriad of utilities and diagnostics. Besides greatly simplifying construction, it also minimizes the number of penetrations and increases shielding effectiveness. The other major difference concerns the method of igloo construction. To make it possible to install the shielding on TFTR without having to remove major systems, such as the neutral beams, the shielding in the lower machine bays will be constructed of borated concrete bricks, custom-fitted and installed with concrete mortar. The portions above the lintels and the roof panels will be constructed of precasted, reinforced borated concrete panels, shown in Fig. 29. Ebasco Services Incorporated will supply technical personnel to complete the design and oversee the installation of the shielding; the Vacuum Section will continue to provide technical management.

The Vacuum Section also provided high levels of support to the major TFTR machine opening, which began in July. Major tasks included the repositioning

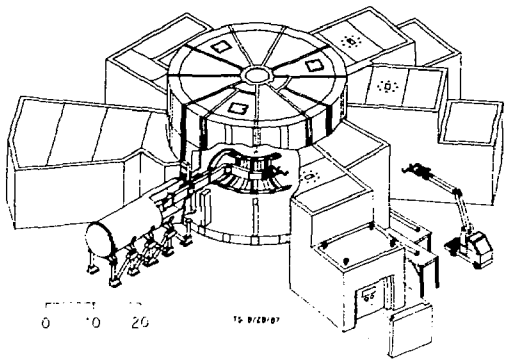

*Figure 28. Deuterium-tritium shielding configuration. (87E1175)*

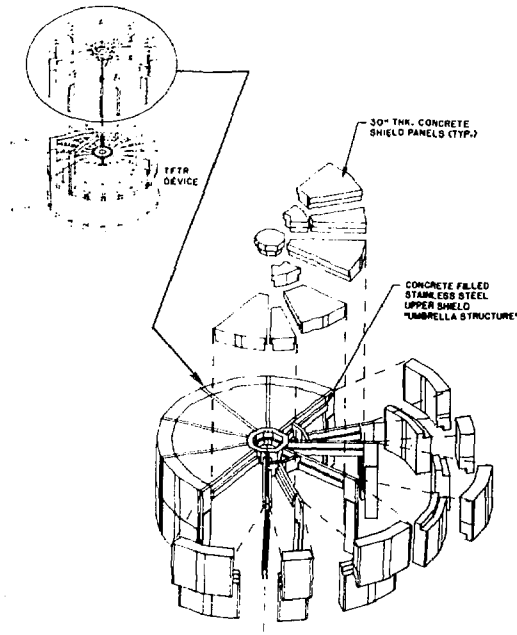


*Figure 29. Details of the upper portion of the deuterium-tritium shield. (87E0099)*

of neutral-beam No. 3 to the No. 1 position and the redesign and fabrication of neutral-beam components to improve the reliability of the neutral beams.

The Vacuum Section provided additional support to the D-T Shielding Program by participating in tritium system design reviews and tritium system planning. During FY87, the Vacuum Section completed work started in the previous year on the passive coil fabrication, poloidal coil vacuum enclosures, and coil supports for the PBX-M Program. The PBX-M is currently undergoing initial tests. The Vacuum Section also completed the fabrication of vacuum enclosures for the S-1 EF-P coils. The S-1, with the new coils installed, also underwent initial testing.

## Cryogenics Section

The Cryogenics Section operates the 1070-watt helium liquifier which supplies liquid helium to the four neutral-beam cryopumping systems. During FY87, the liquifier system operated with an appreciable improvement in availability, with essentially no TFTR downtime attributable to lack of liquifier availability. This system has now operated for a total of approximately 11,00 hours.

## References


[1]S.L. Davis, N.R. Sauthoff, and W. Stark, "Overivew of the TFTR Computer System," *IEEE Transactions on Nuclear Science* (Proc. 5th Conf. on Real-Time Comput. Applications, 1987), Vol. *NS-34* (IEEE, San Francisco, 1987) 718.

[2]J. McEnerney, N. Arnold, J. Chu, *et al.*, "TFTR Control System Applications—An Overview," in *Fusion Engineering* (Proc. IEEE 12th Symp., Monterey, CA, October 1987), to be published.

[3]J. Montague, L. Lagin, J. McEnerney, *et al.*, "The Evolution of the TFTR Master Clock System," in *Fusion Engineering* (Proc. IEEE 12th Symp., Monterey, CA, October 1987), to be published.

[4]L. Randerson, J. Chu, C. Ludescher, *et al.*, "TFTR Data: File Structure, Distribution, Archival, and Retrieval," in *Fusion Engineering* (Proc. IEEE 12th Symp., Monterey, CA, October 1987), to be published.

[5]J. Thompson, J. Murphy, and K. Frank, "SGLIB-A Library for Scientific Graphing," in *Fusion Engineering* (Proc. IEEE 12th Symp., Monterey, CA, October 1987), to be published.

[6]W.A. Rauch, W. Bergin, and P. Sichta, "TFTR CAMAC Systems and Components," *IEEE Transactions on Nuclear Science* (Proc. 5th Conf. on Real-Time Comput. Applications, 1987), Vol. *NS-34* (IEEE, San Francisco, 1987) 970.

[7]N.D. Arnold, G. Schobert, D. Bashore, *et al.*, "Preliminary Design of the TFTR Tritium Remote Control and Monitoring System," in *Fusion Engineering* (Proc. IEEE 12th Symp., Monterey, CA, October 1987), to be published.

[8]P. Sichta and J. Mervine, "TFTR ICRF Computer System," in *Fusion Engineering* (Proc. IEEE 12th Symp., Monterey, CA, October 1987) to be published.

[9]P. Mathe, R. Mika, G. Oliaro, *et al.*, "The PBX-M Control System," in *Fusion Engineering* (Proc. IEEE 12th Symp., Monterey, CA, October 1987), to be published.

[10]W.M. Davis, P. Roney, T. Gibney, *et al.*, "Software Strategies and Hardware Upgrades to the PPPL Data Acquisition System (DAS)," in *IEEE Transactions on Nuclear Science* (Proc. 5th Conf. on Real-Time Comput. Applications, 1987), Vol. *NS-34* (IEEE, San Francisco, 1987) 775.

[11]L. Lagin, J. McEnerney, N. Arnold, *et al.*, "The TFTR Neutral Beam Control and Data Acquisition System," *IEEE Transactions on Nuclear Science* (Proc. 5th Conf. on Real-Time Comput. Applications, 1987), Vol. *NS-34* (IEEE, San Francisco, 1987) 772.

[12]N.R. Sauthoff, W. Stark, L. Drucker, *et al.*, "Computer Support for the CIT Physics," in *Fusion Engineering* (Proc. IEEE 12th Symp., Monterey, CA, October 1987), to be published.

[13]W. Rauch, S. Hayes, J. Lowrance, *et al.*, "CIT Diagnostic Computer Interface Studies," in *Fusion Engineering* (Proc. IEEE 12th Symp., Monterey, CA, October 1987), to be published.

[14]R.J. Goldston, V. Arunasalam, M.G. Bell, *et al.*, "Energy Confinement and Profile Consistency in TFTR," Princeton University Plasma Physics Laboratory Report PPPL-2425 (April 1978) 16 pp.

[15]C.R. Ancher, "PBX-M Field Shaping Power Supplies," in *Fusion Engineering* (Proc. IEEE 12th Symp., Monterey, CA, October 1987), to be published.

# PROJECT PLANNING AND SAFETY OFFICE

## PROJECT PLANNING OFFICE

The Project Planning Office assumed the responsibility for budget and planning for the Compact Ignition Tokamak (CIT) Project during this fiscal year. The first draft of the CIT Project Management Plan was produced, budgets for fiscal years 1987 and 1988 were established, and a preliminary project schedule was issued. Planning was done for the Project performance measurement system (PMS) and the reporting system.

## PROJECT AND OPERATIONAL SAFETY BRANCH

This office worked closely with the Tokamak Fusion Test Reactor (TFTR) Project and with other Princeton Plasma Physics Laboratory (PPPL) projects. As in past years, heavy emphasis was placed on day-to-day interactions and on close support of project personnel. Coordination of preparations for the Deuterium-Tritium (D-T) Amendment to the TFTR Final Safety Analysis Report (FSAR) was started with the D-T Systems Division. Input was supplied for future projects, especially in the areas of environmental and safety concerns for the Compact Ignition Tokamak. Extensive review of and detailed comments on the draft CIT Environmental Assessment (EA) and draft CIT Preliminary Safety Analysis Report Format and Content Guide were provided. Reviews of various CIT issues were reported at topical meetings.[1-4] In May, PPPL published its fifth Annual Environmental Report.[5] This document reports on PPPL's environmental monitoring program and reviews PPPL's compliance with governmental regulations. A permit for groundwater discharge and for a treatment works in relation to our retention basin and oil separator, applied for in 1986, are still under consideration by the N.J. Department of Environmental Protection (NJDEP).

The Radiological Environmental Monitoring Laboratory (REML) received certification from the Environmental Protection Agency (EPA) in 1986 for its tritium analyses. An inspection and review in April 1987 by NJDEP recertified this analytical process. This laboratory is located in the New Guggenheim Building at B-Site on the Forrestal Campus. It will be relocated to a modular building at C-Site in the fall of 1987. The Differential Atmospheric Tritium Sampler (DATS) reported on in 1986, was tested in a field experiment in Ontario, Canada in June 1987. Valuable experience was gained in its use as an operational environmental tritium sampler and also in laboratory chemical recovery procedures. A patent is pending on this device's unique features.

A program is in place to continue to revise and update PPPL's Health and Safety Directives (HSD's). HSD-5008, Supplement 10-5 on radiation training was updated and approved by the Executive Safety Board (ESB) in FY87. The electrical safety section of HSD-5008 is still under review, and a new HSD-5012 on Environmental Protection was initiated.

Health physics surveys, electrical inspections, mechanical/cryogenic inspections, interlock testing, and overall safety reviews continued for all PPPL projects. A Safety Assessment Document (SAD) for the Princeton Beta Experiment-Modification (PBX-M) was written and reviewed and will be approved and published in early FY88. Training programs were expanded in radiation safety and electrical employees were instructed in the 1987 National Electrical Code changes. A tutorial on Overpotential Testing practices and procedures is being prepared. Capacitor bank accessor training and recertification continues. The scope of inspection and testing of personal protective equipment expanded sufficiently to justify some modest, temporary on-site high-voltage testing facilities. The Project and Operational Safety Branch is also completing a program to provide low-voltage rubber gloves to each of PPPL's electrical employees. Extensive reviews and participation in TFTR project safety and environmental issues is reported on in the TFTR section.

## OCCUPATIONAL SAFETY BRANCH

Fiscal year 1987 has been a year characterized by both change and accomplishment for the Occupational Safety Branch. During that time the Branch (formerly the Safety Branch of Occupational Medicine and Safety) became a part of the Safety Office under the Deputy Director for Technical Operations and was renamed the Occupational Safety Branch (OSB).

Particularly noteworthy is the improved capability of the OSB in the industrial hygiene area. The position of industrial hygienst, which was vacant for several months, was filled with a highly qualified and capable individual who has already made many improvements in the program during his short tenure. Asbestos handling procedures were revised to comply with new Occupational Safety and Health Administration (OSHA) standards; new confined-space permit forms

were developed to clarify responsibilities; the number of surveys for health and environmental hazards was sharply increased and assistance was provided in developing procedures for specific instances of hazardous material handling.

In the industrial safety area, in addition to the many ongoing activities such as investigating and reporting on accidents, conducting internal safety audits, publishing Safety Bulletins and HOTLINE articles, monitoring construction projects and inspecting work areas, a Working Alone Policy was developed and approved by the Executive Safety Board.

In both safety and hygiene, a major effort of OSB has been in the training area. During the year over 100 training sessions were conducted with over 2,000 total in attendance. In addition to the training already available, new courses were added or improvements made to existing courses in the areas of confined-space training, asbestos handling, respiratory protection, and safety orientation. A trailer scheduled for salvage was acquired to help temporarily resolve a very real problem of lack of available classroom space; general interest safety programs were initiated with the New Jersey Safety Council's Seat Belt Convincer and mandatory bimonthly Area Safety Coordinator training meetings were approved by the Executive Safety Board and implemented by the OSB.

In the area of fire protection, the Laboratory continued to make good progress in complying with the recommendations of the Factory Mutual Report. At the start of the year, 16 of the recommendations had been closed either through completion or exemption. During the year, an additional 10 were closed and, of the remaining 10, two are nearly done and six have been funded or planned for the near future. In addition to coordinating and reporting this work, the OSB completed numerous fire safety reviews of facility plans and inspected and observed tests of fire system installations.

Branch administration was significantly improved. The file system was revised to make it more functional and an OSB file maintenance procedure was written. Organization of the safety library is well under way and will continue this year. Most important in this area is the improved system for obtaining and handling Material Safety Data Sheets (MSD's), including a computerized index of all MSD's on file to enable expeditious location of the appropriate data sheet when only a product name or chemical name is known. Following the completion of this data base, several hundred MSD's were distributed to field organizations from a backlog of requests. With increased radiation levels at TFTR the film badge administration work load increased substantially. This increase was absorbed without increase in staff through the use of a personal computer.

## References


[1]J.R. Stencel, R.B. Fleming, J.C. Commander, and M.A. McKenzie-Carter, 1987. "Health Physics Considerations for the Compact Ignition Tokamak." *Proceedings of the 20th Midyear Meeting of the Health Physics Society, Reno, Nevada, February 8-12*, pp 356-64.

[2]M.A. McKenzie-Carter and J.R. Stencel, "Environmental Assessment for the Compact Ignition Tokamak," in *Fusion Engineering* (Proc. 12th Symp., Monterey, CA, October 1987), to be published.

[3]R.B. Fleming, J.R. Stencel, E.C. Selcow, and R.E. Lyon, "Control of Activated Air and Nitrogen Coolant for the Compact Ignition Tokamak," in *Fusion Engineering* (Proc. 12th Symp., Monterey, CA, October 1987), to be published.

[4]M.E. Norris, F. Beane *et al.*, "CIT Grounding for Power, Equipment, and Personnel Safety," in *Fusion Engineering* (Proc. 12th Symp., Monterey, CA, October 1987), to be published.

[5]J.R. Stencel, "Environmental Monitoring Report for Calendar Year 1986," Princeton University Plasma Physics Laboratory Report PPPL-2442 (May 1987) 78 pp.

# QUALITY ASSURANCE AND RELIABILITY

Quality Assurance and Reliability (QA/R) continued to refine in-place systems established in 1986. In addition, QA/R was actively involved in Compact Ignition Tokamak (CIT) planning, Tokamak Fusion Test Reactor TFTR reliability improvement, and in a certification program designed to enhance the skill levels of the QA/R personnel.

## COMPACT IGNITION TOKAMAK

In FY87, the CIT Project issued CIT-G005, "The CIT Quality Assurance Requirements." These requirements were tailored from the American Society of Mechanicl Engineers' (ASME's) NQA-1 and they "baseline" the quality assurance (QA) program for the Laboratory, other Project participants, and major subcontractors of CIT. A considerable effort was directed to such issues as the reliability, availability, and maintainability of CIT. This effort is expected to be completed in FY88 with the issuance of a reliability and maintainability (RAM) plan for CIT.

## TOKAMAK FUSION TEST REACTOR

Because of the planned use of tritium in TFTR in 1990, the emphasis of the Quality Assurance and Reliability organization switched to the concerns associated with tritium, primarily in the area of reliability. Due to the neutron activation of the system once tritium is used, access to the tokamak will be greatly limited and repairs difficult, if not impossible. In addition, the number of tritium pulses will be limited. Therefore, it is important to increase the probability that a shot attempt completed successfully and produce all the desired data. Working closely with TFTR Project personnel, significant effort began in 1987, and will continue throughout fiscal year 1988, to identify those system components that have the greatest risk of failure during tritium operation so that the problems may be averted. This effort has three significant components:

First is a major effort of the engineering organizations to review the system components that are currently within the igloo, the area in which access will be most limited during tritium operations. The reviews involve analysis of these components in an attempt to define in advance potential problem areas and recommendations for modifications and improvements.

Second is a major effort spearheaded by QA/R to model the critical TFTR systems, obtain detailed data about failures within these systems as they occur, and predict the reliability performance of these systems. One of the most time consuming efforts involved has been to develop the Critical Parts Lists of all systems contained within the Test Cell and Igloo. This list determines to what level of hardware components reliability statistics will be maintained.

Third is a major effort to improve data about TFTR performance during actual operations and to improve the information maintained and analyzed about the success or failure of each shot attempt and the causes of the failure. The manually maintained TFTR Operations Log was automated by QA/R in early spring, 1987. This allows easier analysis of system failures and easier analysis of shot statistics. The system is currently being enhanced to include better refinement of the data. The upgrade is expected to be available in spring, 1988.

Parallel efforts to the above occurred throughout the year. Audits were performed on the documentation associated with the Tritium Storage and Delivery System and will occur in fiscal year 1988 on other components of the tritium system. Reliability analyses were performed on the 908 CAMAC module. Working with engineering, the reliability of the 908 CAMAC modules was significantly increased.

## CERTIFICATION

A significant effort was undertaken to enhance the skill levels and improve the expertise and capabilities of various PPPL personnel, from the quality control inspectors in the field to the PPPL personnel performing special processes. Significant progress has been made.

First, the inspectors received training and certification in various nondestructive inspection techniques, specifically visual, dye penetrant, mass spectrometer, and ultrasonic testing, according to the standard of the American Society for Non-Destructive Testing, identified as SNT-TC-1A. While these skills are of general importance to the Laboratory, they will be most useful when witnessing leak testing for TFTR or inspecting the welds in the R&D program of bonding Inconel to Copper. In addition, the quality control inspectors received training for the in process inspection of electronic cable terminations and electronic soldering according to Laboratory standards.

Training is not limited to the quality control staff. Special process Princeton Plasma Physics Labor-

atory (PPPL) personnel also received training in electronic cable connectors and electronic soldering, according to the PPPL standards.

The certification process will continue in fiscal year 1988. Plans exist to formally certify all inspectors according to American National Standards Institute (ANSI) standards (both electrical and mechanical) and to formally certify all engineers according to the American Society of Quality Control standards. Finally, the QA/R organization is assisting Laboratory management in setting up a welding and brazing certification program for PPPL welders and brazers.

# ADMINISTRATIVE OPERATIONS

In FY87, the administrative effort focused on the accomplishment of the move of all Laboratory activities out of A- and B-Sites and the consolidation of most activities at C- and D-Sites, as a consequence of contractual agreements between the U.S. Department of Energy (USDOE) and Princeton University. The "move" involved:

- vacating 350,000 square feet of space at A- and B-Sites,
- finding new space for and moving 350 people, and
- relocating, or disposing of, large quantities of plant, equipment, and material.

About 100 people were absorbed by upgrading existing space in C- and D- Sites, while 250 were housed off-site in commercially leased space about two miles from the Laboratory at 307 and 305 College Road East. The cost of the move, including construction of new high-bay engineering space at C-Site, refurbishing office space at C-Site, moving heavy equipment, etc. is estimated at over $5 million in FY87. To accommodate this effort, many normal maintenance and General Plant Projects (GPP) construction activities were deferred to future years, thus increasing the backlogs of work carried into FY88. Much of the move had to be accomplished by subcontract personnel.

During FY87, total Princeton Plasma Physics Laboratory (PPPL) employment continued to be reduced through attrition and workload management from 1,040 at the start of the year to 1,010 at the end. The 1,010 compares to the peak employment of 1,293 in October 1984, and is a reduction of 22%. The composition of the Laboratory by staff on September 30, 1987 is shown in Table I.

Other administrative accomplishments of note in FY87 were:

- With DOE and University support, the Laboratory began serious planning for an additional office building at C-Site that would house the Engineering Department staff which, in the "move," had to be located off-site at 307 College Road East. A proposal to construct a 60,000-square-foot office building under a third party financing arrangement was submitted to DOE for approval.
- A new administrative computing center based on an IBM 4381 was planned, tested, and placed into operation by year's end. The use of this facility, in conjunction with personal computer clusters, increased capacity and productivity and brought substantial reductions in PPPL computing costs.
- The Laboratory successfully adjusted its accounting and reporting operations to enter data as required into DOE's Financial Information System (FIS) at year's end.
- A number of other steps were taken during the year to improve productivity and reduce costs, including consolidation of stockrooms, introduction of a desktop publishing system in Information Services, contracting out automotive maintenance, and reduction in office supply inventories through a direct delivery contract.
- Steps were taken to strengthen administrative support for the Compact Ignition Tokamak (CIT) Project, particularly in the procurement area.
- Medical evaluations by the Occupational Medical Office were extended to include a larger portion of the staff, and planning for expanded wellness/fitness activities was initiated.
- The Laboratory implemented an in-house Employee Development and Training Program with courses to foster career growth and skill enhancement.
- Management and supervisory training was increased. A one-day training course on compensation to be attended by all supervisors was initiated; it was about two-thirds completed by year's end.

**Table I. Fiscal Year 1987 Staff Composition.**

| | |
|---|---|
| Faculty | 2 |
| Physicists | 116 |
| Engineers | 209 |
| Technicians | 465 |
| Administrative | 120 |
| Office and Clerical Support | 98 |
| Total | 1,010 |

# ADMINISTRATIVE DEPARTMENT

## Plant Maintenance and Engineering

The Plant Maintenance and Engineering (PM&E) Division is a technical and administrative support organization. Its function and purpose is to support the Laboratory's research programs by operating, repairing, constructing, and modifying physical facilities, systems, and equipment at A-, B-, C-, and D-Sites. As of October 1, 1987, A- and B-Sites had been vacated; consequently, support in FY88 and beyond will be only for C- and D-Sites and minor support of off-site leased facilities at 307 and 305 College Road East. Table II shows the gross square feet (GSF) maintained by PPPL at each site during FY87 and the new GSF starting in FY88.

**Table II. Gross Square Feet Occupied by PPPL at the Beginning and End of FY87.**

The PPPL FY87 Square Foot Occupancy at the Beginning of FY87.

| Location | GSF |
|---|---|
| A-Site | 209,811 |
| B-Site | 140,088 |
| C-Site | 483,028 |
| D-Site | 218,723 |
| Trailers (C- and D-Sites) | 18,470 |
| Total | 1,070,120 |

The PPPL FY87 Square Foot Occupancy at the End of FY87.

| Location | GSF |
|---|---|
| A-Site | —0— |
| B-Site | —0— |
| C-Site | 483,028 |
| D-Site | 218,723 |
| Modules & Trailers (C- and D-Sites) | 20,836 |
| Off-Site Leased Facilities | 48,862 |
| Total | 771,449 |

### Project Engineering

The Project Engineering Branch is responsible for the planning, engineering, and coordination of General Plant Projects (GPP), as well as for energy studies and conservation projects. Table III summarizes the number and value of active projects at year's end.

In FY87, emphasis was primarily directed toward implementation of energy conservation projects, addressing energy conservation refinements in the physical plant preventative maintenance operation, and vacating A- and B-Sites.

### Energy Conservation

In FY87, the Energy Monitoring and Control System and the Power Line Carrier System were clearly PPPL's "leading edge" of energy conservation management and control. A result of the energy conservation efforts was an impressive energy consumption reduction of 14.5% in the FY87 Laboratory's Buildings Energy Utilization Index (Btu/ft$^2$) versus the FY85 Base Year. (This compares with a DOE-mandated goal of a 10% reduction from the FY85 Base Year by fiscal year 1995.) Reflected within these statistics are a 17.9% reduction in building electrical usage and a 3.9% reduction in building fuel oil usage. These reductions, when normalized, resulted in a savings of $400k in electric and $54k in fuel oil costs (FY87 versus FY85 Base Year) for the Laboratory.

These significant reductions were chiefly attributed to prudent energy management of A- and B-Sites, while occupied and during move-out phases, and to two distinctly different types of energy management systems, which were in operation during FY87: the Energy Monitoring and Control System (EMCS) and the Power Line Carrier System (PLCS). These energy management methods/systems established conservation control of energy-consuming loads and produced both reductions in energy consumption and cost of energy for the Laboratory.

Some of the larger energy retrofit projects completed in FY87 were: Energy-Efficient Motors—Phase II, Variable Frequency Drives for Large Motors, and C-Site Natural Gas/Boilers Central Plant Conversion. Energy studies also completed in FY87 were: Process Deionized Chilled Water Survey for C- and D-Sites and Battery Load Leveling Study.

To keep maintenance personnel up-to-date in energy conservation, equipment operations, and procedures, periodic training sessions were conducted. Also, in order to enhance and implement energy management and conservation measures, special in-depth energy conservation seminars were attended by PPPL engineers.

Public relations interface with Laboratory staff was maintained through the *PPPL HOTLINE* Newsletter. Energy awareness month, using the DOE theme, "Energy Security-Our Future Depends On It," was conducted at the Laboratory in October, 1987. Posters

Table III. Fiscal Year 1987 Project Engineering Summary.

| | No. of Projects | Value ($K) |
|---|---|---|
| **Energy Conservation** | | |
| Conservation | | |
| Previous Fiscal Year | 7 | $2,083 |
| Current FY87 | 2 | 531 |
| Studies | | |
| Previous Fiscal Year | 1 | 77 |
| Current FY87 | 1 | 80 |
| SUBTOTAL | 11 | $2,771 |
| **General Plant Projects (GPP)** | | |
| Authorized | | |
| Previous Fiscal Year | 5 | 348 |
| Current FY87 | 7 | 2,146 |
| Proposed | | |
| Conceptual Design Studies | 7 | 70 |
| SUBTOTAL | 19 | $2,564 |
| **Other Engineering Support*** | 30 | 1,250 |
| TOTAL ALL CATEGORIES | 60 | $6,585 |

*Includes engineering support for relocating A- and B-Site facilities to C- and D-Sites and to 307 College Road East.

encouraging energy conservation were displayed on bulletin boards throughout the Laboratory. Overall, employee cooperation and energy conservation awareness is high. These efforts contributed to an effective Laboratory-wide Energy Management and Conservation Program that produced outstanding results.

Additionally, PPPL, in an effort to preserve Laboratory funds, went into contract renewal in May with PSE&G for interruptible electric service. This three-year contract will be adjusted annually on the basis of the previous summer's kilowatt demand peak average; a saving of over $1 million in electricity costs were realized in FY87 because of this contract.

## Plant Maintenance

The Plant Maintenance and Engineering Division's work force was reduced for the third consecutive year. Full-time equivalent (FTE) employees within PM&E dropped from a high of 150 in FY84 to 102 in FY87 (a 28% reduction over the three years). This was done at a time when the Laboratory was in full operation and great demands were made to provide smooth, uninterrupted operating time for TFTR. Curtailment of nonessential services, reductions in preventive maintenance, careful selection of work projects, and work procedural changes aimed at greater efficiency were initiated in order to keep the level of operations safe and acceptable.

An extra burden placed on the Laboratory as a whole, and particularly PM&E, during FY87 was the relocation of all PPPL personnel and activities from A- and B-Sites. It was mandated by Princeton University and the DOE that this be accomplished in the twelve months prior to October 1, 1987.

A large segment of the relocation was accommodated by the construction of the large (20,750 sq. ft.) high-bay Research Equipment Storage and Assembly (RESA) Building to house the vacuum and coil shops. Another large group (primarily Engineering personnel) was relocated by a commercial mover to leased space in nearby Forrestal Center. To accommodate the remainder, a substantial shuffling of personnel took place at C-Site: trailers near the CAS Building were relocated to D-Site to make room for the new RESA Building; Personnel and Information Services were moved to the Laboratory Office Building (LOB), necessitating a chain reaction of relocations; Modules I and II were completely renovated to house Procurement, Information Resource Management, and Accounting; new trailers and modules were purchased and installed for Quality Assurance, Health Physics, and Materiel Control; the Print Shop was moved into remodeled space formerly occupied by the Computer Division; and so on.

To accomplish all of this work in the time allotted required the hiring of approximately 16 FTE temporary employees; this does not include the many people who were employed through subcontractors. The planning, coordination, and scheduling of this work were made possible by expanded use of the computerized maintenance work order program. In FY87 there were 4,503 service calls, 3,617 major work orders (requiring four or more hours of labor to complete), and 939 preventive maintenance work orders, for a total of approximately 81,000 scheduled man-hours. Table IV shows how the number of work orders and personnel compare with previous fiscal years.

The 2% increase in major work orders between FY86 and FY87 is largely the result of the renovation of spaces and preparation required to vacate A- and B-Sites. The decrease in preventive maintenance is also the result of pressures of the "move" and vacating buildings and equipment at A- and B-Sites.

A significant cost saving was made with the procurement of the preventive maintenance software for D-Site. Previously, any change to the preventive maintenance procedures had to be done by the outside vendor at additional cost. The primary saving was an annual fee of over $30,000 for the software. Operation and updating the computerized preventive maintenance program is now completely in-house. Changes and additions are now expedient and inexpensive. Previously, the C-Site preventive maintenance system was a separate operation done on a word processor. At the beginning of FY87, the C-Site preventive maintenance system was incorporated into the same computerized system as D-Site.

### Maintenance Training

As the manpower reductions continued in FY87, the need for training became more critical to the operation of Plant Maintenance. Radiation training was given to all of the maintenance people who work in the areas where radiation is present. Two additional electricians received training in pyrotronics and one in electrical crane maintenance. Boiler Operations staff received training on the water treatment process, which is also critical to an efficient operation. Safety training continued to receive strong support, with all PM&E mechanics attending monthly training sessions. Additionally, two supervisors attended courses to enhance their abilities in handling people in a safer and more productive manner.

### Maintenance Safety Support

Through meetings and monthly safety inspections, the Area Safety Coordinator (ASC) Program continued to provide adequate safety support in FY87. In addition to 62 "formal work orders," the safety inspection program generated a total of 82 "service requests" in FY87. Safety-related work orders continue to be monitored and tracked through the PM&E work order system to insure prompt and appropriate corrective actions.

The PM&E Division's record of 975 consecutive days without a lost time accident ended on October 5, 1986, with a scraped leg by an employee in the Transportation Services Section.

The Administration Department held a total of 30 safety meetings during FY87 with a combined attendance of 84.7% of the available Administration Department employee population. This met the Laboratory goal of an 85% attendance rate.

## Library

Library operations and activities continued apace in FY87 as 2,430 books, 824 journal articles and 400 technical reports were circulated to PPPL staff. A total of 1,017, or 28% of these materials, were borrowed from other libraries, most from within the Princeton University system. A total of 1,150 fusion-related journal articles and 882 technical reports were cataloged by the Assistant Librarian, and cards were produced for the card catalog and monthly acqui-

**Table IV. Comparison of Work Orders by Fiscal Year.**

| | FY84 | FY85 | FY86 | FY87 |
|---|---|---|---|---|
| **Type of Work Order** | | | | |
| Service Requests | 4,467 | 4,512 | 4,425 | 4,503 |
| Major | 3,024 | 2,751 | 3,008 | 3,617 |
| Preventive Maintenance | 1,318 | 1,500 | 1,100 | 939 |
| Work Force (FTE) including temporaries | 150 | 127 | 108 | 118 |

sitions lists using the SPIRES data base system on the IBM 3081 mainframe computer on main campus.

### Computerized Information Retrieval Systems

Welcome additions to the Library's resources have been the two public terminals which give our users access to the Online Catalog of the Princeton University Library system and a printed union list of the more than 10,000 science serial titles owned by Princeton University. The Online Catalog includes books and other library materials cataloged from January 1980 to the present, and currently contains over 400,000 titles. Our next objective is to make available to our users an on-line catalog of fusion-related journal articles and technical reports.

## Information and Administration Services

The Information and Administrative Services Branch includes all Laboratory services supporting *the preparation and dissemination of information* pertaining to PPPL's program. Included are photography, graphic arts and technical illustration, word processing, printing, duplicating, technical information, and public and employee information. Various administrative services—specifically, telecommunications, mail, and travel services—are also provided.

### Public and Employee Information

The Public and Employee Information Section of the Information and Administrative Services Branch is responsible for providing up-to-date information on PPPL's program for members of the general public, the news media, representatives of government and industry, and employees of the Laboratory. The section maintains an information kit consisting of brochures and information bulletins that are written for the layman; in addition, an employee newsletter, *PPPL HOTLINE*, is published. The staff coordinates an active speakers' bureau, Laboratory tour program, as well as media relations and community outreach activities.

The PPPL employee attitude survey conducted by Opinion Research Corporation in FY86 indicated a need to improve management/employee communications generally. In response, a commitment was made, early in FY87, to increase the frequency *HOTLINE* from once monthly to at least twice. During FY87, 22 issues of *HOTLINE* were published. To insure that this frequency would be maintained and to aid in the production of Information Bulletins, PPPL Digests, and other brochures, a desktop publishing network was installed in the spring of 1987. The system includes MacIntosh personal computers linked to an Apple Laserwriter. Plans call for staff to be trained in the utilization of PageMaker software early in FY88. Availability of the system will allow all PPPL's public and employee publications to be composed and layed out in-house, thereby significantly reducing production time and lowering costs.

Media relations activities during FY87 focused on the Compact Ignition Tokamak (CIT) Project. A news release was issued in January 1987 announcing that funding for CIT was included in President Reagan's FY88 budget, and that the device would be built at PPPL. In conjunction with this news release, a fact sheet was written providing a description of the device and its mission in the U.S. fusion program. Later in the year, a more elaborate three-color CIT overview booklet was written and published.

Access to the Tokamak Fusion Test Reactor (TFTR) for public tours is expected to be limited in FY89 and beyond, especially when tritium operations begin. With this is mind, USDOE approval was obtained for the production of a 20-minute video movie on TFTR. A script was nearly completed by the end of FY87, with plans to submit for approval early in FY88. The video will provide a vicarious tour of TFTR for visitors and will be made available to educators and others for showings off-site. In a similar fashion during FY87, PPPL's existing slide/sound show was copied onto video tape and distributed to physics teachers throughout the State of New Jersey.

PPPL's Community Outreach Program was initiated in 1982 with the goals of fostering a broad base of local public understanding of the Laboratory's program and forging closer communication links to local government, industry, and educational institutions. As part of this program, meetings were held throughout FY87 with government representatives from the State of New Jersey and from several area municipalities to discuss the Laboratory's program and plans for CIT. Further, staff members and their families attended a Family and Community Day open house on Saturday, May 3rd to view experimental areas and displays set up by CIT, TFTR, X-Ray Laser, PLT, PBX, S-1, Engineering, and Computer Division personnel. Over 2,200 attended.

Also, as part of its Community Outreach effort, PPPL repeated its successful Science-on-Saturday seminar program. Over 150 high school students, parents, and teachers attended the eight-week series of lectures at PPPL that covered a variety of scientific subjects.

The Summer Science Awards program was expanded in FY87. Sixteen outstanding high school students were hired for eight weeks and assigned to assist the Laboratory's physicists and engineers. As in previous years, both the students and their PPPL supervisors found the experience to be very rewarding.

### Graphic and Photographic Services

During FY87, PPPL's video recording/editing capability was rounded out with the purchase of professional quality audio recorders and the establishment of a separate studio for video work. A large screen video projection system was installed in the M.B. Gottlieb Auditorium. Together, these facilities allow PPPL to produce video movies completely in-house and display these productions to large audiences.

Substantial progress has been made in the technology of computer-aided graphics. During FY87, an Ad Hoc Committee on Computer-Aided Graphics was formed to ascertain the state-of-the-art and determine its suitability for PPPL. A report was issued in August 1987 recommending the purchase of a MacIntosh II computer system during FY88. This hardware will eventually be used to generate two- and three-dimensional graphics for technical reports, journal articles, and presentations. The MacIntosh II will have the major advantage of complete compatibility with the MacIntosh desktop publishing system recently installed.

### Technical Information and Word Processing

In early FY87, the NBI Operations Center was relocated to the third floor of the LOB, requiring extensive recabling and reconfiguration of the entire network, which was accomplished with minimal downtime to users. In July 1987, the A-Site NBI network was moved to C-Site where it was interlinked with the existing system, increasing the number of terminals and printers on the C-Site network by approximately one-third. In conjunction with this consolidation, the entire software level was upgraded and an interface added to support an NBI PC Pilot Program. At the start of the NBI PC Pilot Program, nine IBM PCs were networked to the NBI system. Progress of the pilot program towards meeting its objectives will be discussed in a six-month interim report and a final report after one year of operation.

The Reports and Patents section was recombined with the technical typing section, i.e., word processing services, to improve backup of staff in both areas. The use of the NBI system to automate Reports and Patents tracking, processing, and reporting requirements was implemented in mid-1987 and has proved to be very useful.

### Copiers, Duplication, and Printing

There was a great deal of office-copier coordination in FY87 due primarily to the relocation of many departments. With a 57 copier inventory at the beginning of FY87, 15 were excessed, 14 purchased or newly installed, and 18 transferred or exchanged, resulting in a net decrease to 48 copiers at the end of FY87.

Duplication Center production in FY87 increased slightly (by 3%) over FY86 to 4.6 million impressions. The most significant change in FY87 for the Duplication Center was its relocation to a newly renovated, centralized area opposite the PPPL Library at C-Site.

The number of individual printing procurements through the US Government Printing Office in FY87 totaled 34 with a total dollar outlay of $48,208.

### Telecommunication Services

The Telecommunications Services Section of the Information and Administrative Services Branch is responsible for the provision of cost-effective voice communication services. The section recommends hardware and supervises and coordinates repairs, installation, and the billing process. During FY87, the staff handled 3,500 requests for moves, installations, and changes in telephone service.

Several major projects were under way or completed during FY87, including:

- The procurement to purchase a digital telephone system was canceled due to the move of 170 employees to 307 College Road East. This move required a reappraisal of the Laboratory's telephone requirements. The least costly, most efficient method was to install a Centrex III Telephone System, leased from N.J. Bell. The first cutover occurred at 307 College Road East in September 1987. The second cutover will occur at C/D-Sites in December 1987. The installation of Centrex III will provide one telephone system at both sites and will make available to the Laboratory the latest in communication technology.
- Installation of the UHF Radio System was completed and the system accepted in FY87.
- Selection of an Equal Access Carrier for PPPL's toll calls was completed and the contract awarded to AT&T in February 1987.

## Personnel

### Great Adventure Picnic

The Laboratory's Annual Picnic was held this year at the Great Adventure Amusement Park. Over five-hundred employees and their families attended. The decision to hold the picnic in late September and to do something "different" was based on responses received from a questionnaire sent to all employees. The questionnaire solicited suggestions for improving the Laboratory's social activities.

Feedback on the picnic was positive, since Great Adventure offered something for everyone: amusement rides, shows, a picnic lunch, and the safari park.

### Employee Recognition Program

A pilot Employee Recognition Program was implemented in Administrative Operations to provide a method of recognizing and rewarding outstanding employees and teams of employees for their quality of contributions and achievements.

The following milestones were achieved during the course of implementing the program:

- Official announcement of the program within Administrative Operations,
- Peer review panels selected,
- Information session and training of panel members,
- *PPPL HOTLINE* article completed.

This program is now in progress with initial candidates scheduled for selection during the fall of 1987.

### Round Tables

Informal meetings between the Deputy Director for Administrative Operations and small groups of employees began during the fourth quarter of FY87. The purpose of these meetings is to increase the flow of communications between employees and top management, improve exposure of top management, and to demonstrate responsiveness to and concern about employee problems. The initial pilot sessions involved first-line supervisors in both an effort to address their concerns and to solicit their support of the program. These early sessions were very effective in meeting the objectives established for them. Hopefully, after several additional Round Tables, the process will be adopted as a regular communication medium and its application will be expanded to other operational organizations.

### Compensation Workshops

A series of workshops were developed by Personnel for managers and supervisors to familiarize them with compensation policy and practice at the Laboratory. A pilot session was held early in the year and was enthusiastically received by those participating. Since then, approximately one half of the Laboratory's supervisors have attended the one-day course. These workshops are designed to provide every supervisor and manager with information about compensation at PPPL, to help them feel good about the thoroughness of the process, and to equip and encourage them to explain the process to the employees they supervise.

### Training

A broad effort in training and development of Laboratory employees began with the introduction of the Employee Development Program in February. Courses range from remedial English and basic mathematics to specific courses in the application of computer software and to the study of such advanced engineering courses as finite element analysis and data and computer communications.

Subcommittees comprised of employees of the various Laboratory staffs were established to review educational needs, make recommendations, select sponsors for courses, and evaluate course success. Additionally, approximately 60 managers and supervisors participated in a Training Needs Analysis conducted during the summer.

### Actions Resulting from the Employee Opinion Survey

Summary results from the Employee Opinion Survey conducted during the summer of 1986 were reviewed by Opinion Research Corporation (ORC) with the Laboratory's General Council.

A Response Task Force was assembled to address the major issues raised by employees and management in the survey. To address the issue of credibility, ORC prepared feedback of survey findings for distribution to all employees and conducted feedback sessions with Division-level managers who have the coordinating and communication responsibility within their organizations. The Response Task Force, subdivided into five subject-area working teams, is implementing steps to meet the commitments made by the Laboratory Director.

## Occupational Medicine Office

In April 1987, a reorganization transferred the responsibility for all safety and industrial hygiene functions to Technical Operations. This left the Medical Branch, renamed The Occupational Medicine Office, within Administrative Operations.

### Clinical Programs

The Occupational Medicine Office continued to offer basic services in health evaluations, health counseling, diagnosis and treatment of occupational injuries and illness, consultation in personal health problems, and treatment of minor nonoccupational illness. In addition, periodic health evaluations were offered to all employees 50 years of age and older. Approximately 60% of those eligible responded.

### Computerized Data Bases

The health evaluation scheduling function was reduced to an electronic base by which individual employees could be kept current in their necessary medical surveillance procedure, such as hearing conservation, evaluations to identify any health abnormalities that might be related to work exposures, and evaluations to assure the continued ability of employees in specific job categories to meet the physical demands of their work. This enabled us to assure that these were done in the most time-effective manner. Another data base was established to record the medical diagnoses arising from health evaluations and from employees returning to work from disability leave of absence. This will eventually become a valuable epidemiological tool. Data bases were also constructed for office management functions, such as procurement.

### New Programs

The Employee Assistance Program was evaluated and recommendations made to effectively broaden its scope and increase employee awareness of it. These changes will be implemented as management approval is finalized.

A need has been felt for an employee wellness/fitness or health management program at PPPL. A contract was let to a consulting company to analyze our needs and resources and submit appropriate recommendations. Elements of such a program will be addressed in FY88.

## Office of Public Safety

In Fiscal Year 1987, the Department of Public Safety continued to provide the Laboratory with professional security and emergency services. During the year, the Department responded to 82 fire alarms, 30 first aid calls, and 8 hazards materials incidents. In addition, Public Safety Officers issued 1,157 flame permits to work crews.

During this year, the following actions took place:

- Fire and security systems were developed for PPPL facilities at 307 College Road East.
- A comprehensive training program of the Emergency Preparedness Plan was developed and implemented.
- A procedure was implemented to fulfill Laboratory responsibilities in complying with a contract between PPPL and Public Service Electric and Gas Company to reduce energy consumption during periods of peak usage.
- A procedure for defining various levels of security for PPPL in response to various external threats was written and is being reviewed by Laboratory management.
- An improved system of internal written communications was developed for the Department of Public Safety.
- The Emergency Services Unit and the Security Unit were equipped with UHF radios. These radios enhanced coverage and, for the first time, enabled two units to directly communicate with each other.

## Procurement

The mandate that the Laboratory vacate all buildings at A- and B-Sites by September 30, 1987 impacted Procurement Division activities throughout the year. In order to accommodate the relocation of 85,000 square feet of shop space, it was necessary to contract for the design and construction of a 20,000 square foot heavy-load-bearing, high-bay RESA building on an expedited basis. This effort, from award of the Architect/Engineering subcontract to the acceptance of the completed building, was accomplished in 9 months.

In addition to the shop relocation, it was necessary to find office facilities in close proximity to the Laboratory for over 200 people. This was accomplished through a competitive procurement to lease approximately 43,000 square feet of office space, which included an option to lease an additional 30,000 square feet at a later date at the same rate as the base lease. In anticipation of CIT requirements, this option was exercised in mid-September of 1987.

Through the combined efforts of the Materiel Control Office and the Procurement Division, a competitive subcontract was entered into with a stationery supply house to provide "desk top" service for office and stationery supplies. This allowed the Laboratory to liquidate approximately $200,000 of inventory and free up stockroom space for more common use spares.

The second phase of the Division's four-year plan to automate its operations through the use of a personal computer-based local area network was completed. In addition, some of the workstations were made NBI/IBM-PC compatible to utilize a network based on the OASys 64 Word Processing System.

In June 1987, the Laboratory was awarded plaques from the Secretary of Energy for exceeding its small business and disadvantaged business goals for 1985 and 1986. Again in 1987, the Laboratory was successful in exceeding its goals of 50 percent for small business and 5 percent for disadvantaged business. The actual results were 55 percent for small business and 5.3 percent for disadvantaged business.

During the third quarter of FY87, the Chicago Operations Office conducted a Contractor Purchasing System Review. It was the opinion of the review team that the procurement system was considered to be adequate for the award and administration of subcontracts and purchase orders and for controlling the expenditure of government funds.

## Materiel Control Office

The primary objective of Materiel Control during FY87 was to complete the Laboratory move and closeout of A- and B-Sites. The "Move Project" was a year-long effort that consisted of relocating the equipment, material, and furniture for approximately 300 people in 20 buildings. Walk-throughs were conducted throughout A- and B-Sites, plans developed, and actions undertaken for the disposal of all surplus materials, equipment, and scrap. The safe disposal of hazardous waste generated by the move resulted in release of the sites in an environmentally acceptable condition. Each building and outside area was inspected by University, DOE, and PPPL officials prior to release from PPPL custody. In every instance, the areas passed review with favorable remarks being received from reviewing officials. The project was completed on September 28, 1987 when the last building was turned over to the University. The teamwork and commitment demonstrated by the Materiel Control staff were major factors in making the move a successful effort.

In other Materiel Control activities, on June 1, 1987 the Stores Operations Branch implemented a new system of direct-vendor supply of Laboratory office supplies. With the implementation of this new system, the Stores inventory budget was reduced $200k and 2,500 square feet of space was released. The reduction of 540 office supply items from inventory and the corresponding reduction of 1,500 requisitions and receipts enabled the Stores Operations Staff to concentrate stockroom support on Technical Operations requirements.

A comprehensive review of Maintenance Spares was also performed by Stores Operations to identify and report items that would no longer be needed due to the Laboratory consolidation. As a result of the

review, 315 maintenance items totaling $11k were excessed. Other stores activities included sales of $1.3M with 69,000 withdrawals being processed. The Spares Parts Section had receipts totaling $343k and withdrawals valued at $393k.

In Warehouse Operations, the Property Administration Office completed the inventory of 3,590 sensitive equipment items in the possession of 993 people. There were also 1,249 new equipment items added, 2,451 revisions, and 4,799 transfers of assets. DOE approval was obtained for the elimination of Computer-Automated Measurement Control Modules and for raising the threshold of sensitive equipment from $50.00 to $100.00. These actions resulted in a reduction of 2,663 equipment items valued at $4,170,277.65.

The Excess Property Section initiated sales of used government equipment to the public (and PPPL employees) resulting in the disposal of 250 items and return of $20k to PPPL. In addition, returns on sales of scrap metals were $54k from 112 shipments; excess equipment reported to DOE/General Services Administration for reutilization was 626 items valued at over $6.5M; and retirements of equipment from PPPL records included 500 items valued at $3.3M.

The Hazardous Material Section relocated their operation from the Warehouse Annex to the new Materials Storage Building at C-Site. The A- and B-site move heavily impacted this area resulting in the safe disposition of over 25 tons of hazardous waste. Increased emphasis on source reduction of hazardous waste helped off-set the rising costs of waste disposal and stricter regulations.

Safety continued to be an important topic during FY87. The Materiel Control Office conducted ten safety meetings and ten safety inspections. An excellent safety record was achieved this year, with only one reportable accident. The improved safety performance was the result of a higher level of safety awareness on the part of Materiel Control supervisors and personnel.

## CONTROLLER'S OFFICE

The Controller's Office is responsible for Laboratory Planning and Budgeting, Accounting and Financial Control, and Information Resource Management.

Funding reductions were a dominant factor in FY87. Despite staffing reductions, increased efficiency permitted the Controller's Office to maintain operations without markedly changing the essential services provided by its various units. Significant benefits resulted from improvements in data management and in the software that operates the Laboratory's management information systems. These improvements included the implementation of a new microcomputer-based Receiver System and the complete restructuring of the Performance Measurement System (PMS) information management system. Restructuring permitted PMS to make better use of more modern technology and to better fit within the overall Laboratory management information systems.

Table V summarizes the financial activities of the Laboratory for the last five years.

**Table V. PPPL Financial Summary**
**(Thousands of Dollars)**

| | FY83 | FY84 | FY85 | FY86 | FY87 |
|---|---|---|---|---|---|
| **OPERATING (Actual Costs)** | | | | | |
| Department of Energy | | | | | |
| TFTR Tokamak Operations | $ 18,029 | $ 16,725 | $ 18,988 | $20,035 | $14,009 |
| TFTR Tokamak Flexibility Mod | 17,725 | 19,358 | 13,658 | — | — |
| TFTR Computer Facility (CICADA) | 8,588 | 10,327 | 9,578 | 6,817 | 3,664 |
| TFTR Heating (Neutral Beams) | 24,410 | 22,166 | 23,475 | 16,091 | 24,896 |
| TFTR Physics Program (Exp. Research) | 5,682 | 5,422 | 4,776 | 6,179 | 3,085 |
| TFTR Diagnostics | 14,143 | 13,146 | 10,124 | 11,343 | 13,059 |
| TFTR D-T Systems | 366 | 3,570 | 3,357 | 2,639 | 8,083 |
| PLT/PDX/PBX | 17,846 | 18,501 | 14,425 | 13,785 | 11,403 |
| RF Development | 742 | 617 | 361 | 185 | — |
| ACT-I/CDX | 458 | 408 | 408 | 269 | 301 |
| S-1 | 3,703 | 3,561 | 3,270 | 3,047 | 2,566 |
| Compact Ignition Tokamak | — | 2,744 | 1,205 | 2,094 | 4,004 |
| Theory | 2,808 | 3,061 | 3,162 | 2,629 | 2,773 |
| Applied Physics | 1,352 | 655 | 833 | 519 | 502 |
| Other Operating | 418 | 457 | 1,379 | 190 | 898 |

**Continued**

*Table V. PPPL Financial Summary (Continued)*
**(Thousands of Dollars)**

| | FY83 | FY84 | FY85 | FY86 | FY87 |
|---|---|---|---|---|---|
| Change in Inventories | (3,169) | (599) | (721) | (173) | (295) |
| X-Ray Laser Development | 313 | 16 | 743 | 1,543 | 1,327 |
| Energy Management Studies | 47 | 125 | 146 | 67 | 139 |
| Department of Defense | 77 | 278 | 228 | 343 | 488 |
| Work for Others | 893 | 1,880 | 2,837 | 903 | 923 |
| Total Operating | $114,431 | $122,418 | $112,232 | $88,505 | $91,825 |
| **EQUIPMENT (Budget Authorization)** | | | | | |
| Capital Equipment not Related to Construction | $ 10,285 | $ 8,896 | $ 5,920 | $ 6,350 | $ 4,555 |
| **CONSTRUCTION (Budget Authorization)** | | | | | |
| TFTR | $ 1,800 | $ 255 | — | — | — |
| General Plant Projects | 1,000 | 1,000 | 1,532 | 874 | 1,300 |
| Energy Management Projects | 499 | 1,049 | 847 | 192 | 531 |
| Total Construction | $ 3,299 | $ 2,304 | $ 2,379 | $ 1,066 | $ 1,831 |

## Budget Office

The Budget System's usefulness to Laboratory management for budget status and control continued to improve during FY87. The preparation of the Field Task Proposals for DOE funding in FY89 again utilized information from PMS to help formulate the proposals. The Budget Office was also asked to prepare and submit a National Field Task Proposal for Compact Ignition Tokamak (CIT) Project funds, combining data from all the project participants into one uniform submission. The proposals were submitted to DOE ahead of schedule.

The projects enter spending plans into the Laboratory financial systems through the Performance Measurement System. This procedure enables each project to develop mission-oriented plans with funding needs, staffing, and other programmatic factors free from the institutional constraints that are present when considering the Laboratory as a whole. The project spending plans are reviewed and consolidated by the Program Committee, which in conjunction with the Budget Office develops a Laboratory program within institutional and funding boundaries.

The Budget Office, in support of the Laboratory's Budget and Manpower Committee, plays a major role in manpower planning. During FY87, PPPL staffing was reduced from 1,040 to 1,010 by attrition. Subcontract labor was used to meet peak demands during this period.

The indirect expenses at the Laboratory continued to attract management attention during the FY87 period. Careful review and analysis of the real needs in the indirect area continued via quarterly Indirect Cost Reviews organized and administered by the Budget Office.

## Performance Measurement System

PPPL's Performance Measurement System (PMS) continued to be utilized by both project and engineering departments for determining performance and controlling cost and schedule. Ongoing efforts during FY87 included:

- Formal work planning, estimating, and authorization processes, including the processing and control of over 800 jobs.
- Formal monthly progress status and reporting (Fig. 1).
- Utilization of PMS data for both the monthly management meetings and in the PPPL budgetary process.

In addition to ongoing system maintenance, the additional accomplishments were as follows.

- Scheduling support increased for the CIT Project, with concentration on Level I milestone schedules, Level II project schedules (Fig. 2), and short-term schedules used in weekly status meetings.
- TFTR summer shutdown activities were planned in detail to determine manpower requirements and to help coordinate daily fabrication, installation, and test activities (Fig. 3).

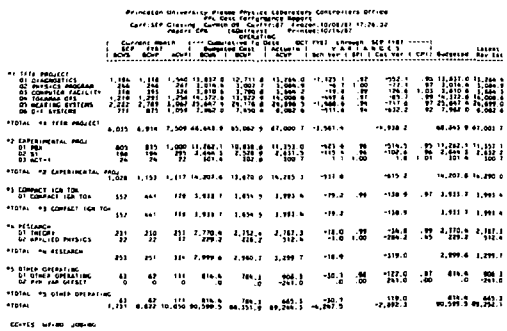

*Figure 1. Sample page of monthly progress status report. (87A0513)*

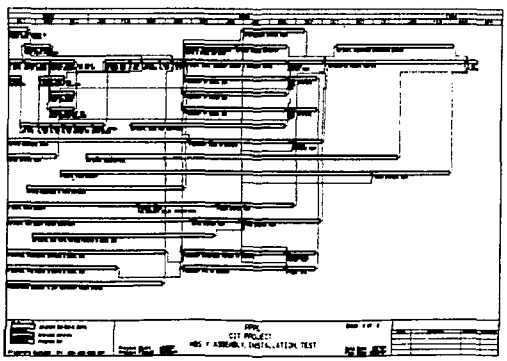

*Figure 2. Sample of Level II project schedule. (87A0511)*

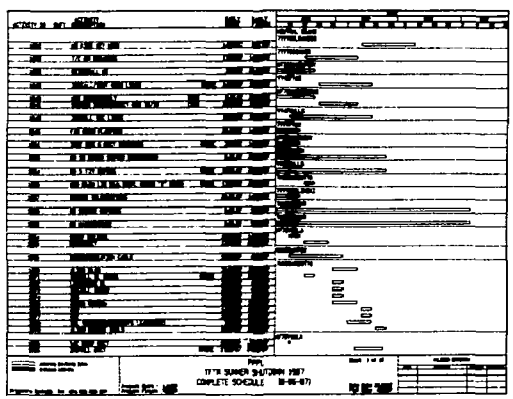

*Figure 3. Sample TFTR shutdown planning sheet. (87A0510)*

- Larger scale plotting capabilities were developed for schedules to provide management with graphical presentations of project plans and schedules (Figs. 2 and 3).

The DOE plans to validate the Laboratory PMS system during 1988 as part of the overall accreditation of the CIT Project at Princeton. Preliminary steps have been taken to prepare for this by examining the Laboratory system in light of the DOE criteria for performance management.

## Information Resource Management

In FY87, the Information Resources Management (IRM) Division continued its maintenance and support of the Laboratory's major data systems by developing programming for both the Financial Information Subsystem (FIS) and the automated system which reconciles the University's and PPPL's accounting records.

The FIS allows the Laboratory to report financial data to the DOE in a balance sheet format consistent with submissions from other integrated laboratories. The system supercedes the DOE Cost Management Report (Form 65), and is expected to improve the integration of PPPL records with the DOE.

Automating the accounting reconciliation process will permit electronic transmission of journal voucher and interdepartmental invoice data between the University and PPPL. Automation will improve upon current manual procedures for determining when accounting entries are recorded in either system, and will provide the basis for an automated reconciliation between the Laboratory and the University.

The greatest effort in FY87 involved acquisition of an IBM 4381 mainframe computer to replace the existing IBM 4361. Thus far, all of the existing 4361 load has been transferred to the 4381, and a major Material Control Subsystem (OASIS) was moved from the University computer to the 4381. Most of the ground work and testing has been completed to relocate all major systems to the 4381 from the University's IBM 3081, which will result in over $200k per year of cost savings.

Installation of the 4381 will benefit PPPL in the areas of:

- **Resource availability**—The University computer is a large-scale IBM 3081 computer with sufficient capacity to meet an *average* workload. However, certain peak processing periods that occur on the computer hinder PPPL's timely processing of essential data. The 4381 will eliminate these computing saturation peaks while providing a reliable and predictable resource for PPPL.
- **Change control**—Currently, it is difficult to coordinate changes required to support PPPL's administrative users with University Computer Center personnel. The local 4381 will be devoted exclusively to PPPL's use, permitting changes to be made without regard to their impact on a larger user base.
- **Cost reduction**—Over the past five years, IRM has demonstrated that it is less expensive to develop and run systems on a local processor such as the 4381 than it is to purchase time from the University's computer. The conversion should further reduce administrative computing costs per transaction (Fig. 4).

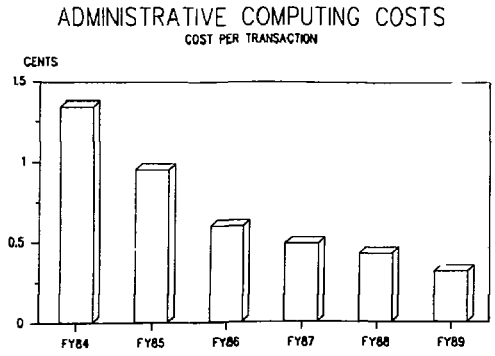


*Figure 4. Graph showing administrative computing costs per transaction. (87A0509)*

## Accounting and Financial Controls

In FY87, the Accounting and Financial Controls Division responded to several changes mandated by the five-year extension of PPPL's DOE contract. The new contract modification required the Laboratory to adopt the Federal Travel Regulations. The Accounting and Financial Controls Division developed procedures, published guidelines, and provided training to the Accounting staff and Laboratory employees on the new procedures. The Accounting Division also became a member of the DOE Laboratories Travel Officers Group, whose primary objective is to exchange information on effective means of adhering to the Federal Travel Regulations.

The contract modification also requires the Laboratory to report its financial data through the Financial Information System. The Accounting and Financial Controls Division carried out this project by modifying its accounting procedures and designing a reporting system that accomplishes the objective. Major advances have also been made in the effort of reconciling PPPL records with Main Campus.

The Accounting staff was further reduced by two permanent employees. This reduction was made possible by continued computerization of manual tasks, reevaluation of procedures, and reassignment of duties.

As its main objectives for FY88, the Accounting and Financial Controls Division will attempt to automate the Accounts Payable process and complete Phase II of the FIS reporting system. Continued effort will also be devoted to achieving further improvements in quality, user responsiveness, and efficiencies resulting in cost reductions.

# PPPL Invention Disclosures for Fiscal Year 1987

| Title | Inventor(s) |
|---|---|
| Solid Metallic Tube Sheath Remover for Coaxial Hard Line Cables | R. Pope |
| Portable Payout Stand for 300' Rolls of Computer Printer Paper | R. Pope |
| Shaft Oil Seal Extractor for Use in Confined Areas | R. Pope |
| An Extractor for Removing Pressed in Lock Barrels from Slide Bolt Blocks | R. Pope |
| Sensitive Leak Test Telescope | W. Blanchard<br>J. Hemmerich<br>T. Winkel |
| 'Spark Plug' Impurity Injection Diagnostics | D. Meyerhofer |
| Round Nosed Locking Pliers | W. Persely<br>R. Pressburger |
| Load Carrying Fixture with Load Rotation Feature | E. DuBois<br>J. Frangipani<br>K. Mann<br>A. Patterson |
| Tomographic Scanner Using Induced Synchrotron Radiation | N. Fisch<br>P. Efthimion<br>T. Luce |
| Low Temperature Injection Cooling Method | J. McDade<br>H. Gentzik |
| Boxcar Photograph | G. Greene |
| Universal Master Times | L. Meixler |
| UV-XUV Dual Multichannel Spectrometer (UXS) | Y.J. Chung<br>P. Lemaire<br>S. Suckewer |
| Rogoski Probe Junction | J. Bilinski |
| Fiber Optic Current Monitor | G. Renda |
| Chip Stopper | L. Darazio |
| Windowless High Power KrF Excimer Laser | S. Suckewer<br>L. Meixler<br>W. Tighe<br>J. Goldhar |
| Ultra-High-Field Superconducting Magnets | H. Furth<br>S.C. Jardin |
| Force-Free High-Current Superconducting Cable | H. Furth<br>S. Jardin<br>D. Montgomery |

**(Continued)**

**PPPL Invention Disclosures for Fiscal Year 1987. (Continued)**

| Title | Inventor(s) |
|---|---|
| RF Bakeout Scheme for Carbon Tiles | P. Colestock |
| Bidirectional Scenarios in Lower Hybrid Wave Heating | S. von Goeler<br>J. Stevens<br>S. Bernabei<br>T.K. Chu<br>W. Hooke<br>R. Motley |
| Tokamak with Superimposed $\ell = 1$ Stellarator Field | H. Furth<br>W. Park |
| Process for Positioning Detector in a Bent-Crystal Spectrometer | P. Beiersdorfer<br>S. von Goeler |
| Fast Wave Reflectometry-Alpha Particle Diagnostic | P. Colestock |
| Use of Elemental Sulphur as a Monatomic Adhesive | J. Timberlake |
| Method for Producing (in vacuo) High Velocity Projectiles $>10\mu$ Thick from Laser Ablation | J. Timberlake |

# GRADUATE EDUCATION: PLASMA PHYSICS

The Plasma Physics Program was first offered at Princeton University in 1959 and two years later was incorporated into the Department of Astrophysical Sciences. The constant aim of the Program has been to provide pertinent graduate education in an environment that, over the past three decades, has seen enormous changes in the fields of plasma physics and controlled fusion. In this period, the Program has established its own traditions of education—centered on fundamentals in physics and applied mathematics and training—based on intense exposure to the cutting edge of research in plasma physics.

Graduate students entering the Plasma Physics Program at Princeton spend the first two years in classroom study, acquiring a firm foundation in the many disciplines that make up plasma physics: classical and quantum mechanics, electricity and magnetism, fluid dynamics, hydrodynamics, atomic physics, applied mathematics, statistical mechanics, and kinetic theory. Table I lists the departmental course offered this past academic year. Many of these courses are taught by the members of PPPL's research staff who also comprise the seventeen-member plasma physics faculty (see Table II). The curriculum is supplemented by courses offered in other departments of the University and by a student-run seminar series in which PPPL physicists share their expertise with the graduate students.

Most students hold Assistantships in Research at PPPL through which they participate in the continuing experimental and theoretical research programs. In addition to formal class work, first- and second-year graduate students work side by side with the research staff, have full access to Laboratory facilities, and learn firsthand the job of a research physicist. First-year students assist in experimental research areas, including TFTR diagnostics development, PBX, S-1, CDX, and the X-Ray Laser Project. In a similar fashion, second-year students assist in theoretical research. Following the two years of class work, students concentrate on the research and writing of a Ph.D. thesis, under the guidance of a member of the PPPL staff. Of the thirty-one graduate students in residence this past year, fifteen were engaged in thesis projects—five on theoretical topics and ten on experimental topics. Table III lists the doctoral thesis projects completed this fiscal year under the Plasma Physics Program.

Four students currently in residence hold Magnetic Fusion Science Fellowships and one student holds a Magnetic Fusion Energy Technology Fellowship.

**Table I. Plasma Physics Courses Offered and Instructors.**

| Course Number | Course Title | Instructor |
|---|---|---|
| | **Fall 1986** | |
| AS 551 | General Plasma Physics I | F.W. Perkins |
| AS 553 | Plasma Waves and Instabilities | L. Chen |
| AS 560 | Advanced Magnetohydrodynamics | S.C. Jardin |
| AS 558 | Seminar in Plasma Physics | C.R. Oberman |
| | **Spring 1987** | |
| AS 552 | General Plasma Physics II | R.M. Kulsrud and H. Okuda |
| AS 554 | Irreversible Processes in Plasma | C.F.F. Karney |
| AS 558 | Seminar in Plasma Physics | S. Yoshikawa |
| AS 559 | Nonlinear Interactions in Plasma | J.A. Krommes |

**Table II. Astrophysical Sciences/Plasma Physics Faculty.**

| *Faculty Members* | Title |
|---|---|
| Thomas H. Stix | Associate Chairman, Department of Astrophysical Sciences, and Associate Director for Academic Affairs, PPPL |
| Liu Chen | Principal Research Physicist and Lecturer with rank of Professor |
| Samuel A. Cohen | Principal Research Physicist and Lecturer with rank of Professor |
| Harold P. Furth | Professor of Astrophysical Sciences |
| Stephen C. Jardin | Principal Research Physicist and Lecturer with rank of Professor |
| Charles F.F. Karney | Research Physicist and Lecturer with rank of Associate Professor |
| John A. Krommes | Principal Research Physicist and Lecturer with rank of Professor |
| Martin D. Kruskal | Professor of Mathematics and Astrophysical Sciences |
| Russell M. Kulsrud | Principal Research Physicist and Lecturer with rank of Professor |
| Carl R. Oberman | Principal Research Physicist and Lecturer with rank of Professor |
| Hideo Okuda | Principal Research Physicist and Lecturer with rank of Professor |
| Francis W. Perkins, Jr. | Principal Research Physicist and Lecturer with rank of Professor |
| Paul H. Rutherford | Principal Research Physicist and Lecturer with rank of Professor |
| William M. Tang | Principal Research Physicist and Lecturer with rank of Professor |
| Schweickhard von Goeler | Principal Research Physicist and Lecturer with rank of Professor |
| Roscoe B. White | Principal Research Physicist and Lecturer with rank of Professor |
| Shoichi Yoshikawa | Principal Research Physicist and Lecturer with rank of Professor |

**Table III. Recipients of Ph.D. Degrees.**

**David D. Meyerhofer**

| | |
|---|---|
| Thesis: | Relaxation and Particle Diffusion in the Proto S-1/C Spheromak, December 1986 |
| Advisor: | M. Yamada |
| Employment: | Laboratory for Fusion Studies, Cornell University |

**John A. Lovberg**

| | |
|---|---|
| Thesis: | Ion Energy Balance Determination During $^3$He-Minority ICRH on PLT Using Fusion-Product Diagnostics, August 1987 |
| Advisor: | J. Strachan |
| Employment: | Maxwell Labs |

**Timothy C. Luce**

| | |
|---|---|
| Thesis: | Superthermal Electron Distribution Measurements with Electron Cyclotron Emission, September 1987 |
| Advisor: | P. Efthimion |
| Employment: | GA Technologies |

**Lynn B. Olson**

| | |
|---|---|
| Thesis: | Dependence of MHD Stability of a Plasma on the Ratio of the Densities of Energetic and Background Particles |
| Advisor: | R. Motley |
| Employment: | Department of Physics, UCLA |

In addition, other students hold awards from the National Science Foundation, the Fannie and John Hertz Foundation, and from the Natural Science and Engineering Reserach Council of Canada. Some of these fellowships are supplemented by partial research assistantships.

Overall, the plasma physics graduate studies program in Princeton University's Department of Astrophysical Sciences has had a significant impact on the field of plasma physics. One-hundred and twenty-seven physicists have received doctoral degrees from Princeton. Many have become leaders in plasma research and technology in academic, industrial, and government institutions. And this process continues as the Laboratory trains the next generation of scientists, preparing them to take on the challenging and diversified problems of the future.

# GRADUATE EDUCATION: PROGRAM IN PLASMA SCIENCE AND FUSION TECHNOLOGY

The Graduate Program in Plasma Science and Fusion Technology, which is based within Princeton University's School of Engineering and Applied Science (SEAS), is a major vehicle for collaboration between the Laboratory and Main Campus departments. The Program provides a coupling between the technology needs of the Laboratory and the Main Campus faculty and students doing research in these areas. In addition, and of increasing interest, the Program provides strong interdepartmental/interdisciplinary support for other plasma applications, such as advanced materials fabrication, light sources, and ion thrusters. These areas represent potential technology transfer activities for PPPL, and also comprise important topics within some of the new initiatives of SEAS, such as the Materials Science Center.

During FY87, the number of students enrolled in the Program increased from 10 to 11. These students, along with their departments, advisors, and thesis topics are listed in Table I. Three of the 11 students are supported by fellowships, while 8 are supported by Laboratory funds. Dr. Byron Peterson, a Magnetic Fusion Energy Technology Fellow from the University of Wisconsin, came to PPPL to perform his practicum work with Dr. M. Ono.

In November 1986, the Program's involvement in the U.S. Department of Energy's Magnetic Fusion Energy Technology Fellowship (MFETF) Program was reviewed to ascertain compliance with recommendations made in a 1984 review to correct alleged deficiencies. The review found that the deficiencies had not been sufficiently ameliorated, and as a result, the University was notified in June 1987, that their participation in the MFETF Program was terminated. The review did encourage the University to reapply for the fellowships, and the reapplication procedure was initiated. The two existing MFET Fellows will be allowed to complete their fellowship appointments.

The Program received new funding in May 1987 from the New Jersey Commission on Science and Technology. These funds will support work on low-temperature nonequilibrium plasmas used for deposition and etching of thin films of interest to semiconductor devices. In addition, the Laboratory received matching funding for this work from the SRI/David Sarnoff Research Center in the form of a long-term equipment loan which included a parallel plate radio-frequency plasma system, with vacuum system and two radio-frequency supplies and matching networks. The system has been used for bias sputter deposition and plasma-enhanced chemical vapor deposition.

In July 1987, Dr. R.G. Mills, who was the Director of the Program in Plasma Science and Fusion Technology and had been primarily reponsible for the Program's creation, retired from Princeton. Dr. Mills had been active in collaboration between PPPL and Main Campus for 15 years, holding a joint appointment at PPPL and in the Department of Chemical Engineering. Dr. J.L. Cecchi was appointed as the new Director of the Program, and has also taken over the responsibilities for teaching the plasma-related courses in the Department of Chemical Engineering, including Ch.E. 417, Introduction to Plasmas and Their Applications, and Ch.E. 550, Fusion Reactor Technology. The scope of Ch.E. 417 was broadened to include topics pertinent to plasmas used for enhanced chemical reactions and thin film deposition and etching.

**Table I. Program in Plasma Science and Fusion Technology Graduate Students.**

**P. Pang**

| | |
|---|---|
| Thesis Topic: | Polymers |
| Advisor: | J.K. Gillham |
| Department: | Chemical Engineering |

**K.W. Goossen**

| | |
|---|---|
| Thesis Topic: | High Speed Detectors |
| Advisor: | S.A. Lyon |
| Department: | Electrical Engineering |

**J.S. Lee**

| | |
|---|---|
| Thesis Topic: | Coupled Mechanical/Electrodynamic Force Analysis |
| Advisor: | J.H. Prevost/P.C.Y. Lee |
| Department: | Civil Engineering |

**G.D.C. Dhondt**

| | |
|---|---|
| Thesis Topic: | The Influence of Helium on the Embrittlement of Metals. |
| Advisor: | A.C. Eringen |
| Department: | Civil Engineering |

**R. Myers**

| | |
|---|---|
| Thesis Topic: | Energy Transfer and Acceleration Processes in Low Power Plasma Thrusters |
| Advisor: | R.G. Jahn/A.J. Kelly |
| Department: | Mechanical and Aerospace Engineering |

**J.F. Quanci**

| | |
|---|---|
| Thesis Topic: | Tritium Recovery Experiments |
| Advisor: | J.L. Cecchi/R.G. Mills |
| Department: | Chemical Engineering |

**D.-S. Shen**

| | |
|---|---|
| Thesis Topic: | Semiconductor Research |
| Advisor: | S. Wagner |
| Department: | Electrical Engineering |

**S. Chaturvedi**

| | |
|---|---|
| Thesis Topic: | Quasi-Isobaric Reactor Study |
| Advisor: | J.L. Cecchi/R.G. Mills |
| Department: | Chemical Engineering |

**Y.-G. Kim**

| | |
|---|---|
| Thesis Topic: | Coupled Mechanical/Electrodynamic Force Analysis |
| Advisor: | P.C.Y. Lee/J.H. Prevost |
| Department: | Civil Engineering |

**D.W. Roberts**

| | |
|---|---|
| Thesis Topic: | RF Heating Studies in Tokamaks |
| Advisor: | C.Z. Cheng |
| Department: | Astrophysical Sciences |

**C.-W. Cheah**

| | |
|---|---|
| Thesis Topic: | Deposition of a C:H Films by Plasma Enhanced Chemical Vapor Deposition |
| Advisor: | J.L. Cecchi |
| Department: | Chemical Engineering |

# SECTION COORDINATORS

**Tokamak Fusion Test Reactor**
Steven P. Duritt, Jr.
Kenneth M. Young

**Princeton Beta Experiment Modification**
Kees Bol
Robert A. Ellis, Jr.

**S-1 Spheromak**
Alan C. Janos
*Masaaki Yamada*

**Current-Drive Experiment**
Masayuki Ono

**X-Ray Laser Studies**
Szymon Suckewer
Alain Wouters

**Theoretical Division**
John A. Krommes

**Tokamak Modeling**
Martha Redi

**Compact Ignition Tokamak**
*Milton D. Machalek*

**Engineering Department**
Computer Division
Sally Connell
Michaela Mole
Electronic and Electrical Engineering Division
*Patrick Murray*
Engineering Analysis Division
Robert A. Ellis, III
Mechanical Engineering
Donald S. Knutson

**Project Planning and Safety Office**
Ellis D. Simon

**Quality Assurance and Reliability**
Harry Howard
*Judith A. Malsbury*

**Administrative Operations**
Olga Bernett
Kathleen A. Dunn

**Graduate Education: Plasma Physics**
Thomas H. Stix

**Graduate Education: Plasma Science and Fusion Reactor Technology**
Joseph L. Cecchi

# GLOSSARY OF ABBREVIATIONS, ACRONYMS, SYMBOLS

| | |
|---|---|
| **A** | Ampere |
| **Å** | Angstrom unit; $10^{-8}$ cm |
| **ac** | Alternating Current |
| **ACT-I** | Advanced Concepts Torus-I |
| **ACWP** | Actual Cost of Work Performed |
| **A/D** | Analog-To-Digital |
| **ADP** | Automated Data Processing |
| **ADPE** | Automated Data Processing Equipment |
| **ALARA** | As low as reasonably achievable |
| **Alcator** | A family of tokamak devices being developed and built at the Massachusetts Institute of Technology (from the Italian for high-field torus) |
| **ALT-I** | Advanced Limiter Test on TEXTOR (Jülich, West Germany); Version I |
| **ALT-II** | Version II of ALT |
| **amu** | Atomic Mass Unit |
| **ANL** | Argonne National Laboratory |
| **ANSI** | American National Standards Institute |
| **ASC** | Area Safety Coordinator |
| **ASDEX** | Axially Symmetric Divertor Experiment (Max-Planck-Institut für Plasmaphysik, Garching, West Germany) |
| **ASE** | Amplified Spontaneous Emission |
| **ASME** | American Society of Mechanical Engineers |
| **ATC** | Adiabatic Toroidal Compressor (Princeton Plasma Physics Laboratory, 1970's) |
| **ATF** | Advanced Toroidal Facility (a stellarator at Oak Ridge National Laboratory) |
| **ATF-1** | Advanced Toroidal Facility-1 |
| **AWAFT** | Automatic Work Approval Form Transfer (system) |
| **BALDUR** | A Princeton Plasma Physics Laboratory one-dimensional tokamak transport code |
| **BBGKY** | Bogoliubov Born Green Kirkwood Yvon |
| **BCWP** | Budgeted Cost of Work Performed |
| **BCWS** | Budgeted Cost of Work Scheduled |
| **CAD** | Computer-Aided Design |
| **CADD** | Computer-Aided Design and Drafting (Facility) |
| **CAE** | Canadian Aviation Electronics (known as CAE Electronics Ltd.) |
| **CAMAC** | Computer-Automated Measurement and Control (System) |
| **CAR** | Computer-Assisted Retrieval |
| **CAR** | Cost Analysis Report |
| **CCD** | Capacitor Charge/Discharge |
| **CCD** | Charge-Coupled Device |
| **CDR** | Conceptual Design Review |
| **CDX** | Current-Drive Experiment (at the Princeton Plasma Physics Laboratory) |
| **CEA** | Commisariat A L'Energie Atomique |
| **CEMC** | Continental Electronics Manufacturing Corporation |
| **CENA** | Charge-Exchange Neutral Analyzer |
| **CGE** | Canadian General Electric |
| **CHERS** | Charge-Exchange Recombination Spectrometer |
| **CICADA** | Central Instrumentation, Control, and Data Acquisition (System) |
| **CICS** | Customer Information Control System |
| **CIPREC** | Conversational and Interactive Project Evaluation and Control System |
| **CIT** | Compact Ignition Tokamak |
| **cm** | Centimeter |
| **COO** | Chicago Operations Office |
| **COS** | Console Operating Station |
| **CPC** | Coil Protection Calculator |

| | |
|---|---|
| **CPSR** | Contractor Procurement System Review |
| **CPU** | Central Processing Unit |
| **CRAY** | A brand of computer made by Cray Research, founded by S. Cray |
| **CSR** | Cost and Schedule Review |
| **CTR** | Controlled Thermonuclear Research |
| **CX** | Charge-Exchange |
| **CY** | Calendar Year |
| ° | Degrees |
| **°C** | Degrees Centigrade |
| **°K** | Degrees Kelvin |
| **D/A** | Digital-To-Analog |
| **DARM** | Data Acquisition Room |
| **DAS** | Data Acquisition System (on PLT, PBX, S-1) |
| **DATS** | Differential Atmospheric Tritium Sampler |
| **DAX** | DAS supplemental system (uses a VAX computer) |
| **dc** | Direct Current |
| **D-D** | Deuterium-Deuterium |
| **DDC** | Disruptive Discharge Cleaning |
| **DEC** | Digital Equipment Corporation |
| **DECAT** | Drivers Energy Conservation Awareness Training |
| **DEGAS** | A PPPL computer code for studying the behavior of neutrals in plasma |
| **DEMO** | Demonstration Power Reactor |
| **D&GF** | Design and General Fabrication (Section) |
| **DIALOG** | An interactive online information retrieval system used by the PPPL Library |
| **DIFFUSE** | A computer code used to calculate the one-dimensional diffusion and trapping of atoms in a wall |
| **D-III** | Doublet-III—A tokamak located at GA Technologies, Incorporated |
| **D-III-D** | Doublet-III-D (recent upgrade of D-III, with D-shaped plasma) |
| **DITE** | Divertor and Injection Tokamak Experiment (Culham Laboratory, United Kingdom) |
| **DNB** | Diagnostic Neutral Beam |
| **DOE** | Department of Energy |
| **DOE/RECON** | An interactive online information retrieval system used by the PPPL Library |
| **DPI** | Deuterium Pellet Injector |
| **dpm** | Disintegrations per Minute |
| **D-T** | Deuterium-Tritium |
| **DVC** | Diagnostic Vacuum Controller |
| **EA** | Environmental Assessment |
| **EAD** | Engineering Analysis Division |
| **EAI** | Electronic Associates Incorporated |
| **ECE** | Electron Cyclotron Emission |
| **ECH** | Electron Cyclotron Heating |
| **ECRF** | Electron Cyclotron Range of Frequencies |
| **ECRH** | Electron Cyclotron Resonance Heating |
| **ECS** | Energy Conversion System |
| **EF** | Equilibrium Field |
| **ELM** | Edge Localized Mode |
| **EMCS** | Energy Monitoring and Control System |
| **EPA** | Environmental Protection Agency |
| **EPFL** | École Polytechnique Fédérale de Lausanne |
| **EPRI** | Electric Power Research Institute |
| **ERB** | Engineering Review Board |
| **ERP** | Edge Relaxation Phenomena |
| **ESB** | Executive Safety Board |
| **ESO** | Emergency Services Officer(s) |
| **ESU** | Emergency Services Unit |
| **ETACS** | Equipment Tracking and Control System |
| **ETR** | Engineering Test Reactor |
| **ETS** | Engineering Test Station |
| **eV** | Electron Volt |
| **EZB** | Exclusion Zone Boundary |
| **FAST** | Fast Automatic Transfer System |

| | |
|---|---|
| **FCPC** | Field Coil Power Conversion |
| **FEA** | Finite Element Analysis |
| **FED** | Fusion Engineering Device |
| **FEDC** | Fusion Engineering Design Center (Oak Ridge National Laboratory) |
| **FELIX** | An experimental test facility under construction at the Argonne National Laboratory |
| **FEM** | Finite Element Modeling or Finite Element Method |
| **FER** | Fusion Engineering Reactor |
| **FIDE** | Fast Ion Diagnostic Experiment |
| **FIR** | Far-Infrared |
| **FIS** | (Department of Energy) Financial Information System |
| **FLOPSY** | Flexible Optical Path System |
| **FMIT** | Fusion Materials Irradiation Test |
| **FPSTEL** | Computer code used to solve the ripple-bounce-averaged Fokker-Planck equation numerically |
| **FSAR** | Final Safety Analysis Report |
| **FTE** | Full-Time Equivalent |
| **FTS** | Federal Telecommunications System |
| **FWCD** | Fast-Wave Current Drive |
| **FWHM** | Full Width at Half Maximum |
| **FY** | Fiscal Year (October 1 to September 30) |
| **G** | Gauss |
| **G&A** | General and Administrative (cost or expense) |
| **GAO** | General Accounting Office |
| **GAT** | GA Technologies, Incorporated |
| **GDC** | Glow Discharge Cleaning |
| **GHz** | Gigahertz; $10^9$ cycles per second |
| **GJ** | Gigajoule, a unit of energy; $10^9$ joules |
| **gpm** | Gallons Per Minute |
| **GPP** | General Plant Projects |
| **GRD** | General Requirements Document |
| **GSA** | General Services Administration |
| **GSF** | Gross Square Feet |
| **HAIFA** | Hydrogen Alpha Interference Filter Array |
| **HAX** | High-Level Data Analysis (system); used a VAX computer |
| **HEDL** | Hanford Engineering Development Laboratory |
| **HELIAC** | A computer code used to calculate vacuum magnetic surfaces in nonaxisymmetric three-dimensional toroidal geometries |
| **HERA** | Helically invariant code |
| **HF** | Horizontal Field |
| **HFIX** | High-Field Ignition Experiment |
| **HLDAS** | High-Level Data Analysis System; equivalent to HAX |
| **H-mode** | High-Confinement Mode |
| **HPA** | High Power Amplifier |
| **HPP** | High Power Pulsing (Operations) |
| **HSD** | Health and Safety Directive |
| **HTA** | Hard Tube Amplifier |
| **HV** | High Voltage |
| **HVAC** | Heating, Ventilating, and Air Conditioning |
| **HVE** | High-Voltage Enclosure(s) |
| **HVST** | High-Voltage Switch Tube |
| **IAEA** | International Atomic Energy Agency, Vienna, Austria |
| **IBW** | Ion-Bernstein Wave |
| **IBWH** | Ion-Bernstein-Wave Heating |
| **ICH** | Ion Cyclotron Heating |
| **ICRF** | Ion Cyclotron Range of Frequencies |
| **ICRH** | Ion Cyclotron Resonance Heating |
| **IGNITOR** | Ignited Torus |
| **IMAPS** | Interstellar Medium Absorption Profile Spectrograph |
| **INEL** | Idaho National Engineering Laboratory |
| **INTOR** | International Tokamak Reactor |
| **I/O** | Input/Output |

| | |
|---|---|
| **IPA** | Intermediate Power Amplifier |
| **IPP** | Initial Protective Plates |
| **IPP** | Institut für Plasmaphysik at Garching, West Germany |
| **IPSG** | Ignition Physics Study Group |
| **IR** | Infrared |
| **IRM** | Information Resource Management |
| **ISP** | Ignition Studies Project |
| **ISS** | Internal Support Structure |
| **ISX** | Impurity Study Experiment (at Oak Ridge National Laboratory) |
| **ITER** | International Thermonuclear Engineering Reactor |
| **ITOC** | Ignition Technical Oversight Committee |
| **ITR** | Ignition Test Reactor |
| **JAERI** | Japan Atomic Energy Research Institute |
| **JET** | Joint European Torus |
| **JT-60** | JT stands for JAERI Tokamak and 60 means plasma volume in $m^3$. An energy breakeven plasma testing device in Japan |
| **kA** | Kiloamperes |
| **keV** | Kilo-Electron-Volts |
| **KFA** | Kernforschungsanlage Jülich, W. Germany |
| **KFK** | Kernforschungszentrum Karlsruhe, W. Germany |
| **kG** | Kilogauss |
| **kHz** | Kilohertz |
| **kJ** | Kilojoule |
| **ksi** | Kilopounds Per Square Inch (Pressure, Stress) |
| **kV** | Kilovolt |
| **kV A** | Kilovolt Ampere |
| **kW** | Kilowatt |
| **kW h** | Kilowatt Hour |
| **LANL** | Los Alamos National Laboratory |
| **LBL** | Lawrence Berkeley Laboratory |
| **LBM** | Lithium Blanket Module |
| **LC** | Inductance Capacitance |
| **LCC** | Lithium Comparison Code |
| **LCCs** | Local Control Centers |
| **LCFS** | Last Closed Flux Surface |
| **LCP** | Large Coil Program |
| **LED** | Light Emitting Diode |
| **LENS** | Low Energy Neutral System |
| **LEO** | Low Earth Orbit |
| **LH** | Lower Hybrid |
| **LHCD** | Lower Hybrid Current Drive |
| **LHe** | Liquid Helium |
| **LHRF** | Lower Hybrid Range of Frequencies |
| **LHRH** | Lower Hybrid Resonance Heating |
| **LITE** | Laser Injected Trace Element (System) |
| **LITE** | Long-Pulse Ignited Test Experiment (at the Massachusetts Institute of Technology) |
| **LLNL** | Lawrence Livermore National Laboratory |
| **L-mode** | Low-Confinement Mode |
| **LO** | Local Oscillator |
| **LOB** | Laboratory Office Building |
| **LOTUS** | Nuclear testing facility at École Polytechnique Fédérale de Lausanne in Switzerland |
| **LPIS** | Long-Pulse Ion Source |
| **$\mu$m** | Micrometer; equivalent to micron |
| **$\mu$sec** | Microsecond |
| **m** | Meter |
| **MA** | Megamperes |
| **MARFE(s)** | Region(s) of enhanced edge radiation localized poloidally on the inner-major-radius side of a plasma |
| **MARS** | Mirror Advanced Reactor Study (Lawrence Livermore National Laboratory) |
| **Mb** | Megabyte |
| **MCNP** | Monte-Carlo Neutron and Proton Code |

| | |
|---|---|
| **MED** | Mechanical Engineering Division |
| **MeV** | Mega-Electron-Volt |
| **MFAC** | Magnetic Fusion Advisory Committee |
| **MFE** | Magnetic Fusion Energy |
| **MFETF** | Magnetic Fusion Energy Technology Fellowship (Program) |
| **MFTF-B** | Mirror Fusion Test Facility at Lawrence Livermore National Laboratory |
| **MG** | Motor Generator |
| **MHD** | Magnetohydrodynamics |
| **MHz** | Megahertz |
| **mil** | A unit of length equal to 0.001 inch |
| **MIRI** | Multichannel Infrared Interferometer |
| **MIST** | A computer code which follows impurity species through various stages of ionization, charge-exchange, radiation, and transport within the plasma |
| **MIT** | Massachusetts Institute of Technology |
| **MJ** | Megajoules |
| **mm** | Millimeter |
| **MPa** | Mega-Pascal (Pressure, Stress) |
| **MPE** | Most Probable Earthquake |
| **MSDS** | Material Safety Data Sheet |
| **msec** | Millisecond |
| **MTL** | Material Test Laboratory |
| **MVA** | Megavolt Ampere |
| **mW** | Milliwatt |
| **MW** | Megawatt |
| **NA** | Neutron Activation (system) |
| **NASA** | National Aeronautics and Space Administration |
| **NASA/RECON** | An interactive online information retrieval system used by the PPPL Library |
| **NASTRAN** | A structural analysis code |
| **NB** | Neutral Beam |
| **NBETF** | Neutral Beam Engineering Test Facility |
| **NBI** | Neutral Beam Injection |
| **NBI** | NBI, Incorporated (word-processing equipment and service company) |
| **NBLs** | Neutral Beamlines |
| **NBPS** | Neutral Beam Power Supply |
| **NBTC** | Neutral Beam Test Cell |
| **NCR** | Nonconformance Report |
| **NET** | Next European Torus |
| **NJDEP** | New Jersey Department of Environmental Protection |
| **nm** | Nanometer |
| **NMFECC** | National Magnetic Fusion Energy Computer Center |
| **NPB** | Neutral Probe Beam |
| **NRC** | Nuclear Regulatory Commission |
| **nsec** | Nanosecond |
| **NTGD** | Nontritium Gas Delivery |
| **NTIS** | National Technical Information Service |
| **OFE** | Office of Fusion Energy |
| **OH** | Ohmic Heating |
| **OMA** | Optical Multichannel Analyzer |
| **OM&S** | Occupational Medicine and Safety |
| **ORC** | Operations Review Committee |
| **ORNL** | Oak Ridge National Laboratory |
| **ORR** | Operational Readiness Review |
| **OSB** | Occupational Safety Branch |
| **OSES** | Operations System Engineering Support |
| **OSHA** | Occupational Safety and Health Administration |
| **OSR** | Operational Safety Requirements |
| **PADS** | Procurement Automated Data Processing System |
| **PAP** | Plasma "Apprentice" Program |
| **PBX** | Princeton Beta Experiment |
| **PBX-M** | Princeton Beta Experiment Modification |
| **pC** | Pico Coulomb |

| | |
|---|---|
| **PC** | Personal Computer |
| **PDC** | Pulse-Discharge Cleaning |
| **PDR** | Preliminary Design Review |
| **PDX** | Poloidal Divertor Experiment |
| **PEST** | Princeton Equilibrium, Stability, and Transport Code |
| **PF** | Poloidal Field |
| **PFC** | Plasma Fusion Center (at the Massachusetts Institute of Technology) |
| **PHA** | Pulse-Height Analysis |
| **PIV** | Plenum Interface Valve |
| **PLANET** | A two-dimensional transport code used to study the scrape-off region created by divertors and limiters |
| **PLC** | Programmable Logic Controller |
| **PLCS** | Power Line Carrier System |
| **PLT** | Princeton Large Torus |
| **PM** | Preventive Maintenance |
| **PM&E** | Plant Maintenance and Engineering |
| **PMS** | Performance Measurement System |
| **PMS** | Performance Management System |
| **P&OS** | Project and Operational Safety |
| **PP-Lasers** | Power, Picosecond Lasers |
| **PPM** | Parts per Million |
| **PPPL** | Princeton Plasma Physics Laboratory |
| **psec** | Picosecond |
| **PSE&G Co.** | Public Service Electric and Gas Company (New Jersey) |
| **psi** | Pounds Per Square Inch |
| **PUBSYS** | PPL Public Information System (installed on the Princeton University IBM 3081 computer) |
| **PUCC** | Princeton University Computer Center |
| **QA** | Quality Assurance |
| **QA/R** | Quality Assurance and Reliability |
| **QMS** | Quadpole Mass Spectrometer |
| **RAM** | Reliability and Maintainability |
| **RAX** | TFTR off-line data reduction system (uses a VAX computer) |
| **R&D** | Research and Development |
| **RDAC** | Research and Development Activity |
| **REML** | Radiation Environmental Monitoring Laboratory |
| **RESA** | Research Equipment Storage and Assembly |
| **rf** | Radio Frequency |
| **RFBA** | Request for Baseline Adjustment |
| **RFP** | Request for Proposal |
| **RFP** | Reversed-Field Pinch |
| **RFTF** | Radio-Frequency Test Facility |
| **RGA** | Residual Gas Analyzer |
| **RIF** | Reduction-in-Force |
| **RIV** | Rapid Intervention Vehicle |
| **RLIN** | Research Libraries Information Network |
| **rms** | Root-Mean-Square |
| **RPI** | Repeating Pellet Injector also Repeating Pneumatic Injector |
| **rpm** | Revolutions Per Minute |
| **RTD** | Resistive Thermal Detector |
| **S-1 Spheromak** | A compact toroid device (at the Princeton Plasma Physics Laboratory) |
| **S-1 Upgrade** | |
| **SCR** | Silicon Controlled Rectifier |
| **SAD** | Safety Assessment Document |
| **S/DB** | Small and Disadvantaged Businesses |
| **SDS** | Safety Disconnect Switch(es) |
| **SEAS** | School of Engineering and Applied Science |
| **sec** | Second |
| **SEM** | Scanning Electron Microscope |
| **SF** | Shaping Field, equivalent to EF |
| **SHEILA** | Australian Heliac |
| **SIMS** | Secondary-Ion Mass Spectroscopy |

| | |
|---|---|
| **SNAP** | Time-independent power equilibrium code |
| **SNL** | Sandia National Laboratories |
| **SOP** | Safe Operating Procedure |
| **SOXMOS** | Soft X-Ray Monochromator Spectrometer |
| **SPARK** | A general geometry computer code that calculates transient eddy currents and the resulting fields |
| **SPEB** | Subcontract Proposal Evaluation Panel |
| **SPICE** | A general purpose circuit simulation code |
| **SPRED** | Survey, Power Resolution, Extended Domain Code |
| **SPS** | Surface Pumping System |
| **Sr** | Steradian |
| **SR** | Safety Requirements |
| **SRD** | System Requirements Document |
| **START-UP** | A computer code which evaluates free boundary axisymmetric equilibria and transport |
| **STEP** | Stellarator expansion equilibrium and stability code |
| **Supershots** | Low-current, high-density plasma discharges combined with intensive neutral-beam heating that are fired in a machine where the walls have been scrupulously conditioned via high-power discharges to remove adsorbed deuterium. |
| **SBD** | Surface Barrier Diode |
| **SURFAS** | A fast between-shot moments code |
| **TAC** | Technical Advisory Committee |
| **TCV** | Tokamak Condition Variable—a tokamak under construction at École Polytechnique Fédérale de Lausanne in Switzerland |
| **TDC** | Taylor-Discharge Cleaning |
| **TEA** | *T*ransverse *E*lectrical excitation at *A*tmospheric pressure |
| **TEXT** | Texas Experimental Tokamak |
| **TEXTOR** | Tokamak Experiment for Technologically Oriented Research (Jülich, West Germany) |
| **TF** | Toroidal Field |
| **TFCD** | Tokamak Fusion Core Device |
| **TFCX** | Tokamak Fusion Core Experiment |
| **TFD** | Telemetry Fault Detector |
| **TFM** | TFTR Flexibility Modification |
| **TFTR** | Tokamak Fusion Test Reactor |
| **TIBER** | Tokamak Ignition/Burn Experiment |
| **TiC** | Titanium Carbide |
| **TIV** | Torus Interface Valve |
| **TLD** | Thermoluminescent Dosimeters |
| **TMPs** | Turbo-Molecular Pumps |
| **TMX** | Tandem Mirror Experiment at Lawrence Livermore National Laboratory |
| **TMX-U** | Tandem Mirror Experiment Upgrade (at Lawrence Livermore National Laboratory) |
| **TORE-SUPRA** | Tokamak at Cadarache, France |
| **Torr** | A unit of pressure equal to 1/760 of an atmosphere |
| **TOS** | Teleoperator System |
| **TOS** | Terminal Operating Station |
| **TPI** | Tritium Pellet Injector |
| **TPOP** | Tritium Proof of Principle |
| **TRANSP** | Time-dependent transport analysis code |
| **TRECAMS** | Tritium Remote Control and Monitoring System |
| **TSC** | Tokamak Simulation Code |
| **TSCALE** | A computer code that scales plasma equilibrium parameters over a wide range of major radius and aspect ratio |
| **TSDS** | Tritium Storage and Delivery System |
| **TSTA** | Tritium Systems Test Assembly |
| **TVPS** | Torus Vacuum Pumping System |
| **TVTS** | TV Thomson Scattering |
| **UCLA** | University of California at Los Angeles |
| **UHF** | Ultrahigh Frequency |
| **USC** | User Service Center; implemented on a Digital Equipment Corporation (DEC) PDP-10 computer |
| **USGS** | United States Geological Survey |
| **USNRC** | United States Regulatory Commission |

| | |
|---|---|
| **UV** | Ultraviolet |
| **V** | Volt |
| **VAX** | Digital Equipment Corporation computer; "Virtual Address Extention" |
| **VC** | Variable Curvature |
| **VCD** | Viscous Current Drive |
| **VF** | Vertical Field |
| **VHF** | Very High Frequency |
| **VIPS** | Visible Impurity Photometric Spectrometer |
| **VSOP** | Variable Specification Omni Processor |
| **VSWR** | Variable Standing Wave Ratio |
| **VUV** | Vacuum Ultraviolet |
| **VXCS** | Vertical X-Ray Crystal Spectrometer |
| **W** | Watt |
| **WAF** | Work Approval Form (system) |
| **WBS** | Work Breakdown Structure |
| **WHIST** | A $1\frac{1}{2}$-dimensional transport code developed by the Oak Ridge printer National Laboratory |
| **WKB** | Wentzel-Kramers-Brillouin. (A method for analyzing wave behavior if propagation characteristics depend on position) |
| **W-VIIAS** | Wendelstein VII Stellarator Modified (at Garching, W. Germany) |
| **XCS** | X-Ray Crystal Spectrometer |
| **XIS** | (Horizontal) X-Ray Imaging System |
| **XUV** | Extreme Ultraviolet |
| **ZrAl** | Zirconium-Aluminum |
| **ZT-H** | A 4-MA reversed-field pinch experiment at the Los Alamos National Laboratory |

# Princeton Plasma Physics Laboratory Reports
# Fiscal Year 1987

**PPPL-2266, October 1986, 43 pp.**

Propagation of a Non-Relativistic Electron Beam in a Plasma in a Magnetic Field

H. Okuda, R. Horton, M. Ono, M. Ashour-Adballa

**PPPL-2365, October 1986, 7 pp.**

Designs for a TFTR Full-Power Pumped Limiter

R. Budny

**PPPL-2368, March 1987, 53 pp.**

Transport Simulations of Ohmic TFTR Experiments Models for $\chi_e$ and $\chi_i$

M.H. Redi, W.M. Tang, P.C. Efthimion, D.R. Mikkelsen, G.L. Schmidt

**PPPL-2372, October 1986, 28 pp.**

MHD Stable Regime of the Tokamak

C.Z. Cheng, H.P. Furth, A.H. Boozer

**PPPL-2378, October 1986, 20 pp.**

Long- and Short-Term Trends in Vessel Conditioning of TFTR

P.H. LaMarche, H.F. Dylla, M.G. Bell, F.P. Boody, C.E. Bush, R.J. Groebner, R.J. Hawryluk, K.W. Hill, D. Mueller, D.K. Owens, A.T. Ramsey, J.F. Schivell, S. Sesnic, B.C. Stratton, M. Ulrickson

**PPPL-2379, October 1986, 17 pp.**

Experimental Results from Detached Plasmas in TFTR

J.D. Strachan, F.P. Boody, C.E. Bush, S.A. Cohen, B. Grek, L. Grisham, F.C. Jobes, D.W. Johnson, D.K. Mansfield, S.S. Medley, W. Morris, H.K. Park, J. Schivell, G. Taylor, K.L. Wong, S. Yoshikawa, M.C. Zarnstorff, S.J. Zweben

**PPPL-2383, October 1986, 33 pp.**

An Algorithm for the Analysis of Inductive Antennas of Arbitrary Cross Section for Heating in the Ion Cyclotron Range of Frequencies

I.S. Lehrman, P.L. Colestock

**PPPL-2385, October 1986, 12 pp.**

Stabilization of Sawtooth Oscillation by Island Heating

W. Park, D.A. Monticello, T.K. Chu

**PPPL-2386, October 1986, 44 pp.**

Plasma-Material Interactions in TFTR

H.F. Dylla, M.G. Bell, W.R. Blanchard, F.P. Boody, N. Bretz, R. Budny, C.E. Bush, J.L. Cecchi, S.A. Cohen, S.K. Combs, S.L. Davis, B.L. Doyle, P.C. Efthimion, A.C. England, H.P. Eubank, R. Fonck, E. Fredrickson, L.R. Grisham, R.J. Goldston, B. Grek, R. Groebner, R.J. Hawryluk, D. Heifetz, H. Hendel, K.W. Hill, S. Hiroe, R. Hulse, D. Johnson, L.C. Johnson, S. Kilpatrick, P.H. LaMarche, R. Little, D.M. Manos, D. Mansfield, D.M. Meade, S.S. Medley, S.L. Milora, D.R. Mikkelsen, D. Mueller, M. Murakami, E. Nieschmidt, D.K. Owens, H. Park, A. Pontau, B. Prichard, A.T. Ramsey, M.H. Redi, J. Schivell, G.L. Schmidt, S.D. Scott, S. Sesnic, M. Shimada, J.E. Simpkins, J. Sinnis, F. Stauffer, B. Stratton, G.D. Tait, G. Taylor, M. Ulrickson, S. von Goeler, W.R. Wampler, K. Wilson, M. Williams, K.L. Wong, K.M. Young, M.C. Zarnstorff, S. Zweben

**PPPL-2387, October 1986, 20 pp.**

$^3$He Functions in Tokamak-Pumped Laser Systems

D.L. Jassby

**PPPL-2388, October 1986, 39 pp.**

Diffusion of a Plasma Subject to Neutral Beam Injection

H. Okuda, S. Hiroe

**PPPL-2389, November 1986, 70 pp.**

Physics Aspects of the Compact Ignition Tokamak

D. Post, G. Bateman, W. Houlberg, L. Bromberg, D. Cohn, P. Colestock, M. Hughes, D. Ignat, R. Izzo, S. Jardin, C. Kieras-Phillips, L.P. Ku, G. Kuo-Petravic, B. Lipshultz, R. Parker, C. Paulson, Y-K.M. Peng, M. Petravic, M. Phillips, N. Pomphrey, J. Schmidt, D. Strickler, A. Todd, N. Uckan, R. White, S. Wolfe, K. Young

**PPPL-2390, October 1986, 36 pp.**

Experimental Results from the TFTR Tokamak

R. Hawryluk, V. Arunasalam, J.D. Bell, M.G. Bell, M. Bitter, W. Blanchard, F. Boody, N. Bretz, R. Budny, C.E. Bush, J.D. Callen, J.L. Cecchi, S. Cohen, R.J. Colchin, S.K. Combs, J. Coonrod, S.L. Davis, D. Dimock, H.F. Dylla, P.C. Efthimion, L.C. Emerson, A.C. England, H.P. Eubank, R. Fonck, E. Fredrickson, L.R. Grisham, R.J. Goldston, B. Grek, R. Groebner,

H. Hendel, K.W. Hill, D.L. Hillis, E. Hinnov, S. Hiroe, R. Hulse, H. Hsuan, D. Johnson, L.C. Johnson, R. Kaita, R. Kamperschroer, S.M. Kaye, S. Kilpatrick, H. Kugel, P.H. LaMarche, A. Little, C.H. Ma, D.M. Manos, D. Mansfield, M. McCarthy, R.T. McCann, D.C. McCune, K. McGuire, D.M. Meade, S.S. Medley, S.L. Milora, D.R. Mikkelsen, W. Morris, D. Mueller, M. Murakami, E. Nieschmidt, D.K. Owens, V.K. Pare, H. Park, B. Prichard, A. Ramsey, D.A. Rasmussen, M.H. Redi, A.L. Roquemore, N.R. Sauthoff, J. Schivell, G.L. Schmidt, S.D. Scott, S. Sesnic, M. Shimada, J.E. Simpkins, J. Sinnis, F. Stauffer, B. Stratton, G.D. Tait, G. Taylor, C.E. Thomas, H.H. Towner, M. Ulrickson, S. von Goeler, R. Wieland, J.B. Wilgen, M. Williams, K.L. Wong, S. Yoshikawa, K.M. Young, M. Zarnstorff, S. Zweben

**PPPL-2391, October 1986, 11 pp.**

Loss of Confinement Following a Sawtooth Internal Disruption in PBX Tokamak

H. Takahashi, W. Morris, S. Sesnic, K. Bol, R. Fonck, B. Grek, G. Gammel, W. Heidbrink, R. Kaita, S. Kaye, H. Kugel, B. LeBlanc, M. Okabayashi, S. Paul, M. Reusch, D. Ward

**PPPL-2392, November 1986, 33 pp.**

Positron Deposition in Plasmas by Positronium Beam Ionization and Transport of Positrons in Tokamak Plasmas

T.J. Murphy

**PPPL-2393, October 1986, 15 pp.**

Impurity Transport on Ohmic- and Neutral-Beam-Heated TFTR Discharges

B.C. Stratton, S.A. Cohen, F.P. Boody, C.E. Bush, R. Ellis III, R.J. Fonck, E. Fredrickson, B. Grek, R.J. Groebner, K.W. Hill, R.A. Hulse, D. Johnson, B. LeBlanc, E.S. Marmar, K. McGuire, D. McNeill, A.T. Ramsey, J.F. Schivell, S. Sesnic, J. Timberlake

**PPPL-2394, November 1986, 32 pp.**

Measurements of Fusion Product Emission Profiles in Tokamaks

J.D. Strachan, W.W. Heidbrink, H.W. Hendel, J. Lovberg, T.J. Murphy, E.B. Nieschmidt, G.D. Tait, S.J. Zweben

**PPPL-2395, November 1986, 28 pp.**

Neutron Ion Temperature Measurement

J.D. Strachan, H.W. Hendel, J. Lovberg, E.B. Nieschmidt

**PPPL-2396, October 1986, 14 pp.**

Geometrical Effects in X-Mode Scattering

N. Bretz

**PPPL-2397, November 1986, 19 pp.**

Application of Small-Signal Fusion Energy Gain

D.L. Jassby

**PPPL-2398, November 1986, 10 pp.**

Loss of Beam Ions to the Inside of the PDX Tokamak During the Fishbone Instability

W.W. Heidbrink, P. Beiersdorfer

**PPPL-2399, October 1986, 30 pp.**

The Coupling of Mechanical Dynamics and Induced Currents in Plates and Surfaces

D.W. Weissenburger, J.M. Bialek

***PPPL-2400, April 1987, 76 pp.***

An Algorithm for the Calculation of 3-D ICRF Fields in Tokamak Geometry

D.N. Smithe, P.L. Colestock, R.J. Kashuba, T. Kammash

**PPPL-2401, December 1986, 153 pp.**

Theory of Current-Drive in Plasmas

N.J. Fisch

**PPPL-2402, March 1987, 67 pp.**

Tokamak Physics Studies Using X-Ray Diagnostic Methods

K.W. Hill, M. Bitter, S. von Goeler, P. Beiersdorfer, E. Fredrickson, H. Hsuan, K. McGuire, N.R. Sauthoff, S. Sesnic, J. Stevens

**PPPL-2403, October 1986, 54 pp.**

Tokamak X-Ray Diagnostic Instrumentation

K.W. Hill, P. Beiersdorfer, M. Bitter, E. Fredrickson, S. von Goeler, H. Hsuan, L.C. Johnson, S-L. Liew, K. McGuire, V. Pare, N.R. Sauthoff, S. Sesnic, J.E. Stevens

**PPPL-2404, November 1986, 17 pp.**

Scrape-off Profiles and Effects of Limiter Pumping in Tore Supra

R. Budny

**PPPL-2405, January 1987, 53 pp.**

Measurements of Beam-Ion Confinement During Tangential-Beam Driven Instabilities in PBX

W.W. Heidbrink, R. Kaita, H. Takahashi, G. Gammel, G.W. Hammett, S.M. Kaye

**PPPL-2406, January 1987, 29 pp.**

Recent Progress on the Compact Ignition Tokamak (CIT)

D.W. Ignat

**PPPL-2407, January 1987, 30 pp.**

HAIFA: A Modular, Fiber-Optic Coupled, Spectroscopic Diagnostic for Plasmas

A.T. Ramsey, S.L. Turner

**PPPL-2408, February 1987, 20 pp.**

Satellite Spectra of Heliumlike Nickel

H. Hsuan, M. Bitter, K.W. Hill, S. von Goeler, B. Grek, D.W. Johnson, L.C. Johnson, S. Sesnic, C.P. Bhalla, K.R. Karim, F. Bely-Dubau, P. Faucher

**PPPL-2409, February 1987, 9 pp.**

A Rotating Arc Plasma Invertor

M.F. Reusch, K. Jayaram

**PPPL-2410, February 1987, 53 pp.**

A Spectroscopic Study of Impurity Behavior in Neutral-Beam and Ohmically Heated TFTR Discharges

B.C. Stratton, A.T. Ramsey, F.P. Boody, C.E. Bush, R.J. Fonck, R.J. Groebner, R.A. Hulse, R.K. Richards, J. Schivell

**PPPL-2411, February 1987, 29 pp.**

Measurement of the Local Particle Diffusion Coefficient in a Magnetized Plasma

D.D. Meyerhofer, F.M. Levinton

**PPPL-2412, February 1987, 9 pp.**

Theory of Resistive Magnetohydrodynamic Instabilities Excited by Energetic-Trapped Particles in Large-Size Tokamaks

H. Biglari, L. Chen, R.B. White

**PPPL-2413, February 1987, 37 pp.**

Anisotropic Pressure Tokamak Equilibrium and Stability Considerations

E.R. Salberta, R.C. Grimm, J.L. Johnson, J. Manickam, W.M. Tang

**PPPL-2414, February 1987, 33 pp.**

Plasma Transport in a Compact Ignition Tokamak

C.E. Singer, L-P. Ku, G. Bateman

**PPPL-2415, February 1987, 25 pp.**

Simulation of a Compact Ignition Tokamak Discharge (CIT-2L)

D.P. Stotler, G. Bateman

**PPPL-2416, February 1987, 27 pp.**

Current Relaxation Time Scales in Toroidal Plasmas

D.R. Mikkelsen

**PPPL-2417, February 1987, 18 pp.**

TFTR Plasma Regimes

R.J. Hawryluk, V. Arunasalam, M.G. Bell, W.R. Blanchard, N.L. Bretz, R. Budny, C.E. Bush, J.D. Callen, S.A. Cohen, S.K. Combs, S.L. Davis, D.L. Dimock, H.F. Dylla, P.C. Efthimion, L.C. Emerson, A.C. England, H.P. Eubank, R.J. Fonck, E. Fredrickson, H.P. Furth, G. Gammel, R.J. Goldston, B. Grek, L.R. Grisham, G.W. Hammett, W.W. Heidbrink, H.W. Hendel, K.W. Hill, E. Hinnov, S. Hiroe, R.A. Hulse, H. Hsuan, K.P. Jaehnig, D.L. Jassby, D.W. Johnson, L.C. Johnson, R. Kaita, R. Kamperschroer, S.M. Kaye, S.J. Kilpatrick, R.J. Knize, H. Kugel, P.H. LaMarche, B. LeBlanc, R. Little, C.H. Ma, D.M. Manos, D.K. Mansfield, M.P. McCarthy, R.T. McCann, D.C. McCune, K. McGuire, D.H. McNeill, D.M. Meade, S.S. Medley, D.R. Mikkelsen, S.L. Milora, W. Morris, D. Mueller, V. Mukhovatov, E.B. Nieschmidt, J. O'Rourke, D.K. Owens, H. Park, N. Pomphrey, B. Prichard, A.T. Ramsey, M.H. Redi, A.L. Roquemore, P.H. Rutherford, N.R. Sauthoff, G. Schilling, J. Schivell, G.L. Schmidt, S.D. Scott, S. Sesnic, J.C. Sinnis, F.L. Stauffer, B.C. Stratton, G.D. Tait, G. Taylor, J.R. Timberlake, H.H. Towner, M. Ulrickson, V. Vershkov, S. von Goeler, F. Wagner, R. Wieland, J.B. Wilgen, M. Williams, K.L. Wong, S. Yoshikawa, R. Yoshino, K.M. Young, M.C. Zarnstorff, V.S. Zaveriaev, S.J. Zweben

**PPPL-2418, February 1987, 13 pp.**

Microinstability-Based Models for Confinement Properties and Ignition Criteria in Tokamaks

W.M. Tang, C.M. Bishop, B. Coppi, S.M. Kaye, F.W. Perkins, M.H. Redi, G. Rewoldt

**PPPL-2419, March 1987, 58 pp.**

High-Resolution Duo-Multichannel Soft X-Ray Spectrometer for Tokamak Plasma Diagnostics

J.L. Schwob, A.W. Wouters, S. Suckewer, M. Finkenthal

**PPPL-2420, March 1987, 40 pp.**

Ideal MHD Stability Properties of Pressure-Driven Modes in Low Shear Tokamaks

J. Manickam, N. Pomphrey, A.M.M. Todd

**PPPL-2421, April 1987, 17 pp.**

Impurity and Particle Transport and Control in TFTR

K.W. Hill, V. Arunasalan, M.B. Bell, W.R. Blanchard, N.L. Bretz, R. Budny, C.E. Bush, J.D. Callen, S.A. Cohen, S.K. Combs, S.L. Davis, D.L. Dimock, H.F. Dylla, P.C. Efthimion, L.C. Emerson, A.C. England, H.P. Eubank, R.J. Fonck, E. Fredrickson, H.P. Furth, G. Gammel, R.J. Goldston, B. Grek, L.R. Grisham, G.W. Hammett, R.J. Hawryluk, W.W. Heidbrink, H.W.

Hendel, E. Hinnov, S. Hiroe, R.A. Hulse, H. Hsuan, K.P. Jaehnig, D.L. Jassby, D.W. Johnson, L.C. Johnson, R. Kaita, R. Kamperschroer, S.M. Kaye, S.J. Kilpatrick, R.J. Knize, H. Kugel, P.H. LaMarche, B. LeBlanc, R. Little, C.H. Ma, D.M. Manos, D.K. Mansfield, M.P. McCarthy, R.T. McCann, D.C. McCune, K. McGuire, D.H. McNeill, D.M. Meade, S.S. Medley, D.R. Mikkelsen, S.L. Milora, W. Morris, D. Mueller, V. Mukhovatov, E.B. Nieschmidt, J. O'Rourke, D.K. Owens, H. Park, N. Pomphrey, B. Prichard, A.T. Ramsey, M.H. Redi, A.L. Roquemore, P.H. Rutherford, N.R. Sauthoff, G. Schilling, J. Schivell, G.L. Schmidt, S.D. Scott, S. Sesnic, J.C. Sinnis, F.L. Stauffer, B.C. Stratton, G.D. Tait, G. Taylor, J.R. Timberlake, H.H. Towner, M. Ulrickson, V. Vershkov, S. von Goeler, F. Wagner, R. Wieland, J.B. Wilgen, M. Williams, K.L. Wong, S. Yoshikawa, R. Yoshino, K.M. Young, M.C. Zarnstorff, V.S. Zaveriaev, S.J. Zweben

**PPPL-2422, May 1987, 89 pp.**

Rigorous Upper Bounds for Transport Due to Passive Advection by Inhomogeneous Turbulence

J.A. Krommes, R.A Smith

**PPPL-2423, February 1987, 31 pp.**

Numerical Solution of Three-Dimensional Magnetic Differential Equations

A.H. Reiman, H.S. Greenside

**PPPL-2424, April 1987, 15 pp.**

Eigenmode Analysis of Compressional Waves in the Magnetosphere

C.Z. Cheng, C.S. Lin

**PPPL-2425, April 1987, 16 pp.**

Energy Confinement and Profile Consistency in TFTR

R.J. Goldston, V. Arunasalam, M.G. Bell, W.R. Blanchard, N.L. Bretz, R. Budny, C.E. Bush, J.D. Callen, S.A. Cohen, S.K. Combs, S.L. Davis, D.L. Dimock, H.F. Dylla, P.C. Efthimion, L.C. Emerson, A.C. England, H.P. Eubank, R.J. Fonck, E. Fredrickson, H.P. Furth, B. Grek, L.R. Grisham, G.W. Hammett, R.J. Hawryluk, W.W. Heidbrink, H.W. Hendel, K.W. Hill, E. Hinnov, S. Hiroe, R.A Hulse, H. Hsuan, K.P. Jaehnig, D.L. Jassby, D.W. Johnson, L.C. Johnson, R. Kaita, R. Kamperschroer, S.M. Kaye, S.J. Kilpatrick, R.J. Knize, H. Kugel, P.H. LaMarche, B. LeBlanc, R. Little, C.H. Ma, D.M. Manos, D.K. Mansfield, M.P. McCarthy, R.T. McCann, D.C. McCune, K. McGuire, D.H. McNeill, D.M. Meade, S.S. Medley, D.R. Mikkelsen, S.L. Milora, W. Morris, D. Mueller, V. Mukhovatov, E.B. Nieschmidt, J. O'Rourke, D.K. Owens, H. Park, N. Pomphrey, B. Prichard, A.T. Ramsey, M.H. Redi, A.L. Roquemore, P.H. Rutherford, N.R. Sauthoff, G. Schilling, J. Schivell, G.L. Schmidt, S.D. Scott, S. Sesnic, J.C. Sinnis, F.L. Stauffer, B.C. Stratton, G.D. Tait, G. Taylor, J.R. Timberlake, H.H. Towner, M. Ulrickson, V. Vershkov, S. von Goeler, F. Wagner, R. Wieland, J.B. Wilgen, M. Williams, K.L. Wong, S. Yoshikawa, R. Yoshino, K.M. Young, M.C. Zarnstorff, V.S. Zaveriaev, S.J. Zweben

**PPPL-2426, May 1987, 46 pp.**

Lower Hybrid Experiments on PLT Using Grills Having Various $n_{\parallel}$ Spectral Widths

J. Stevens, R. Bell, S. Bernabei, A. Cavallo, T.K. Chu, P.L. Colestock, W. Hooke, J. Hosea, F. Jobes, T. Luce, E. Mazzucato, R. Motley, R. Pinsker, S. von Goeler, J.R. Wilson

**PPPL-2427, April 1987, 21 pp.**

Vectorizing and Macrotasking Monte Carlo Neutral Particle Algorithms

D.B. Heifetz

**PPPL-2429, July 1987, 18 pp.**

Boxcar Photography

G.J. Greene, G. Cutsogeorge, M. Ono

**PPPL-2430, April 1987, 19 pp.**

Effects of High Power Ion Bernstein Waves on a Tokamak Plasma

M. Ono, P. Beiersdorfer, R. Bell, S. Bernabei, A. Cavallo, A. Chmyga, S.A. Cohen, P.L. Colestock, G. Gammel, G.J. Greene, J. Hosea, R. Kaita, I. Lehrman, G. Mazzitelli, E. Mazzucato, D.H. McNeill, K. Sato, J. Stevens, J.R. Timberlake, J.R Wilson, A.W. Wouters

**PPPL-2431, April 1987, 41 pp.**

Gyrokinetic Particle Simulation of Ion Temperature Gradient Drift Instabilities

W.W. Lee, W.M. Tang

**PPPL-2432, April 1987, 31 pp.**

Operation of a Tangential Bolometer on the PBX Tokamak

S.F. Paul, R.J. Fonck, G.L. Schmidt

**PPPL-2435, April 1987, 19 pp.**

Coherent and Turbulent Fluctuations in TFTR

K. McGuire, V. Arunasalam, M.G. Bell, W.R. Blanchard, N.L. Bretz, R. Budny, C.E. Bush, J.D. Callen, S.A. Cohen, S.K. Combs, S.L. Davis, D.L. Dimock, H.F. Dylla, P.C. Efthimion, L.C. Emerson, A.C. England, H.P. Eubank, R.J. Fonck, E. Fredrickson, H.P. Furth, G. Gammel, R.J. Goldston, B. Grek, L.R. Grisham, G.W. Hammett, R.J. Hawryluk, W.W. Heidbrink, H.W. Hendel, K.W. Hill, E. Hinnov, S. Hiroe, R.A. Hulse, H. Hsuan, K.P. Jaehnig, D.L. Jassby, D.W. Johnson, L.C. Johnson, R. Kaita, R. Kamperschroer, S.M. Kaye, S.J. Kilpatrick, R.J.

Knize, H. Kugel, P.H. LaMarche, B. LeBlanc, R. Little, C.H. Ma, D.M. Manos, D.K. Mansfield, M.P. McCarthy, R.T. McCann, D.C. McCune, D.H. McNeill, D.M. Meade, S.S. Medley, D.R. Mikkelson, S.L. Milora, W. Morris, D. Mueller, V. Mukhavatov, E.B. Nieschmidt, J. O'Rourke, D.K. Owens, H. Park, N. Pomphrey, B. Prichard, A.T. Ramsey, M.H. Redi, A.L. Roquemore, P.H. Rutherford, N.R. Sauthoff, G. Schilling, J. Schivell, G.L. Schmidt, S.D. Scott, S. Sesnic, J.C. Sinnis, F.L. Stauffer, B.C. Stratton, G.D. Tait, G. Taylor, J.R. Timberlake, H.H. Towner, M. Ulrickson, V. Vershkov, S. von Goeler, F. Wagner, R. Wieland, J.B. Wilgen, M. Williams, K.L. Wong, S. Yoshikawa, R. Yoshino, K.M. Young, M.C. Zarnstorff, S.J. Zweben

**PPPL-2436, May 1987, 30 pp.**

Characteristics of Solid-Target Charge-Exchange Analyzers for Energetic Ion Diagnostics on Tokamaks

P. Beiersdorfer, A.L. Roquemore, R. Kaita

**PPPL-2437, May 1987, 24 pp.**

Fast Current Ramp Experiments on TFTR

E. Fredrickson, K. McGuire, R.J. Golston, M.G. Bell, B. Grek, D.W. Johnson, W. Morris, F.L. Stauffer, G. Taylor, M.C. Zarnstorff

**PPPL-2438, May 1987, 48 pp.**

Injection and Propagation of a Nonrelativistic Electron Beam and Spacecraft Charging

H. Okuda, J. Berchem

**PPPL-2439, May 1987, 16 pp.**

Formation and Maintenance of a Tokamak Discharge Via DC Helicity Injection

M. Ono, G.J. Greene, D. Darrow, C. Forest, H. Park, T.H. Stix

**PPPL-2440, June 1987, 16 pp.**

Solitary Alfvén Wave Envelopes and the Modulational Instability

C.F. Kennel

**PPPL-2441, May 1987, 17 pp.**

Ion Radial Transport Induced by ICRF Waves in Tokamaks

L. Chen, J. Vaclavik, G.W. Hammett

**PPPL-2442, May 1987, 80 pp.**

Environmental Monitoring Report for Calendar Year 1986

J.R. Stencel

**PPPL-2443, May 1987, 23 pp.**

Prospects for Alpha Particle Studies on TFTR

S.J. Zweben

**PPPL-2444, May 1987, 35 pp.**

Gamma Ray Measurements During Deuterium and $^3$He Discharges on TFTR

F.E. Cecil, S.S. Medley

**PPPL-2445, June 1987, 14 pp.**

Asymptotic Stability Boundaries of Ballooning Modes in Circular Tokamaks

L. Chen, A. Bondeson, M.S. Chance

**PPPL-2446, July 1987, 15 pp.**

Polarized Advanced Fuel Reactors

R.M. Kulsrud

**PPPL-2447, July 1987, 17 pp.**

Application of Polarized Nuclei to Fusion

R.M. Kulsrud

**PPPL-2448, May 1987, 32 pp.**

Conditioning of the Graphite Bumper Limiter for Enhanced Confinement Discharges in TFTR

H.F. Dylla, P.H. LaMarche, M. Ulrickson, R.J. Goldston, D.B. Heifetz, K.W. Hill, A.T. Ramsey

**PPPL-2449, May 1987, 39 pp.**

Effect of Deuteron Temperature on Iron Forbidden Line Intensities in RF-Heated Tokamak Plasmas

K. Sato, S. Suckewer, A.W. Wouters

**PPPL-2450, July 1987, 25 pp.**

MIRI: A Multichannel Far-Infrared Laser Interferometer for Electron Density Measurements on TFTR

D.K. Mansfield, H. Park, L.C. Johnson, H.M. Anderson, R. Chouinard, V.S. Foote, C.H. Ma, B.J. Clifton

**PPPL-2451, June 1987, 17 pp.**

Diagonal Padé Approximations for Initial Value Problems

M.F. Reusch, L. Ratzan, N. Pomphrey, W. Park

**PPPL-2452, June 1987, 16 pp.**

Electron Heating Using Lower Hybrid Waves in the PLT Tokamak

R. Bell, S. Bernabei, A. Cavallo, T.K. Chu, T. Luce, R. Motley, M. Ono, J. Stevens, S. von Goeler

**PPPL-2453, June 1987, 24 pp.**

Damping of Electron Cyclotron Waves in Dense Plasmas of a Compact Ignition Tokamak

E. Mazzucato, I. Fidone, G. Granata

**PPPL-2454, June 1987, 8 pp.**

Fission-Detector Determination of D-D Triton

Burnup Fraction in Beam-Heated TFTR Plasmas

D.L. Jassby, H.W. Hendel, Cris W. Barnes, S. Bosch, F.E. Cecil, D.C. McCune, E.B. Nieschmidt, J.D. Strachan

**PPPL-2455, June 1987, 8 pp.**

Reduction in TFTR Fusion Reaction Rate by Unbalanced Beam Injection and Rotation

H.W Hendel, D.L. Jassby, M. Bitter, G. Taylor

**PPPL-2456, June 1987, 19 pp.**

Theory of Magnetospheric Hydromagnetic Waves Excited by Energetic Ring-Current Protons

L. Chen, A. Hasegawa

**PPPL-2457, June 1987, 8 pp.**

Inverse Problem for Incremental Synchrotron Radiation

N.J. Fisch

**PPPL-2458, August 1987, 29 pp.**

The Generalized Balescu-Lenard Collision Operator: A Unifying Concept for Tokamak Transport

H.E. Mynick

**PPPL-2459, July 1987, 9 pp.**

Rigorous Upper Bounds for Fluid and Plasma Transport Due to Passive Advection

J.A. Krommes, R.A. Smith, C.-B. Kim

**PPPL-2460, July 1987, 29 pp.**

Parabolic Approximation Method for the Mode Conversion-Tunneling Equation

C.K. Phillips, P.L. Colestock, D.Q. Hwang, D.G. Swanson

**PPPL-2461, August 1987, 27 pp.**

Course/Workshop on Muon Catalyzed Fusion and Fusion with Polarized Nuclei

R.M. Kulsrud

**PPPL-2462, August 1987, 15 pp.**

Current Drive, Anticurrent Drive, and Balanced Injection

S. von Goeler, J. Stevens, P. Beiersdorfer, R. Bell, S. Bernabei, M. Bitter, A. Cavallo, T.K. Chu, H. Fishman, K. Hill, W. Hooke, R. Motley, J.R. Wilson

**PPPL-2463, August 1987, 18 pp.**

Sawtooth Effects in INTOR and TIBER

D.P. Stotler, D. Post, G. Bateman

**PPPL-2464, August 1987, 31 pp.**

Nonperturbative Analysis of the Two-Level Atom—Applications to Multiphoton Excitation

R.E. Duvall, E.J. Valeo, C.R. Oberman

**PPPL-2465, August 1987, 11 pp.**

The Spheromak - a Prototype for Ultra-High-Field Superconducting Magnets

H.P. Furth, S.C. Jardin

**PPPL-2466, August 1987, 27 pp.**

Gas Utilization in TFTR Neutral Beam Injectors

J.H. Kamperschroer, G. Gammel, H. Kugel, L.R. Grisham, T.N. Stevenson, A. von Halle, M. Williams, T.T.C. Jones

**PPPL-2467, August 1987, 8 pp.**

Differential Form of the Collision Integral for a Relativistic Plasma

B.J. Braams, C.F.F. Karney

**PPPL-2468, September 1987, 21 pp.**

Feedback Stabilization of the Axisymmetric Instability of a Deformable Tokamak Plasma

N. Pomphrey, S.C. Jardin

**PPPL-2469, September 1987, 64 pp.**

A Nonvariational Code for Calculating Three-Dimensional MHD Equilibria

H.S. Greenside, A.H. Reiman, A. Salas

**PPPL-2470, August 1987, 12 pp.**

Neoclassical Diffusion of Heavy Impurities in a Rotating Tokamak Plasma

K.L. Wong, C.Z. Cheng

**PPPL-2471, August 1987, 29 pp.**

Calculation of Fusion Angular Correlation Coefficients for Fusion Plasmas

T.J. Murphy

**PPPL-2472, September 1987, 15 pp.**

Quenching of Spontaneous Emission Coefficients in Plasmas

Y. Chung, P. Lemaire, S. Suckewer

**PPPL-2473, September 1987, 41 pp.**

Magnetic Fluctuations CAN Contribute to Plasma Transport, "Self-Consistency Constraints" Notwithstanding

J.A. Krommes, C.-B. Kim

**PPPL-2474, September 1987, 15 pp.**

Electron Temperature Profiles in High Power Neutral-Beam-Heated TFTR Plasmas

G. Taylor, B. Grek, F.L. Stauffer, R.J. Goldston, E. Fredrickson, R. Wieland, M.C. Zarnstorff

**PPPL-2476, September 1987, 49 pp.**

Ion Temperature from Tangential Charge Exchange Neutral Analysis on the Tokamak Fusion Test Reactor

C.L. Fiore, S.S. Medley, G.W. Hammett, R. Kaita, A.L. Roquemore, S.D. Scott

**PPPL-2477, September 1987, 94 pp.**

Collisional Processes of Hydrocarbons in Hydrogen Plasmas

A.B. Ehrhardt, W.D. Langer

## Notice



Available from
National Technical Information Service
U.S. Department of Commerce
5285 Port Royal Road
Springfield, Virginia 22161

Price: Printed Copy $*; Microfiche $4.50

| *Pages | NTIS Selling Price |
|---|---|
| 1-25 | $ 7.00 |
| 26-50 | 8.50 |
| 51-75 | 10.00 |
| 76-100 | 11.50 |
| 101-125 | 13.00 |

---

**Editor:** Carol A. Phillips

**Editorial Assistant:** Ann Lengyel

**Graphic Arts:** Terry Birch
Kim Burke
Greg Czechowicz
Bernie Giehl
Steve Lengyel

**Photography:** Linda Fahner
Ed Farris, Jr.
John Peoples